UNIVERSITY OF NAIROBI

THE GEOLOGY AND HYDROCARBON POTENTIAL OF LUGH-MANDERA BASIN (SOMALIAN SECTOR)

WARSAME MOHAMED ATTEYEH

I56/14689/2018

A DISSERTATION SUBMITTED IN PARTIAL FULFILLMENT OF THE REQUIREMENTS FOR DEGREE OF MASTERS OF SCIENCE IN GEOLOGY (PETROLEUM GEOLOGY) IN THE DEPARTMENT OF EARTH AND CLIMATE SCIENCES.

DEPARTMENT OF EARTH AND CLIMATE SCIENCES

NOVEMBER, 2021.

DECLARATION

This research project is my original work and has not been presented for any degree or academic work in any other university.

Signature _____   Date 29/11/2021_____

Warsame Mohamed Atteyeh

Reg. No.: I56/14689/2018

This dissertation has been submitted for examination with my knowledge as the university supervisor.

Signed …………………………….   Date 29/11/2021……………….

Dr. Daniel Dennis Waga

University Of Nairobi

Department Of Earth and Climate Sciences

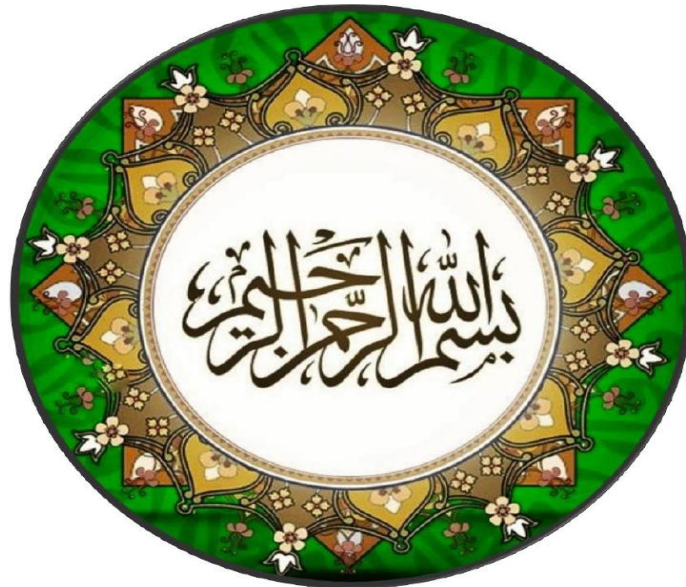Signed ……………………………   Date 29/11/2021……….

Dr. Edwin Wandubi Dindi

University Of Nairobi

Department Of Earth and Climate Sciences

DEDICATION

I dedicate this thesis to the Almighty Allah for the grace and strength He has offered me. I also thank my wife, parents, relatives and friends for their unwavering support, encouragement and guidance during my Master's study at the University of Nairobi. Lastly, I dedicate this project to my late Uncle who was an instrumental person in my life.

In the name of
ALLAH
The most Beneficent &
the most Merciful

ACKNOWLEDGEMENTS

ABSTRACT

This study attempts to evaluate the petroleum potential of the Somalian sector of the broad Lugh-Mandera basin based on the available geological and geophysical (Seismic) data sets. The basin has not been studied in detail, and is classified as a frontier exploration area with only 3 wells drilled in an area of approximately $70,000 Km^2$. It is infilled with thick Jurassic-Cretaceous formations whose source, reservoir, and sealing configurations and distribution are still poorly understood. The main aim of this research was to undertake an integrated structural and stratigraphic study of all geological data, in particular, interpretation of fourteen (14) 2D seismic profiles with a total length of 605 km and tied to the Hol-1 well and also evaluates the source rock potential of several levels of interest through Time-Temperature Index (TTI) Modeling. In addition, the investigations also undertook a regional correlation with formations from neighboring Ogaden basin in Ethiopia. Some of the tasks of the objectives that guided this study included: a) determination the of rock units succession and the types of proven petroleum systems within the basin compared to the neighboring Ogaden basin found in Ethiopia, through interpretation of the seismic sections and well log data; b) understanding the aspects of structural style and it's impact on hydrocarbon entrapment, and delineate the subsurface target horizon in the study area by using (depth maps, thicknesses maps, and the interpreted fourteen (14) seismic profiles); c) to evaluate the hydrocarbon potential of the area by creating and analysing burial curves of the source rock intervals of the basin by calculating the TTI values.

The stratigraphy of Hol-1 well encountered mainly the Jurassic section and lowermost of Cretaceous formations. The lithologies are commonly represented by interbedded layers of grey limestone, lime mudstone, shales, sandstones, pale marls, with minor dolomite and anhydrite occurrences.

The result of the seismic interpretation shows that the deformed Garbaharey fold belt formed as a result of wrench tectonics and comprises anticlines with a wavelength of about 10 km that are associated with a transpressional right strike slip movement. The presence of positive flower structures that are viable hydrocarbon traps can be observed from the interpreted seismic profiles.

A TTI analysis was done for the Lower Jurassic source rock interval encountered by Hol-1 well and yielded a value of 1,319. This value corresponds to Vitrinite Reflectance (Ro) of more than 2. Which indicates that these source rocks are over mature and are located within the dry gas window, which initiated in the Sinemurian (approximately 196 Ma) times? Maturation and expulsion began in the Aalenian (172 Ma). The Middle Jurassic source rock interval gives a TTI value of 20 which suggests maturation within the peak oil window. The Upper Jurassic source rock is positioned within the early oil window, as indicated by a TTI value of 5.1, maturation and outflow began Oxfordian (159 M.a) and is still ongoing. Faulted anticlines formed after the initial hydrocarbon expulsion and migration might have occurred and entrapment relies on only re-distribution of hydrocarbons.

Potential hydrocarbon traps developed in the Somalian sector of the Lugh-Mandera basin are presented by structural (wrench faults, folds), and hydrodynamic types (Baidoa formation). The current study proposes other drilling locations in the south-eastern part of the study area that will test the pontential of the supposed hydrodynamic trap.

TABLE OF CONTENTS

LIST OF FIGURES

LIST OF TABLES

LIST OF ABBREVIATIONS

3D: Three dimentional

2D: Two dimensional

BGR: Federal Institute for Geosciences and Natural Resources

CGG: CGG Robertson Geospec Data Services

MPMR: Ministry of Petroleum and Mineral Resources

SEGY: Society of Exploration Geophysicists y-format

      Seismic Project

Ma: Million years

.LAS: .las well data format

SP: Shot Point

TWT: Two way travel time

TTI: Time Temperature Index

TOC: Total Organic Carbon

PSE: Petroleum System Element

DST: Drill Stem Test

TAI: Thermal Alteration Index

J_a: Jurassic (Adigrat Formation)

J_u: Jurassic (Uanei Member)

J_b: Jurassic (Baidoa Member)

J_{g1}:   Jurassic (L.Goloda Member)

J_{g2}:   Jurassic (U.Goloda Member)

J_{an}:   Jurassic (Anole Formation)

J_{ug}:   Jurassic (Uegit Formation)

K_b: Cretaceous (Busul Member)

CHAPTER 1 : BACKGROUND INFORMATION

1.1. Introduction

This study area was undertaken over the Lugh-Mandera basin of SW Somalia (Figure.1.1), and attempts to assess the hydrocarbon potential of this part of the country. Over the years, hydrocarbon prospects in Somalia have motivated a number of oil exploration firms to set base in the country in hope of finding oil and gas. The history goes back to, 1950s, when Agip (Italian) and Sinclair Oil Corporation (American) companies begun the geochemistry survey of Somalia and drilled several wells for stratigraphic purposes and commercial objectives. This paved the way for other companies to rush to enter the country.. In the late fifties (1950's) and sixties (1960's), Somalia led in exploration intensity in Africa. Amerada Company surveyed and drilled a couple of wells in north Somalia. Western companies ceased their operations in Somalia in the seventies (1970's), however, returned later in the eighties when Somalia started to open its economy for foreign investors. At present, six (6) sedimentary basins have been identified (Figure.1.1).
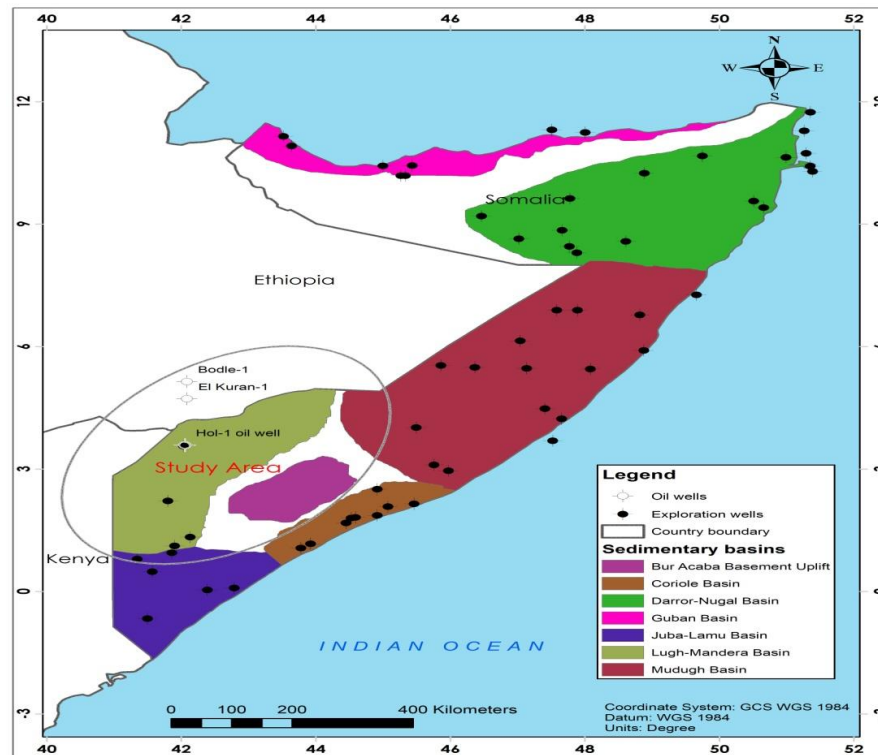
Figure 1.1: Somalia Hydrocarbon Basin Discoveries (Modified after Harms and Naleye, 1993).

These are: Lugh-Mandera, Juba-Lamu, Coriole, Mudugh, Darror-Nugal, and Guban basin (Harms et Naleye, 1993).

Somalia petroleum exploration has progressed with interruptions for the last 60-years, with the initial assessment wells, Sagaleh-1 and Hobyo-1, spudded in 1956. As of 2012, a total of 63 wells with only oil and gas shows had been drilled. None of them, however, has proven to be financially viable (Harms and Brady, 2002).

1.1.1. Reasons why previous exploration did not reach a commercial discoveries

The territory of Somalia has not been studied in detail. This is evidenced by low drilling density, with wells widely spread from one another at a distance of 50 to 100 kilometers in some cases up to 400 kilometers, in others (Barnes, 1976). The explanations for this are;

i.   Early geological models were inaccurate- whereby many wells were wrongly located.

ii. The preliminary data was of low quality and could not accurately determine the structural nature of the research area and the placement of wells. Most of the historical studies were conducted using outdated or insufficient seismic data. Future exploration activities are likely to utilise the modern and advanced geophysical methods and exploration strategies.

iii. Technology limitation- Exploration has become more plausible as a consequence of technical advancements in seismic surveys and other fields of discovery.

iv. Since the legislative body approved a new Petroleum Legislation Act in 2006 that clarifies sharing agreements, which create a better environment for exploration, discovery, development, production, and export of hydrocarbon products.

v.   Low well density or drilling density with only 63 historical wells drilled across vast sedimentary basins.

1.1.2. Oil and Gas Potential

The Jurassic to Miocene successions covers most of the territory of Somalia, ranging from two to five kilometres in thickness making it ideal for a petroleum generation, migration, and accumulation. The potential reservoirs are presented by the carbonate and

clastic varieties which developed at different stratigraphic levels (Barnes, 1976). The infill thickness of the six sedimentary basins that have shown huge hydrocarbon potential and development varies greatly (Harms and Naleye, 1993). Some of the basins have a complete working petroleum system.

The collapse of Eastern Gondwana super continent began in the Carboniferous and lasted in Jurassic Times, while the breakup of Madagascar and India took place in the early Late Jurassic, and the development of the Gulf of Aden occurred in the mid-Tertiary. These events contributed to the primary structural components seen in this region. Late Cretaceous to mid-Tertiary faulting and warping can be observed in southern and central Somalia. The Gulf of Aden rifting that led to Africa split from the Arabian Peninsula is responsible for the majority of deformation in the north part of the country (Bosellini and Alfonso, 1989; Barnes, 1976; Kamen-Kaye and Barnes, 1979 and Whiteman, 1981).

In a diversity of geological contexts, hydrocarbon source rocks coexist with prospective reservoirs and structures (Bosellini and Alfonso, 1989). The rift basins, regional arches, carbonate platform margins, deltaic complexes, and faulted basin edges are all attractive exploitation targets (Barnes, 1976).

Drilling density of Somalia basins is very low by comparison to other similar basins in the world. Table (1.1) shows the area of each of the six sedimentary basins and the number of wells drilled in them. Drilling density ranges from one well for every 2,300 km^2 to one well for every 23,000 km^2.

In some places, a distance between the exploratory wells is more than 100 km, leaving many opportunities for additional exploration. Despite the low well density, the contribution of petroleum exploration to the knowledge of geology of Somalia has been significant. The seismic, gravity, and magnetic surveys and drilling exercises have all added significantly to the understanding of structure and stratigraphy.

Table 1.1: Exploration in Somali sedimentary basins (Harms and Naleye, 1993)

No	Sedimentary basins	Area in Km^2	Wells drilled	Drilling Density= Area/Wells
1	Lugh-Mandera	70,000	3	23,000
2	Juba-Lamu	45,000	6	7500
3	Coriole	25,000	11	2300
4	Mudugh	150,000	16	9400
5	Darror-Nogal	160,000	14	11,400
6	Guban	35,000	7	5000

N.B.   The last two wells drilled in the Darror Valley of Puntland are included.

The questions arising about the discovery of oil in Somalia, particularly in the south-western part of the country, derive favourable responses due to the following few reasons:

i.   The presence of several significant oil seeps (Tarbaj Oil Seepage) in north-eastern Kenya and (Genale Oil Seepage) eastern Ethiopia (Barnes, 1976; Kamen-Kaye and Barnes, 1979).

ii.   The discovery of gas by Tenneco Oil Corp at the Calub and Halala fields (Wardheer, Ethiopia), which are close to Galinsoor in Galmudugh (Kamen-Kaye and Barnes, 1979).

iii.   The advancements by Tenneco Oil Corp in discovering non-commercial oil at El Kuran, near the Somalia-Ethiopia border, highlighted the hydrocarbon potential of the area (Biro, 1974).

It is apparent from the preceding facts that Lugh-Mandera basin is a potential area for hydrocarbon generation, with its economic viability still unrevealed. The current investigation focused on the wrench fault tectonics that has been identified by previous scholars (Beltrandi and Pyre, 1973).   An in-depth scrutiny of physical structure, stratigraphy, and time temperature index of Lugh-Mandera basin led to the decision to investigate the influence of wrench fault tectoics on the petroleum system.

The path is clear for investors and multinational oil corporations to actively consider exploring the Lugh-Mandera basin for oil and gas. The Lugh-Mandera basin is a large

sedimentary basin with a thick infill including Jurassic-Early Cretaceous sediments of more than 4 km in thickness.

These thick and diverse strata are products of extensional tectonics that happened between 200 and 130 million years ago. Wrench faulting led to facies alterations, positive flower fault structures, and folds. Combinations of trap, reservoir, seal, and source rock may be conceivable due to tectonics (Harms and Naleye, 1993).

1.2. Problem Statement

Lugh-Mandera basin of the SW Somalia is one of the remaining frontier exploration basins and is infilled with thick Jurassic-Cretaceous formations whose source, reservoir, and sealing configurations and distribution are still poorly understood.

Despite the fact that the basin has gained an increasing attention during the last decades, mainly due to the successful gas discoveries in its western part of Ethiopia, the area has an extremely sparse well control comprising only 3 wildcat wells, as such, not much is known about the geology of this vast, largely unexplored territory.

This project is dedicated to investigate its tectonic history, structural architecture and subsurface stratigraphy based on an integrated interpretation of both seismic and well log data. To accomplish this, the following tasks were undertaken during the study:

- ➢ Seismic stratigraphy analysis of the Jurassic-Early Cretaceous formations from the Somalian sector of the Lugh Mandera Basin
- ➢ Establishment and classification of the Petroleum Systems (PS) developed within the Somalian sector of the Lugh Mandera Basin
- ➢ Evaluation of the source rock potential of the Jurassic-Early Cretaceous intervals, and their comparisons with contemporaneous formations developed in neighboring Ogaden basin of Ethiopia.
- ➢ Identification of the dominating structural style of the basin and evaluation of structural and hydrodynamic types of hydrocarbon entrapment
- ➢ Proposal of future infill drilling sites based on subsurface geological and structural mapping interpretations.

1.3. The Study Area

1.3.1. Location

The Lugh-Mandera basin is located in SW Somalia, trends in N.E.-S.W directions and is considered a synclinal feature with dimensions approximately 500 kms by 300 kms (310 miles x185miles) (Figure 1.2). Accordingly, the basin can be described as a massive syncline known as the Tomalo syncline, with branches that only drop a few degrees (Ali Kassim et al., 2002).
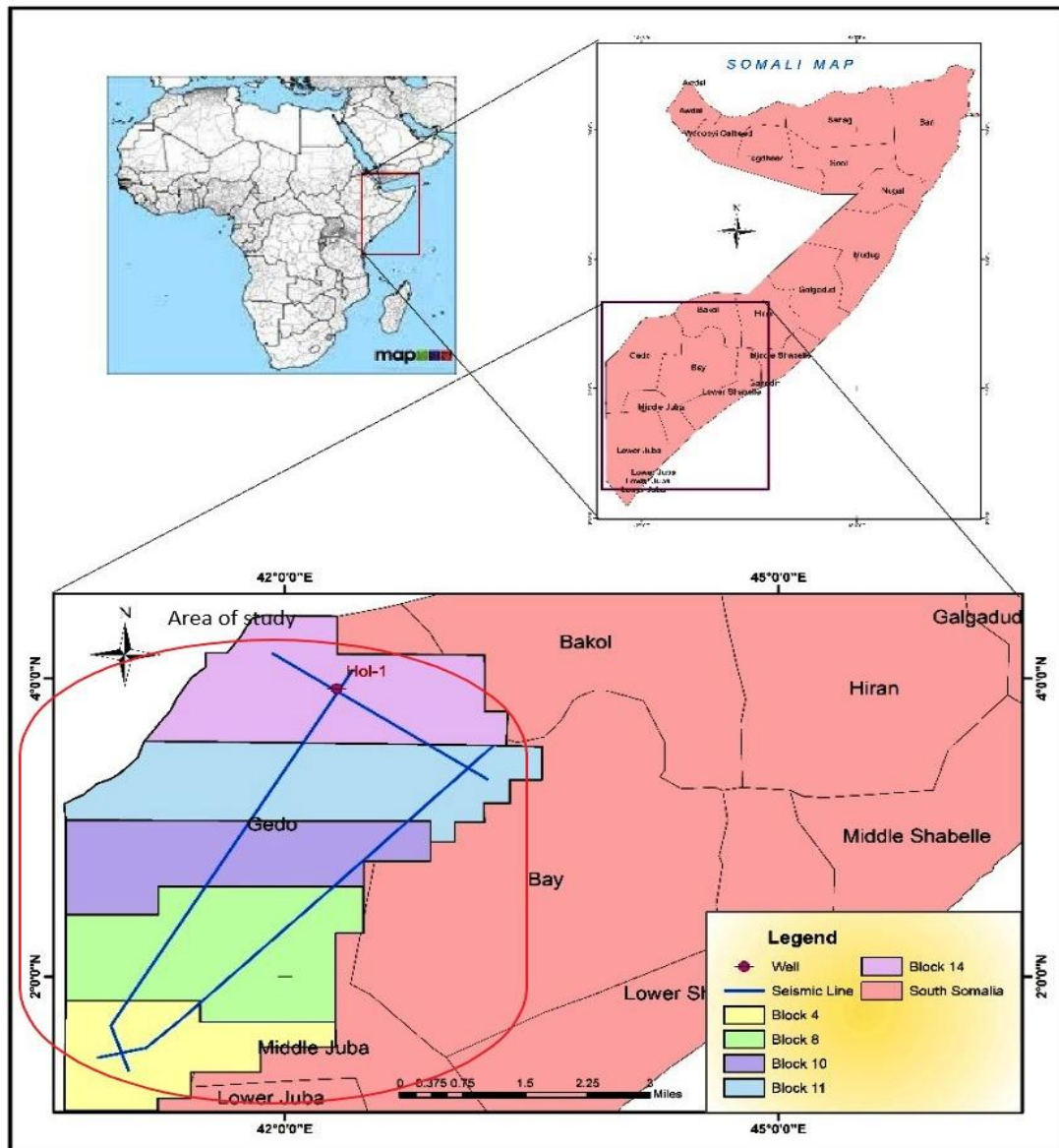
Figure 1.2: Location of Lugh-Mandera basin in south western Somalia with the fourteen seismic profiles used in the study area and the position of Hol-1 well indicated.

6

It is the third largest sedimentary basin in Somalia following Mudugh and Nogal basins (Harms and Naleye, 1993). Its sedimentary infill exceeds 4 km based on the results from the 3 exploratory wells that have been drilled in the basin.

1.3.2. Climate

The region is characterized by dry climate, spanning over wide, flat, and gently sloping plains. The Jubba valley is situated approximately 160 m above the sea level. The region is also characterized by two rainy seasons, with rainfall amounts varying between 200-2000 mm per year particularly in regions bordering Ethiopia in Bakool, Hiiraan and Gedo. The long rain season usually occur between April and June, while the short rain season spans between October and December. However, because the Jilal season is wet at the coast, there is a distinct rainy season from March to September, which is fully shaped by the SW monsoon winds. The peak rainfall amount, as reported by Fantoli (1960) based on data from Kismayu station, was in June and had a rainfall range of 300–600 mm/yr; this can occasionally exceed 600-700 mm/yr in the South. However, as near the Kenyan border, the volume of rain drops. A mean monthly rainfall of 50 mm and is considered as the limit between dry and humid months (Rizzo, 1977). The annual mean temperature is in the range of 26–27 ℃ with low seasonal fluctuations.

1.3.3. Physiography, Vegetation and Drainage

The south-western area of Somalia is marked by morphological maturity, with vast, level, or slightly sloping plains. The thalweg of the Jubba valley, which is 160 meters above sea level in Lugh and around 100 meters above sea level in Baardheere, highlights the small height variations in the area. The average altitude of the area is about 200–300 m a.s.l. and alluvial deposits are found at altitudes of 150–200 m (Ali Kassim et al, 2002),

The topography is characterized by bushes, scub land, shallow rivers of dry sand beds and low trees and grasslands during rainy seasons. The environment is very ideal for pastoralism (Acacia Researchers, 2008).

In the Somali coastal zone, the open woodland vegetation (''boscaglia'' in Italian; Pichi-Sermolli, 1957) is characterized by sparse umbrellalike treelets and thorny shrubs, both principally consisting of species of the Acacia family.

The Juba drainage basin is approximately 64,744 km^2 and is mainly built in the Middle Juba, Lower Juba and Gedo regions (Swalim, 2007). Juba River is the main stream that flows into the basin and crosses the study area as shown in figure 1.3.

The Juba River, which originates from the upper catchments of the Juba basin in neighboring Ethiopia, flows in a valley and its waters are used for irrigation purposes. The quantity of the river water that flows here is twice that of R. Shabelle and it remains the main source of water for the population. Due to the increased consumption, the river waters downstream are significantly reduced (Swalim, 2007).
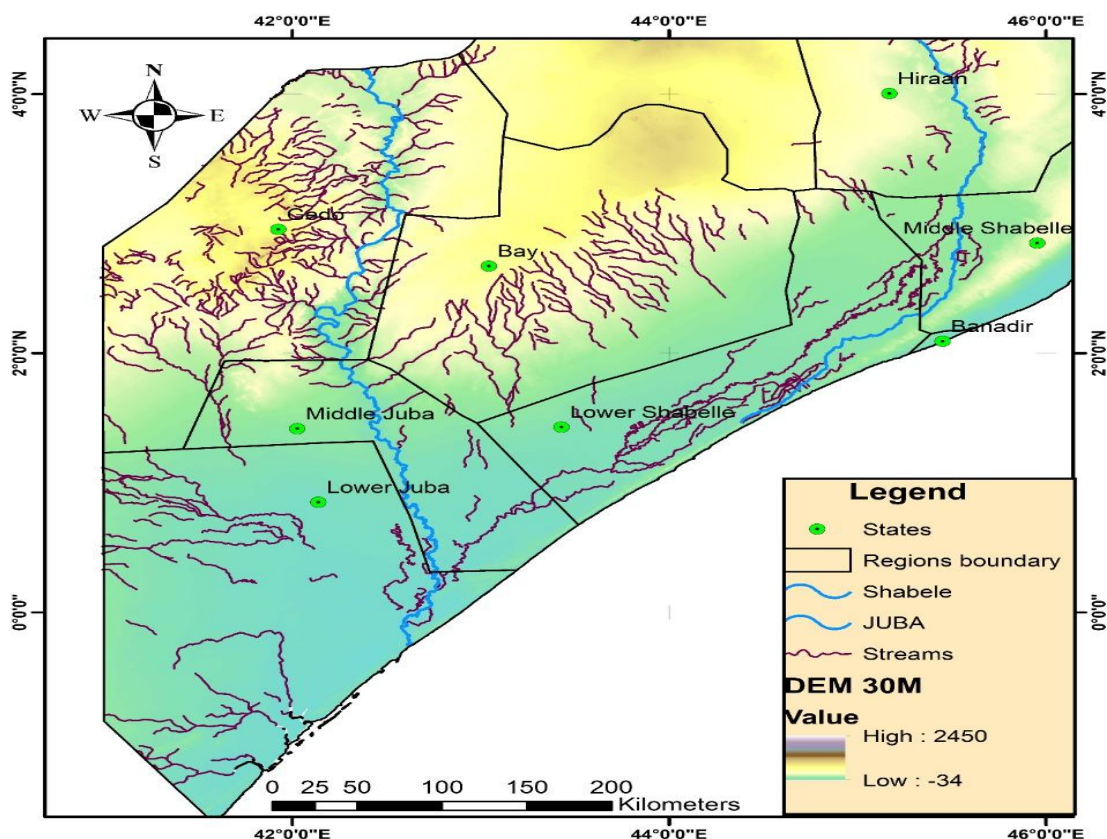
Figure 1.3: Coverage of the Juba River and numerous streams in Lugh-Mandera basin.

1.4. Justification and Significance

The Lugh-Mandera basin is one of Somalia's least investigated basins. Understanding the basin will greatly improve the understanding of the controlling the structural-stratigraphic components of the entire region.

Stratigraphic studies should be able to reveal the true thicknesses of the Jurassic and Cretaceous sequences. Geological time is a critical aspect in the trapping and preservation of hydrocarbons. Therefore, structural analysis will assess the time-aspect of hydrocarbon entrapment. The timing of oil expulsion from the source rocks is a key moment and a tool for use to evaluate the potential of their entrapment. As such, the evaluation of the geo-history of the basin through TTI analysis is a crucial step in determining the efficiency of hydrocarbon generation and entrapment within the basin.

This basin has similar geology with the neighboring Ogaden basin in Ethiopi (Beltrandi and Pyre, 1973; Whiteman, 1981). One of the aspects that make Lugh-Mandera basin look very promising are the discoveries of commercial natural gas deposits in neighboring Ethiopia (Calub gas field) and the close vicinity of natural oil seepages (Tarbaj) in N.Kenya and (Genale) in Ethiopia serve as encouraging indications of the presence of a working petroleum system.

This research has selected at least three potential petroleum systems that correspond to the oil systems of neighboring Ogaden basin. These are:

a) Adigrat-Lower Hamenlei PS which corresponds to the transition zone- Adigrat oil/gas system of the Ogaden basin (Hunegnaw et al., 1998).
b) Middle-Upper Hamenlei PS.
c) Uarandab-Upper Hamenlei PS corresponding to Uarandab-Gabredarre oil system of Ogaden basin (Hunegnaw et al., 1998).

The interpretation of seismic data was expected to provide relevant structural and geological information that would improve the understanding of both the geology and spread of Somalia's oil and gas exploration capabilities. The discoveries of hydrocarbons in the zone will likely spur socio-economic advancements and promote the oil sector in the East African region, in general.

1.5. Aim and Objectives

1.5.1. Aim

The goal of the project was to use all available data that would enable to interpret seismo-stratigraphy, structural styles, and to determine the sub-surface structures in relation to wrench tectonic mechanisms, to asses their probable hydrocarbon entrapment potential and delineate promising locations within the Somalian sector of the Lugh-Mandera Basin (LMB).

1.5.2. Objectives

i. To determine the succession of rock units and the types of proven petroleum systems within the basin compared to the neighboring Ogaden basin found in Ethiopia, through interpretation of 2D seismic and well log data..

ii. To understand the aspects of structural style (wrench fault tectonics), it's impact on hydrocarbon entrapment, and delineate the subsurface target horizon in the study area by using (depth elevation maps, Isochore & Isopach thickness maps, and the interpreted fourteen (14) seismic profiles).

iii. To evaluate the hydrocarbon potential of the area by creating and analysing burial curves of the source rock intervals of the basin through calculating the Time-Temperature Index (TTI) values.

iv. From objectives (1), (2) and (3) above, determine the occurrence and map the extent of structural, stratigraphic and possible combination of hydrocarbon traps and select hydrocarbon target areas (prospect and plays).

To achieve the above mentioned aims and objectives all available seismic, well log data and other geological were applied.

.

1.6. Thesis Format

The presented dissertation consists of next chapters following the Introduction.

 Chapter two reviews in details of the geological setting of the study area. This commences with the short overview of regional geology focusing particularly on the geology of Lugh-Mandera basin and its tectonic setting and also tectonic evolution, and the stratigraphy of the Hol area.

Chapter three describes the methodology, the data set used, the software's applied includes; base map of the Hol area, interpretation of the seismic data such as (horizon and fault interpretation), preparation of time and depth elevation maps, and (Isochore and Isopach) thickness maps for the study area

Chapter four provides the results of the seismic stratigraphy analysis and interpretations made from the integrated well and seismic data, focuses on the stratigraphy and petroleum system elements of Lugh-Mandera basin, hydrocarbon traps and prospective areas, seismic stratigraphy, structural analysis, subsurface geological mapping, the Lopatin-Waples Technique used in Time-Temperature Index (TTI) Modeling for Hol-1, Bodle-1, and Elkuran-1 wells. It specifies the mature source rock intervals and predicts the time of expulsion-migration-entrapment/accumulation of hydrocarbons (Hc's) in relation to the seismic stratigraphy and structural geology interpretation, and finally concludes the discussion of the results.

Chapter five concludes the dissertation and presents a list of key points drawn from the overall study. Conclusions were made based on an integrated interpretation of stratigraphic and structural analysis within the study area and final provides recommendations and suggestions for future exploration activities.

CHAPTER 2 : LITERATURE REVIEW

2.1. Introduction

Missions to investigate and collect fossils in SW Somalia were initiated by British geologists (Currie, 1925; Weir, 1929) in the early 20 century. Between 1936 and 1957, the Italian oil company AGIP conducted reconnaissance geological studies and produced a series of geologic maps depicting the rock formations of the key geological features of Somalia and the Ogaden area (Azzaroli and Merla, 1959).

All these preliminary studies were followed by detailed paleontological research (Barbieri, 1968).

The systematic analysis of aerial photo in the 1960s provided the right conditions for the development of modern geologic maps of the Somalia region, which displays the formation units. The preliminary steps that were followed in investigating the hydrocarbons involved sampling, exploration, airborne geophysical and gravimetric surveys (Barbieri, 1968; Beltrandi and Pyre, 1973).

More detailed work was done by the Somalia Gulf Oil Company geologists who measured and described a large number of well exposed outrop sections developed along as NE-SW trend which is parallel to the axis of the basin. The results of this work were incorporated into a paper (Beltrandi and Pyre, 1973). Surface geological work done by Hammar Petroleum Co. and Burmah Oil Somalia Ltd. followed and largely confirmed the Gulf Oil Company studies.

A surface geological study by Mobil Oil Company was expanded to cover the East side, across the Oddur Arch into the Lugh-Mandera basin. Studies by the Kenyan geological surveys have also captured the western side of the basin. Photogeological maps covering the southernmost part of the Lugh-Mandera basin were prepared for Hammar Petroleum Company-by Trollinger, Go-sney and Associates, but since this area is largely covered by superficial deposits little information is given on the solid geology. Domino (1966) who was an employee of Hammar Petroleum Company prepared sets of photogeological maps of the Baidoa- Oddur and Garbaharey areas and made field checks on his interpretations.

Geological mapping and interpretation of the Somalian side of the basin was completed in 1970 by Hammar Petroleum Company. Limited magnetic, gravity and seismic surveys were carried out in the Lugh-Mandera basin by the Somalia Gulf Oil Company. The data from these surveys was later re-interpreted by Hammar Petroleum Company.

The well Hol-1 was spudded by Burmah Oil in 1973 in the axial zone in the northern part of Lugh-Mandera basin and encountered a fluvio-deltaic sequence of Hettangian-Toarcian (Lower Jurassic) age to a depth of 13,258' (4,042 m). The Micropaleontology and palynology studies were undertaken by paleoserrvices (1973, 1975) and Bocal (1972). Their reports are reviewed and discussed in this study.

The Hol-1 oil well proved to be non-commercial. The Upper Jubba valley has seen a significant interest from international geologists (Kamen-Kaye and Barnes, 1979; Bignell, 1977; Barnes, 1976), and some Somalian researchers from the Somalia National University's Faculty of Geology. The latest geophysical surveys were done by Rapolla et al. (1995a,b).

Some scholars have also noted that basement fault interactions and reactions of evaporate flows in the pre-Jurassic were responsible for the folding (Beltrandi & Pyre, 1973). Such a system of folds was observed in the Garbaharey-Mandera and Mata-Arba outcrops in the western side, as well as the eastern side in Fafadun and El Wak. They suggest that old normal Triassic faults (the two marginal faults of the basin?) may have been reactivated as wrench faults after the Early Cretaceous or are probably related to the East African Rift System (EARS).

Between 1982 and 1990, additional geological studies were conducted in the south-western regions by the Faculty of Geology of the Somalia National University, and the Italian Cooperation for Developing Countries funded by the Italian Ministry of Foreign Affairs and led by Carmignani. However, the civil war that erupted in 1990 forced these studies to be halted.

Geochemical analyses were undertaken on sample cutting from Hol-1 well at the request of Esso Exploration (E.A.850014, May 1, 1985) to assist in the evaluation of the source

rock potential of the Esso/Shell license area (Morgan, 1985). In the same year, a paleontological study was undertaken by Freudenthal and Hochuli (1985).

2.2. Regional Geology

Lugh-Mandera basin has a general NE-SW orientation and can be classified according to Klemme's (1980) classification as an extra continental down-warp trough basin. Both Kenya's Precambrian bedrock and southwestern Somalia's Bur Uplift bind the basin. To the south the basin is covered by younger sediments of the Lamu Embayment, while to the northeast passes into the Ogaden and the Mudugh basins of eastern Somalia.

Purcell (1979) and St John (2016) concluded that the development of some basins was related to the triple-junction rift system in the Late Paleozoic-Mesozoic epochs, and that thick Karoo sediments had filled the rift troughs. Examples of such troughs are found in the Mandera-Bodle Rift, the Calub Saddle of the Ogaden basin, and the Blue Nile rift to the northwest (Figure. 2.1).
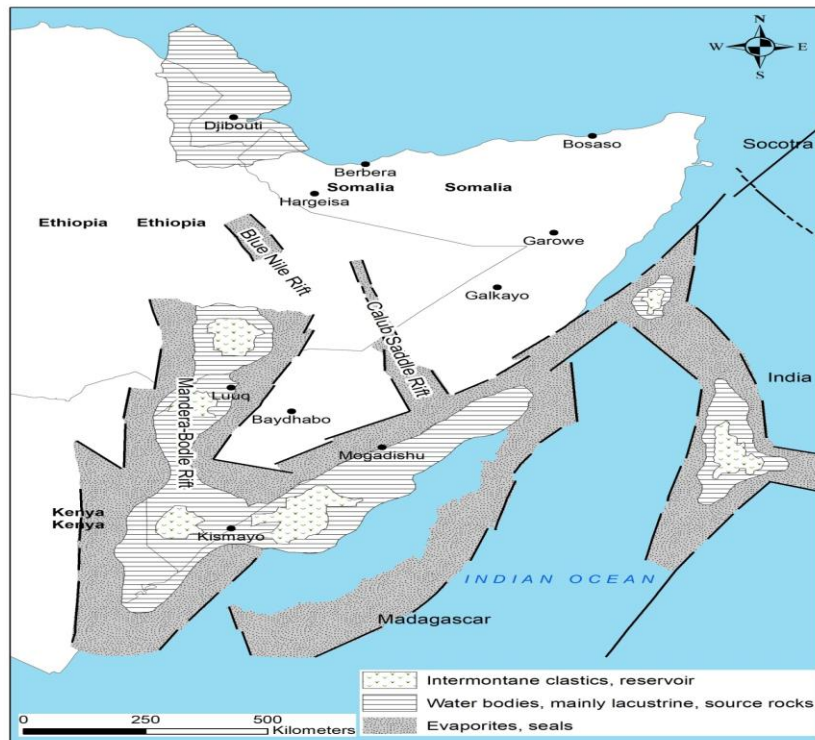
Figure 2.1: Modified Karoo Rift System in East Africa, Madagascar, Socotra, and India (after Bosellini, 1989), only major rifts are shown: 1) Mandera-Bodle Rift; 2) Calub Saddle Rift; 3) Blue Nile Rift.

14

- The Mandera-Bodle Rift is one of failed arms of the triple-junction rift system oriented SSW-NNE, which is bordered by transcurrent faults. Bosellini (1989) estimates that the sequence in the central part of the Lugh-Mandera basin is more than 29,520' (9000 m) in depth.

- The Calub Saddle, located on the north eastern edge of the basin and trending from NE-SW to ENE-WSW, includes the North Shillabo and is bordered by faults. The expansion of the NW-SE faults is responsible for its formation, while the Bur high separates it from Somalia coastal basins.

- The SE segment of the sloping Blue Nile splits at NW-SE in the NW part. The depth of the bottom grows SE wards along the southern border of the Blue Nile Rift, from 2,952' (900m) in the Gerbi-1 well region to roughly 16,400' (5,000m).

The Lugh-Mandera basin originated in the Late Paleozoic during the early phases of Gondwana separation and grew gradually throughout the Mesozoic when Madagascar drifted away from Africa. The Karoo rift in the Late Carboniferous (Catuneanu et al., 2005) continued to develop for 150 million years until the spreading episode between the Madagascar- E. Africa sea floor spreading in the Early-Middle Jurassic (Coffin and Rabinowitz, 1987; Eagles and Konig, 2008). Around 120 Ma (Rabinowitz et al., 1983) or 130 Ma (Rabinowitz et al., 1983; Kent, 1982), the Madagascar-East-Africa sea floor spreading came to a halt, exposing the area to significant tectonic deformation and uplift due to volcanic activities (Coffin and Rabinowitz, 1987). As such, the rifted basins were formed.

Rifted basins tend to form as a result of continental fracture, Localized subsidence and the deposition of syn-rift sediments is caused by heating and thinning of the continental lithosphere during rifting (e.g. McKenzie, 1978; Buck et al., 1999; Lavier and Manatschal, 2006). The heated and thinned lithosphere cools when rifting stops and post-rift sediments accumulate.

2.2.1. Plate Tectonics

The Plate Tectonic history of Gondwanaland and the development of the Indian Ocean are fundamental to understanding the regional structural and stratigraphic setting of

onshore Somalia. According to several academic researchers, such as Whiteman (1981). the area has been divided into numerous major uplifts and sedimentary basins due to tectonic development that has persisted since the Late Paleozoic (Karoo) period. The Bur Acaba, Nogal, and Northern uplifts, on the other hand, are crucial to comprehending these formations.

Permo-Triassic (298.9Ma-237Ma): Early Karoo rifting of the Gondwana supercontinent created intracontinental rift basins in which Karoo sands, organic rich lacustrine mudstones and coals were deposited (Norton and Sclater, 1979; Bosellini, 1989). The Lugh-Mandera basin's advancement is linked to the fragmentation of Gondwanaland, where most of these rifts 'failed' and did not reach the drift phase.

Late Triassic-Early Jurassic (237Ma-174.1Ma): East Gondwana rifted from the African mainland of West Gondwana. East Gondwana comprised the Seychelles, Madagascar, India, Antarctica and Australia. The accepted plate reconstruction (Coffin and Rabinowitz, 1992; Bosellini, 1992) places Madagascar adjacent to the Somali coast making the NW Madagascar and South Somalia/NE Kenya to become conjugate passive rift margins (Figure 2.2). A restricted marine setting existed in the rift valleys and resulted in the development of marine shales (e.g. Meregh Fm. in Somalia), and evaporites known from Tanzania and NW Madagascar.

Mid Jurassic-Early Cretaceous (174.1Ma-120Ma): Open marine conditions existed from the Mid Jurassic. The Davie Fracture Zone was an active right-lateral (dextral) transform fault from Mid Jurassic (160 Ma) to Aptian (120 Ma), as East Gondwana moved southwards relative to West Gondwana, and where Madagascar reached its current position. During this period the Somali Basin continued to open and sea-floor spreading produced an oceanic crust between Madagascar and mainland Africa.
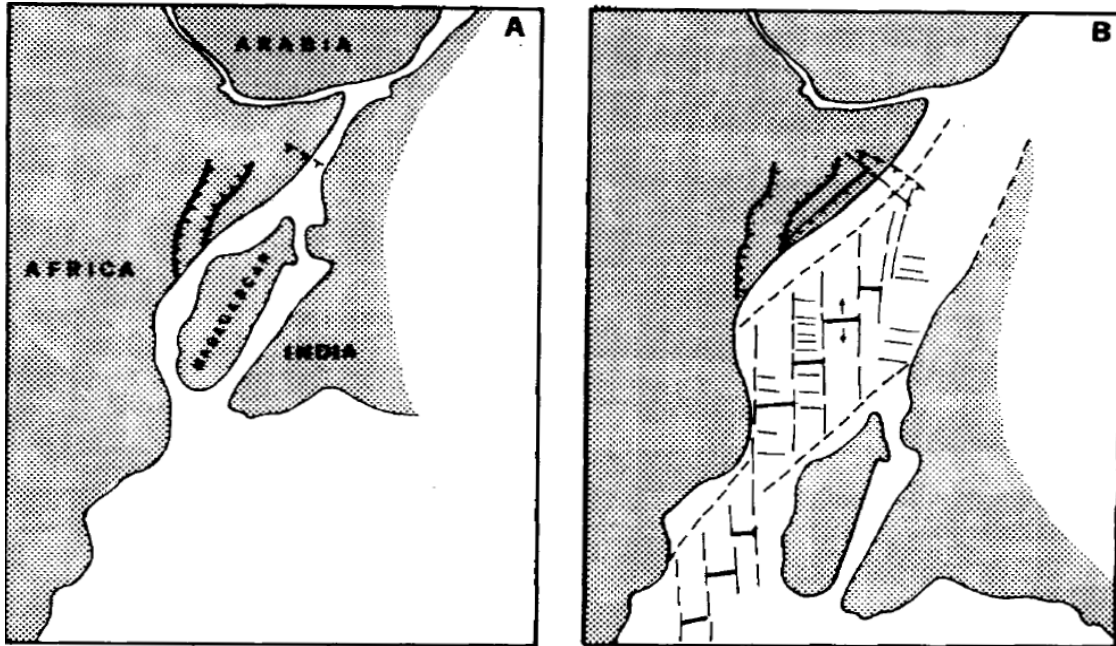
Figure 2.2: Plate Positions: Late Triassic to Early Cretaceous (after Norton and Sclater 1979; Masson et al., 1982 Rabinowitz d al., 1983).

Figure **(A)** depicts the Continental blocks' initial position (Triassic) around **251 Ma** prior to their break-up. It also depicts the start of the Lugh-Mandera basin's creation.

Figure **(B)** depicts the scenario at around **120 Ma**, when Madagascar's southerly migration came to an end (southern migration ceased)

2.2.2. Geology of Lugh-Mandera basin

The Lugh-Mandera basin is underlain by Precambrian basement rocks, while the overlying succession predominantly consists of Mesozoic sedimentary rocks. Figure 2.3 depicts the main geological features of southwestern Somalia, including the research area. The Lugh-Mandera basin, which is the study region, is made up of the following succession rock units from oldest to youngest:

The oldest formation are presented by the Triassic sequence and is made up of the Adigrat Sandstone formation, followed by the Jurassic sequence consisting of Iscia-Baidoa Formation (Uanei, Baidoa and Goloda Members), Anole and Uegit Formations, and finally, by the Cretaceous sequence which comprises the Garbaharey Formation.

17

Numerous researches on the subject that provides more in-depth explanation of Eastern Africa's geodynamic evolution can be found on (Ali Kassim M. et al., 2002). Some of the notable research includes that of Norton and Sclater (1979), Coffin and Rabinowitz,(1983-88), Bosellini (1986-92), Piccoli (1986) and Boccaletti et al., (1988).
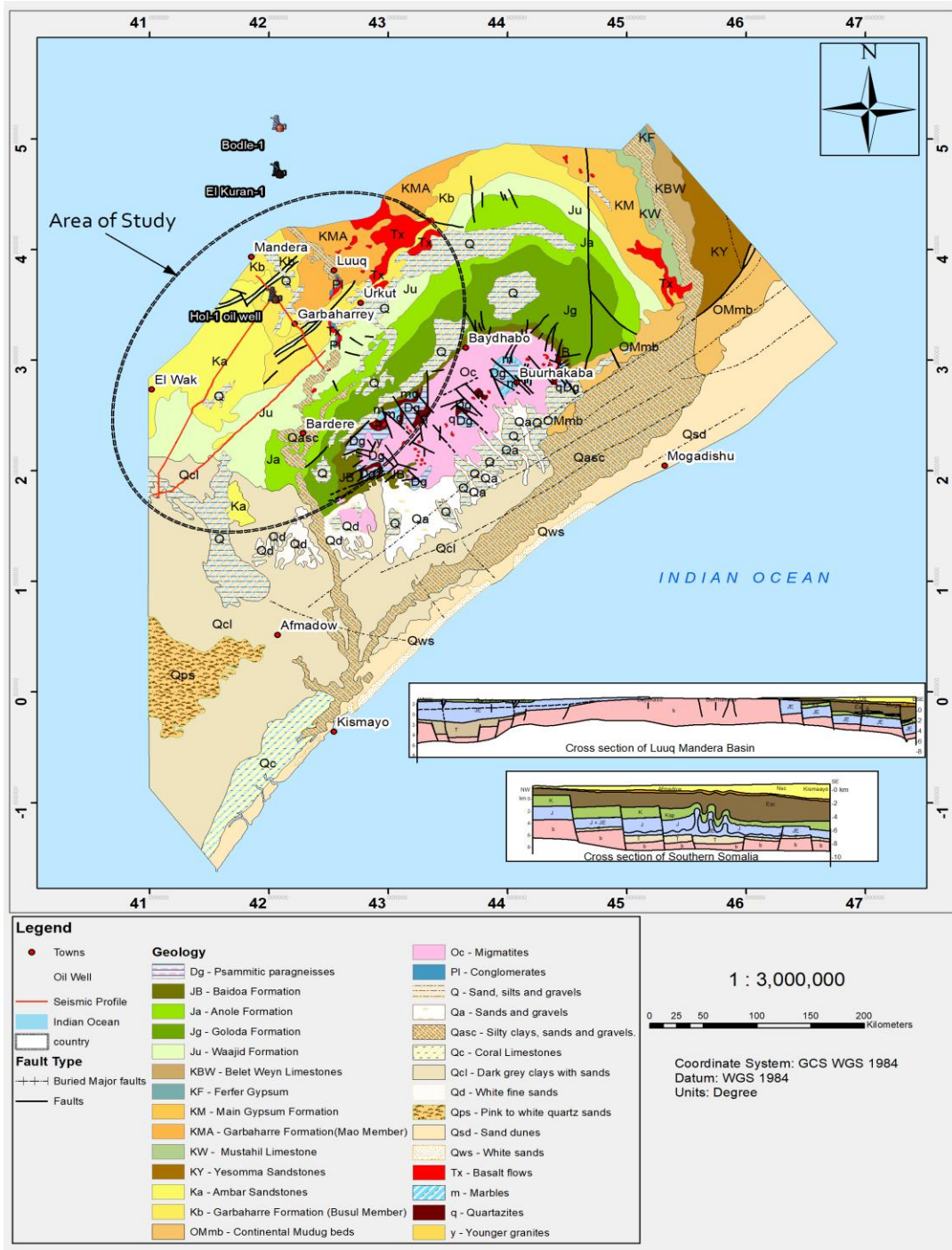
Figure 2.3: Modified Geological sketch map of southern Somalia (after Abbate et al., 1993).

2.3. Generalized Stratigraphy of Lugh-Mandera basin

The study of Somalian onshore is based on drilling results of about 30 well sections, as illustrated in the studies of (Barnes, 1976; Ali Kassim et al., 2002; and Bosellini, 1986, 1989, 1992; and among others).   The analysis of the Burmah Hol-1 Oil well revealed that the sedimentary cycle of the south western Somalia and the neighboring Kenyan Mansa Guda formations began in the Triassic period during the crustal movements with the Adigrat Sandstone (Beltrandi and Pyre, 1973). Thus, the Liassic (Early Jurassic period), represents the start of marine incursion, which is particularly noticeable in the SW region. The high rate of subsidence that took place around 165 Ma, prompted the marine transgression that enabled the deposition of predominantly carbonates with subordinate shales, sandstones and gypsum (Baidoa, Anole, and Uegit formations) during the Jurassic (Piccoli et al. 1986; St John, 2016). These carbonates are vast, extending over 1000 kilometers onshore over to Ethiopia's Ogaden basin as well as into Yemen (Al Thour, 1997).

The period of Early Cretaceous saw the sea retreating, ceasing further deposition of sedimentary rocks, and allowing the development of the Main Gypsum (evaporates) of the Garbaharey formations in the basin. In addition, the developments led to the lateral grading of the continental deposits in the western most region bordering Kenya, for instance Ambar formation.

Subsidence and sedimentation of the Lugh-Mandera basin ceased in the Early Cretaceous with marine deposition restricted only to the coastal region, regressive towards S/E and W of the Bur uplift and also to the long the existing depression of the Mudugh and Ogaden basins. This period coincides with the ceasing of the southern Madagascar drift, which is dated at around 115- 120 Ma (Rabinowitz et al.*, 1983).

In spite of the generally poor surface exposures and sparse drilling, the lithological subdivision of the outcropping Jurassic-Cretaceous succession in the Lugh-Mandera is well documented both in Somalia and Kenya. However, problems do arise when correlation between outcrop and axial zone of the basin in time is attempted. This reflects the facts that fossil groups have been used in the two areas are distant apart from each other where successions and ranges of fossils have been established.

Consequently, more work is necessary before a satisfactory system of dating (level of correlations) is established in the Lugh-Mandera basin.

A simplified cross section map illustrating the difference in lithological deposition between the basinal section of the Lugh-Mandera basin and the outcrop as shown in Figure 2.4.
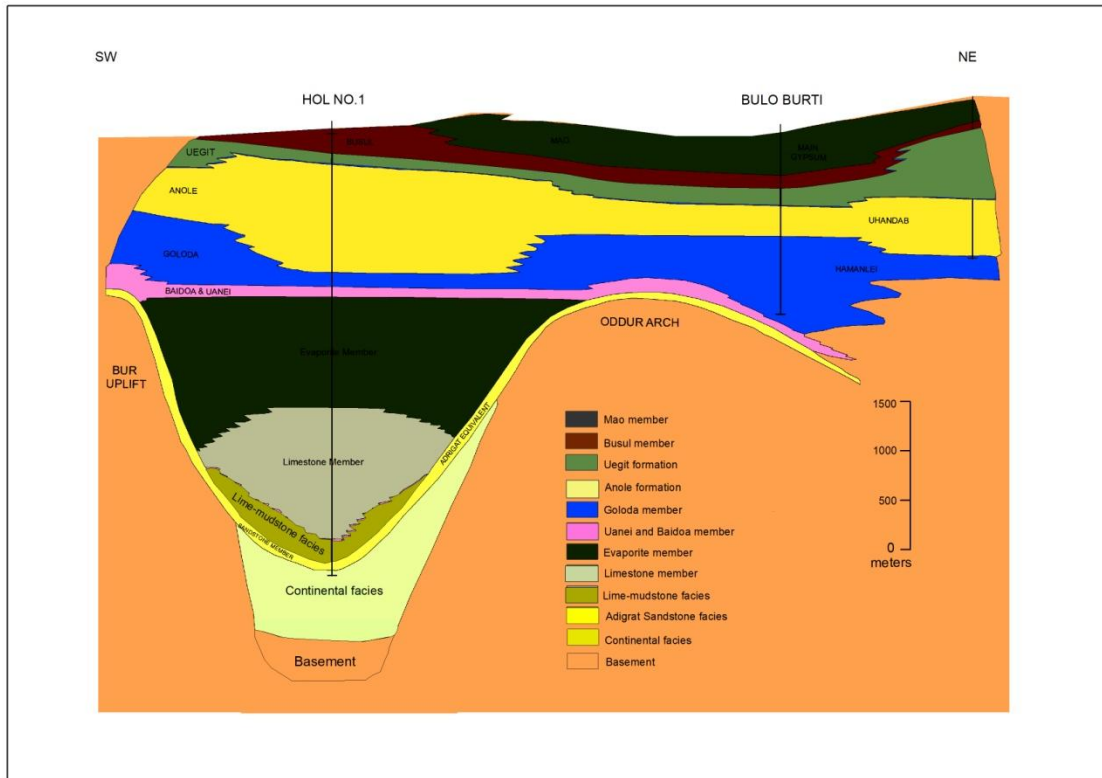
Figure 2.4: An out-of-scale modified, schematic cross section showing the stratigraphic column of the edge and axis of Lugh-Mandera basin after (Burmah Oil Co, 1972).

Stratigraphy of Lugh-Mandera basin is known based on information from previous studies on the outcrops and the Hol-1 well section. The stratigraphy from Jurassic to Early Cretaceous is reviewed below:

2.3.1. Precambrian Basement

The basement in the southern part of the country is significantly exposed by about 300 kilometers in a severely peneplaned landscape between Mogadishu and the Jubba Valley,

and thus known as "Bur" or "Bur Crystalline Basement" because of the isolated inselbergs and presence of two high grade metamorphic complexes. The first geologists to study the rocks and characterize their properties were Stefanini and Paoli (1916); Aloisi and De Angelis (1938); Azzaroli and De Angelis (1965); Borsi (1965); Daniels (1965); Ilyin (1967); Bellieni et al., (1980); Haider (1983); Warden and Horkel (1984); Dal Piaz and Sassi (1986); Haider (1993), and many others.

According to Harms and Brady (1989), the Karoo sediments lie directly on metamorphic basement and are Late Permian to Late Triassic in age. Karoo beds are fluvial and lacustrine deposits and have been drilled extensively in the Ogaden area of Ethiopia.

2.3.2. Sequence of Triassic age (Continental deposit)

Overlying the Karoo beds are Triassic–Lower Jurassic basal clastics or the Deleb Adigrat Sandstone Formation. It consists of interbedded continental sands and shales. The sands are dominantly fluvio-lacustrine deposits, and are usually of felspathic composition, well cemented and with poor to fair porosity, although coarse, better quality sand layers do exist. These sands are not always distinctive from underlying Karoo beds and they may be equivalent in age to the Upper Karoo. The transition from the Karoo Series to Adigrat Sandstone was diachronous and controlled by rift-affected faults in Early Jurassic (Bosellini, 1992).

The Hol-1 well is situated in the Lugh-Mandera basin (3 3502300N, 42 0205800E). Burmah Oil Co. (1973) reported it to be 4,042 meters (13,258 ft) deep. According to Bosellini (1989) the thickness of these deposits is over 9000 m below the Hol-1 well site. The Lugh-Mandera has no known outcropping sections with the Permian-Triassic formations. It is believed that there was strong differential vertical movement between the basin axis and surrounding areas at this time that coarse rocks derived from nearby basement areas are probably dominant (Burmah Oil Co, 1973, Figure. 2.4).

a) Deleb Adigrat Sandstone Formation

This is the basal sandstone in Somalia and is present throughout East Africa, and was named by W. T. Blanford in 1870 (Arkell, 1956). This formation consists of silty shales,

slightly argillaceous sandstones, and fine to coarse grained quartzite sandstones. The latter are clean, well sorted, and consist of rounded quartz grains which are completely cemented together by authogenic quartz overgrowths Berry (1974). The Adigrat characterizes a weakly bedded fine to medium-grained sandstone that is up to 60 meters thick in Ethiopia, and generally quartzitic and unfossiliferous Migliorini (1948).

The sandstones and conglomerates of Mansa Guda formation in NE Kenya are almost certainly continental in origin, and a similar origin is suggested for the 'red beds' found at the basal section of the Hol-1 well.

The palynological analysis from the well data has yielded several very poorly preserved small spores like hardly identifiable structures. Also there is no evidence to confirm a possible Triassic age which was suggested by Burmah geologists (Bocal, 1972). According to Kassim et al. (2002), this formation developed in the Early Liassic (J_1). Its depositional environment was probably continental (fluvio-deltaic).

2.3.3. Jurassic sequences

Consist of three main formations such as: Iscia-Baidoa, Anole, and Uegid Formations.

b) The Iscia-Baidoa Formation

In addition, many researchers have extensively investigated the outcrop section in the eastern part of the basin (Buscaglione et al., 1993; Ali Kassim et al., 1987). The stratigraphic succession of the outcropping section in south-western Somalia, above the crystalline basement, was established as follows, from bottom:

Early Jurassic sediments have been encountered in Hol-1 well section, are represented by an extremely thick series of dark colored carbonates, containing anhydrate and dolomites in its upper part. The strata in the axial sections of the Lugh-Mandera basin, which primarily consist of detrital, carbonates, and evaporate lithologies, have no outcrops. The initial transgressive sequence consists of dolomite/claystone unit which was probably deposited in lagoon conditions. The succeeding limestone unit which is probably remarkable for (i) lack of lithological variation and (ii) lack of fossils of the whole of its 1,300 m thickness: which indicate unfavorable conditions to life? It is considered

unlikely that this thick unvarying succession formed in a restricted lagoon environment (Burmah Oil Co, 1973).

- **Early Jurassic (Lias) sequences**

In early Jurassic times there was widespread transgression of the sea across northeast Africa from the open marine area off the east coast. The Lugh-Mandera basin subsidence continued along the basin axis but there was apparently little uplift on its flanks, and not much of terrigineous material reached the Hol Area (Friedman, 1972).

Uanei Member

The lithologies that make up the Uanei Member are: marls with quartz clasts and gray marly limestones in the lowermost parts; marls and marly limestones alternate with calcarenitic bioturbed layers in thick strata of gray and bioclastic calcilutites (in the Middle section); and the bioclastic and peloidal packstone–grainstones that make up the calcarenite sheets, which are tens of centimeters thick (in the uppermost section) (Buscaglione et al., 1993).

Bivalves, gastropods, brachiopods, benthic foraminifers, and ammonite fossils may all be found in this collection.

Baidoa Member

Fossils of gastropods, lamellibranchs, foraminifers, ostracods, echinoderms, radiolarians, and sponge spicules are among the fossils found. The fossil collection suggests an age of Aalenian to early Bajocian range. The rocks consist of packstones/bioclastic grainstones, peloidal and oncoidal grains which includes oolithic grainstone layers and frequent crossbedding (Buscaglione et al., 1993).

- **Mid Jurassic (Dogger) sequence**

The rifting and separation of Gondwanaland continued during the Middle Jurassic (Dogger) time that led to the development of very thick successions of carbonate in the area of South Western Somalia.

At Hol area during the Dogger time, the rate of deposition in the basin axis overtook the rate of subsidence and shallower water conditions prevailed. As a result, the precipitated sulphates were preserved in the form of the Evaporite unit. It is considered that more open marine conditions probably prevailed at the northeastern and southern ends of the basin, and that zones of sedimentation in which mainly milestones dolomite were deposited, existed in these areas (Burmah Oil Co, 1973).

Goloda Member

The Goloda Member depicts the carbonate series in southern Somalia. Greyish calcilutites, sedimentary rocks, and brownish dolomites characterize the base, while yellow–brown calcarenites and bioturbed calciluts characterize the top. The common fossils encountered in this member are bivalves, gastropods, echinoderms, calcareous algae, foraminifers, and corals. The setting is that of a narrow platform, with a transition up section to an open platform environment (Buscaglione et al.1993). The component's thickness at Baidoa is 137m while at Hol region is 1159m.

This member is dated to the late Bathonian–Early Callovian based on paleontological evidence. At Hol area these sediments lithologically compose of fine to medium grained fossilfereous lime mudstone and skeletal wackstones, and medium grained oolitic grainstones. This zone act as a good reservoir rock and it is the most important stratigraphic package of study area. Characterizing high energy oolitic grainstones of the Goloda Member, where intergranular porosities in excess of 30% were common before cementation or the dolomitized interval occur (Berry, 1974).

- **Late Jurassic (Malm) sequences**

The period of maximum transgression is represented by marine mudstones of Anole formation, which was apparently deposited below the wave base in open marine conditions in the Late Jurassic (Malm). The onset of the regressive phase is represented by the shallow water limestones associated with Uegit formation and by the lagoonal and littoral carbonates, evaporates and clastics of the Garbaharey formation.

c) Anole Formation

The gray-green marls in the formation's 30-meter-thick layers alternate with thin micritic and occasionally marly limestone beds and calcarenites. In the marls, brachiopods are common, but in the micrites, foraminifers, ammonites, belemnites, and structures such as burrows are common.

These were all open water sediments that were accumulated below the wave base during the Jurassic sea's greatest ingression. The deposit is 400 meters thick. These sediments were deposited during a period of widespread regression that is geodynamically linked to the breakup of Africa and Madagascar, as well as the subsequent expansion of ocean floor (Coffin and Rabinowitz, 1987). Fossils date from the early Kimmeridgian through the late Callovian periods (Kamen-Kaye, 1978). These sediments are thick in the Hol-1 well section around 488m (Burmah Oil co., 1973).

This formation has proved source rock properties capable of generating hydrocarbons throughout country in general, and particularly, in the Lugh-Mandera basin (Morgan, 1985).

d) Uegit Formation

The lithologies that dominate the Uegit Formation include well-bedded calcarenites, usually oolitic (in the lowermost part), and light gray fossiliferous micritic limestones. Fine-grained calcarenites in m-thick strata with numerous mollus cremnants are also less prevalent. In the intermediate portions, micrites intercalated with dark gray marls define calcarenite strata bearing cm-sized oncolites. Huge ostreids and large turricolate gastropods, as well as coral colonies in growth (in the uppermost of the section) were reported here by Barbieri (1968). According to Angelucci et al. (1983), the Uegit Formation is roughly 350 m thick,). These sediments have been encountered in the Hol-1 well section with thickness of around 589m. The deposition environment varies from a shallow shelf to a lagoon.

2.3.4. Lower Cretaceous (Neocomian) sequences

The pattern of deposition at this stage was complicated by the supply of clastic sediment to the southwestern end of the basin and the resulting facies variation has necessitated the

definition of a variety of restricted lithologies subdivisions for this area. The final phase of deposition resulted the development of marine/marginal marine and perhaps continental sandstones of the Ambar formation at the southwestern end of the basin, and in the evaporitic facies of the Mao member to the northeast.

e) Garbaharey Formation

Rocks of Garbaharey Formation have been encountered in Hol-1 well as a thin section. Barbieri (1968) split the strata into two Members: the Busul Member and the Mao Member, which outcrop in the northeastern part. The Busul member is mostly composed of yellow dolomites in meter-thick layers with reddish, laminated quartz arenites with mollusc lumachelle intercalations. The thickness of this component is roughly 300 meters. The top boundary of the Busul Member is abrupt, and it can coexist with either the Mao Member or the Ambar Sandstone Formation. The Lugh region's cyclic alternation of sandstones, calcarenites, and micritic limestones implies that this component accumulated in a shallow sea coastal environment over a series of transgressive/regressive events. This member can be assigned to the Neocomian based on the presence of bivalves.

In the Early Cretaceous times the onshore sector of Somalia and neighboring Ogaden basin of Ethiopia represented a shallow restricted marine basin with the development of Main Gypsum beds accumulating in a sabkha setting (Barnes, 1976).

The supply of clastic sediments into the Lugh-Mandera basin towards end of the Jurassic period is indicative of another period of differential vertical movement between the basin axis and the surrounding area. This phase of movement apparently reached its climax in Early Cretaceous times and probably also corresponds to the time at which the main faults and folds in the basin were formed by slight relative movement of basement blocks. Terrigenous material entering the basin from the southeast was deposited during Early Cretaceous times resulting in the accumulation of Amber and Lugh-Mandera sandstones under marginal marine to continental conditions. The sea apparently withdrew towards the northeast and it is in this area that the restricted marine evaporitic facies of the Mao formation (potential seals) are deposited. Subsidence of the Lugh-Mandera basin

stopped in the Early Cretaceous. The marine deposition in the region was entirely restricted to the coastal region south and to the east of the Bur Uplift, and also to the long existing depression of the Mudugh and Ogaden basins. This evaporitic formation acts as a perfect sealing component ensuring the preservation of expelled hydrocarbons from the Anole formation. Figure 2.5 illustrate the stratigraphy and the depositional environments of outcrops developed in the Lugh-Mandera basin.

The Ambar Sandstone Formation has a thickness of 1968.5' (600m) near the Kenya-Somalia border and develops further towards south west region of the North-eastern Kenya (Baker and Saggerson, 1958). In addition along the Kenyan border, the conditions were more continental, and thus, formed the main source of clastic sediment materials.
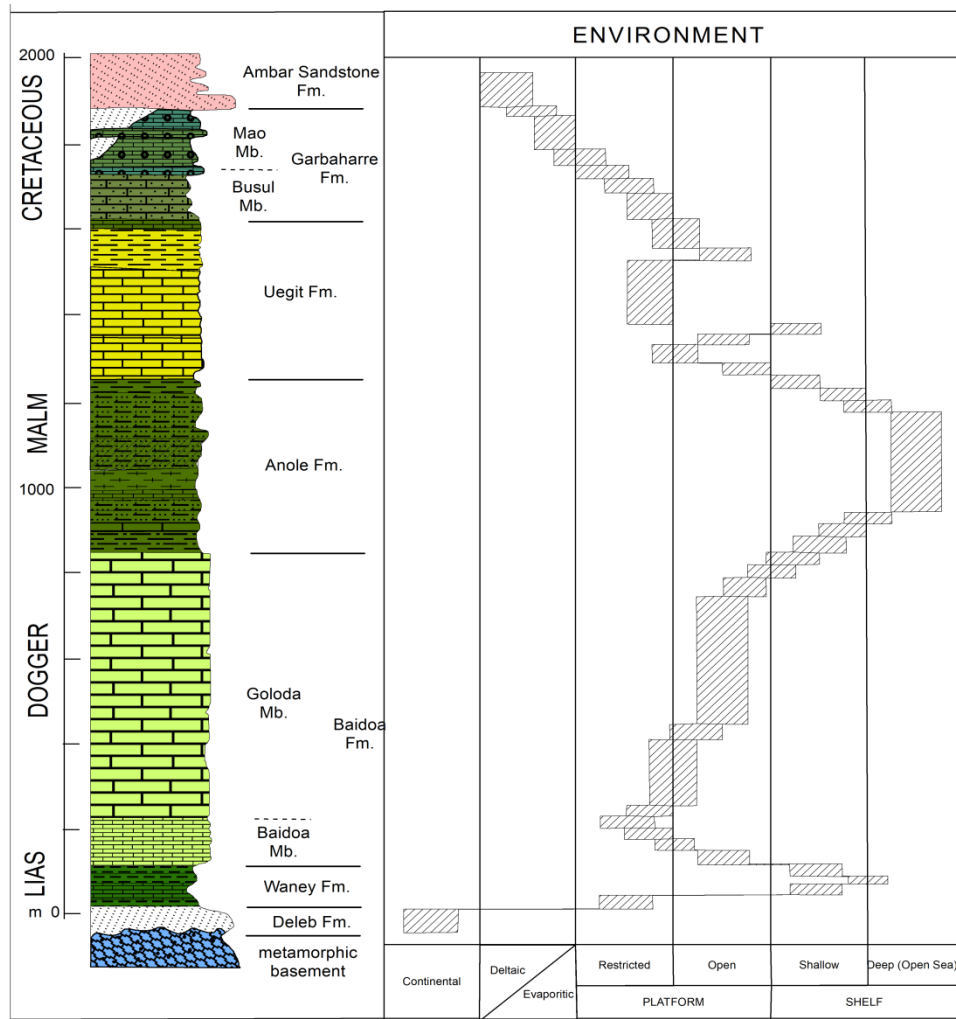
Figure 2.5: Modified stratigraphy and environmental interpretation of the Lugh-Mandera basin (after Bruni and Fazzuoli in Ali Kassim et al., 1987).

2.4. Structural Geology of Lugh-Mandera basin

The area Horn of Africa is presented (covered) by the Ogaden, Lugh-Mandera, and Tertiary coastal basins (or Mogadishu Basin), as well as the Bur Acaba, Nogal, and Northern uplifts of the Precambrian or early Paleozoic (Barnes, 1976). The Bur Acaba uplift is bounded on the southeast, southwest, and northwest flanks by vertical underground faults (Beltrandi and Pyre, 1973; Kamen-Kaye and Barnes, 1979). The fault process spreads towards the west connecting Lugh-Mandera basin as a series of north-trending valleys and ridges structures ranging in age from Early Mesozoic to pre-Tertiary.

The Bur Acaba uplift first developed in pre-Jurassic times and later in the Late Jurassic and Early Cretaceous times when Lugh-Mandera basin experienced folding and formed vertically uplifted as indicated in figure 2.6 (Beltrandi and Pyre, 1973; Barnes, 1976).

Whiteman (1981) suggested that Lugh-Mandera basin trough consists of up to 8,000 m (25,000 ft) of rocks deposits along its fault line in pre-Middle Jurassic time.
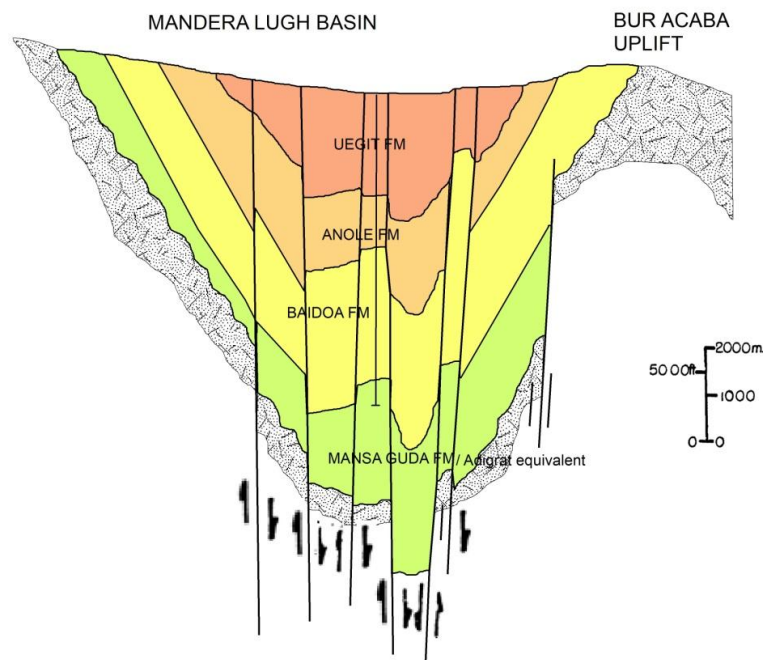
Figure 2.6: Modified West-East structural-stratigraphic cross-section, showing sedimentary facies and structural features. (after Beltrandi & Pyre, 1973; Kamen-Kaye & Barnes, 1979).

Lamu embayment is separated from the Lugh-Mandera basin by an east-west basement crest that was identified through geophysical studies. Lamu embayment structural pattern and Somalia coast regions are characterized by deposited sediments. Geophysical survey results shows that rock fractures and pre-Tertiary highs occur in the sub-surface as well as the presence of salt-assisted structures (Walters and Linton, 1973; Whiteman, 1981).

The noticeable distinct sections are the eastern and western sectors. The former is a region trending in the NNE-SSW and ENE-WSW direction, located north of Bur, between Uegit and Garbaharey. The latter trends in the NNW-SSE and N-S direction between Bardera and the outcropping Kenyan basement. The sectors are separated by a NW-SE trends of fault systems that originates from the SW to NW of the Bur. (Figure. 2.7) depicts the interpretation of Landsat images and air photos showing both the synclinal and anticlinal folds axes (Beltrandi and Pyre, 1973; Carmignani *et* al., 1983).

The Sengif-Mata Arba mountain range is among the most complicated formations on the planet (Figure 2.7). It features a fold in both sectors, with gradually sloping flanks of 30º-40º, culminating in box-fold formations in certain cases. Normally, the axial orientations are undulating, indicating torsional stresses. The Mata Arba-Sengif anticline, Garbaharey anticline, and Tomalo syncline are depicted on the map. It also illustrates structures that, although following the major trends are regarded as weak cover undulations.
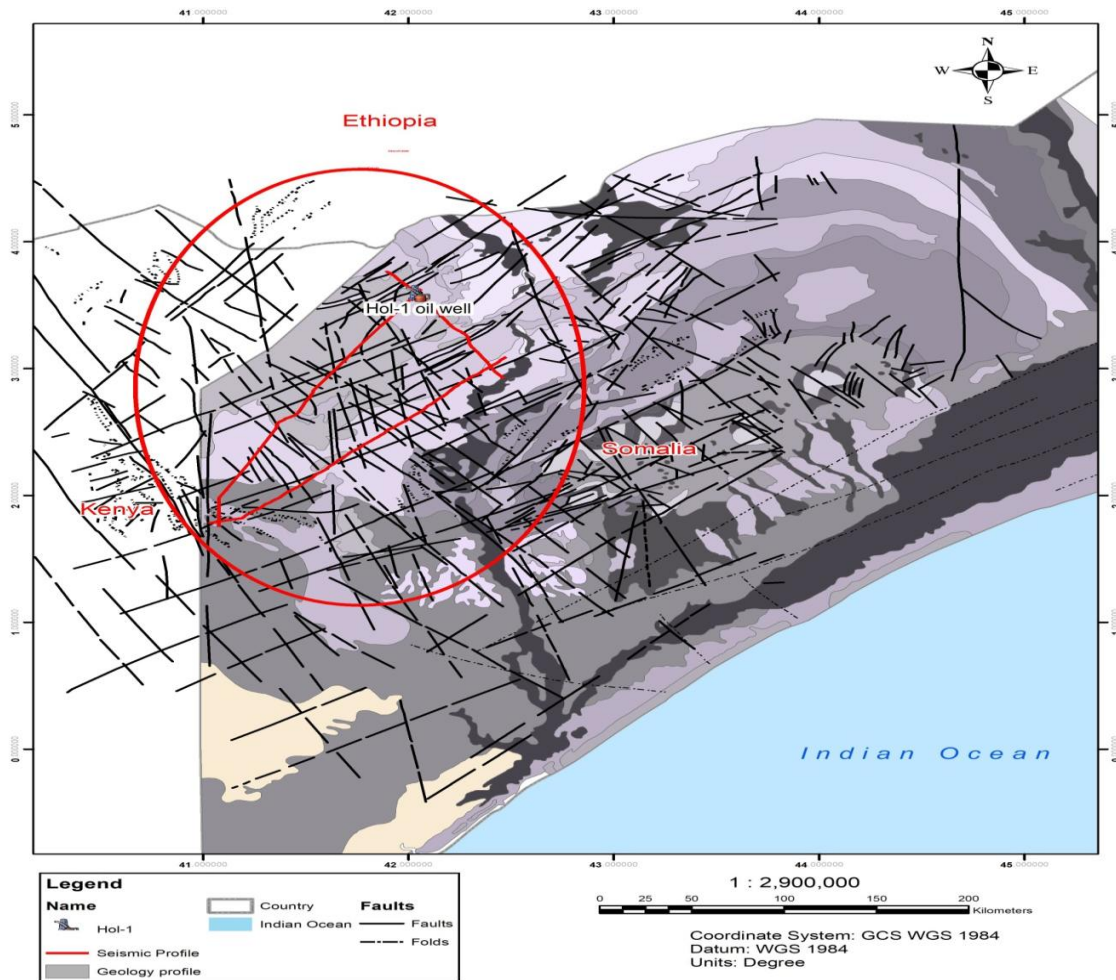
Figure 2.7: Modified geological-structural map of SW Somalia and NE Kenya (after Boccaletti et al 1988).

The simple regional structures of Lugh-Mandera basin is complicated by the strike-slip movements along vertical faults in the Sengif and Garbaharey belts (Figure 2.8), and highlights the major tectonic events in the study area and throughout SW Somalia (Beltrandi and Pyre, 1975) . The deformation curvature is concentrated within the narrow strip that runs NE–SW for more than 100 kilometers along the Tomalo Syncline and including various systems of faults and folds, sometimes with steeply dipping limbs. The relations between these systems indicate that the structural setting of the Garbaharey belt is due to wrenching tectonics with a transpression component.

The two belts cut across an enormous practically undeformed area and are the most interesting tectonic structures of the region.

The general geological setting of the Garbaharey belt indicates that the large anticlines have been complicated by flower structures which are also products of wrench (strike-slip tectonics).
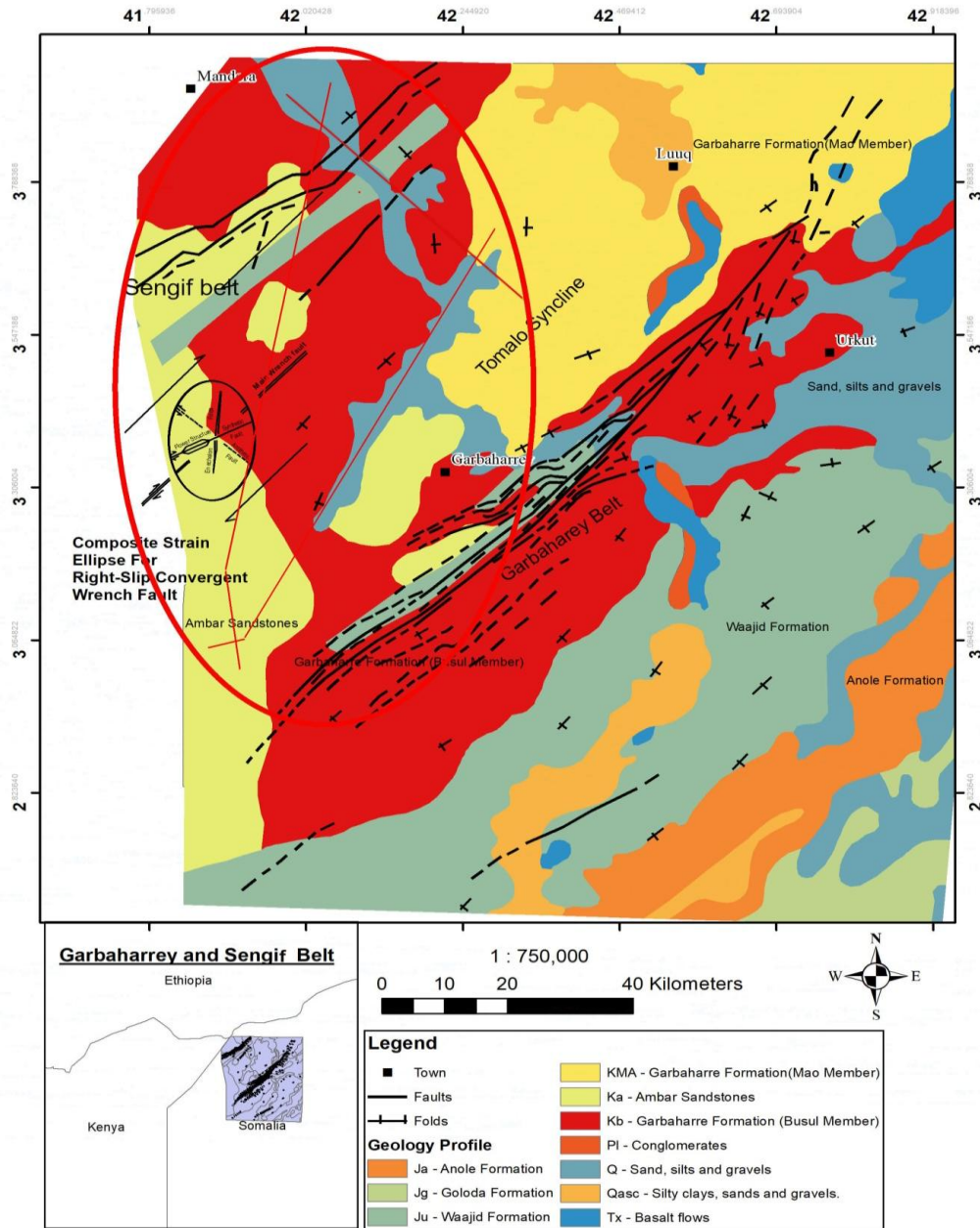
Figure 2.8: Modified Geological map of Sengif and Garbaharey belts and composite strain ellipse for right-slip convergent wrench fault (after Beltrandi and Pyre, 1975).

2.4.1. Structural Geometry

This involves the identification of the faults such as (vertical or subvertical faults), anticlines and flower structures in the reflection patterns on the seismic sections of the basin.

The interpretation of the vertical seismic displays of Hol area revealed that the Lugh-Mandera basin has a asymmetric cross-sectional sedimentary sequence. This indicated that deposition occurred at the time when the crust was thinning, thus got thickened at the basinal zone and thin along the edges as shown in (figure 2.9).
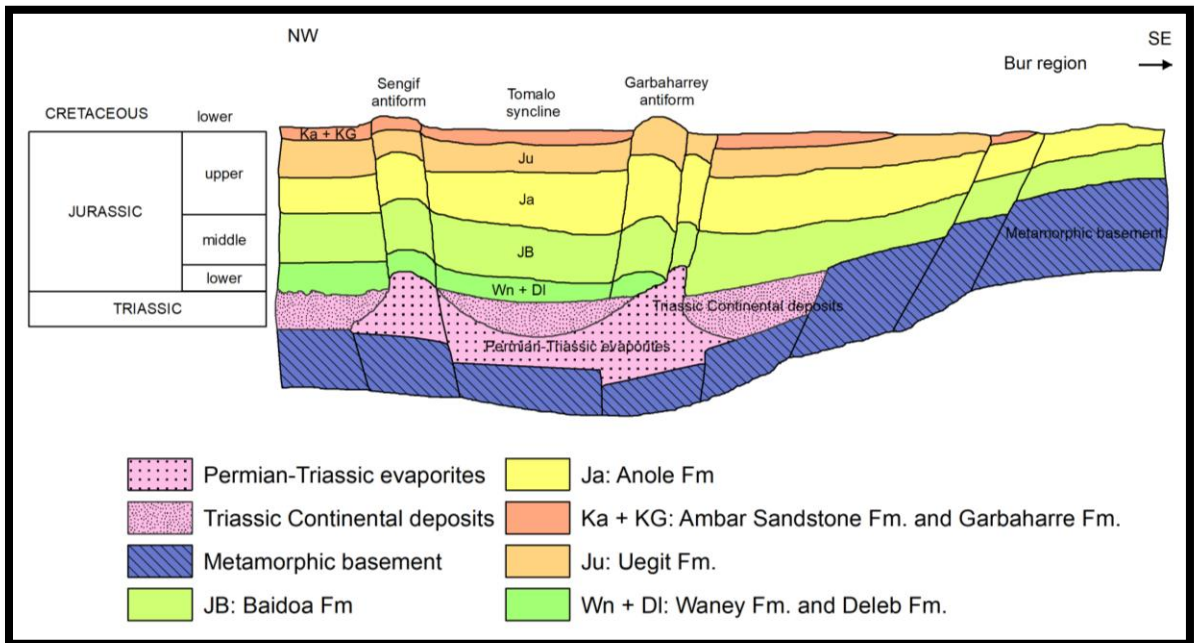
Figure 2.9: Schematic section of the Lugh-Mandera basin (Modified after Beltrandi and Pyre, 1973).

As a result, the basin resembles a massive syncline with limbs that only dip a few degrees. The Tomalo syncline is depicted in its entirety. The Sengif and Garbahaarrey belts both of which stretch for more than 100 kilometers and run parallel to the basin's axis, disrupt this regular pattern.

The main tectonic trends within the basin parallel what appears to be its main axis i.e. the structures trend NE-SW in the northeastern area and NNW-SSE in the southwest (Burmah Oil Co., 1973). There are three structural highs in the area. The structural highs are as follows; 1) Hol high 2) Cursi high 3) El God high, and broad Tomalo Syncline that deepens towards the north and can be observed from the generated gravity map (Figure 2.10).

The Hol high yielded a -8.36 mGal anomaly which located at a top of topographic high in the northern Lugh-Mandera basin. The Cursi and El God highs yield an anomaly of about 11.56 mGals and located to the east/south of the basin depression, while Tomalo syncline goes up to -48m Gal.

The Hol, Cursi, and El God structural highs in the Lugh-Mandera basin have also been depicted in the generated satellite gravity map.
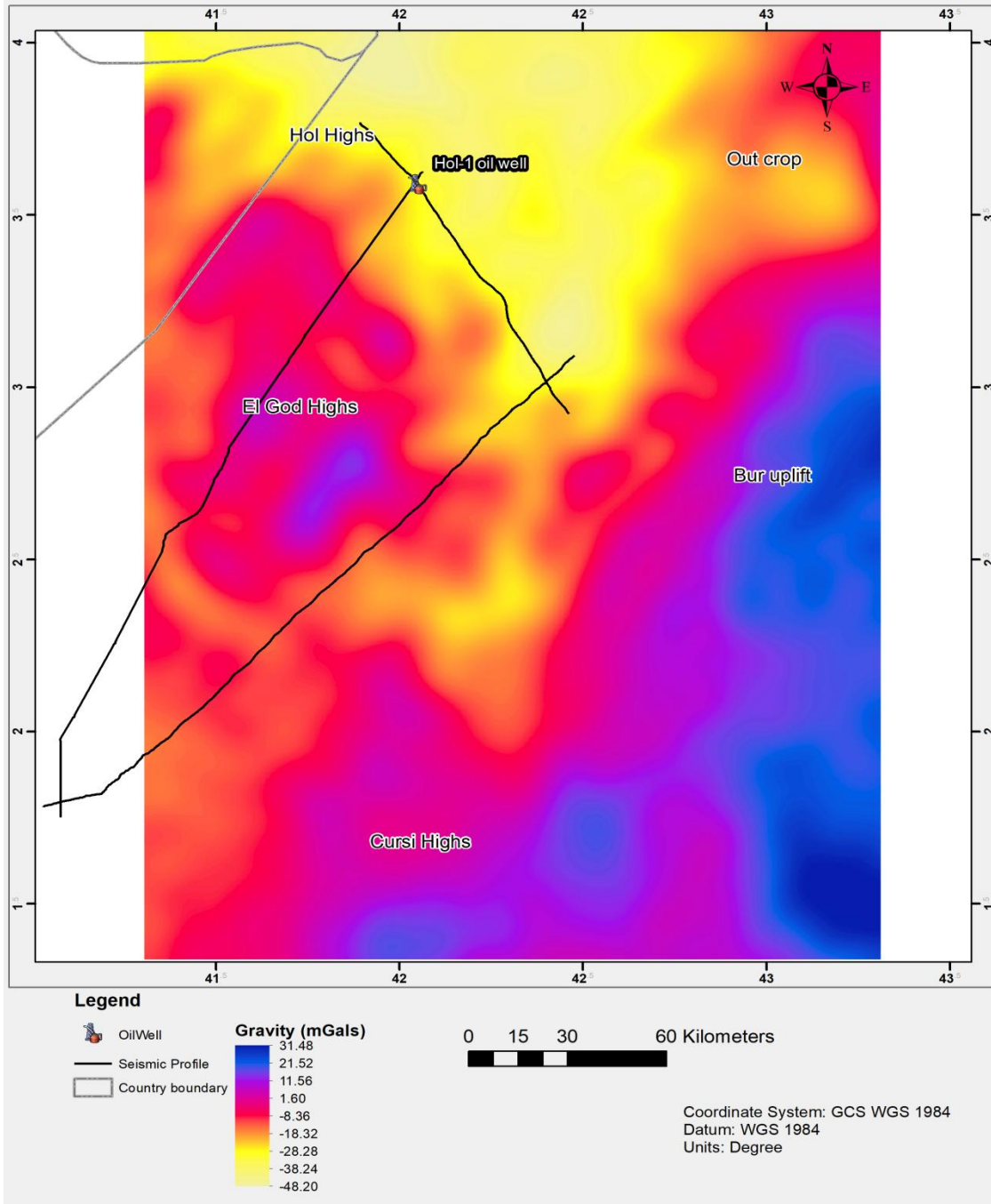
Figure 2.10: A 2D DTEM Satellite gravity map of the Lugh-Mandera basin shows, three structural highs and one visible syncline located in the northern part of the study area. Source: http://topex.ucsd.edu/cgi-bin/get_data.cgi.

2.5. Petroleum System

2.5.1. Potential Reservoir Rocks

The primary prospective reservoir rocks have been established based on sedimentological research on carbonate rocks and carbonate outcrop field studies by Berry (1974). Syn-rift grainstone/packstones and dolomites contain the majority of the carbonates in the Middle and Upper Hamenlei Formations. None or barely cemented limestones, as well as dolomitized intervals all have good petrophysical (porosity, permeability) properties.

2.5.2. Source Rocks

Several Geochemical studies (Morgan, 1985) have shown that the top Adigrat-base Lower Hamenlei and the Uarandab Formation are the most promising source-rock intervals. TTI Modeling was used to obtain the maturation parameters in the next section, as well as predictions of the timeframe of hydrocarbon generation, migration, and accumulation.

According to geochemical data (Morgan, 1985), The grey lime mudstone zone developed between 12,980 and 13,250 feet has a TOC of 0.93, which qualifies as a poor to marginal source rock, Vitrinite Reflectance (Ro) studies show that this section is mature (0.9 – 1.04 Ro). While Thermal Alteration Index (TAI) data suggests that the kerogen in this zone is definitely over matured (3.9 - 4) and corresponds to the Ogaden basin's transition zone-Adigrat oil/gas system (Hunegnaw et al., 1998).

The Uarandab Formation (L.Callovian - Oxfordian) is composed of 30- to 120-meter thick dark, laminated mudstones deposited in the open floor of the ocean environment. These mudstones are the best source rocks in Somalia and it's environ. Majority of the area has the potential to produce hydrocarbon accumulations.

2.5.3. Traps

The research area contains a number of potential structural, combinational, and stratigraphic type of traps. Fault traps on the sides of deep rocks, folded and faulted structures linked to transpressional wrench tectonics, the pinch-out of the Goloda Member reservoir on the basin's margin. Likely presence of hydrodynamic type of traps towards southeastern part of the study area due to the dead network drainage.

2.5.4. Seals

The Adigrat, Middle and Upper Hamenlei reservoir units are sealed by Middle Hamenlei evaporite rocks and Uarandab shales all of which have a regional development and good (excellent) sealing capacities.

2.6. Wrench Fault Tectonics

The aim of this subchapter is to provide a broad overview of the complicate/complex nature of wrench (transcurrent/strike-slip) tectonics, and its control on hydrocarbon accumulations.

As acknowledged previously by (Beltrandi and Pyre, 1973), the study area has experienced wrench fault tectonic. Nonetheless, wrench faults have been, and will be, important for the oil and gas industry.
In addition to this, the reader is referred to several other important volumes which cover related topics of strike-slip fault tectonics (Sylvester, 1988); continental transpressional and transtensional tectonics (Holdsworth et al. 1998); the role of strike-slip fault systems at plate boundaries (Woodcock N.H. 1986); and Seismic characteristics and identification of negative flower structures, positive flower structures, and positive structural inversion (Harding T.P, 1985).

Wrench faults, by definition, are older structures based in basement rocks that are frequently buried by newer sedimentary cover and reactivated as simple shears over time. Wrench faults are particularly essential in the development of sedimentary basins and

petroleum accumulation because of the reactivation process, which is why the term "wrench" fault became widespread (Moody and Hill, 1956; Wilcox et al., 1973). In the mid-nineteenth century, this was especially true in southern California. These faults are billions of years old and mostly inactive today in the interior of continents.

Kennedy (1946) and Anderson (1951) coined the term wrench fault to define ruptures in the earth's crust where relative motion of one block to the next is horizontal and the fault planes are almost vertical. The term is derived from the German "blatt," and was first used by Suess (1885) which is nearly the same with transcurrent faults.

As defined by Hill (1947), right and left lateral correspond to the actual relative movement of which the right lateral denotes clockwise separation while left lateral denotes counterclockwise separation. Strike slip systems are not but almost vertical, narrow wrench zones where two neighboring blocks shift sideways, parallel to the fault zone's position. They're made at transform tectonic plate borders, for example, where plates slide past each other horizontally (Figure 2.11). There is no net increase or decrease in the crust's area (Sylvester, 1988). Strike slip faulting is thought to take place in a three dimensional shear force, with the highest and lowest principal stresses occurring in the horizontal and vertical plane for example sinistral (anti clockwise) and dextral (clockwise) (Hill, 1947).
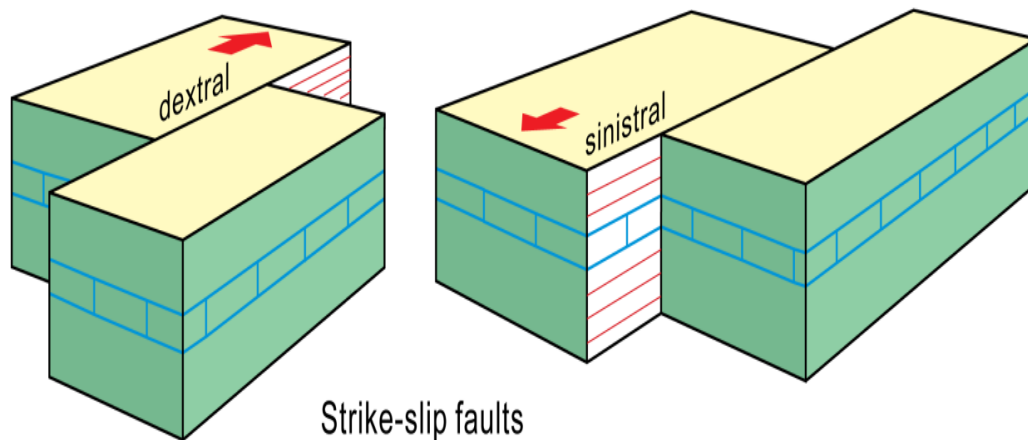
Figure 2.11:Types of Strike slip faulting, sinistral (anti clockwise) and dextral (clockwise) after (Hill, 1947).

2.6.1. The Basic Structure of Wrench Tectonics

Analogue experiments have successfully reproduced strike slip faulting. Riedel shears are secondary fractures that do not extend far from the main fault but are yet contemporary. On a large-scale fault system, Riedel shear can refer to up to five direction groups of associated fractures (Figure 2.12). Individual fractures in this scenario stay active after the other types have evolved, allowing for coordinated movement across all fractures to accommodate fault zone strain. Riedel shears' geometrical arrangement suggests that movement inside the wrench zone is therefore commonly employed for kinematic evolution analysis (Hill, 1947).
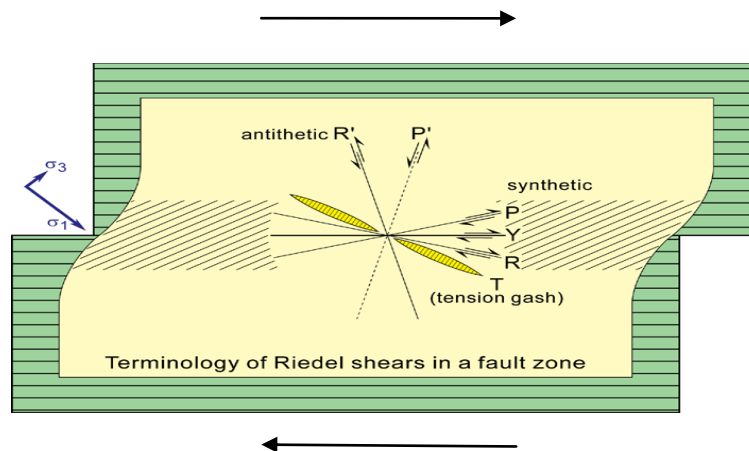
Figure 2.12: Illustration of theoretical orientation of wrench fault after (Hill, 1947).

R Riedel shears are the most common secondary fractures, and they usually form the most conspicuous pair. On a right-lateral fault, they form at an acute angle of 10 to 20 degrees clockwise, while on a left-lateral fault, they form at an acute angle of 10 to 20 degrees anticlockwise.

R' shears are antithetic faults parallel with the R (riedel) shears and orientated at a high angle at about 75°. They tend to form in the overlap zone and they frequently connect these two R shears.

P Shears are synthetic minor faults symmetrically orientated to the R shears with regard to the fault plane (anticlockwise and clockwise faults respectively). P shears can also be used to create an en échelon array with R shears and link them together. P-shears compress as shearing progresses to account for fault parallel shortening. They're not as

frequent as R and R' shears, and they might take a little longer to form. As for R Riedel shears, there may be **P' shears** conjugate with P shears but these have relative minor importance and are difficult to separate, in terms of orientation, from R-shears.2φ.

Y shears are synthetic microfaults, which appear to be the last to emerge and run parallel to the main fault.

- **Predictive Clay Model**

Clay models are used to investigate the mechanics of wrench faulting. Wrench faults form on the earth's surface as a result of horizontal shearing of surface brittle rocks and are consequently reproduced in clay models by a thin layer of clay underneath them (Cloos, 1955). The movement of crustal blocks in the opposite direction causes wrenching.

En echelon (folds and faults) are common features in the wrench zones formed during the migration process and are home to hydrocarbon traps. They also characterize the end of a wrench (Harding, 1973). The clay models given in Figures 2.13 and 2.14 shows a right-lateral wrench where a fault displacement results in movement of a non-stationary block in the right of the stationary one. The breadth and kind of mud coat employed, as well as the lateral displacement, define the sort of model created.

An increasing magnitude of stress during wrenching leads to splitting of the folds, first by fractures then leads to faulting, as illustrated in Figure 2.13C. In addition, the side sections of the fold are offset in the sequence and one fold side is moved over lengthy period of geologic time to a completely new location.

Folds appear when a thin sheet of clay film with a thickness of 0.0005-in is interlayered in the clay, resulting in a well-articulated clay-wrench model. Figure 2.13A, presents a clay model with discrepancies between the original fold trend line and the reflected one, thus revealing the thin plastic sheet that affected the folding process. The film hinders the prediction of the wrench fault in the model as shown in Figure 2.13.
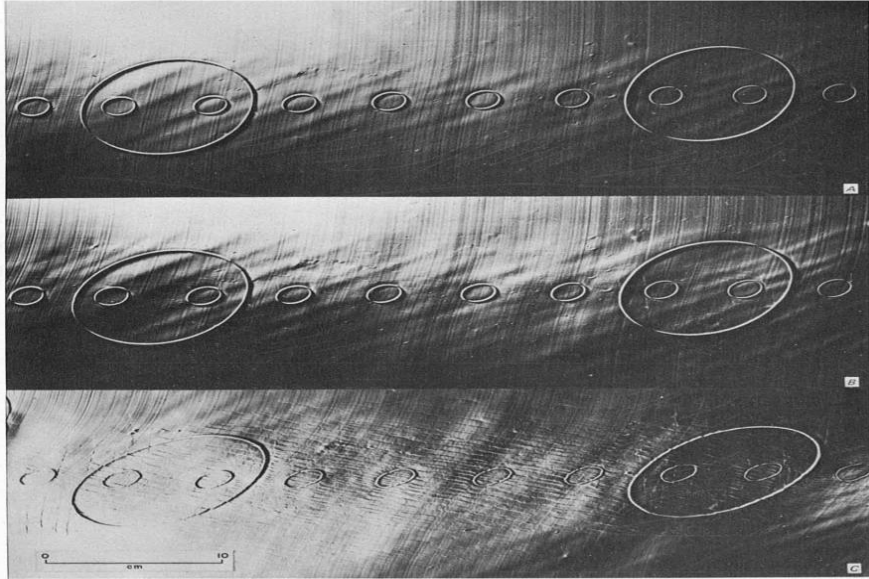
Figure 2.13: Clay model of parallel right-lateral wrench fault with layer of thin plastic film embedded 0.25 in. below surface to enhance en echelon folds (A-C = three stages, vertical views) from Wilcox et al. (1973).

In the early stages of movement of the clay model of a convergent wrench fault, Wilcox et al. (1973), ''en echelon'' folds will develop together with a few synthetic fractures. At later stages, the ''en echelon'' folds are offset along the Synthetic faults and Antithetic faults are also formed, as seen one of the models (Figure 2.14C). The model also revealed a complex thrusting of the wedges squeezed off the wrench zone by convergence. Folds and thrusts generally occur along the ellipse in en échelon displaying sharp slant to the key fault. Depending on the amount of transpression or transtension, Clay models that lack plastic film have the axes of folds and eclipse lying parallel to one another *(e.g.* Figure 2.14B).
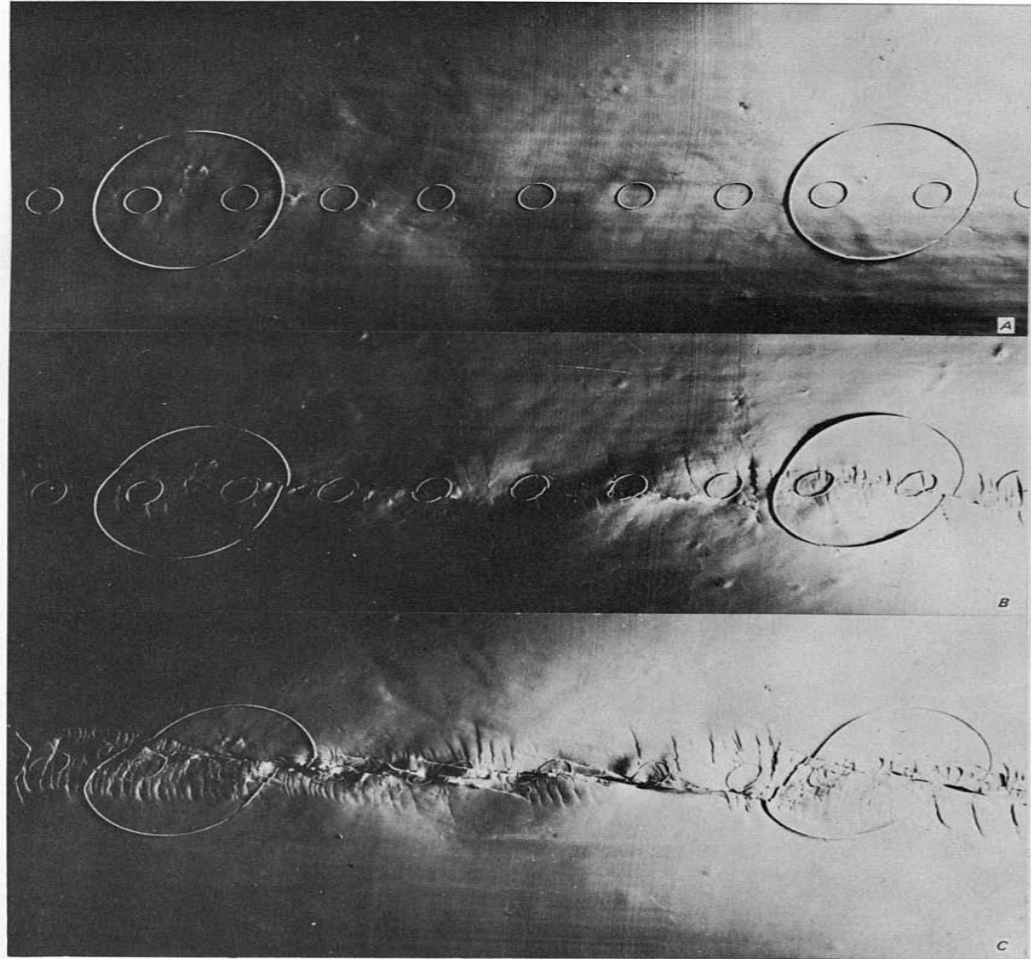
Figure 2.14: Clay model of parallel right-lateral wrench fault (A-C = three stages, vertical views) Wilcox et al. (1973).

2.6.2. Transpression and Transtension

Transtension refers to the deformation component of bulk strike-slip faulting. Shortening across a mostly strike-slip fault on the other hand is referred to as compression. Individual regional boundary conditions, such as, horizontal convergence or divergence at plate borders, as well as environmental characteristics (Holdsworth et al., 1998), as shown in (figure 2.15).
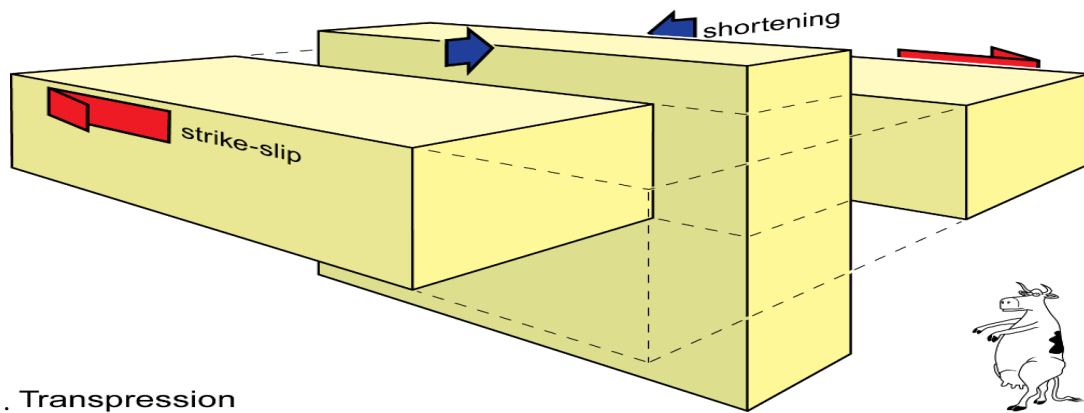
Figure 2.15: Transpressional strike slips movement (after Holdsworth et al., 1998).

The fault zone defines transpression and transtension, respectively. The findings of the experiments demonstrate a clear distinction between structures generated at 15° and 30°degees. For small values the consistency of the faults and distortion is restricted to steep faults (dipping > 70°). According to the regime, faults that create unequal rifts on thrusts or basins on fault lines are more likely to have substantial deformation.

2.6.3. Flower Structures

Flower structures have the following properties respectively:

- At depth, fan-like, relatively steep faults merge into a single one
- The deep main fault (the **stem**) is subvertical.
- On both sides of faults, facies and thickness vary dramatically for the same stratigraphic strata.
- The relative fault movement causing normal and reverse offsets along a single fault plane.

A flower structure is the upward splay shape of subsidiary faults. (Figure 2.16) shows substantial changes along the same wrench system in different sections.

It curves upward with minimal dips near the surface when the vertical component is reversed. A positive or reverse flower structure produces an elevated, antiformal region (a rhomb horst or push-up). This upward-diverging flaw produces an upward shape resulting positive flower formations are also referred to as palm-tree structures (Harding, 1985).
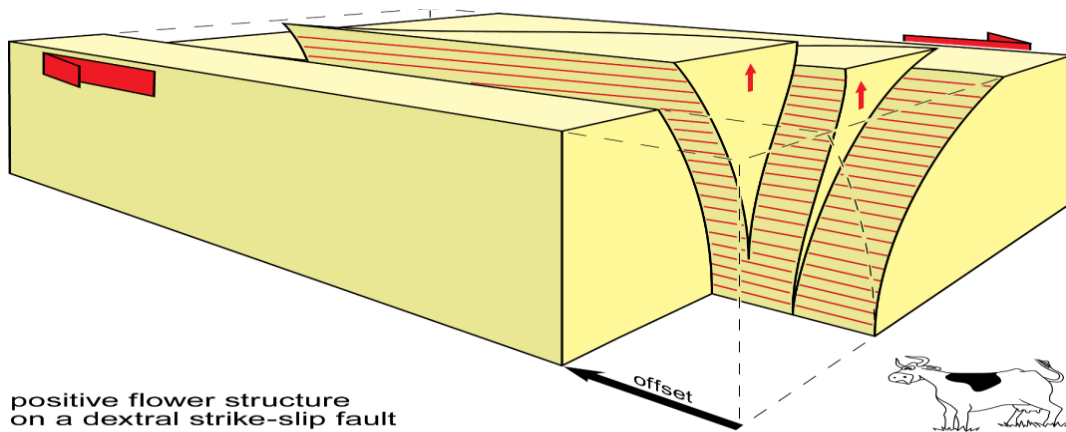
Figure 2.16: The flower structure of the palm tree is connected with strike slip movement (after Harding, 1985).

2.6.4. Relationship between Folds and Strike-Slip Faults

- **Passive En Échelon Folds**

Non-cylindrical, doubly plunging, and generally short folds associated with wrench fault systems are common, with sharply descending axial planes. They are structured spatially so that the peaks and valleys of succeeding folds are aligned to form angles with roughly parallel fold axes. They are considered to be arranged en échelon because they are stepped and regularly overlap (Woodcock, 1986). Figure 2.17 illustrates the relationship between the folds and strike-slip fault movement. The distribution of the axial planes, which are broadly orthogonal to the shortening direction, allows for the identification of the possible fault linking them.
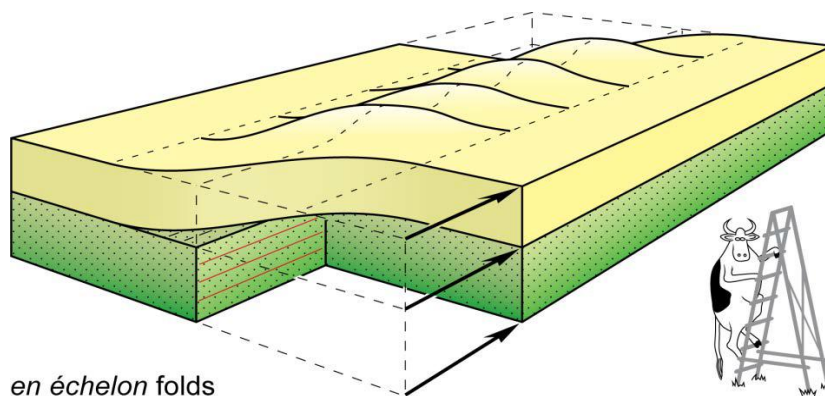
Figure 2.17: Relationship between folds and strike-slip faults movement (after Woodcock, 1986).

43

2.6.5. Occurrence of wrench fault tectonics

The widespread existence of long, generally straight, and geomorphically noticeable strike-slip faults, which are a kinematic consequence of large-scale tectonic plate motions on a sphere is one of the Earth's crust's most notable tectonic features (Wilson, 1965). In continental and oceanic transform plate boundaries, faults can occur as transfer zones connecting normal faults in rift systems and thrust faults in fold–thrust belts (Woodcock ,1986; Sylvester, 1988; Yeats et al., 1997). Strike-slip faults also are common in obliquely convergent subduction settings where interplate strain is partitioned into arc-parallel strike-slip zones within the fore-arc, arc or back-arc region (Beck, 1983). When strike-slip faults initiate in natural and experimental settings, they commonly consist of en echelon fault and fold segments (Wilcox et al., 1973).

2.6.6. Identification of Wrench Faults from Surface and Subsurface

Billings (1954) provided an excellent discussion of wrench fault recognition criteria. the following discussions are related to his work with a focus on wrench problems. Aerial pictures, with their straight trails, are extremely useful in locating prospective wrench faults.

Slickensides, stream offsets, and offsets in structures and outcrop patterns are the most common manifestations of strike-slip components of movement along fault planes. In certain instances, modern movement along these faults is associated with earthquakes.

The interpretation of seismic profiles can be used to identify wrench fault tectonics in the subsurface (Anderson, 1951). Firstly, various criteria from both profile and map associations are applied in the first stage. Secondly, alternative styles are identified, and their validity is assessed using additional criteria. Third, the working interpretation is put to the test against criteria that directly contradict the proposed wrench fault interpretation. The second and third steps are where one's interpretation is put to the ultimate test.

2.6.7. The Importance of Wrench Faults in Petroleum System

Knowledge of the wrenching structural style is extremely valuable in exploration. In general, the structures and structural traps found in a wrench terrane can be predicted to a great degree of accuracy (Figure 2.18). The associated folds have the potential for trapping hydrocarbons because of their early formation and because they frequently give the most closures, which are genetically, linked to wrenching (Harding, 1973).

The wrench fault tectonic settings are known for prominent hydrocarbon discoveries with classical examples, such as, Newport-Inglewood trend and Whittier Field in the Los Angeles Basin, oil fields of the San Joaquin Valley in California, Scipio-Albion Oilfield in Michigan basin, oilfields of central and south Sumatra in Harding (1973), and Panuco field in Mexico, Ellenburger structure of the Triple 'N' field in Texas, among many others.

SW   NE

Figure 2.18: Structure of Whittier oil field. Northeast closure is provided by Whittier fault, upplunge closure by tar seal in outcrops of producing sands. Production on northeast side of fault is marginal and comes from tight older Miocene sands (After Gaode, 1964)

2.7. Literature Review Gaps

Many researchers have extensively investigated the stratigraphic succession on both the outcropping section in south-western Somalia, and the axis of the Lugh-Mandera basin (Stefanini, 1931d; Barbieri, 1968; Beltrandi and Pyre, 1973; Angelucci et al., 1983; Canuti et al., 1983; Buscaglione et al., 1993; Ali Kassim et al., 1987; Ali Kassim et al., (2002); Burmah Oil Co., 1973; Berry (1974) Compared to the neighboring Ogaden basin in Ethiopia. But no study has been done on the types of proven petroleum systems within the basin .

In addition, little is known about the wrench fault tectonic structures in the Lugh-Mandera basin. Geologists from Burmah Oil Co. (1973) and Beltrandi and Pyre (1973) acknowledged the presence of wrench tectonic structures in the Lugh-Mandera basin. Burmah Oil Co. (1973) studied the main tectonic trends within the basin, and suggested that the angles of intersection of faults and fractures are similar to those which might be expected in a wrench fault system. They postulated that the structural trends may be inherited from a much earlier wrench fault system, and concluded that the age of the fault is unknown, but predates the overlying sediments. Beltrandi and Pyre (1973) made an attempt at interpreting the two belts of the Gedo region by using seismic data and assumed that the old normal Triassic faults may have been reactivated as wrench faults after the Early Cretaceous. They concluded that the Garbaharey belt has a relatively complex structure in which various systems of faults and folds may be recognized due to wrench tectonics with a transpression component. Ali Kassim et al. (1993), studied tectonic transpression in the same Gedo region where they gave a detailed mapping which showed that each belt (Garbaharey and Sengif) contains a pattern of folds and faults similar to those occurring in a right wrench zone with a transpression component. They concluded that the structural characteristics of the Garbaharey belt indicated right-hand movement accompanied by shortening normal to the wrench zone. No study has established the impact of wrench tectonics on the petroleum system of the basin, through the interpretation of available data, including subsurface maps (Isochore and Isopach maps) and the interpreted of the fourteen 2D seismic profiles.

Morgan (1985) studied geochemical analyses that were undertaken on cutting samples from Hol-1 well, at the request of Esso Exploration (E.A.850014, May 1, 1985) to assist in the evaluation of the source rock potential of the Esso/Shell license area by using rock eval analysis. However, no studies have been undertaken to evaluate the quality and the source rock potentiality of the basin by applying Time-Temperature Index (TTI) modeling.

CHAPTER 3 : MATERIAL AND METHODS

3.1. Introduction

Right before the initiation of this thesis work, various activities were scheduled. It began with the literature and previous reports reviewing and then followed by problem identification. Next the objectives were set and the methods to be adopted have been selected. Seismic and well data has been collected, and finally the data were analyzed and interpreted.

3.2. Seismic Data Acquisition Parameters

The seismic data in the Hol area were obtained using vibroseis of sweeps 12, 48 fold spilt spread 10-56 Hz, 96 trace and sweep length of 4 Seconds. A geophone spacing of 135 m and shot (vibroseis) spacing of 37.5m was used. Data was acquired for 6 seconds at a 4-millisecond sampling rate.

3.3. Background to Seismic Reflection Surveys

Seismic methods are a form of geophysical approach that is used to map sedimentary basins on a large scale as well as on a micro scale for detailed exploration and development (Bjorlykke, 2010). Seismic delineations are essential because they relate surface seismic data to subsurface stratigraphy and sedimentary facies (Gadallah & Fisher, 2009).

Seismic data is generated through recording of reaction times of a directed artificial acoustic energy into the earth. The traces on a seismic section are a representative of the reflected energy. Figure 3.1 depicts a seismic line from a modest reflector, whereas Figure 3.2 depicts a deeper reflector. The traces are detected on the x axis, while the y-axis shows the Two Way travel Time (TWT). A trace characterizes the position of a geophone. The time it takes for a seismic wave to return from a source and a given depth to be recorded by a geophone, is known as Two-Way travel Time (TWT). When visualized, the trace lines are packed closely together.
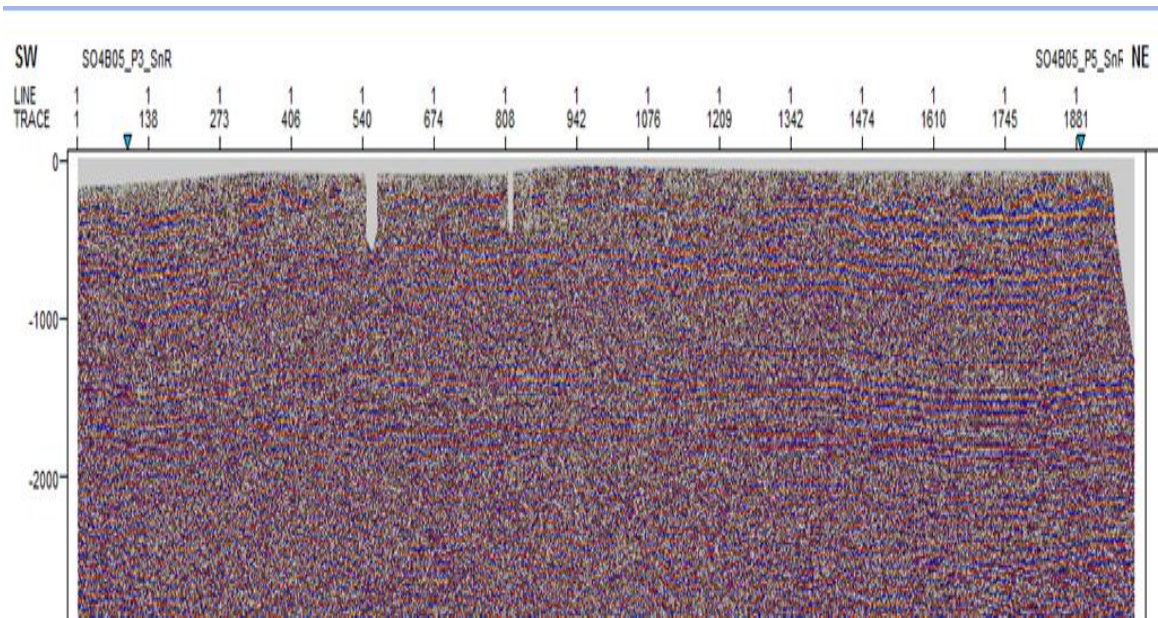
Figure 3.1: Seismic section due to a shallow reflector from seismic line S04B05-P4-SnR in Lugh-Mandera basin (CGG, 2021).
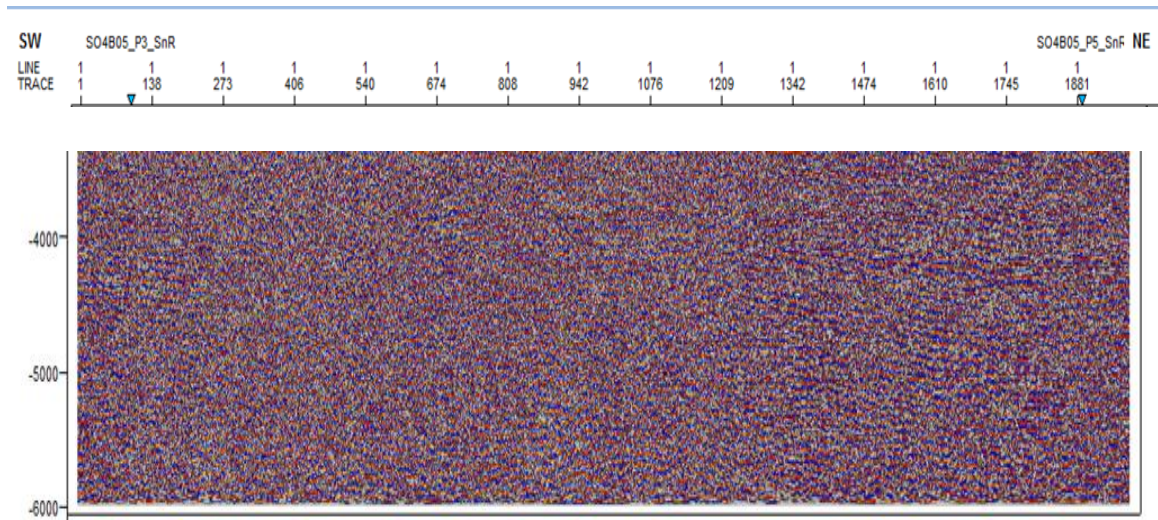
Figure 3.2: Seismic section due to a deep reflector from seismic line S04B05-P4-SnR in Lugh-Mandera basin (CGG, 2021).

The 2D seismic survey data as acquired over the Lugh-Mandera basin by Seismograph Service Ltd on behalf of Burmah Oil Operator covering over three structural highs in the Lugh-Mandera basin these are: Hol, E1 God and Cursi between September 1971 and May 1972. Table 3.1 illustrates the summary of the geophysical survey parameters. The

following line kilometers were recorded during the acquisition time; 337 line miles at Hol, 147.50 km at El God, and 128.27km at Cursi areas, respecively.

Table 3.1: Summary of the acquisition parameters (Burmah oil service)

Date	Company	Acc. Contractor	Source	Instrument	SP Int	Geo Int	Channels	Spread	Fold
Sept/1971	Burmah Oil Somalia Ltd	Seismograph service Ltd.	Vibroseis	DFS V	37.5	135m	96	3788-263-0-262-3787 m.	48

The initial interpretation of this data contributed in the setting the wild cat of Hol-1well.

3.3.1. Two-Dimensional Seismic Reflection Survey Techniques

In 2D data acquisition the reference points and receivers are lined in a straight line when profiling the reflections. The reproduced raypaths fit the profile plane when perpendicularly aligned to the geologic strike (Schuck and Lange, 2007). To capture the lateral positions of the underlying geologic sections, the source point and its corresponding geophone spread are moved in line along the profile line. The source-geophone configurations employed in a 2D seismic reflection study are shown in Figure 3.3.

a) Split spread (split dip) refers to the geophone array being symmetrically arranged on both sides of the source.

Figure 3.3: Commonly used source-geophone arrangements (spreads) for 2D seismic reflection data acquisition (Schuck and Lange, 2007).

3.4. Seismic Reflection Data Processing Parameters

The current investigation was intended to evaluate 2D seismic data that had been acquired, processed and migrated. As the current research objectives are not concerned with the processing of seismic data, here we only give a summary of the status and the quality of the data that is shown in Table 3.2.

Table 3.2: Hol-1 Seismic Data - Processing Parameters (CGG, 2021)

Date	Proc.contractor	Processing	Data Quality	Area	Total (Miles) (Km)
18/2/86	Exxon exapration data processing center Houston, Texas.	Migrated	Excellent	Hol area	337 miles (542.34Km)

3.5. Seismic Data Interpretation Practice

The interpretation of the seismic data is science of gathering the geological information at targeted depth from the seismic data. Depth to the targeting surface is dependent on the thickness and velocity of seismic waves with in the overlying rock layers. The initial significant task for an interpreter of the seismic data is to pick reflectors of targeted horizons, since this will depend on what wiggles from trace to trace are aligned with the reflection from the same horizon. The interpretation of seismic data needs the gathering of all geological and geophysical data into a unified picture that should be more significant. For the achievement of a successful interpretation, it is required that the interpreter should sensibly follow the interpretation work flow described in the following steps:

Step 1: Interpretation plan

Interpreter of seismic data should have a clear idea about the targeting horizons and what is the tectonic regime he/ she is working on. This is done when the interpreter is referred to analyze previous studies available with interpreted reports and thesis.

Step2: Regional tectonic, structural and depositional trends

For the interpretation and identification of actual structures and structural styles from the seismic data, it is necessary for the interpreter to study literature about the tectonic history of the study area.

Step 3: Seismic patterns

Regional seismic pattern can be studied from previous or published interpreted seismic data of the area. This verifies the seismic signature of the target, the location of the mapping horizon, and the adequacy of the time-depth functions.

Step 4: Building and amalgamation of different datasets

After following the steps mentioned above, the assembling and amalgamation of all available datasets is necessary and an important step in seismic data interpretation. The catalogue of all available seismic data acquired at different times should be prepared. This step helps to determine whether available data are significant enough for targeted study.

Step 5: Interpretation

The seismic data to be interpreted can be loaded with the help of specific software selected for the interpretation purpose. For the current study IHS Kingdom Suite 2017 and Schlumberger Petrel 2017 versions software were applied.

According to Dobrin and Savit (1988), Keary and Brooks (2002), there are two approaches for the interpretation of seismic data of any area. The First one, is the stratigraphic interpretation and, the second one, is the structural interpretation. These are dealt with in details in the following chapters.

3.6. Interpretation Process

The interpretation process of the seismic data involved;

- The digitization and typing of the shot point locations into a text file, for easy import into IHS Kingdom Suite software.
- Transferring the typed text file into the IHS Kingdom Suite and Schlumberger Petrel Softwares, to vsualize the orientations as provided later ahead in Figure 3.6.
- Data viewing to identify seismic lines in the header information.

- Data importation to IHS Kingdom Suite and Schlumberger Petrel softwares for further interpretation of the unique seismic lines.

The process of interpreting the seismic data was carried out for each line because of the diverse structural, stratigraphic and hydrocarbon properties, thus allowing easier prospective analysis. A comprehensive flow chart of overall seismic data interpretation is shown in (Figure 3.4).

Seismic Data Interpretation Flow Chart
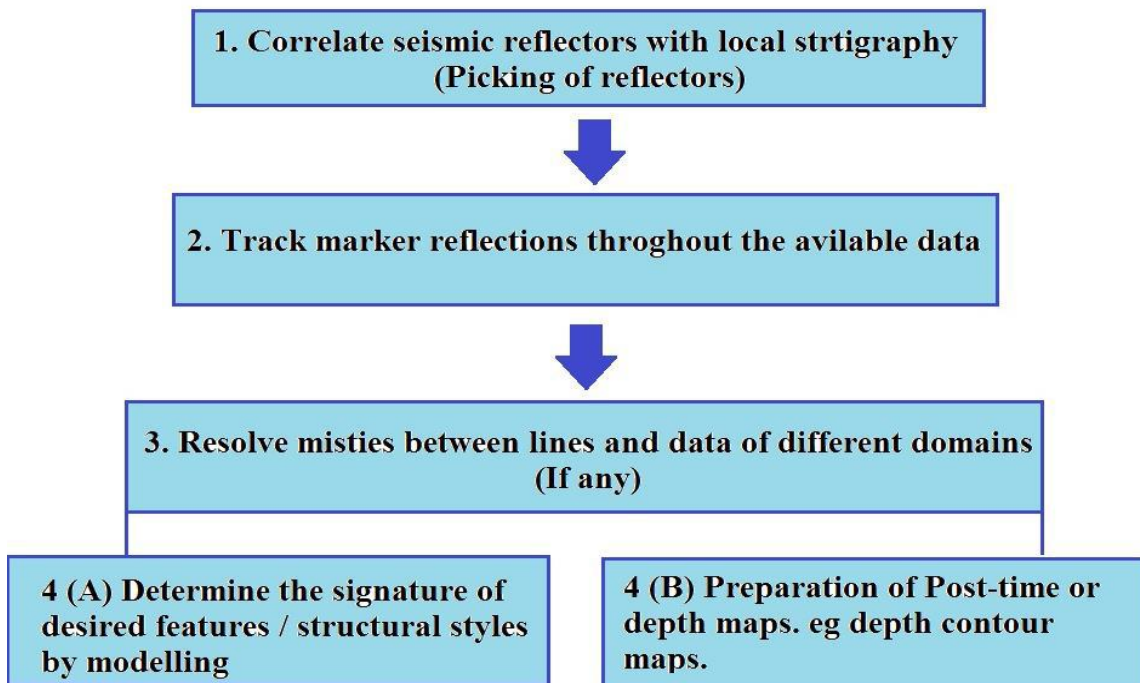
Figure 3.4: Seismic data interpretation flowchart (modified after Dobrin and Savit, 1988).

3.7. Stratigraphic Analysis

Stratigraphic analysis included the interpretation of litho and seismo-stratigraphic properties of the Hol-1 well, and the entire (major part) of the basin. The purpose was to map the seismic formations (facies), unconformities bounding them, and to examine the distribution of the main components of the petroleum sysem (source rock, reservoir, trap, seal, etc). The following sub-chapters highlight the methods used to achieve the objective.

3.7.1. Data Set and Software's

The secondary 2D seismic data sourced from the CGG Robertson database was used for the current research study. The data included fourteen (14) seismic profiles intersecting one well, (Hol-1) section used for seismic well tie procedures. The data record quality for the area is excellent. The data set included a digital recording of the vibroseis reflection seismic survey conducted by seismograph service limited over the Lugh-Mandera basin. The area surveyed was Hol which was covered by approximately 337 line miles of 12 fold multiplicity traverses: 165 miles were traversed at Hol.

The seismic and well data used for the identification and interpretation of stratigraphic and structural styles were obtained from CGG Robertson which is a servicing company managing data for Somalia on behalf of the Ministry of Petroleum and Mineral Resources (MPMR). The data were processed by Exxon exapration data processing center in Houston, Texas, USA. Interpretations of the seismic profiles were done using IHS Kingdom Suite and Schlumberger Petrel interpretation softwares at the Department of Earth and Climate Sciences, University of Nairobi (UoN).

The Hol-1 well information described above was represented by such well log. Las format files: CALD-CALI-DEN_UN-DRHO-DT-GR-LL7-MCAL-MINV-MNOR-NEUT-PML-R16-RHOB-RILD-SNP-SP (Figure 3.5).
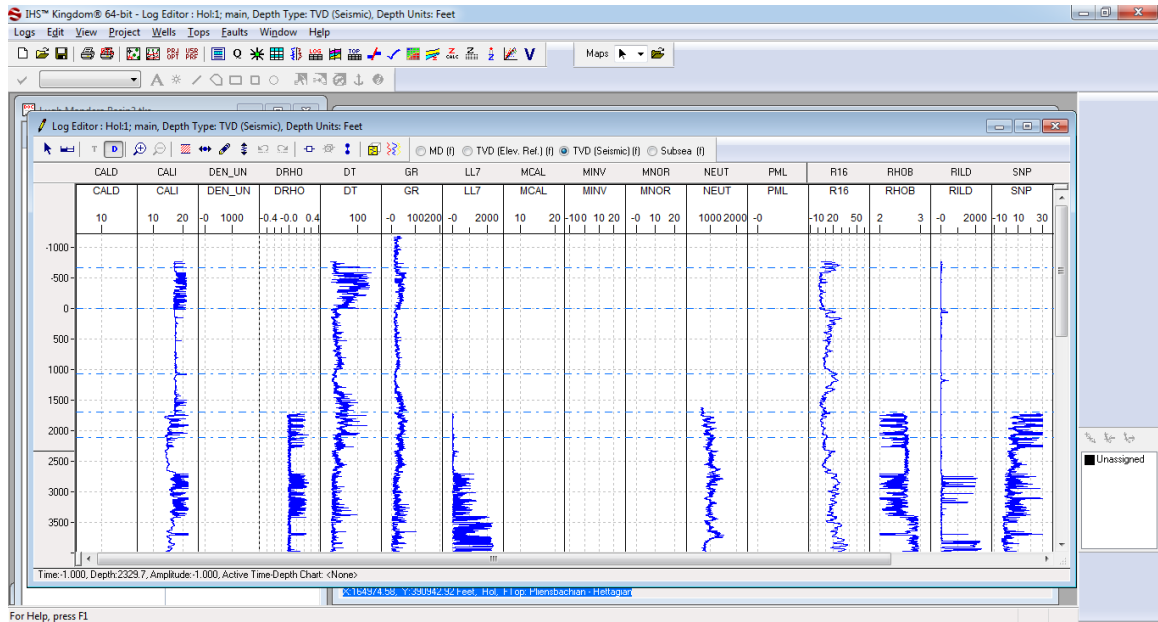
Figure 3.5: Display of the well log data for the upper well section in IHS Kingdom Suite version 2015.

The Lugh-Mandera basinal area hosts the Hol-1 well with the following coordinates of (3_3502300N, 42_0205800E) and was drilled by Burmah Oil Co. to test the Mesozoic structure. The drilling was started 18/12/1972 and completed at 2/1/1973, with a total depth of about 13,258' (4,042 m). Later, it was classified as an abandoned one with some gas shows and oil and gas shows. From the geochemical report data there are four interval zones which indicated a gas shows at (2900', 4900', 8870', and 11950'). There were no cores cut in Hol-1 Well. Also several Drill Stem Tests (DST's) were conducted, but no hydrocarbon recoveries were reported.

3.7.2. Base Map of the Seismic Profiles

The Kingdom Suite software recreates the base map by analysing the wells seismic and log data and thus offers an in-depth conceptualisation of subsurface properties with regard to structure and hydrocarbon potentials. With regard to the study, fourteen profiles (14) of 2D seismic data, which best represented the area of study in terms of access and availability of the basin's digitized data, were used to inform the investigations.The

seismic lines which cover 650.5 km and which are described here comprise fourteen (14) seismic profiles. The locations of the seismic data are given in Figure 3.6 a,b.

In this study, seismic digital SEG-Y data containing two (2) dip lines and nine (9) parallel lines and three (3) perpendicular lines were used for interpretation.

The seismic data lines parameters, such as, seismic line name, orientation, SP, Migration Type, and Line Length (650.5 km) of each seismic line given in Table 3.3.

Table 3.3: Seismic data lines parameters (CGG, 2021)

No	Line no	SP first	SP last	Length (Km)	Strike/Dip/ Parallel	Survey type
1	SO4B05_P1	2010	2399	29.4	Dip	Scanned and reconstructed SEG-Y migration
2	SO4B05_P2	2210	3355	85.7	Parallel	Scanned and reconstructed SEG-Y migration
3	SO4B05_P3	3290	3551	19.5	Parallel	Scanned and reconstructed SEG-Y migration
4	SO4B05_P4	3457	4451	74.1	Parallel	Scanned and reconstructed SEG-Y migration
5	SO4B05_P5	4350	5203	63.9	Parallel	Scanned and reconstructed SEG-Y migration
6	SO4B25_P1	2158	2453	22.1	Dip	Scanned and reconstructed SEG-Y migration
7	SO4B25_P2	2958	3669	53.1	Parallel	Scanned and reconstructed SEG-Y migration
8	SO4B25_P3	2330	3052	54.3	Parallel	Scanned and reconstructed SEG-Y migration
9	S04B25_P4	3569	4223	48.9	Parallel	Scanned and reconstructed SEG-Y migration
10	SO4B25_P5	4124	4721	44.6	Parallel	Scanned and reconstructed SEG-Y migration
11	SO4B25_P6	4609	5078	35.6	Parallel	Scanned and reconstructed SEG-Y migration
12	SO4B30_P1	2002	2981	73.4	Perpendicular	Scanned and reconstructed SEG-Y migration
13	SO4B30_P2	2957	3073	8.6	Perpendicular	Scanned and reconstructed SEG-Y migration
14	SO4B30_P3	3027	3527	37.3	Perpendicular	Scanned and reconstructed SEG-Y migration
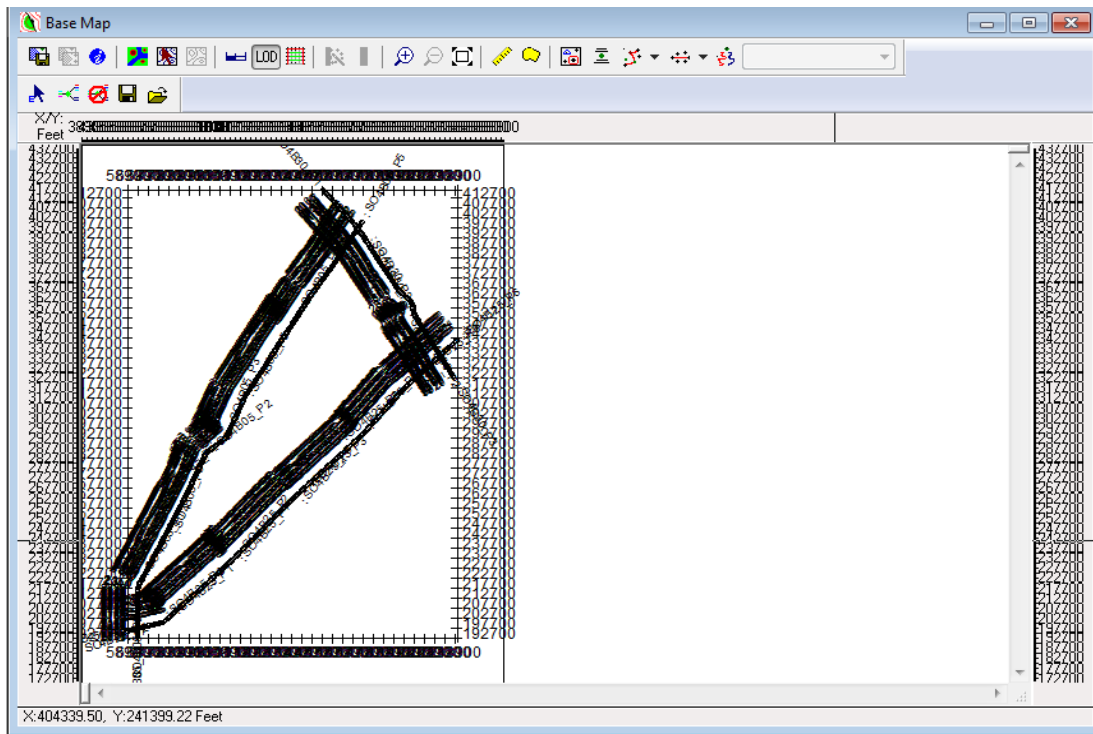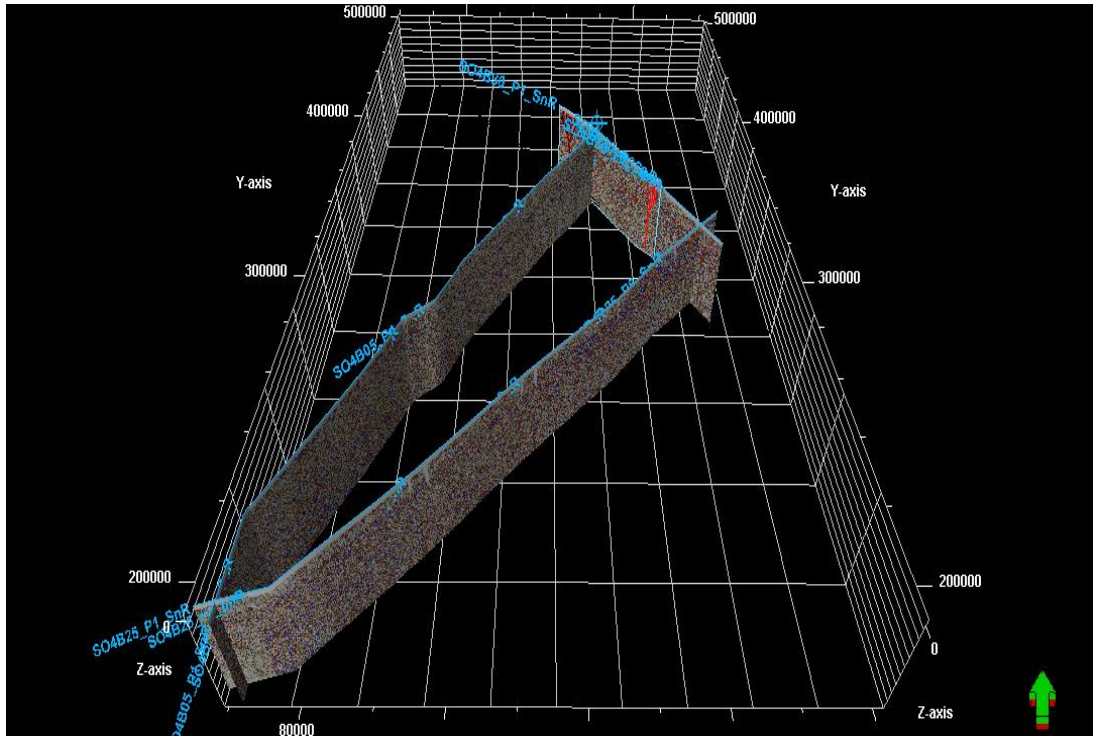
Figure 3.6 a,b: 2D seismic profiles used in the current study displayed in Schlumberger Petrel 2017 (above) and IHS Kingdom Suite 2015 (below). Nine (9) profiles having a trend that is parallel to the axis of the Lugh-Mandera basin (NE-SW), while three (3) profiles, trending (NW-SE) across the basin, and two (2) other profiles have a (N-S) and (W-E) extent respectively.

3.7.3. Petroleum System Elements

The purpose here is to determine the major types of the petroleum system elements (PSE's) in Hol-1 well and the surrounding area. The presence of which is proven or anticipated were done through analyzing the stratigraphy information that obtained from bore hole data and Burmah Oil Co. well reports. A Correlation of these petroleum systems with those of the neighboring Ogaden basin in Ethiopia were also undertaken.

3.7.4. Tying of Synthetic with Seismic Data

Seismic ties with wells is a significant method used for the picking of horizons. In this method, tops of geological horizons identified in a well section with specific reflections are accurately matched with the two-way time seismic profile data. Sonic and density well logs were used to generate a synthetic seismic trace. This is significant approach for the interpretation of seismic data.

The IHS Kingdom Suite and Schlumberger Petrel softwares were used for the interpretation of seismic data allows well to seismic tie as well as generation of synthetic seismogram.

3.7.5. Horizon Picking

The science of interpreting the stratigraphy of the subsurface requires an emphasis on picking the reflectors of targeted formations and isolation of main units, unconformities, and boundaries that are observed on the vertical display. The steps include identifying the observable sets of horizons that are similar, then correlating, tracking them, and finally, digitizing them. The formation tops mapped during the current study are provided in Table 3.4.

Table 3.4: Time Categories of the Hol-1 Formation Tops (Moderated from Palynology Report) from CGG Robertson used for the Seismostratigraphy of Lugh-Mandera basin (LMB).

Top Depth MD (ft)	Top Boundary	Base Depth MD (ft)	Base Boundary	Age
100	Confident	609	Confident	Tithonian – Kimmeridgian
699	Confident	1272	Confident	Lower Kimmeridgian
1,671	Confident	2,349	Confident	Oxfordian

2,400	Confident	2,973	Confident	Oxfordian – Callovian
3,030	Confident	3,390	Confident	Lower Callovian – Bathonian
3,570	Confident	5,400	Confident	Bajocian
5,520	Confident	6,180	Confident	Toarcian
6,360	Confident	13,220	Confident	Pliensbachian – Hettagian

The depth values for these formation tops were identified and mapped using the IHS Kingdom Suite version 2015 software after some convertions generating a Time-Depth Chart for the Hol-1 area (Figure 3.7). The depths were measured in feet and correspond to the Measured Depth (MD) type.
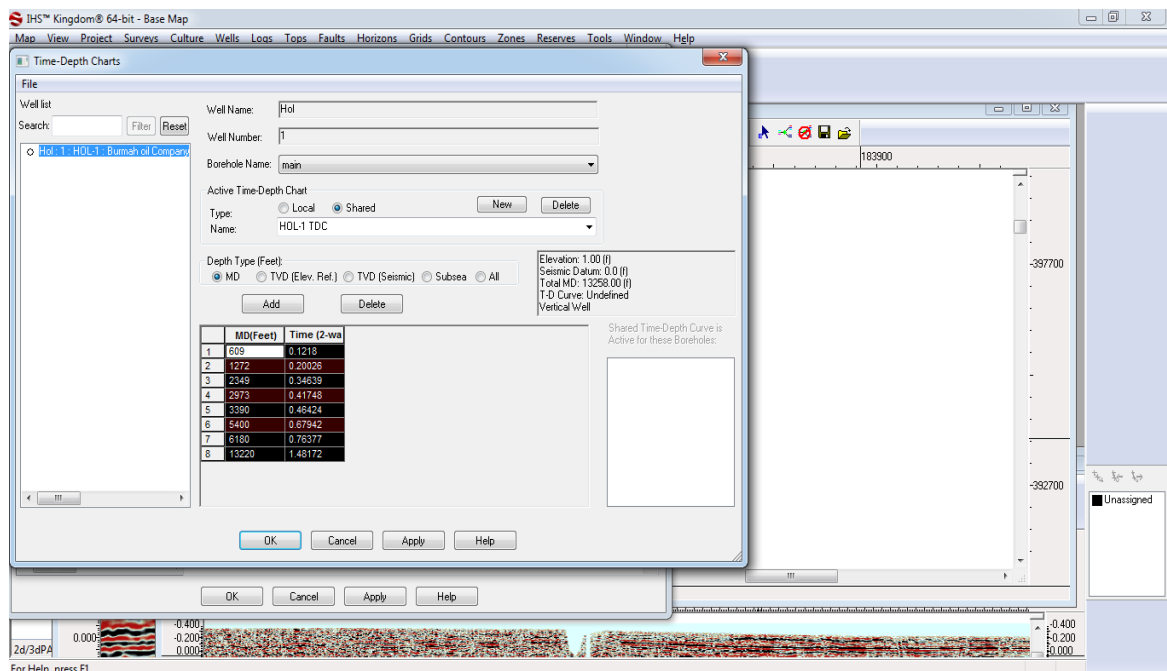
Figure 3.7: Convertion values obtained from the Time-Depth Chart generation for the chosen top formations from Hol-1.

3.8. Structural Analysis

The investigations also entailed examining the structural geometry of the Lugh-Mandera basin given the interpreted 2D seismic data and well logs.

3.8.1. Data set and software's used

The investigations used the IHS Kingdom Suite Software to display the processed 2D seismic lines and examine the geology of the subsurface structure in terms of faults and major horizons mapping (Figure 3.8). Schlumberger Petrel 2017 version was used to generate the structural isochore and isopach maps.
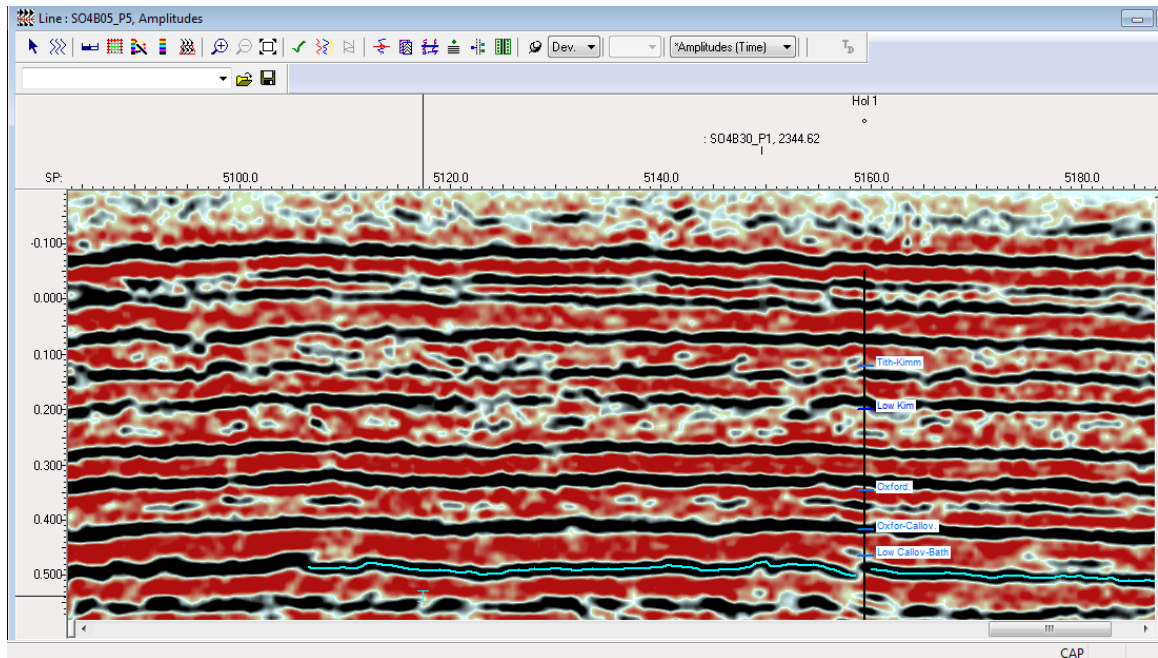
Figure 3.8: Seismic profile SO4B05_P5 –well Hol-1 tying and mapping of selected well top formations using IHS Kingdom Suite version 2015.

3.8.2. Fault interpretation

Faults in a 2D map are characterized by discontinuous horizon reflectors. Marillier et al., (2006) mentions that faults are best characterized by sudden vertical displacement of several reflectors along a plane. With this regard, the current study identified and mapped the main faults lines through interpretation of fourteen (14) 2D seismic profiles. The interpretation of the faults as displayed on the seismic lines called for creation and digitization of the points to compose the fault segment. The most prominent fault line that was easily observable was named as the Garbaharey fault while other synthetic faults were interpreted as convex upward reversed faults which resembled flower structure

(Sylvester et al, 1976). Results of this procedure are discussed in detail in Chapter four (4) Results and Discussion.

The vertical seismic displays of seismic lines, such as, SO4B-05-P5 (Figure 4.3) and SO4B-05-P4 (Figure 4.4) illustrates the development of steep, almost sub vertical faults which splay at the upper levels. These are so-called flower structures that easily recognizable.

3.9. Time-Temperature Index (TTI) Modeling

The application of Lopatin-Waple Technique (TTI) will enable us to understand the maturation history of the potential source rock intervals in the Lugh-Mandera basin. Similar research will be undertaken from El Kuran-1, and Bodle-1 wells, wellsites located in Ethiopia, to have a regional estimate of the source rock capacity for Lugh-Mandera and Ogaden basins.

Analyzing the burial history helps retrace the vertical migratory patterns of the sediments found in a basin. According to Hinte (1978), it is the quantitative description of the basin's geologic antiquity, and as such, the Lopatin-Waples method that encompasses both construction of graphs and calculations of TTI values will be adopted in predicting the start of petroleum generation-migration-accumulation. The scrutiny of the TTI modeling thus reveals the time and hydrocarbon types generated.

3.9.1. Data Set

The major data requirements for the analysis of TTI include;
- Bottom-Hole Temperature (BHT)
- Well formation tops
- Sediment thickness
- Sediment age
- Sedimentation rates

The burial history curves and stratigraphic charts were generated manually and later digitized with the help of Corel Draw Suite 2019/2020 version software.

3.9.2. TTI Analysis

The components of time and temperature greatly influence the organic materials, and as such, the Lopatin-Waples method that utilizes the two elements will be used to determine the time of petroleum generation. The model indicates that the level of oil and gas production doubles for every unit rise in temp. As such, a $10°$ C temp change in either direction of the base point enhances either positively or negatively the rate of generation of petroleum (Barker, 1996; Angengo, 2020). As a result, a temperature function δ is provided for each interval, n where:

$$\text{(Equation 3.1)}$$

As a result, interval n factors in the temperature function δ =where:

$\delta = r^n$

where r = 2

Table 3.5: Temperature factors for every $10°$ C interval (Barker, 1996)

Temperature interval	N	r^n
20-30C°	-8	$1/256$
30 – 40C°	-7	$1/128$
40 – 50C°	-6	$1/64$
50 – 60C°	-5	$1/32$
60 – 70C°	-4	$1/16$
70 – 80C°	-3	$1/8$
80 – 90C°	-2	$1/4$
90 – 100C°	-1	$1/2$
100 – 110C°	0	1
110- 120C°	1	2
120 – 130C°	2	4
190 – 140C°	3	8

The temperature sets of $10°C$ used in the Lopatin-Waples method are tabled above. The technique determines the maturity value by supposing that a rise in maturity over each $10°C$ temperature interval is proportional to the time spent by the source rock, and thus maturity rise is equal to the temperature's n^{th} power.

$$\Delta Maturity\ (TTI) = (\Delta Ti)\ (r^{ni}) \qquad \text{(Equation 3.2)}$$

where Ti= the amount of time spent in the range of temperatures

r^{ni}= factor of temperature in the interval

For each 10°C temperature range, the total maturity is the summation of maturity indexes.

Further, the Lopatin-Waples technique observes the following procedures;

a) Burial graphs, which plot sedimentary layers depth versus age profiles. This step however, does not account for the compaction or water loading.

b) The construction of a temperature grid of 10°C intervals. The geothermal gradient is supposed to remain constant through time. Waples (1980, 1985) similarly tabled the TTI values with corresponding maturity indicators (Vitrinite reflectance, Ro) and types of hydrocarbons as indicated in Table 3.6.

Table 3.6: TTI –Vitrinite reflectance correlation and hydrocarbon type (Waples, 1985)

TTI	Ro	Hydrocarbon type (80% probability)
50	0.90	Normal oil
75	1.00	Normal light oil
180	1.35	Condensate – wet gas
500	1.75	Wet gas
900	2	Dry gas

The temperature factor is reduced by uplifts. Since maturity growth is independent of burial or uplift, the TTI values are likely to remain positive. With elevation and cooling, however, the rate of maturation is expected to slow over time (Waples, 1985).

3.9.3. Age of Formations and Unconformity Record

The micropaleontological data from the Lugh-Mandera basin was collected by Paleoservices in 1973, 1975, while palynology data was provided by Bocal (1972). The chronostratigraphic chart time scale was used to determine the ages of strata deposition as shown in Table 3.7. The rate of sedimentation curve from the Aalenian (174.1 Ma) stage, of the middle Jurassic reveals an uplift and related erosional phase.

Table 3.7: Formation ages, depth thicknesses, sedimentation rate in 1 My, TTI, TOC, Ro, and erosion history for sediments in Hol-1 based on palynological data and sedimentation rate from the sedimentation rate curve, and the GSA geological time scale.

No	Formations	Age (M.A)	Depth thickness (ft)	Sedimentation rate in (m/Ma)	TTI	TOC (wt%)	Ro
1-	**Busul Mb**	Tithonian – Kimmeridgian	100 -- 609	23			
2-	**Uegit FM**						
		Tithonian - Kimmeridgian	699 -- 1272	127.5	1.2		
		Oxfordian	1671 -- 2349	229	2.5		
3-	**Anole FM**	Oxfordian - Callovian	2,400 -- 2,973	416	4.9	0.60%	< 1
	Goloda Mb	Lower Callovian - Bathonian	3,030 -- 3,390	86.9	5.1	0.22%	< 1
	Baidoa Mb	Bajocian	3,570 -- 5,400	1,005	20	0.15%	0.9
	Uanei Mb	Toarcian	5,520 -- 6,180	62.5	20.8	0.48%	1
4-	**Iscia baid Fm** / **Adigrat/Lwr Hamenlei**	Pliensbachian - Hettagian	6,360 -- 13,220	525	1,319	I. (10,400--11,390)= 0.6% II. (12,980--13,250)= 0.6%	>4

Table 3.8: Summary of the data and software used in this study

Task	Output	Software
Desk Study	Digitized Geological map Digitized Drainage map Gravity map	ESRI Arc GIS ESRI Arc GIS ESRI Arc GIS
Structural Interpretation	Seismic sections	IHS Kingdom Suite 2017
	Depth structure maps	Schlumberger Petrel 2016/2017
Stratigraphic Interpretation	Seismic facies sections	IHS Kingdom Suite 2017
	Stratigraphic chart	Corel Draw 2019
Time-Temperature Index (TTI)	TTI Curves SR Curves TTI Comparison chart	Corel Draw 2019 Corel Draw 2019 Corel Draw 2019

CHAPTER 4 : RESULTS AND DISCUSSION

4.1. Stratigraphy and Petroleum System Elements of the Lugh-Mandera Basin

4.1.1. Lithostratigraphy and Biostratigraphy of Mesozoic Strata from Hol-1 well

Hol-1 well encountered mainly Jurassic and lower most Cretaceous formations. The total depth of Hol-1 well 13,258 ft (4,042m) and ends in the Lower Jurassic formation. The lithologies are commonly represented by interbedded layers of grey limestone, lime mudstone, shales, sandstones, pale marls, with minor dolomite and anhydrite occurrences.

Figure 4.1 is based on Hol-1 well lithological and geochemical results adopted from Burmah Oil Company reports. They were modified to include the Petroleum System Elements (PSE's) comparing with those from the neighboring Ogaden basin in Ethiopia and the tectonic events that affected the Lugh-Mandera basin.

- **Lower Jurassic Sediments- 13,258'-5,520' (4,042m-1,683m) interval**

The thickest strata found by the Hol-1 well section of 7,738' (2,359 m) belong to the Lower Jurassic (Liassic) sediments and are subdivided into the subunits listed below:

a) **Pliensbachian-Hettangian (top Adigrat/Lower Hamenlei formations= almost entire Iscia-Baidoa Member)- 13,258'-8,000' (4,042m-2,439m) interval**

Adigrat formation represents the lowermost layer of the strata reached by the well section. It comprises thin layers of red silty shales, siltstones, pink sandstones, fine grained mixed with probably in caved white sandstones, and grey green clays. The Calub-1 well from Ogaden basin encountered significant amount of natural gas in sands of the Adigrat and Karoo formations at a depth of approximately 9000' (2,744 m) (Harms and Naleye, 1993). This section probably corresponds the early rift phase.

The Lower Hamenlei overlies the Adigrat formation and consists of a series of dark grey limestones with interbeddings of light grey and grey green clays, locally fossilfereous at a depth of around 12,600' (3,841m) these are light brown dolomite that appear along with light grey clay-stone and fine grained sand. The sandstone from 12,920' (3,939m)

contains elements composed of dark grey limestone. This formation accumulated in a shallow marine environment with intertidal and lagoonal episodes. Geochemical data indicates that the zone in the depth range of 12,980' – 13,250' (3,957-4,039m) has a TOC value 0.93 wt% characterizing it as a poor to marginal source rock. Vitrinite reflectance (Ro) data indicate that this section is mature (0.9 – 1.04 Ro), while Thermal Alteration Index (TAI) data indicate that the kerogen is probably overmature in this zone corresponding (3.9 - 4). There are some gas shows around 11,950' (3,643m) and 8,875' (2,705m) both from Lower Hamenlei formation.

At a depth of 12,260' (3,738m) the lime mudstone commonly contain type III Kerogen which is mature, suggesting that it has produced natural gas. The average TOC values in the Lower Hamenlei are within the 0.108 - 0.224 wt% range that indicates poor source rock quality. The lime mudstone usually contains a small amount of former solution moldic type of porosity infilled with sparite cement. Additionally, the data from Ogaden basin it shows that this zone 12,880' (3,927m) act as a reservoir rock. Which probably represents the beginning of the Adigrat formation in the transition zone (Hunegnaw et al, 1998)?

b) **Toarcian (mid Middle Hamenlei = top Iscia-Baidoa formation= upper Uanei Member)- 6,180'-5,520' (1,884m-1,683m) interval**

The Lower Middle Hamenlei is a thick section which is composed of a series of dark grey limestones, dolomitic limestones, dolomite, anhydritic dolomite, anhydrite with rare interbeds of black shales and sandstones. The limestone is occasionally psuedoolithic and mainly consists of pelletal wackstones, packstones, and fossilfereous lime mudstones which are often recrystallized. Tectonically, this unit accumulated during the early rift phase.

The Uanei Member appears to be dominated by dark grey and grey-brown, hard,compact lime mudstones which are locally fossilfereous and argillaceous.

Thermal Alteration Index (TAI) suggests that from 4,600' (1,402m) - 6,300' (1,920m) interval it is completely mature (2.6 –3.0) and it is within the Oil zone in transition to the gas zone (3.0—3.8) from 6,300' (1,920m) up to 12,400' (3,780m). The kerogen type in

this zone is predominantly algae, with lesser amounts of woody and biodegraded terrestrial material. The TOC values are anomalously high around 1.51%. This indicates good quality source rock. There is a gas show at a depth of 4900' (1,494m) from the Anole formation. Probably, this thick section contains petroleum system element (PSE)-source rock, reservoir rock, and seal that are combined together. The HILALA-1 Well from Ogaden basin had encountered crude oil that was recovered on test from Upper Hamenlei which correlates to the Hol-1 section (Harms and Naleye, 1993).

No visible porosity has been recorded from this interval in Hol-1 well section, although evidence of former porosities is present in most of the lithological type's desended. The pelletal and oolitic limestone usually contains small amounts of former intergranular and solution moldic porosities, both of which are currently filled with passively precipitated non-ferroen equigranular sparry calcite cement (Berry, 1974). When comparing with Ogaden basin data, it becomes obvious that the equivalent sections to this zone which consists of fracture limestone, and has act as a reservoir rock and at the same time it has a good sealing capabilities due to anhydrite and evaporate series developed within the carbonate unit.

- **Middle Jurassic (Dogger) Sediments 5,400'-2,400' (1,646-732m) interval**

The thicknesses of the Middle Jurassic (Dogger) sediments are 3,000' (915m) and can be subdivided into the units listed below:

c) **Bajocian (lower Upper Hamenlei=Baidoa Member) - 5,400'-3,570' (1,646m-1,088m) interval**

Lithologically, the Baidoa Member is composed of fine to medium grained, fossilfereous lime mudstone and skeletal wackstones, and medium grained oolitic grainstones. The Baidoa Member has increased average TOC values (>0.5 %) at it's lower portion suggesting increased shaliness. In the Ogaden basin, the shales that are intercalated among the carbonates contain kerogen of Type II and are mature enough to generate wet gas.

In Hol-1 section the grainstones show a thicker development at its upper part b/w 4,240' (1,293m) – 4,320' (1,317m) interval. Thin interbeds with of fossilferous lime mudstone and packstones. The lower part of this interval consists mostly of skeletal wackstones, locally oolitic and pelletic. No visible porosity has been identified although there are samples that contain fabrics indicating the former existence of the porosity. After deposition the oolitic grainstones possessed excellent intergranular porosity, but this appears to have been completely infilled by passively precipitated non-ferron calcite or sparite cements. This zone act as a good reservoir rock as indicated from Ogaden basin (Hunegnaw et al, 1998). Tectonically, this part of the section deposited during the syn-rift phase.

d) **Lower   Callovian   -Bathonian   (mid   Upper   Hamenlei=top   Anole formation=Goloda Member)- 3,390'-3,050' (1,033-930m) interval**

Lithologically, the Goloda Member is represented by fine to medium grained lime mudstones/wackstones which contain poorly sorted, subangular to subrounded pelecypod and echinoderms debris together with small amounts of quartz silt. Also there is no visible porosity present. As indicated from the Ogaden basin this section is presented by fractured reservoir interval. In SW Somalia, the Goloda Member is characterized by high permeability properties due to it's increased fracturing.

e) **Oxfordian-Callovian (Upper Hamenlei=Anole formation)- 3,050'-2,400' (930-732m) interval**

Lithologically, the Anole Formation comprises dark grey limestones with shale interbed; fossilferous lime mudstone and skeletal wackstones. This zone is a potential good source rock for the Upper Hamenlei sediments. The van Krevelen diagram from this zone indicates that the kerogen is a mature type II, with lesser amounts of woody and biodegraded terrestrial material. The TAI ranges between (2-3) suggesting that this section is in the oil window. The TOC around (>0.5%) is recorded at 3,050ft, this provides a good quality source rock. Interestingly, a gas show was encountered in this zone at the depth of 2900' (884m). Tectonically, these strata accumulated during the syn-rift phase.

- **Upper Jurassic (Malm) Sediments- 2,400'-570' (732 – 174m) interval**

Upper Jurassic sediments can be subdivided into two the Lower and Upper Uegit Formation. These are presented by interbeddings of grey limestones, shales, sandstones, and sandy limestones. Tectonically, these sediments accumulated during the syn-rift phase.

f) **Oxfordian (Upper Hamenlei =? Lower Uegit formations)- 2,400'-2,050' (732-625m) interval**

Lithologically, the Lower Uegit is mainly presented by silty lime mudstones which are unfossiliferous or flora remains. The limestones are composed of nonferroan calcite. The lime mudstones and siltstones contain no visible porosity. The siltstone is considered to represent a period of increased detrital influx probably into a shallow marine environment.

g) **Kimmeridgian (Uarandab formation=Upper Uegit formation)- 2,050'-570' (625-174m) interval**

The Upper Uegit is commonly composed of fine to coarse grained lime mudstones, wackstones, and packstones. The porosity in this interval is infilled with sparry calcite cement. Data from the Ogaden basin it shows that this interval may act as a source and seal rock simultaneously, which prevents the escape of hydrocarbons that were generated during the Upper Jurassic (Hunegnaw et al, 1998).

- **Lower Cretaceous Sediments- 570'-100' (174-30m) interval**
Lower Cretaceous sediments are the thinnest and uppermost section encountered by the Hol-1 well, since the deposition of sediments in the basin had ceased in the Early Cretaceous. This part of the section is represented by the Garbaharey Formation. Which can be subdivided into two units: the lower part, Busul Member and the upper part, Mao Member.

h) **Tithonian base (Garbaharey Formation/Busul Member)- 570'-100' (174-30m) interval**

This is composed of terrigenous sediments that entered the basin from the southwest and were deposited during the Early Cretaceous times. The Ambar sandstone accumulated under marginal marine to continental conditions. The formation consists of limestones, dolomitic limestones and sandstones. According to our interpretation, this unit will act as overburden rock.
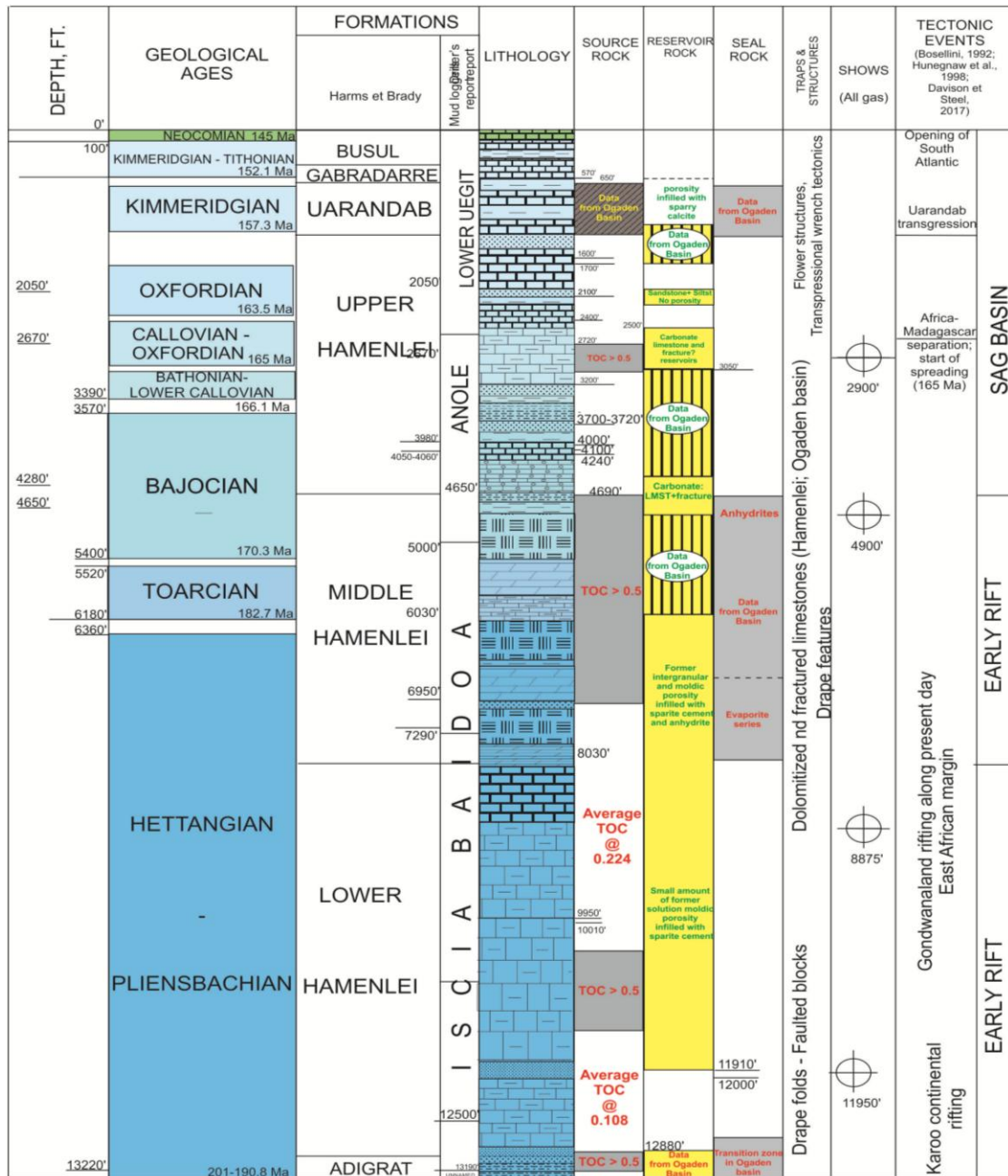
Figure 4.1: A generalized lithological and tectonic sequence chart with corresponding Petroleum System Elements (PSE) for the Hol-1 well (Atteyeh, 2021).

4.2. Hydrocarbon Traps and Prospective Areas

The major hydrocarbon traps in Lugh-Mandera basin are structural in nature (subvertical faults associated with positive flower structure or domal anticlinal traps due to the basement highs), stratigraphic (may be in porosity pinch out of Goloda Member), and also hydro-dynamic traps in nature. If we are to consider the hydrographic network of SW Somalia, the Dead valley which runs over 100 km long and is almost as wide as the present Jubba valley, and flows to the N from the Garbaharey area to the Dawa river, W of Mandera (Paleo-Dawa). We may conclude that the hydrographic network deepened, and this might have eventually leaded to flushing out the crude oil accumulation towards the Bur Acaba area. We assume that, at the south east most hydrocarbons were trapped at fault closures and at fold anticlines.

This research has selected at least three potential Petroleum Systems (PS) corresponding to those of the neighboring Ogaden basin located in Ehiopia, These are:

a) Adigrat-Lower Hamenlei PS which corresponds to the transition zone of the Ogaden basin (Hunegnaw et al, 1998).

The source and seal rocks of the Lower Hamenlei lie above the Adigrat sandstone reservoir. Drag folds linked with wrench tectonic faults are the structural type of hydrocarbon traps. After the early to middle phases, the oil generation, migration, and accumulation occurred, making it conductive to accumulation. The Jurassic-Early Cretaceous deformation altered this petroleum system, reactivating pre-existing normal faults.

According to data from the Ogaden basin, the Adigrat sandstone reservoir is of good quality (especially the lower portion), with porosities varying from 10 to 20%, and permeabilities up to 100 mD, plus a maximum net thickness of 135m (Hunegnaw et al.1998). The grey lime mudstone zone between 12,980' (3,957 m) and 13,250' (4,040 m) has a TOC of 0.93 wt%, which according to geochemical data (Morgan et Davies, 1985) is a poor to marginal source rock. Vitrinite reflectance studies show that this section is mature (0.9 – 1.04 Ro). While TAI data suggests that the kerogen in this zone is definitely over developed (3.9 - 4).

b) Middle-Upper Hamenlei PS.

The reservoir units at the Middle Hamenlei formations serve as a good reservoir. The quality of the reservoirs in the Hol area is rather poor. Good petrophysical characteristics are found in high energy oolitic grainstones of the Goloda Member (Top Anole- Lower Uegit formations) where intergranular porosities are in excess of 30% were common before cementation or dolomitic beds with high porosity and permeability values that can be found as pinch out porosity traps along the basin's margins, especially in the uppermost part of the Upper Iscia-Baidoa Formation (Berry, 1974).

The lime mudstone Uarandab formation that lies over the reservoir rock serves as a good source rock (kitchen) for hydrocarbon generation, and also acts as a seal.
 Kerogen thermal alteration index (TAI) values (2.6–3.0) indicates that it's interval corresponds to a Oil zone between 4,600' (1,402 m) and 6,300' (1,920 m) interval. Before transitioning into a Gas zone (3.0—3.8) from 6,300' (1,920 m) to 12,400' (3,780 m) interval. The kerogen type in this zone is mostly of algae origin, with some woody and biodegraded terrestrial debris. The TOC was unusually high (1.51 wt %) producing an excellent source rock with a gas display. Hilala-1 well from the Ogaden basin has encountered oil recovered on test from the Upper Hamenlei, while better reservoir qualities were identified in Calub Saddle with a high oil generation potential of up to 19 kg HC/ton rock (Hunegnaw et al., 1998).

c) Uarandab-Upper Hamenlei PS corresponding to Uarandab-Gabredarre oil system of Ogaden basin (Hunegnaw et al, 1998).

The Uarandab source rock is located between the Upper Hamenlei limestone reservoir and the Uegit carbonate reservoirs. The structural deformation occurred after the oil generation and it's migration is highly likely. In this zone, the van Krevelen diagram shows a mature kerogen type II, which is mostly presented by organic matter of some woody and biodegraded terrestrial material. This section is in the oil window with TAI corresponding (2-3), at a depth of 3000' (915 m), and the TOC is around 0.46 wt %.

The Uegit reservoir carbonates are underlain by fossilferous lime mudstones which both serve as a source and seal rocks with calcite cement filling. The Uarandab shales are

responsible for the reefs of the Calub Saddle oil cooking zone, as well as the oil shows in Hilala-1 well and the oil seeps in the Genale zone (Hunegnaw et al., 1998).

4.3. Seismic Stratigraphy

The fourteen seismic profiles traverse the Lugh-Mandera basin's thick sedimentary rock infill. Reasonably high quality seismic profiles were generated. The profiles (Figure.4.2) disclose the basins' sedimentary architecture, allowing the syn-rift sequence to be distinguished from the Karoo group sequence and basement formation.
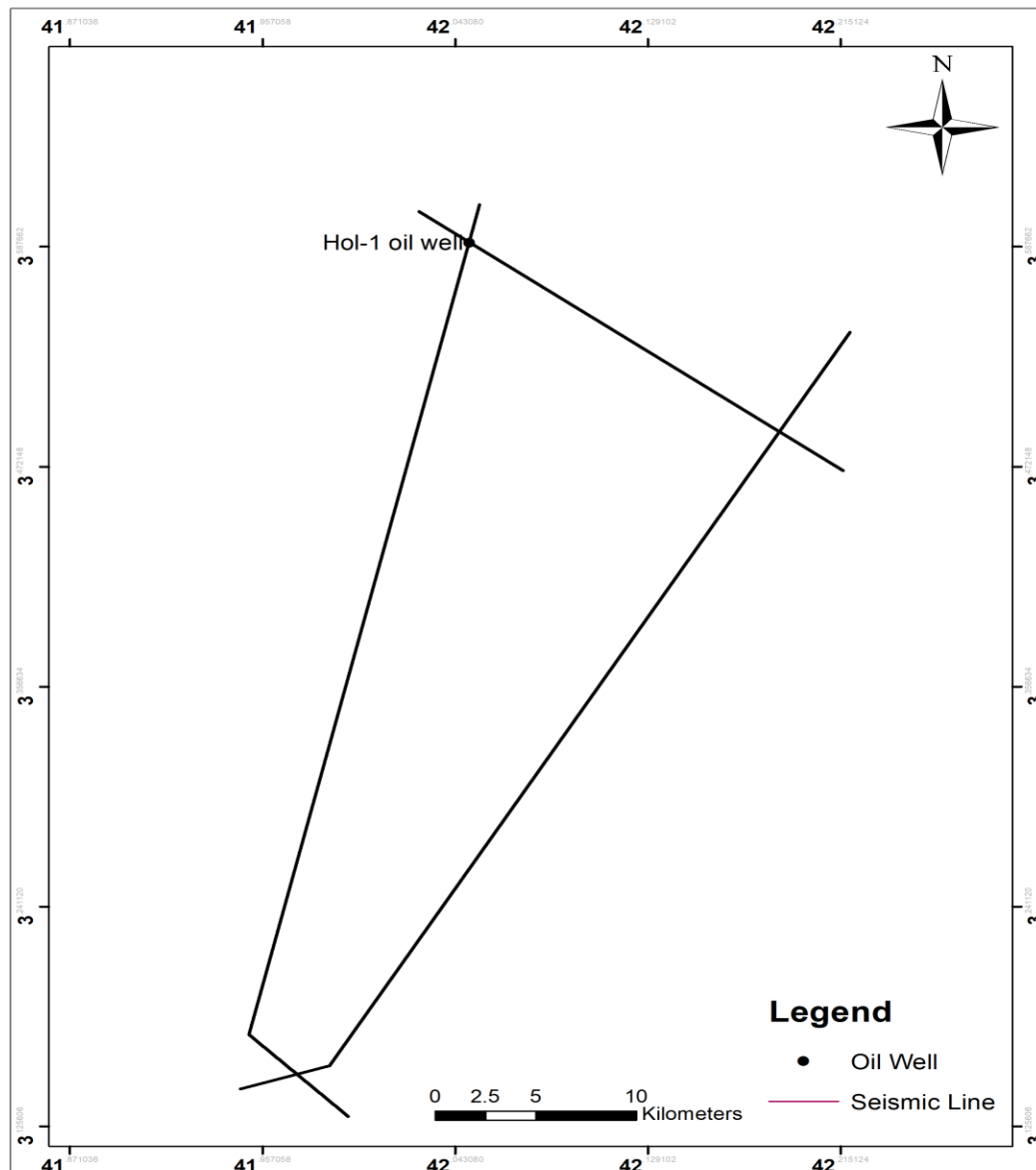
Figure 4.2: Base map of the seismic survey

The well reports paired with wire line logs (gamma ray, resistivity, and sonic) informed the subsurface geology of the well sites, including providing information of the formation characteristics in terms of lithology, geochemistry, and physical properties. As a consequence of well-to-seismic correlations and the lateral continuity of seismic strata, six regionally traceable stratigraphic sequences were identified and illustrated in (Figures 4.3 to 4.16). From bottom to top these include;

a) Pliensbachian – Hettagian base surface
b) Toarcian base surface
c) Bajocian base surface
d) Lower Callovian – Bathonian base surface
e) Oxfordian – Callovian base surface
f) Oxfordian base surface

a) Pliensbachian – Hettagian base surface (top Adigrat/Lower Hamenlei Formations)

The deepest sediments encountered by the Hol-1 well were stratigraphic units of the Early Jurassic that belong to the Adigrat and Iscia-Baidoa formations. The sequence's top and bottommost sections exhibit laterally continuous high reflectors. This sequence reaches its maximum thickness in the Hol region, where it is almost 7,040' (2,146 m) thick in the basin's center. These rock deposits are regularly evident through whole the Lugh-Mandera basin, as shown in (Figures 4.3 and 4.16), and widely observed on the vertical seismic display of the majority of seismic profiles SO4B05 P2, as shown in (Figure 4.12) . The sequence thickens from SW to NE.

b) Toarcian Sediments (Upper Middle Hamenlei-Uanei Member)
The formation top is visible and is an easily traceable reflection with a large amplitude and medium continuity that spans the majority of the research area. The width of the sequence thickens as it approaches the basinal Hol area; here the Toarcian sequence

reaches up to 780' (238 m) thickess in the south-western part of the study area (figure 4.20).

c) Bajocian Sediments (Lower Upper Hamenlei-Baidoa Member)

The Baidoa formation base boundary can be recognized by a series of continuous, high-amplitude parallel reflectors which are easily traceable across the seismic sections. In addition, the sequence includes the Lower Baidoa member consisting of evaporites and disconformable dolomites near the uppermost of the section. This creates laterally continuous, high to moderate amplitude reflectors. They overlie Lower Toarcian sediments. They appear to be thicker than the over and underlying sediments. According to the inferred seismic attributes, these rocks are likely exposed on the basin's southern and south-eastern portion (figures 4.24 and 4.25).

d) Lower Callovian – Bathonian Sediments (Mid Upper Hamenlei- Goloda Member)

This sequence overlie the Bajocian Sediments, may be responsible for hydrocarbon accumulation in the Middle Jurassic sediments. These sediment sequences narrow out as they approach the basin's flexural edges (Figures 4.10, 4.12, 4.26, 4.28) depict the possibility of the distribution of these sediments especially on the basin's northern and north-eastern edges.

e) Oxfordian – Callovian Sediments (Upper Hamenlei=Anole Formation)

The top of this sequence is exposed due to the uplift that affected some of the structures located in the deformed Garbaharey belt. The basal surface, on the other hand, is a traceable high-amplitude, medium-continuity reflector that spans the majority of the research region. The thickness of the sequence gradually increases as it approaches the basinal Hol region.

f) Oxfordian Sediments (Upper Hamenlei-? Lower Uegit Formation)

These sediments were not interpreted on all seismic lines, they seen to thicken towards the Hol basinl area, where they create two depocenters at the NE of the survey area (Figure 4.32). These might be the SW continuation of the Bodle Deep further developed in the Ogaden basin of Ethiopia (Hunegnaw et al., 1998).

Precambrian basement rocks

The interpretion of the seismic profiles demonstrated that the basement rocks are located much deeper probably at a depths corresponding to 8 km, under the thick Karoo deposits. And have larger thicknesses in the Lugh-Mandera basin (LMB) compared to the Ogaden basin.

4.4. Structural Analysis

This chapter includes the results of the seismostratigraphic and structural geology interpretations of fourteen (14) 2D seismic profiles (Figure 4.2). Fault and horizon interpretations were done independently for each seismic profile. The results demonstrated a relatively complex structure of the Somalian sector of the Lugh-Mandera basin. The interpretations resulted in the generation of a series of supporting subsurface base formation and thicknesses (isochore and isopach) maps, all of which provided crucial information in understanding the Mesozoic geological history and structure of the studied sedimentary basin.

4.4.1. Interpreted Seismic Profiles

Profile S04B05-P5-SnR

Figure 4.3: Uninterpreted Seismic Profile SO4B05_P5_Snr (a), Interpreted faults and horizons (b), and the side picture show the location of the seismic line (c).

Figure 4.3 trends the uninterpreted, interpreted, and location map. The line SO4B05_P5 SnR runs parallel to the basin's axis and advances in a NE-SW orientation; it also shows the principle structures and lithologies of the Hol-1 well location and the surrounding area.

The interpreted seismic profile is complicated by a number of splaying almost vertically faults that merge into single vertical faults at depths corresponding to 6000 ms (Figure 4.3b). These structures are products of wrench fault tectonics, and are associated with transpressional right strike slip movement within the study area. There is another visible horizon at a depth around 4000 ms which may represent the basement.

The stratigraphy of the area is dominated by carbonates, such as interbedded mudstones, dolomite, and evaporites. All seismostratigraphic sequence corresponding to the Adigrat-Lower Hamenlei Formation, Uanei Member, Baidoa Member, Goloda Member, Anole, and Uegit Formations were mapped here. The thickness of these formations remains horizontal through out.

Profile SO4B05_P4 SnR

Figure 4.4: Uninterpreted Seismic Profile SO4B05_P4_SnR (a), interpreted faults and horizons (b), and the side picture shows the location of the seismic line (c).

Figure 4.4 trends in a NE-SW direction, which is parallel to the axis of the Lugh-Mandera basin. The seismic profile is cut by a number of positive flower structures. The layering of most mapped formations remains-horizental.

On the middle of the profile, a mild anticlinal structure is also observable. The Jurassic sediments are generally horizontal, which consist carbonates of Iscia-Baidoa formation, followed by shales and marls of Anole formation. The main stratigraphic sequences that were found on the seismic profile are the Adigrat-Lower Hamenlei formation, (Uanei, Baidoa, and Goloda) members, which equivalent to Iscia-Baidoa formation.

Profile SO4B05_P3_SnR

Figure 4.5: Uninterrupted Seismic Profile SO4B05_P3_SnR (a), interpreted faults and horizons (b), and the side picture shows the locations of the seismic line (c).

Figure 4.5 shows the structure and stratigraphy of this section. This profile S04B05-P3 SnR trends to NE-SW direction, which is parallel to the axis of Lugh-Mandera basin, the seismic profile has a lesser concentration of flower structures compared to the previous profiles. The seismo-stratigraphic sequences thin out towards the SW direction of the basin. The main stratigraphic formations that were traced easily through the seismic profile are Adigrat-Lower Hamenlei formation, Uanei, Baidoa, Goloda Members.

Profile S04B05-P2 SnR

Figure 4.6: Uninterpreted Seismic Profiles SO4B05_P2_SnR (a), interpreted faults and horizons (b), and the side picture shows the locations of the seismic line (c).

Figure 4.6 shows that this profile trends in the NE-SSW direction, which is parallel to the Lugh-Mandera depression's axis.the seismic profile is cut by a few flower structures the mapped seismostratigraphic sequences continue to wedge out towards to the SW direction (part) of the LMB. The Jurassic phases produced the observed mild anticlinal structure on the seismic section's northern side. Only two seismo-stratigraphic sequences were found on the seismic profile which represent by the Adigrat-Lower Hamenlei Formation and Uanei Member.

Profiles SO4B05_P1_SnR

Figure 4.7: Uninterpeted Seismic Profiles SO4B05_P1_SnR (a), interpreted faults and horizons (b), and the side picture show the locations of the seismic line (c).

Figure 4.7 demonstrates the extent of the seismic profile S04B05_P1_SnR which has a longitudinal (N-S trend) that is oblique to the trend of the LMB. It is cut by a few flower structures whose splaying faults at a deeper level compared to some previous seismic profiles only two seismo-stratigraphic sequences were mapped here belonging to Adigrat-Lower Hamenlei formation and Uanei Member which is equivalent to Iscia-Baidoa carbonates (interbedded mudstones, dolomite, and oolitic limestone's). As seen from the interpretation both boundaries of the formations are subhorizental, and generally preserve the thickness.

Profile S04B25-P1SnR

Figure 4.8: Uninterpreted Seismic Profile SO4B25_P1_SnR (a), interpreted faults and horizons (b), and the side picture shows the locations of the seismic line (c).

Figure 4.8 trends the uninterpreted, interpreted, and location map. The 2D seismic profile S04B25_P1_SnR that has a latitudinal (E-W) trend which is oblique to the general axis of the LMB. Here two flower structures were encountered. Only two seismo-stratigraphic sequences corresponding to Adigrat-Lower Hamenlei formation and Uanei Member were mapped here. Apparentely, the thicknesses of these formations are slightly reduced towards the western part of the profile, all suggesting the presence of some structural high in this part of the survey area.

This profile is cut only by the splaying faults that converge into one stem at a much deeper level.
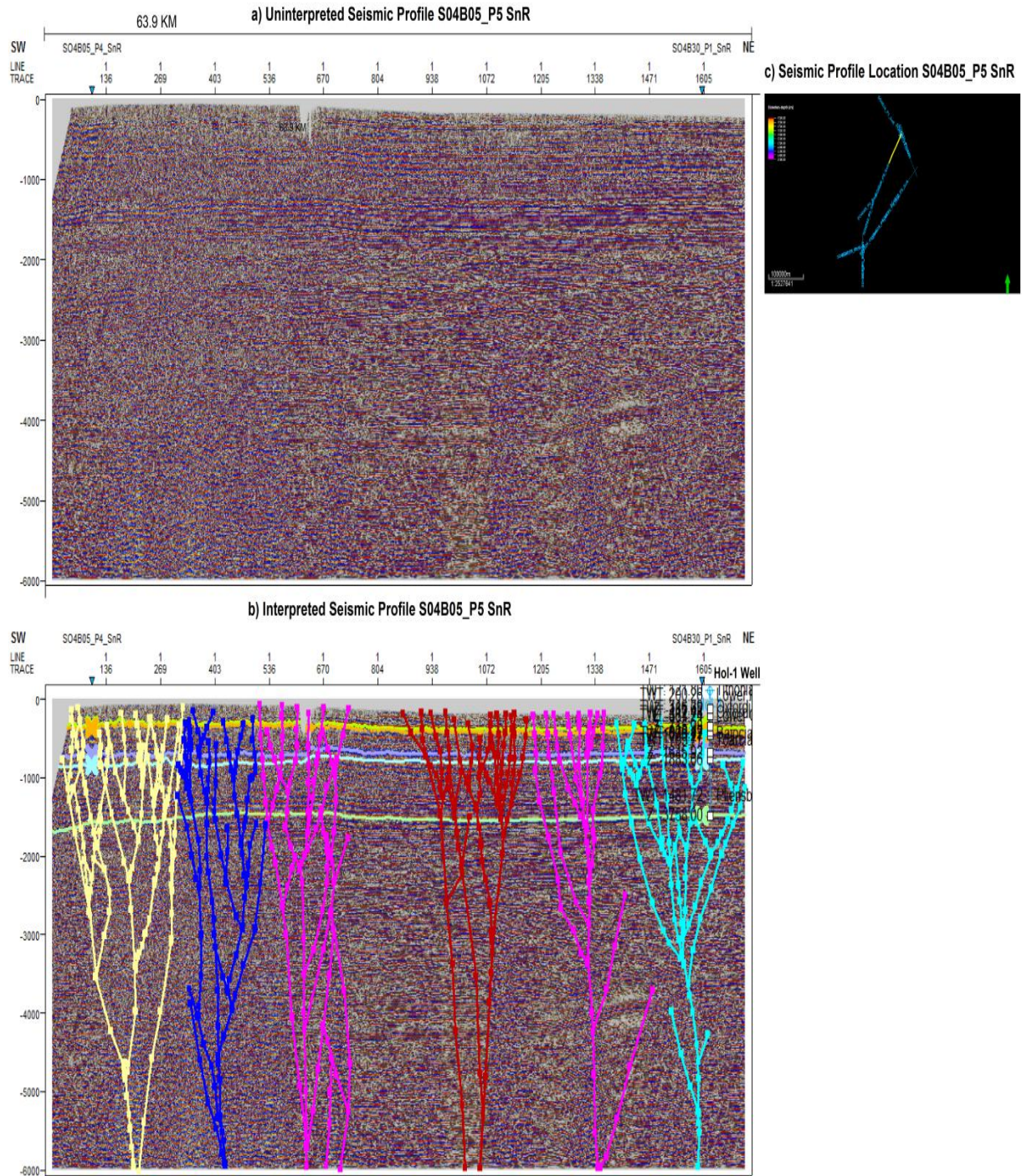
Profile SO4B25_P2_SnR

Figure 4.9: Uninterpreted Seismic Profile SO4B25_P2_SnR (a), interpreted faults and horizons (b), and the side picture shows the locations of the seismic line (c).

Figure 4.9 presents uninterpreted, interpreted, and the location map. The interpreted seismic section of profile S04B25-P2 which runs NE SW direction which is parallel to the basin axis .

The interpreted seismic profile is complicated by a number of splaying almost vertically faults that merge into a single vertical faults at depths corresponding to 6000 ms (Figure 4.12b).

Only two seismostatigraphic boundaries were mapped throughout the profile corresponding to Adigrat-Lower Hamenlei formation, Uanei Member. These formations have constant thicknesses and are subhorizental.

A minor deformation is seen near line trace 270 (Figure 4.12b)
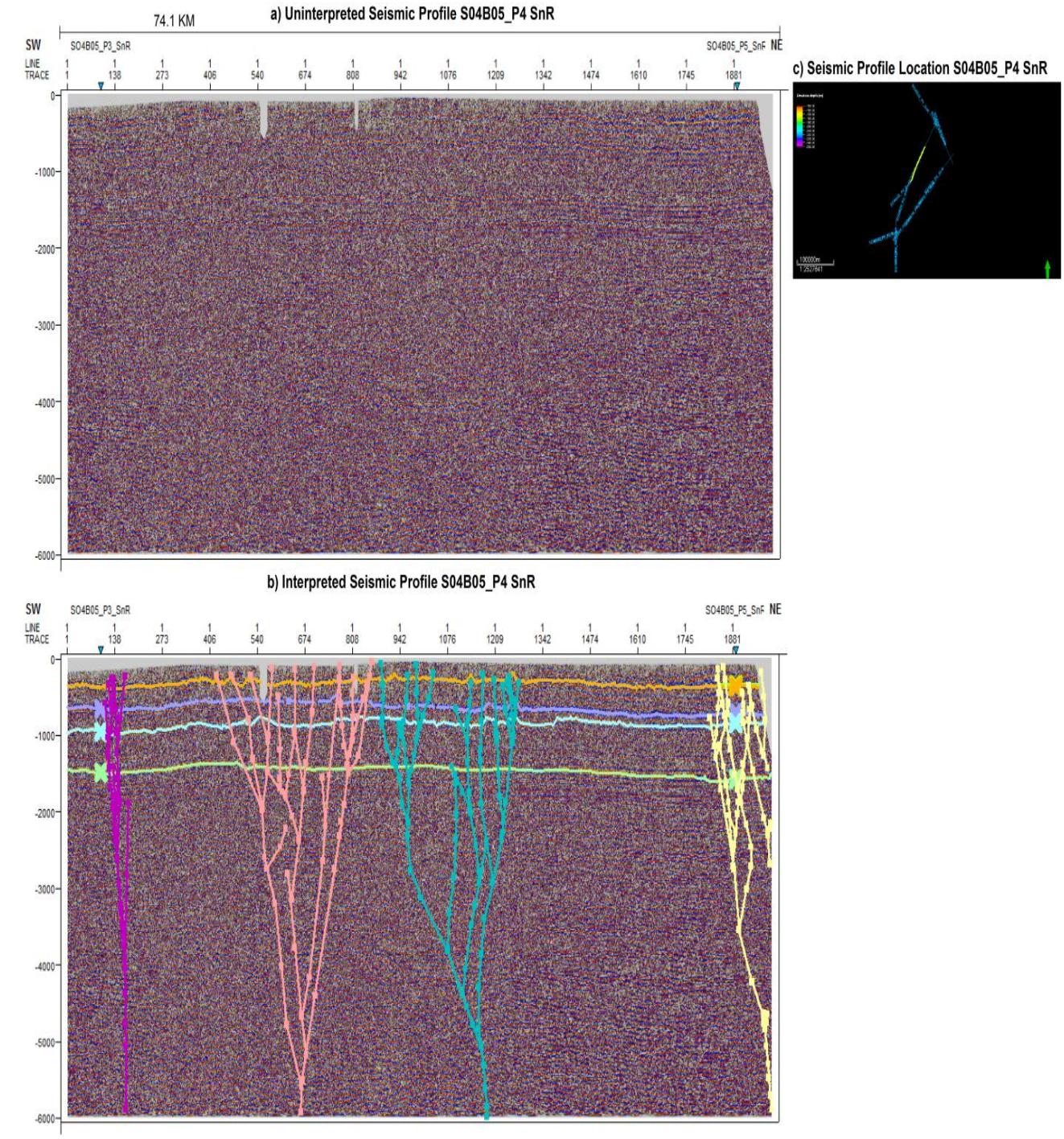
Profile SO4B25_P3_SnR

Figure 4.10: Uninterpeted Seismic Profile SO4B25_P3_SnR (a), interpreted faults and horizons (b), and the side picture show the locations of the seismic line (c).

Figure 4.10 illustrate the uninterpreted, interpreted, and the map location. The seismic profile S04B25_P3 SnR has a NE-SW trend parallel to the axis of LMB.

Compared to the previous interpreted profiles, this one is cut (intersected) by an increased amount of flower structures. The mapped seismostratigraphic sequences are presented by Adigrat-Lower Hamenlei Formation and Uanei Member who generally preserve their thicknesses with a slight reducing trend towards the SW part of the sedimentary basin. The formations are also sub horizontal.

A mild broad anticlinal fold has been mapped on the SW corner of the survey area (Figure 4.10b).
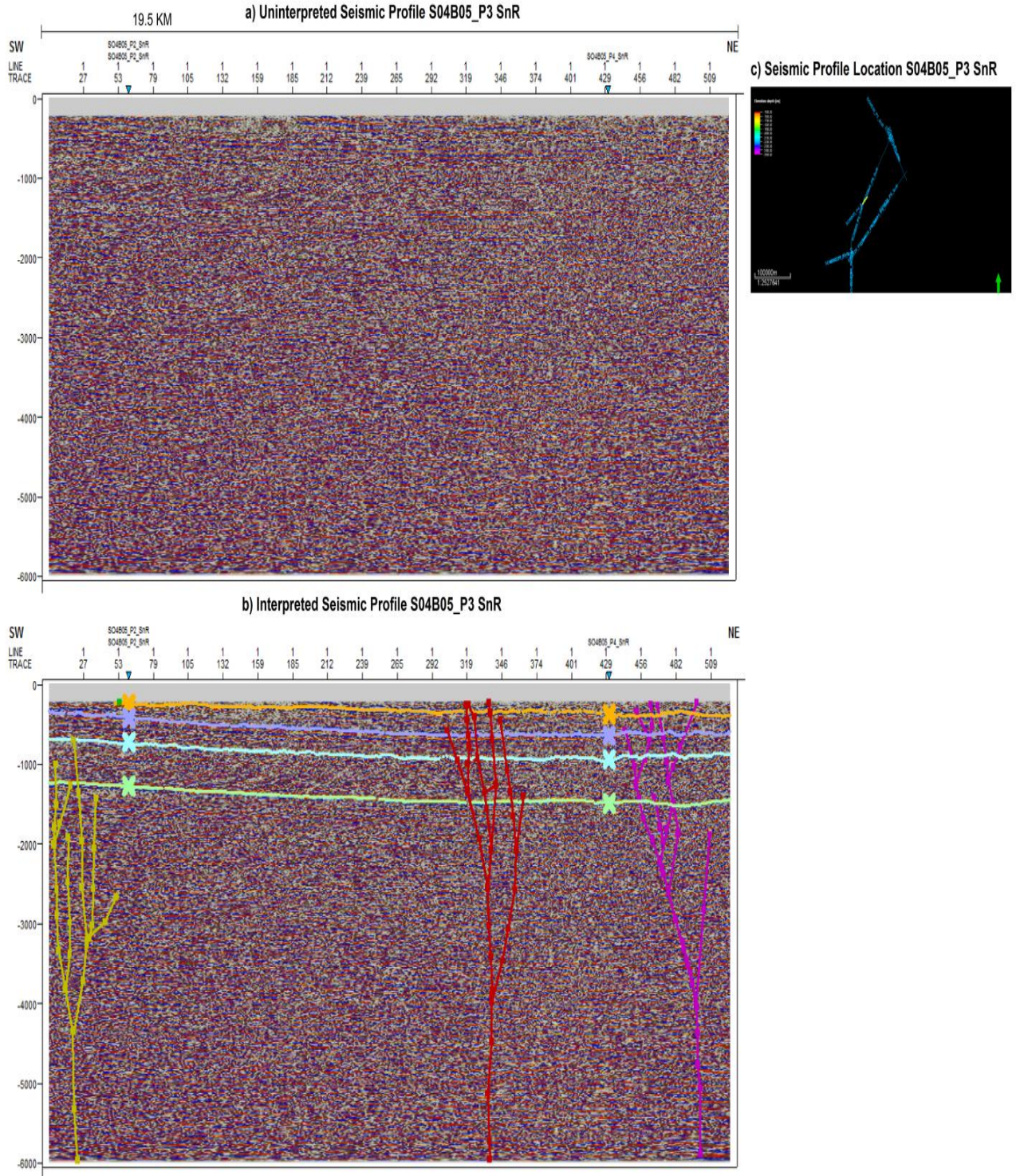
Profile SO4B25_P4_SnR

Figure 4.11: Uninterpreted Seismic Profile SO4B25_P4_SnR (a), interpreted faults and horizons (b), and the side picture show the locations of the seismic line (c).

Figure 4.11 presents the uninterpreted, interpreted, and the location map. It also shows the structure and stratigraphy of this section (Figure 4.11b). This profile S04B05-P4 SnR trends (NE-SW), which is parallel to the axis of Lugh-Mandera basin (Figure 4.11c). Just as the previous profile the concentration of flower structures seems to increase towards the NE part of the survey area.

Two (2) seismostratigraphic sequence base boundaries of the Adigrat-Lower Hamenlei Formation and Uanei Member were mapped in this profile with all preserving their thicknesses and having a subhorizental layering. The splaying faults merge at a deeper level (Figure 4.11b).
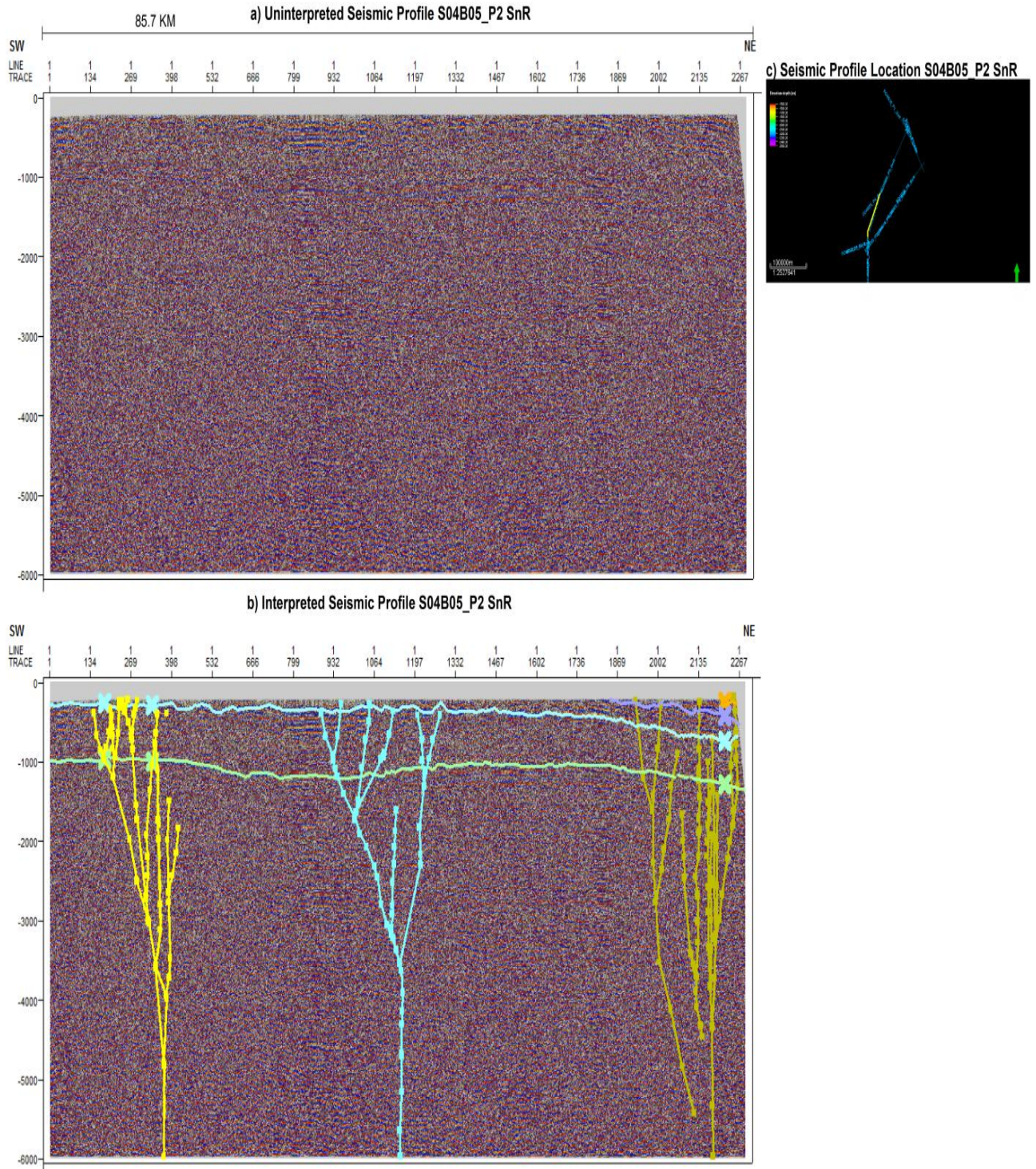
Profile SO4B25_P5_SnR
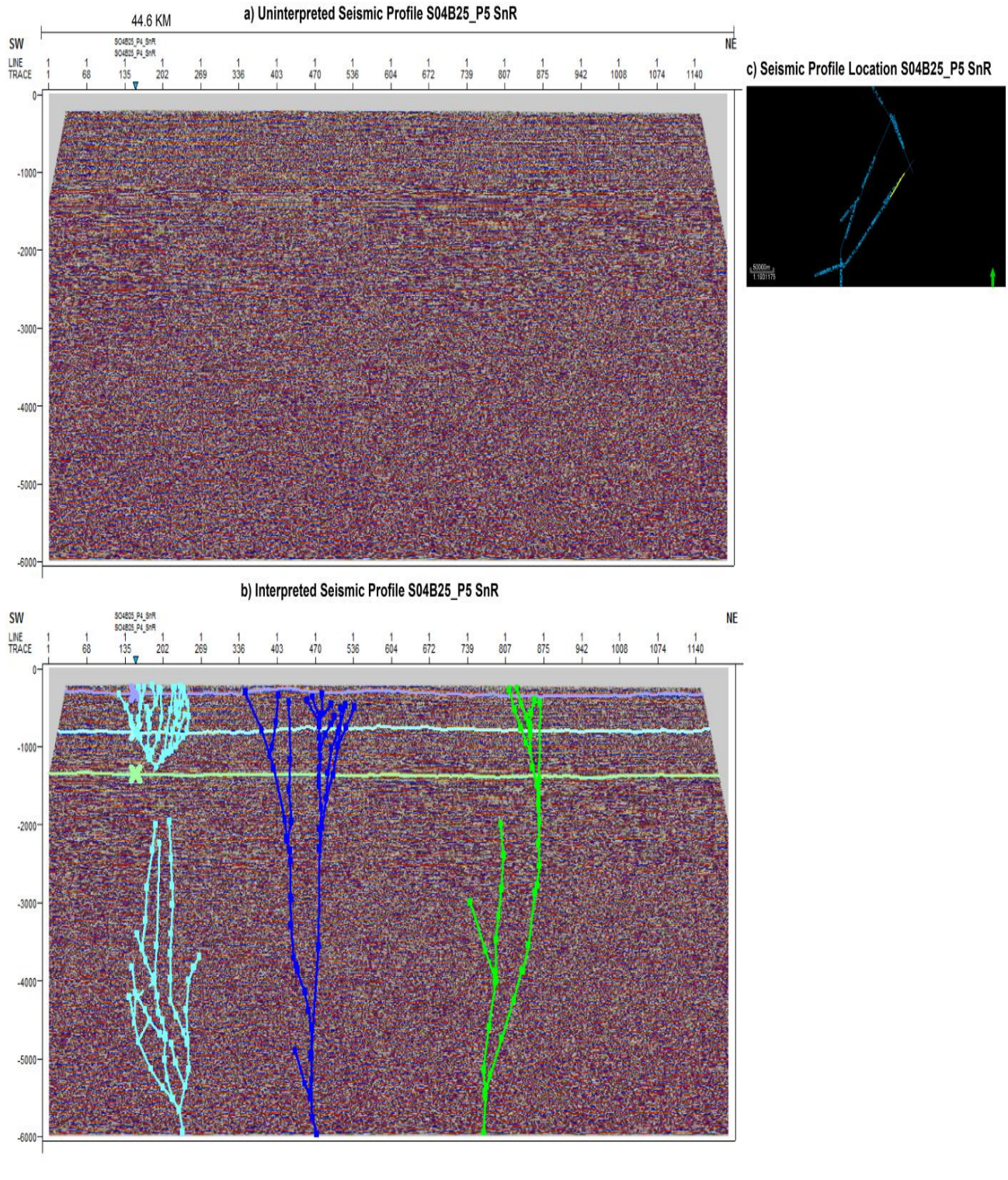
Figure 4.12: Uninterpreted Seismic Profile SO4B25_P5_SnR (a), interpreted faults and horizons (b), and the side picture show the locations of the seismic line (c).

Figure 4.12 demonstrates the uninterpreted, interpreted, and the location map. The seismic profile S04B25-P5 which runs (NE-SW) parallel to the axis of the Lugh-Mandera basin (Figure 4.12c).

The seismic profile is characterized by a lesser concentration of mapped flower structures, but an increased amount of seismostratigraphic sequences base surfaces of Adigrat-Lower Hamenlei formation, Uanei and Baidoa Members (Figure 4.12b).

The mapped seismostratigraphic sequences have constant thicknesses throughout the profile. Splaying faults of the flower structures merge into a singular vertical fault approximately at 6000 ms (Figure 4.12b).
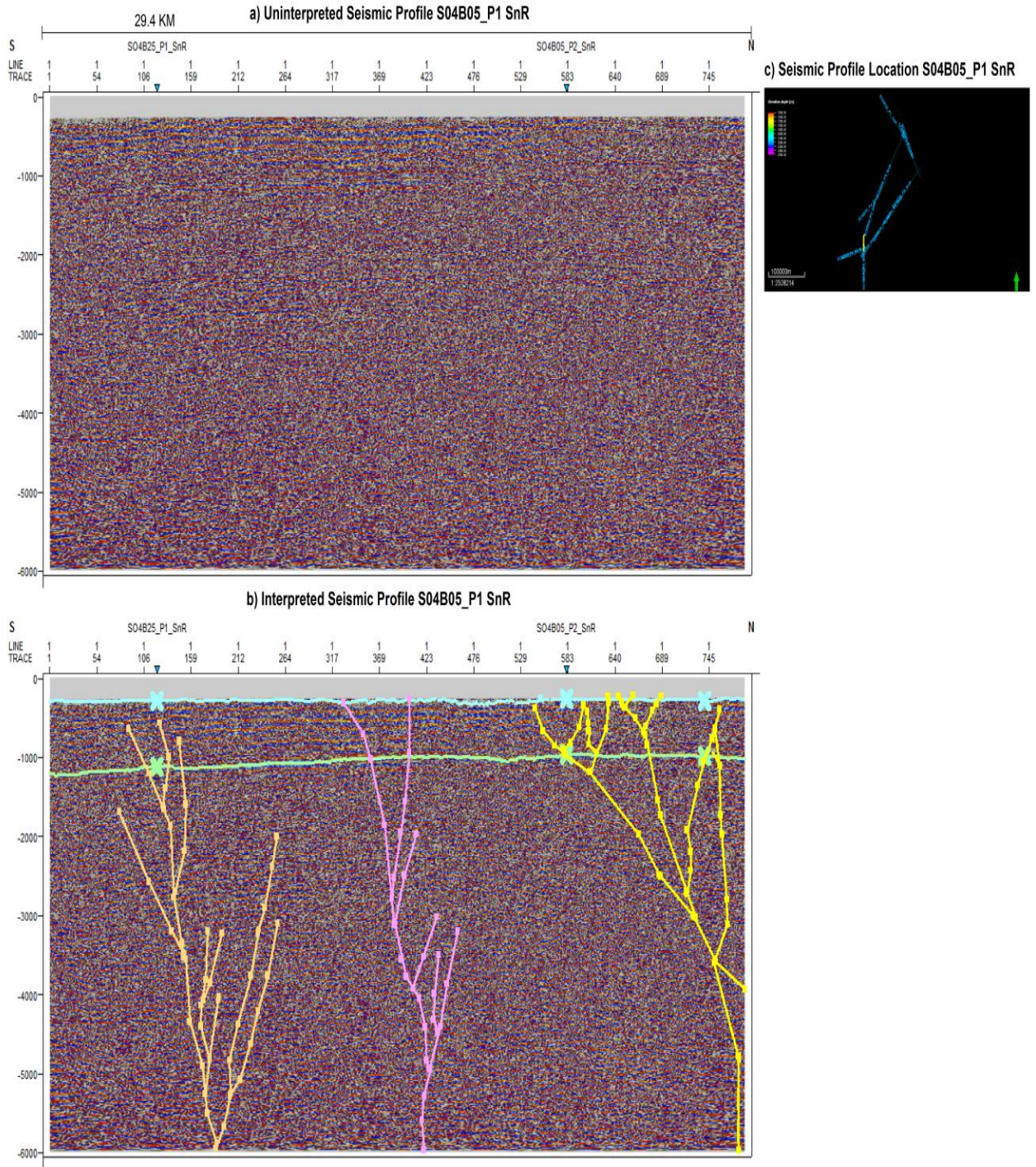
Profiles SO4B25_P6_SnR
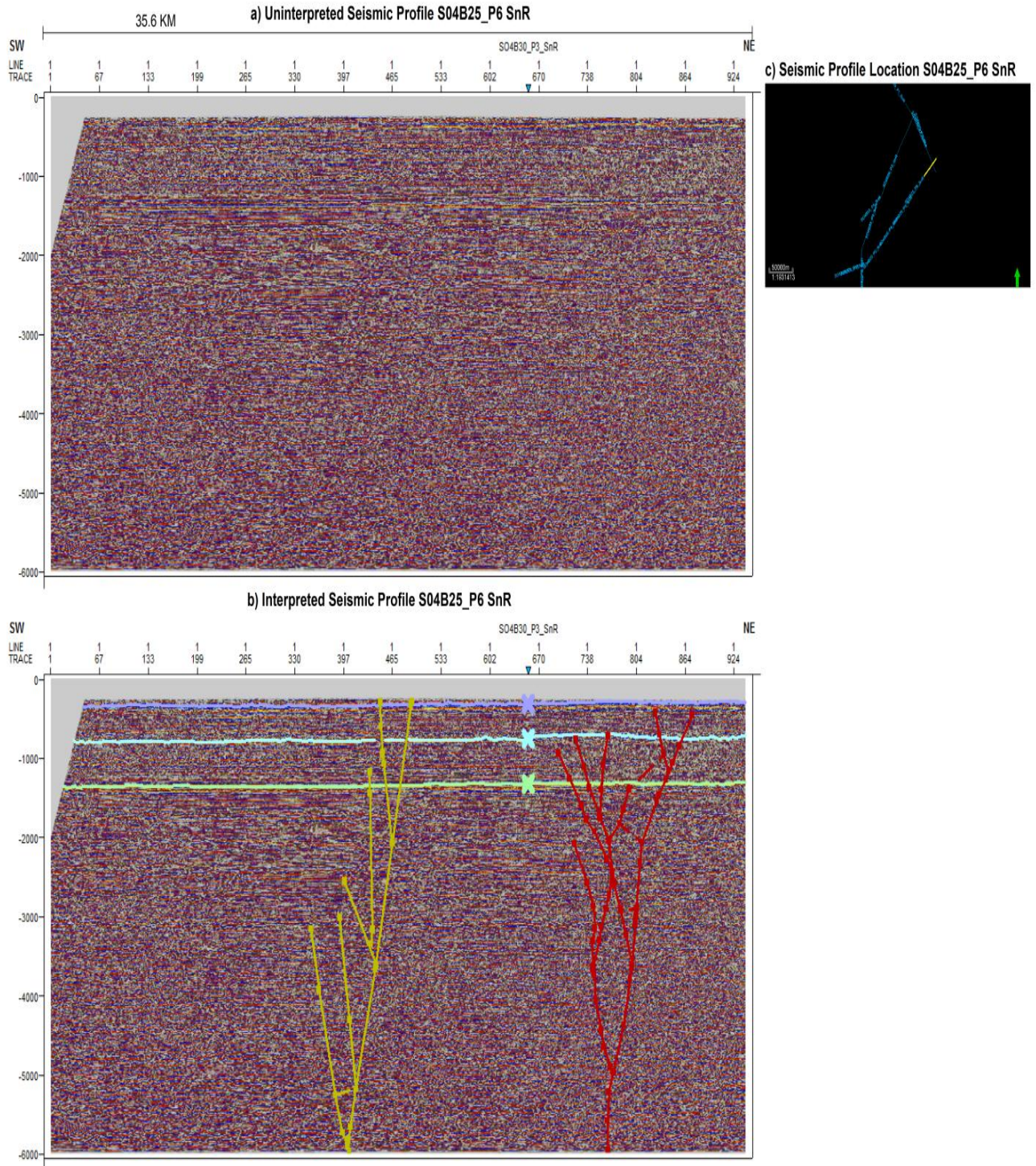
Figure 4.13: Uninterpreted Seismic Profiles SO4B25_P6_SnR (a), interpreted faults and horizons (b), and the side picture show the locations of the seismic line (c).

Figure 4.13 presents the uninterpreted, interpreted, and the location map. It also shows the principle structure and the lithology of the section. The interpreted seismic sections of profile SO4B25_P6_Snr that has a (NE-SW) trend parallel to the axis of Lugh-Mandera basin (LMB).

The seismic profile is cut by two splying flower structures (Figure 4.13b) that merge at a depths corresponding to 5000 to 6000 ms.

Three (3) seismostratigraphic sequences have been mapped along this profile corresponding to Adigrat-Lower Hamenlei Formation, Uanei and Baidoa Members (Figure 4.13b). All mapped formations, shows constant thicknesses along the profile, subparallel and subhorizental.
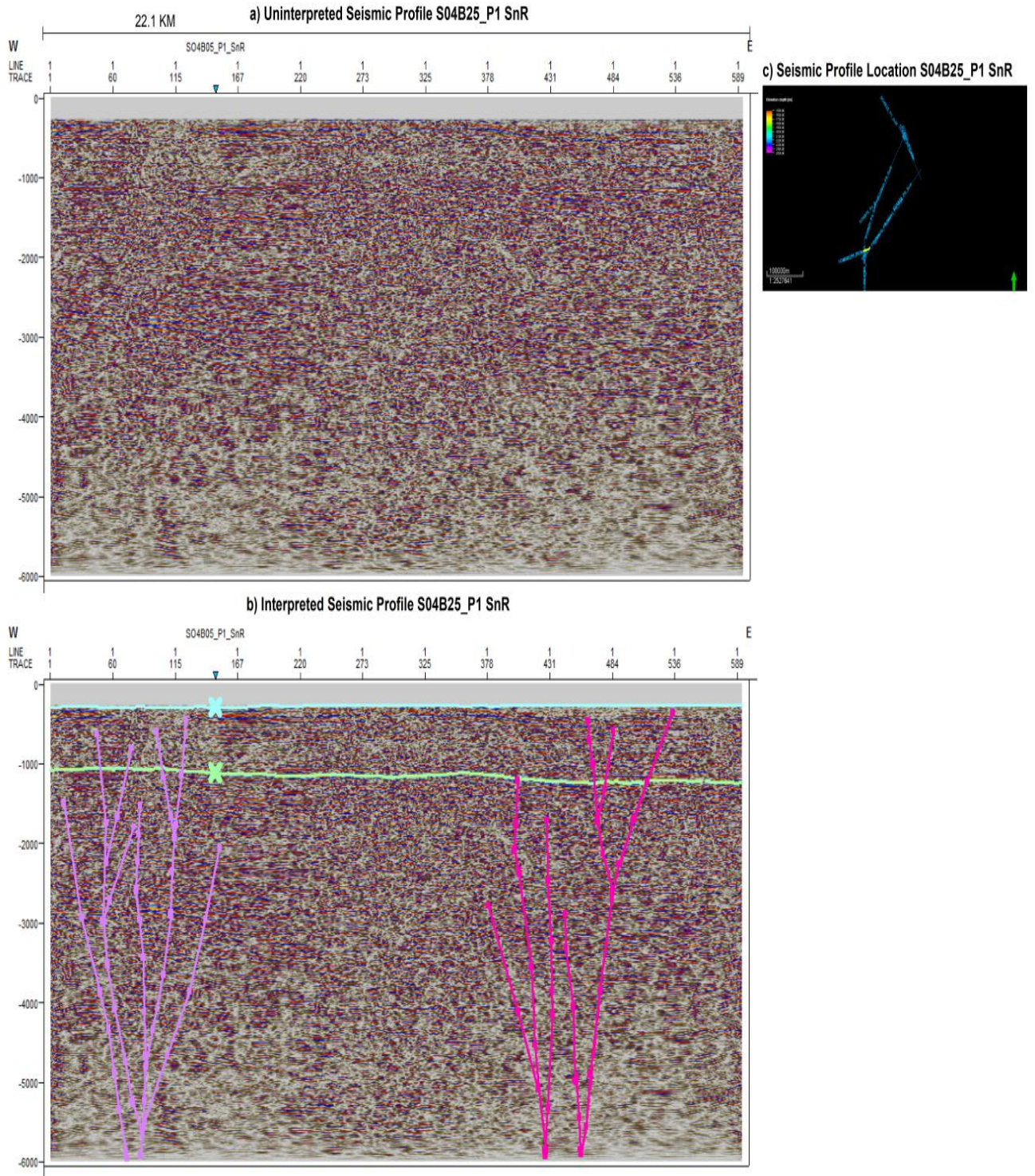
Profiles SO4B30_P3_SnR
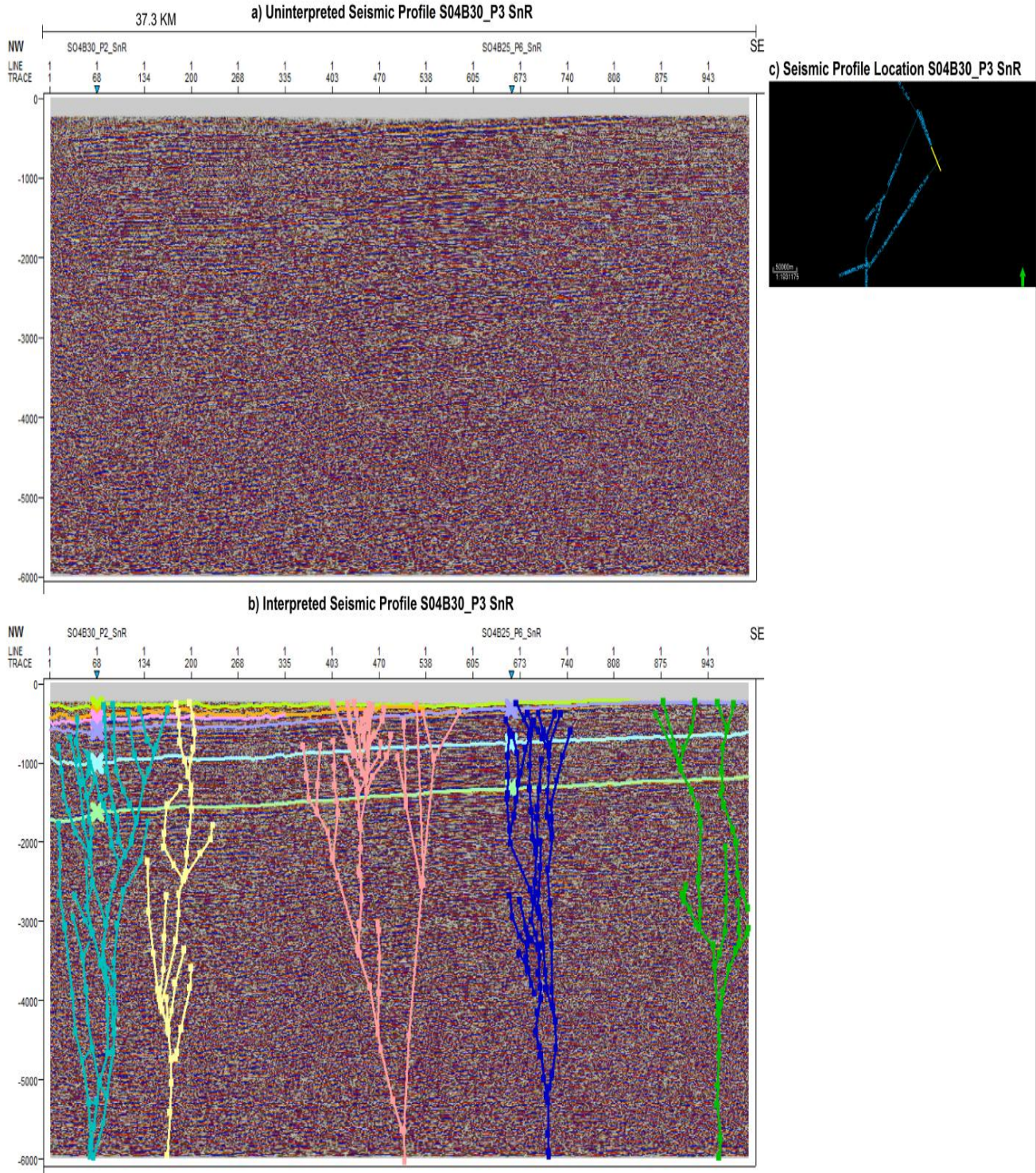
Figure 4.14: Uninterpreted Seismic Profiles SO4B30_P3_SnR (a), interpreted faults and horizons (b), and the side picture show the locations of the seismic line (c).

Figure 4.14 presents uninterpreted, interpreted, and the location map. This line S04B30-P3 runs (NW-SE), which is almost perpendicular to the axis of the Lugh-Mandera basin (Figure 4.14c).

The seismic is complicated by an increased number of almost vertical splaying flower structures (Figure 4.14b) most of which merge to single vertical faults at depths corresponding to 5000- 6000 ms (Figure 4.14b).

Five (5) seismostratigraphic sequences were mapped along the interpreted seismic section. These corresponds to Adigrat-Lower Hamenlei formation, Uanei Member, Baidoa Member, Goloda Member, Anole and Uegit formations that seem to have a shallow dip towards the NW (Figure 4.14b). All formations are subhorizental, subparallel, and wedge out to the SE.
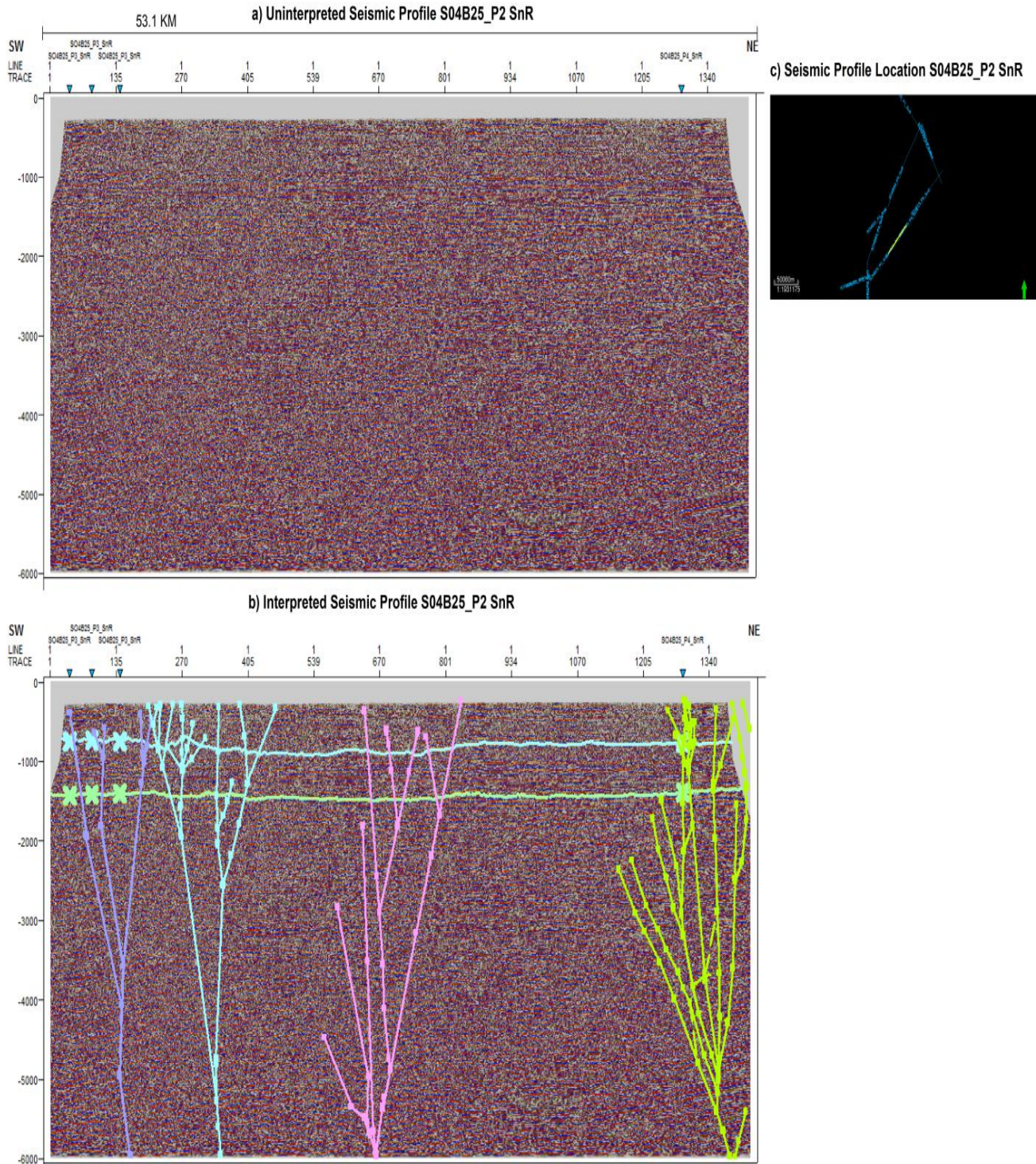
Profiles SO4B30_P2_SnR
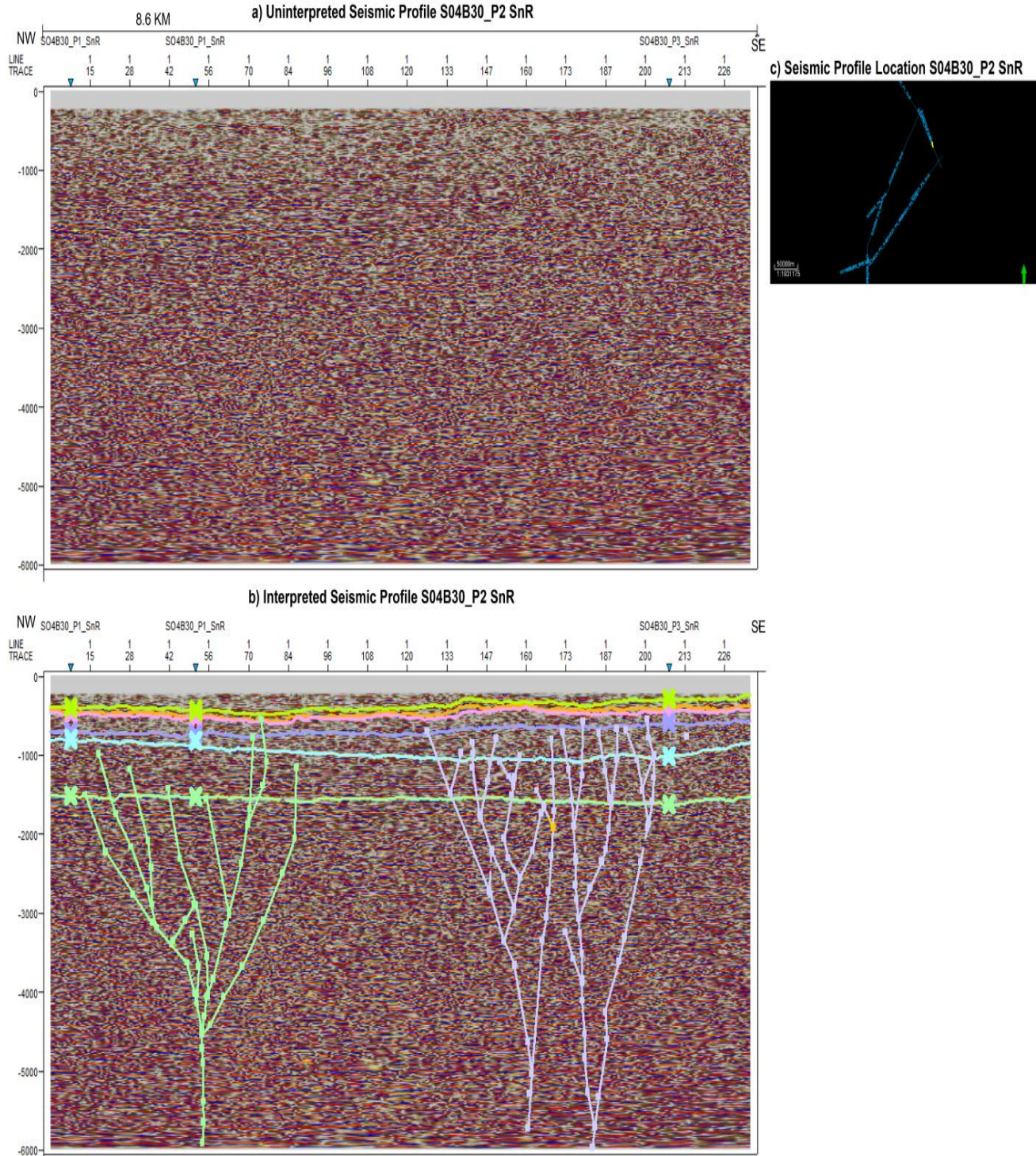
Figure 4.15: Uninterpeted Seismic Profiles SO4B30_P2_SnR (a), interpreted faults and horizons (b), and the side picture shows the locations of the seismic line (c).

Figure 4.15 demostrates uninterpreted, interpreted, and the location map. The interpreted seismic section for profile S04B30-P2 which runs NW-SE direction almost perpendicular to the Lugh-Mandera basin (LMB) axis.

The seismic profile is complicated by two splying flower structures (Figure 4.15b) that merge at depth levels of 5000 to 6000 ms. Mild deformations are associated with these structures.

Five (5) seismostratigraphic sequences have been mapped along this profile. They correspond to Adigrat-Lower Hamenlei formation, Uanei Member, Baidoa Member, Goloda Member, Anole and Uegit formations, which are subparallel and subhorizental.
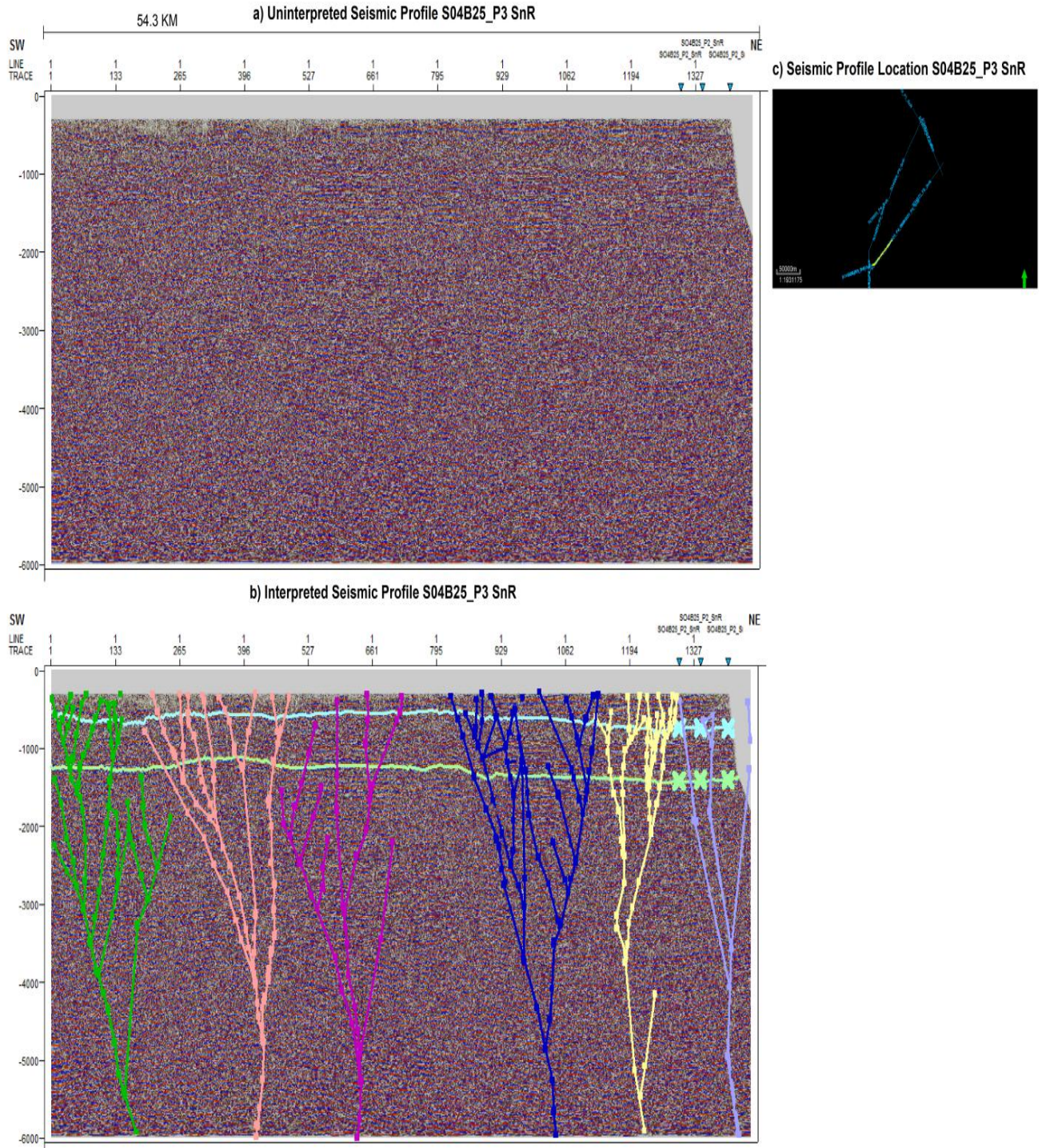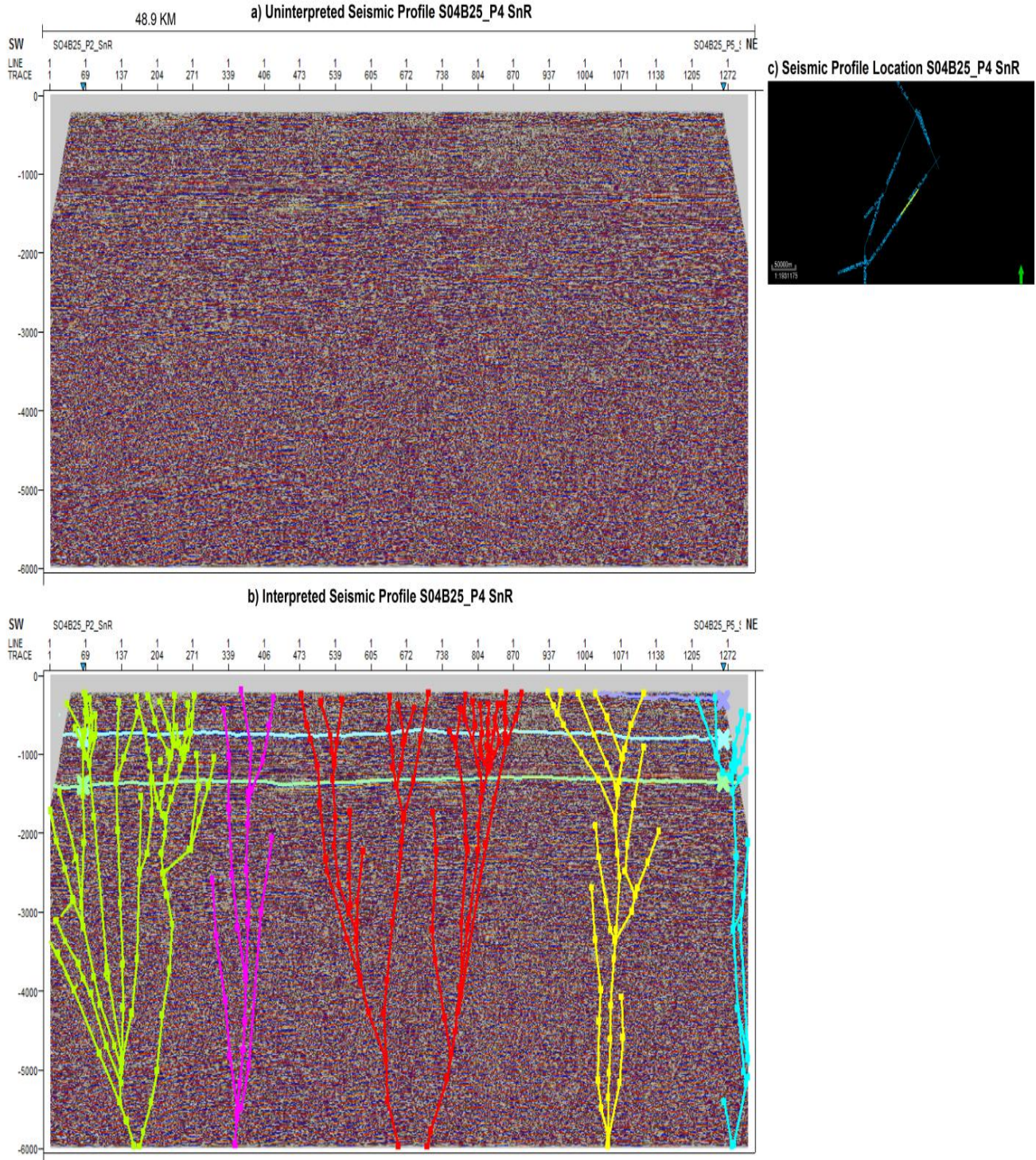
Profiles SO4B30_P1_SnR
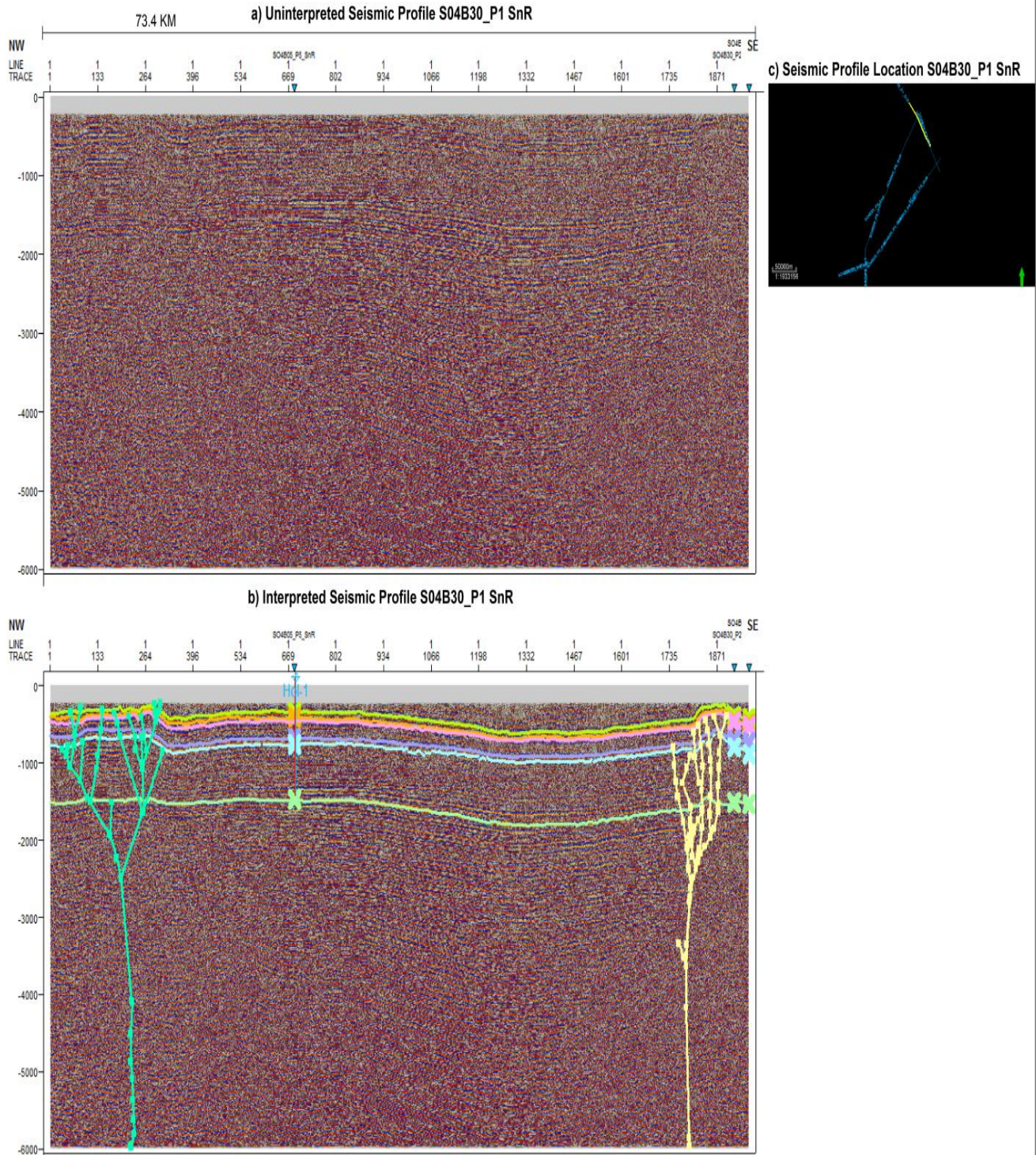
Figure 4.16: Uninterpreted Seismic Profiles SO4B30_P1_SnR (a), interpreted faults and horizons (b), and the side picture show the locations of the seismic line (c).

Fig 4.16 illustrates uninterpreted, interpreted, and the location map. The interpreted seismic section of profile SO4B30_P1_SnR which runs NW-SE direction that is oblique almost perpendicular to the LMB axis (Figure 4.16c).

The seismic line is cut by two positive flower structures developed at both ends of the profile (Figure 4.16b). These two structures represent to Sengif and Garbaharey fold belts mapped at the surface (Beltrandi & Pyre, 1975; Abbate et al., 1993).

At the subsurface these two belts have visible deformations associated with folding approximately to a depth corresponding to 2000 ms (Figure 4.16b).

A total of six (6) seismostratigraphic sequences were mapped and correlated with the log data from Hol-1 well. As mentioned above deformations occur on both ends of the seismic profile while the central portion is occupied by a gentle syncline. this probably corresponds to the Tomalo Syncline mapped at the surface (Beltrandi et Pyre, 1975; Figure 2.8).

This structure is a symmetrical with increasing dip values and axis located near the Garbaharey fold belt (Figure 4.16b) where some increasing thickness can also be observed.

4.4.2. Subsurface Geological Mapping

Subsurface geological maps rely on data supported by well logs and 2D-3D seismic survey data. They are important as they provide geologists with crucial information about the attitudes and distribution of the deep geological formations and structures, and help map potential areas with hydrocarbon traps and reservoirs (leads, prospects, plays, etc.).

Here, we present the results of subsurface geological mapping with surfaces mapped and generated through the seismic interpretation of fourteen (14) 2D seismic profiles from the Somalian sector of the Lugh-Mandera basin (LMB).

We were able to construct six (6) subsurface maps that included (the following base boundaries):

a) Pliensbachian-Hettangian base surface map (top Adigrat/Lower Hamenlei Formations);
b) Toarcian base surface map (Upper Middle Hamenlei=Uanei Member);
c) Bajocian base surface map (Lower Upper Hamenlei=Baidoa Member);
d) Lower Callovian -Bathonian base surface map (mid Upper Hamenlei= Goloda Member);
e) Oxfordian-Callovian base surface map (Upper Hamenlei=Anole Formation);
f) Oxfordian base surface map (Upper Hamenlei =? Lower Uegit Formations).

Due to issues related with the well-tie and synthethic seismogram generation we were not able to map the top most Kimmeridgian (Uarandab Formation=Upper Uegit Formation) and Tithonian base (Garbaharey/Busul Formation boundaries). These complications are related to the well data uncertainties (elevation depth, reference to the drilling floor or rotary table, and seismic profile quality at shallow depths).

a) Pliensbachian-Hettangian base surface map (top Adigrat/Lower Hamenlei Formations)

The depth surface map of Top Adigrat/Lower Hamenlei Formations within the study area is demonstrated in Figure.4.17. The surface map of the top Pliensbachian-Hettangian interval within the Lugh-Mandera basin has (kitchen zone) located at the northeastern side of the study area. The average depth of top Pliensbachian-Hettangian within the survey is approximately 2000 m. According to the well completion report of Hol-1, this part of the section contains the basal clastics of Deleb Adigrat sandstones, shales and the carbonates associated with minor dolomites of the Iscia-Baidoa formations. According to a geochemical data report, the mature source rock is developed in the Lower part of the Formation. The major structural highs are those located in SW and SE areas and represent two distinctive reservoir zones (probably folded Deleb Adigrat sandstone formations) with good vertical closure at the southwestern side of survey area, and also, the minor one at east (Figure 4.17).
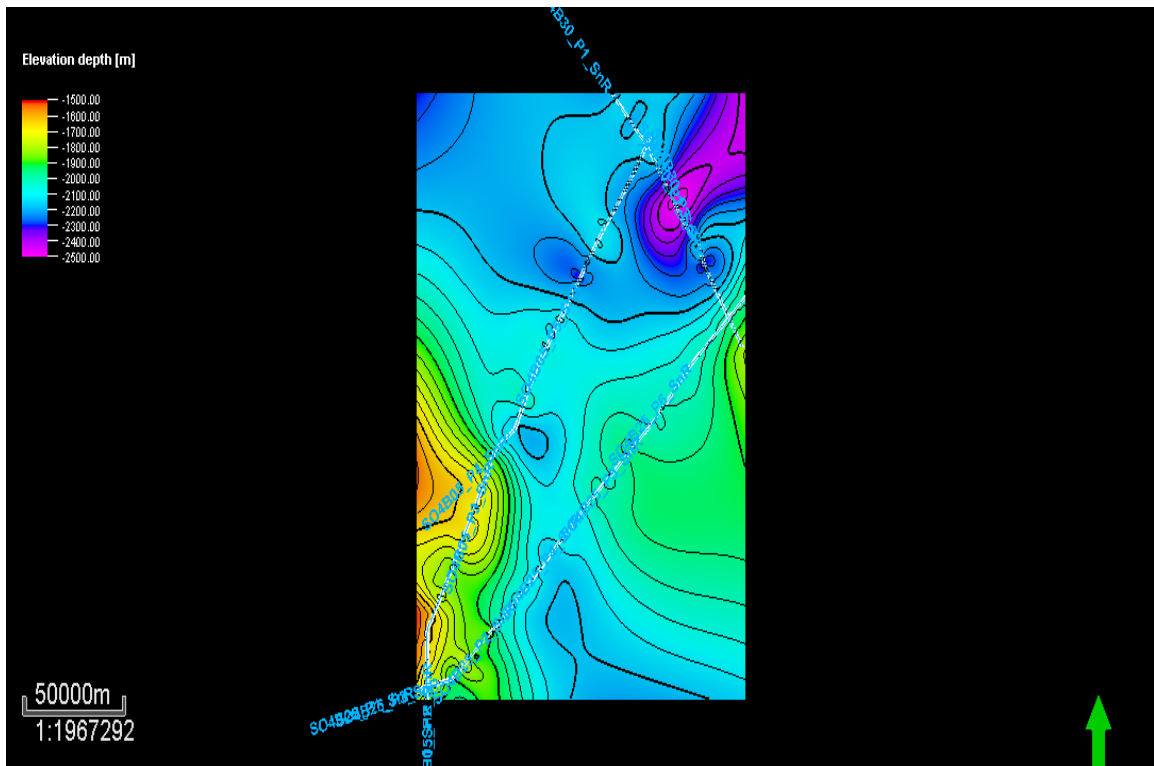
Figure 4.17: 2D view of the Pliensbachian-Hettangian base surface map (top Adigrat/Lower Hamenlei Formations).

Figures 4.18 and 4.19, presents a 3D view of the Pliensbachian-Hettangian base surface map including the poisoning of 2D seismic profiles and exploration wells from neighboring Ogaden basin.
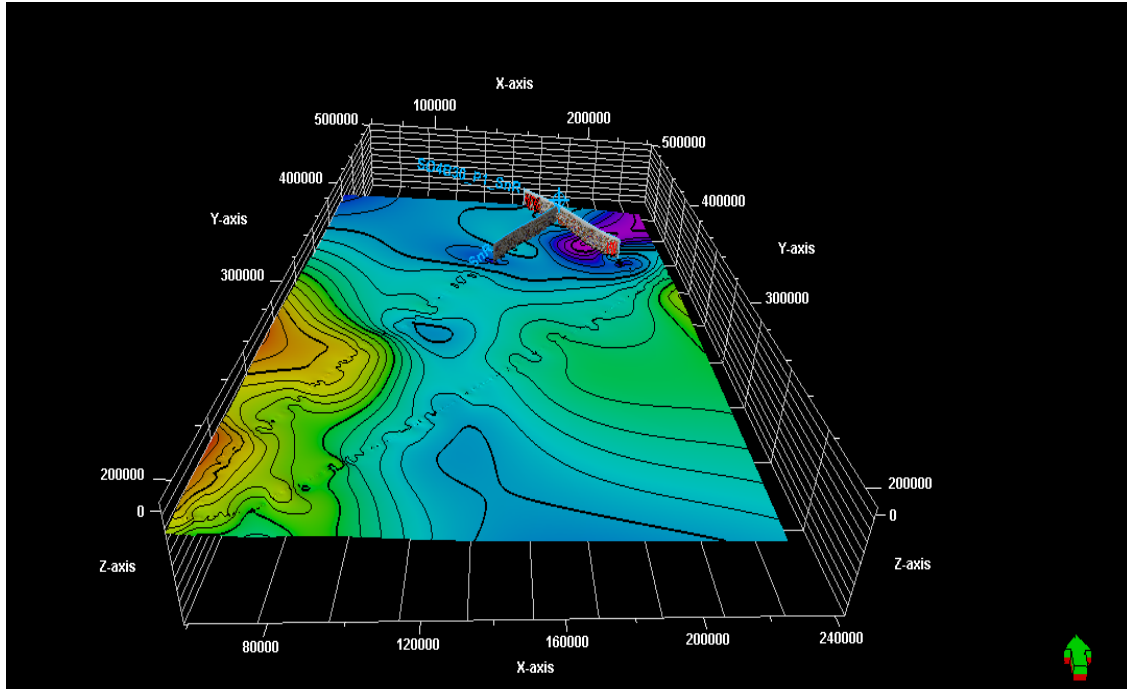
Figure 4.18: 3D view of the Pliensbachian-Hettangian base surface map (top Adigrat/Lower Hamenlei Formations).
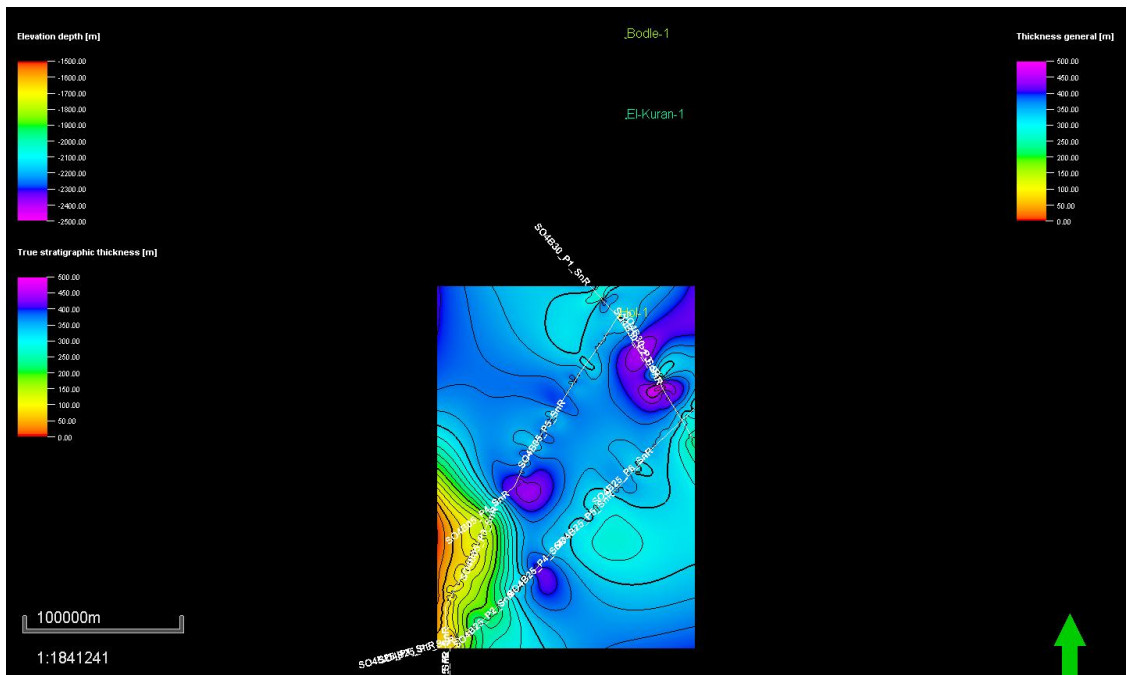
Figure 4.19: Pliensbachian-Hettangian base surface map (top Adigrat/Lower Hamenlei Formations) with seismic profiles and exploration wells from neighboring Ogaden basin.

b) Toarcian base surface map (Upper Middle Hamenlei=Uanei Member);

The depth contour map for the Upper Middle Hamenlei (Uanei Member) points out the presence of structural high at the southwest, as shown in (Figure 4.20). The Toarcian base surface map shows the presence of at least three kitchen zones, two of which are located in the northeastern side of the study area, and the others located at the central and the south areas. The depth contour surface of the Upper Middle Hamenlei Formation was created by connecting the positions of same depth. These depth rates were designated in a color line, which can be utilized to classify the difference in thickness Formations. On the color line, red indicates the uplifted area and purple-blue indicate the deepest sections (part). The structural high located in the SW has probably generated potential hydrocarbon traps to which the expelled oil and gas migrated to from the kitchen source rock zones (Figure 4.20).
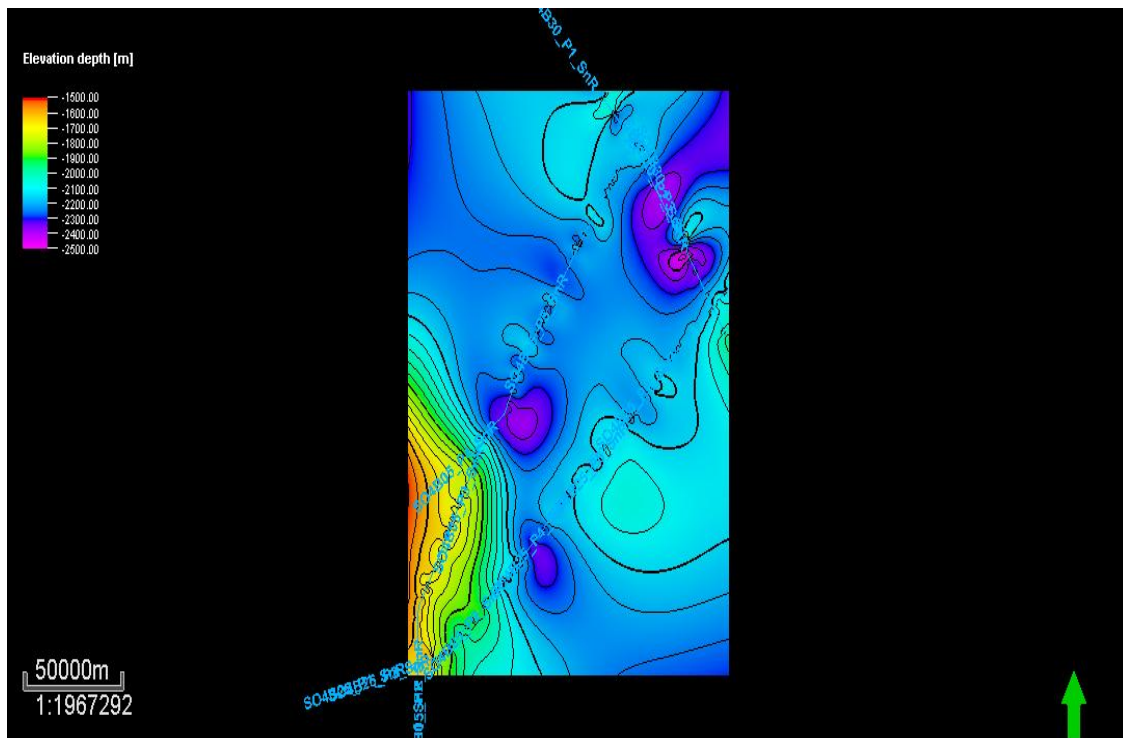
Figure 4.20: 2D view of the Toarcian base surface map (Upper Middle Hamenlei=Uanei Member).

Figures 4.21 and 4.22 provide a 3D view for the Toarcian base surface map and locations of the seismic profiles and exploration wells from neighboring Ogaden basin.
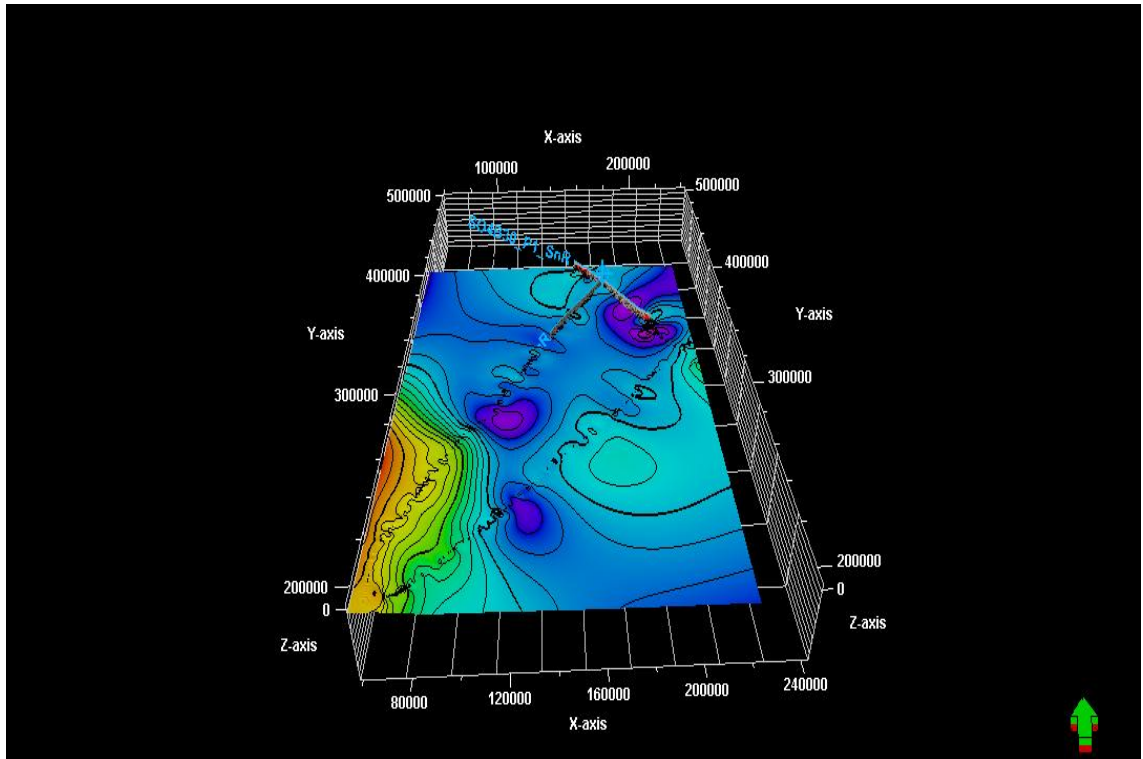
Figure 4.21: 3D view of the Toarcian base surface map (Upper Middle Hamenlei=Uanei Member).
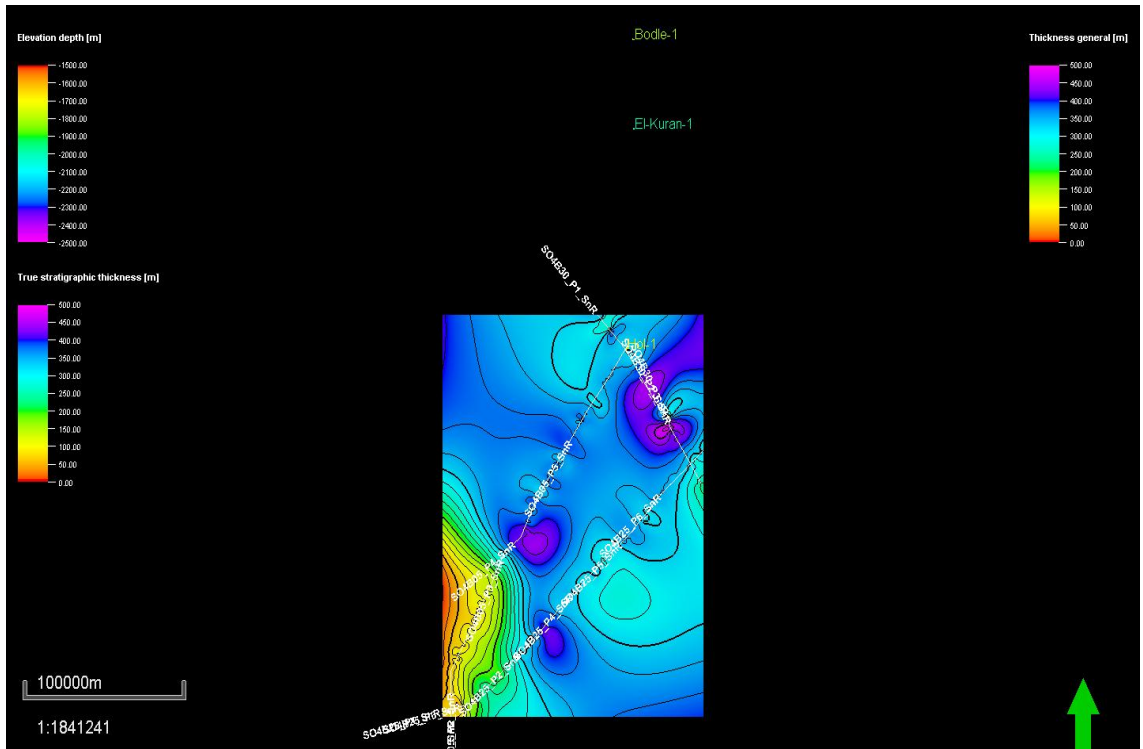
Figure 4.22: Toarcian base surface map (Upper Middle Hamenlei=Uanei Member) with seismic profiles and exploration wells from neighboring Ogaden basin.

c) Bajocian Base Surface Map (Lower Upper Hamenlei=Baidoa Member)

The surface map for the Bajocian (Figure 4.23) demonstrates that the depocenters and potential kitchen zones were developed at the north-east and west arches of the survey area. A structural high has been mapped at the SE corner of the study area. It is likely that the hydrocarbons can potentially be ontrapped in this structure.

The depth contour surface of the Lower-Upper Hamenlei formation was created by connecting the positions of same depth. These depth values were designated in a color line, which can be utilized to classify the difference in thickness formations. On the color line, red indicate the topmost area and purple-blue indicate the lowermost (Figure 4.23).
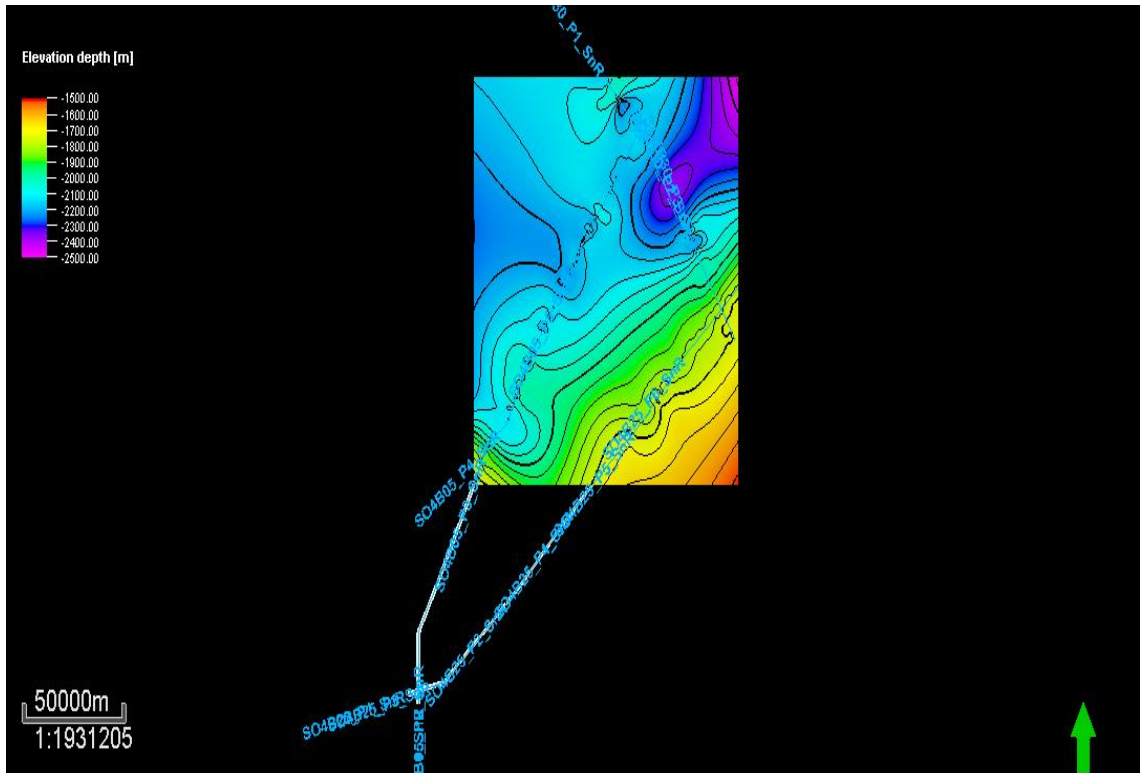
Figure 4.23: 2D view of the Bajocian base surface map (lower Upper Hamenlei=Baidoa Member).

Figures 4.24 and 4.25 provide a 3D view of the Bajocian base surface map and locations of the seismic profiles and exploration wells from neighboring Ogaden basin.
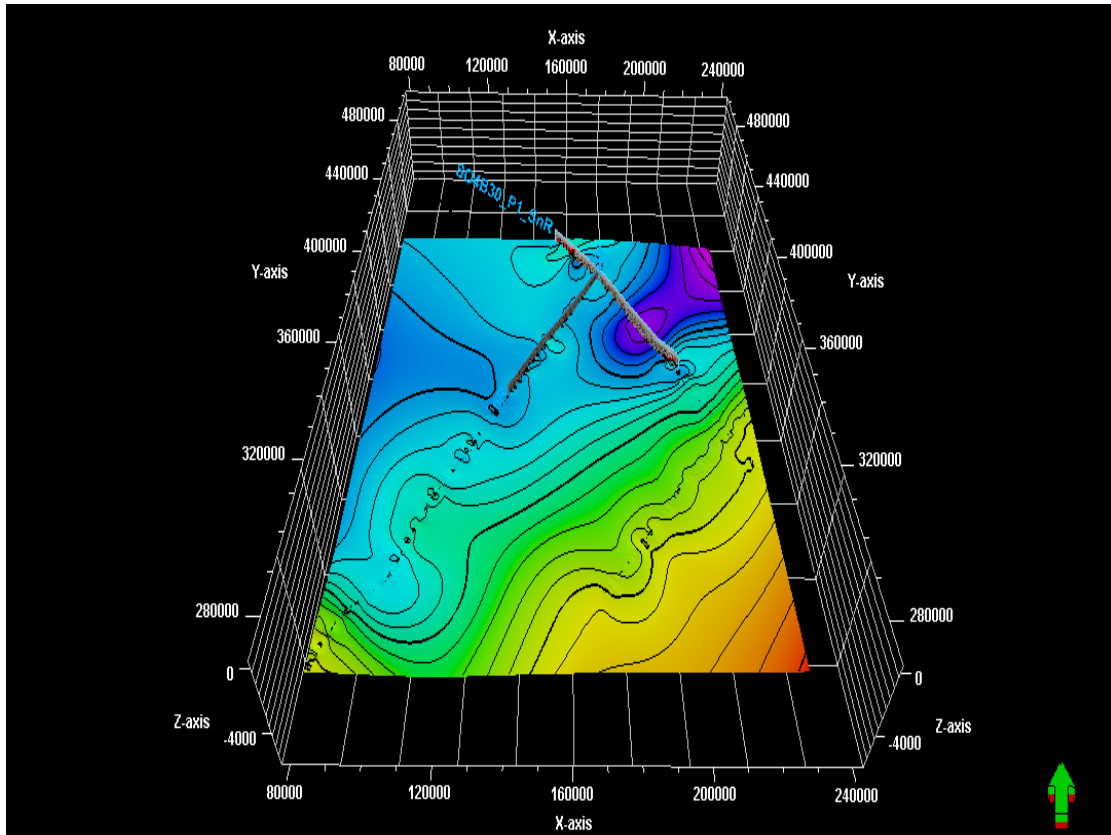
Figure 4.24: 3D view of the Bajocian base surface map (lower Upper Hamenlei=Baidoa Member).
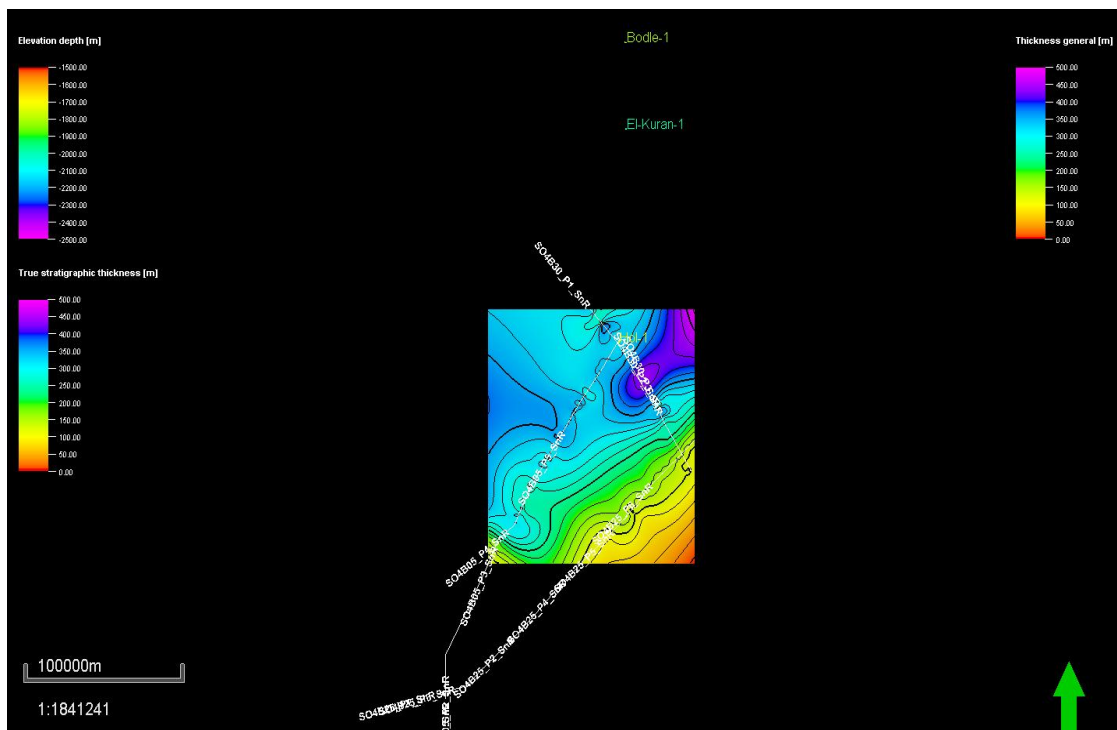
Figure 4.25: Bajocian base surface map (lower Upper Hamenlei=Baidoa Member) with seismic profiles and exploration wells from neighboring Ogaden basin.

111

d) Lower Callovian -Bathonian Base Surface Map (mid Upper Hamenlei= Goloda Member)

The surface map demonstrates the presence of depocenter near the Hol-1 well (Figure 4.26) bounded by two structural highs at the NW and SE. the depocenter may have a SW extension but the current interpretation failed to map its fall extent.

The Goloda member is a potential reservoir rock, and therefore, additional mapping or will be necessary.

Figures 4.27 and 4.28 provide 3D views of the Lower Callovian-Bathonian base surface map and locations of the seismic profiles and exploration wells from eighboring Ogaden basin.
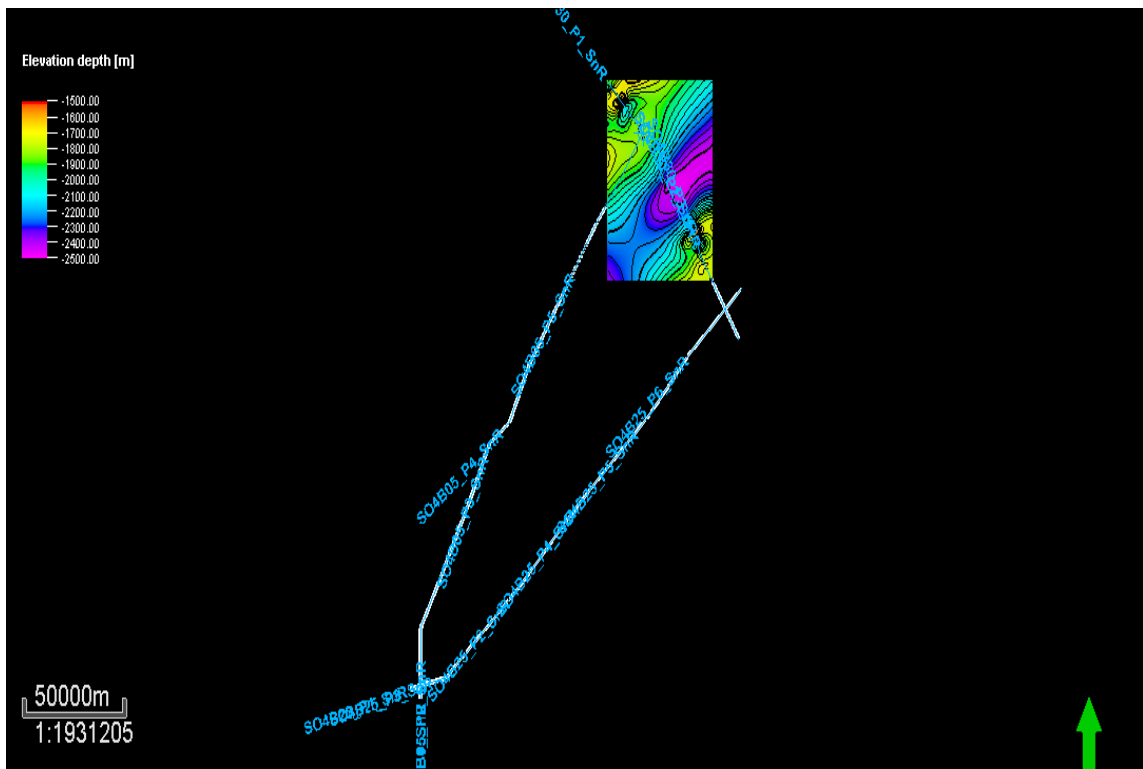
Figure 4.26: 2D view of the Lower Callovian -Bathonian base surface map (mid Upper Hamenlei= Goloda Member).2D view of the Lower Callovian -Bathonian base surface map (mid Upper Hamenlei= Goloda Member).
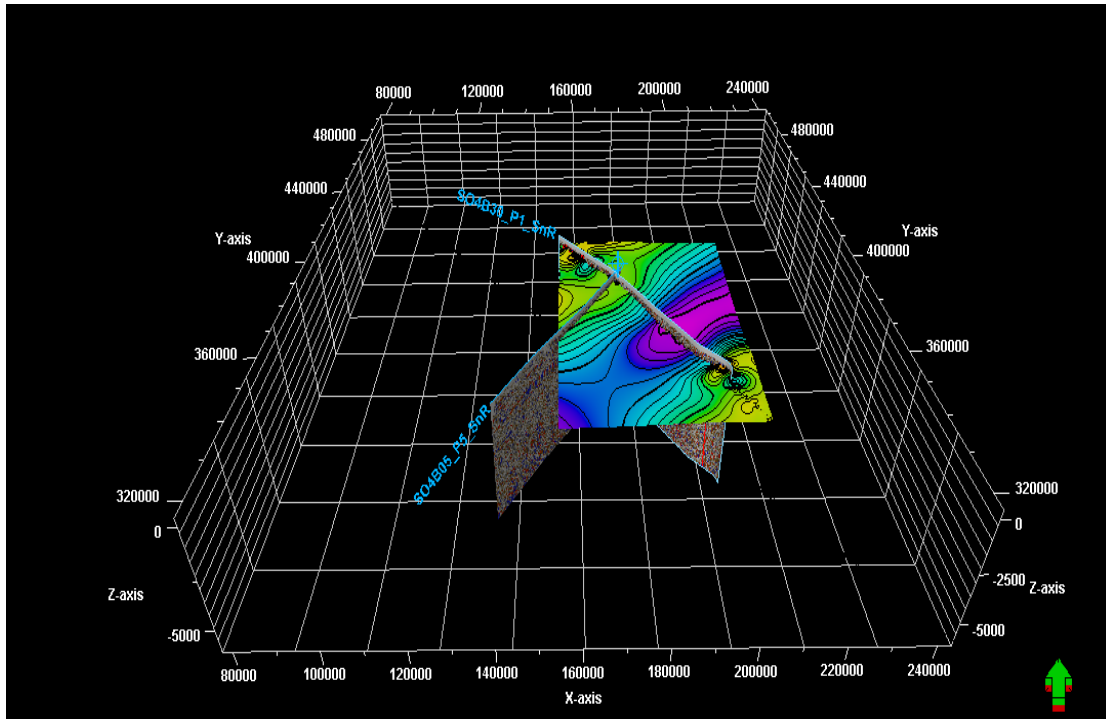
Figure 4.27: 3D view of the Lower Callovian -Bathonian base surface map (mid Upper Hamenlei= Goloda Member).
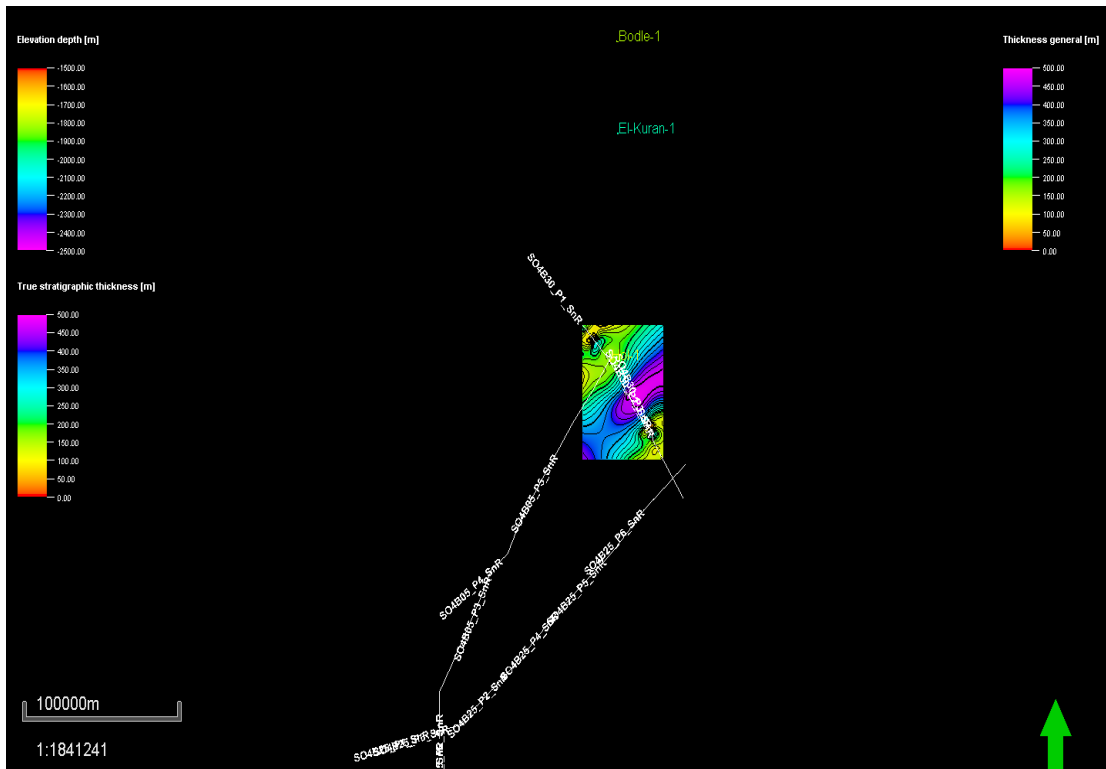
Figure 4.28: Lower Callovian -Bathonian base surface map (mid Upper Hamenlei= Goloda Member) with seismic profiles and exploration wells from neighboring Ogaden basin.

e) Oxfordian-Callovian base surface map (Upper Hamenlei=Anole Formation);
The depth contour map for the Upper Hamenlei Formation within the study area is demonstrated in Figure 4.29. It includes one visible kitchen zone located at the northeastern side of the survey area. The map also shows two potential structural high areas located at the SW and SE of the map. These areas could act as good hydrocarbon traps.

Figures 4.30 and 4.31 provide a 3D view for the Callovian - Oxfordian base surface map and locations of seismic profiles and exploration wells from the neighboring Ogaden basin.
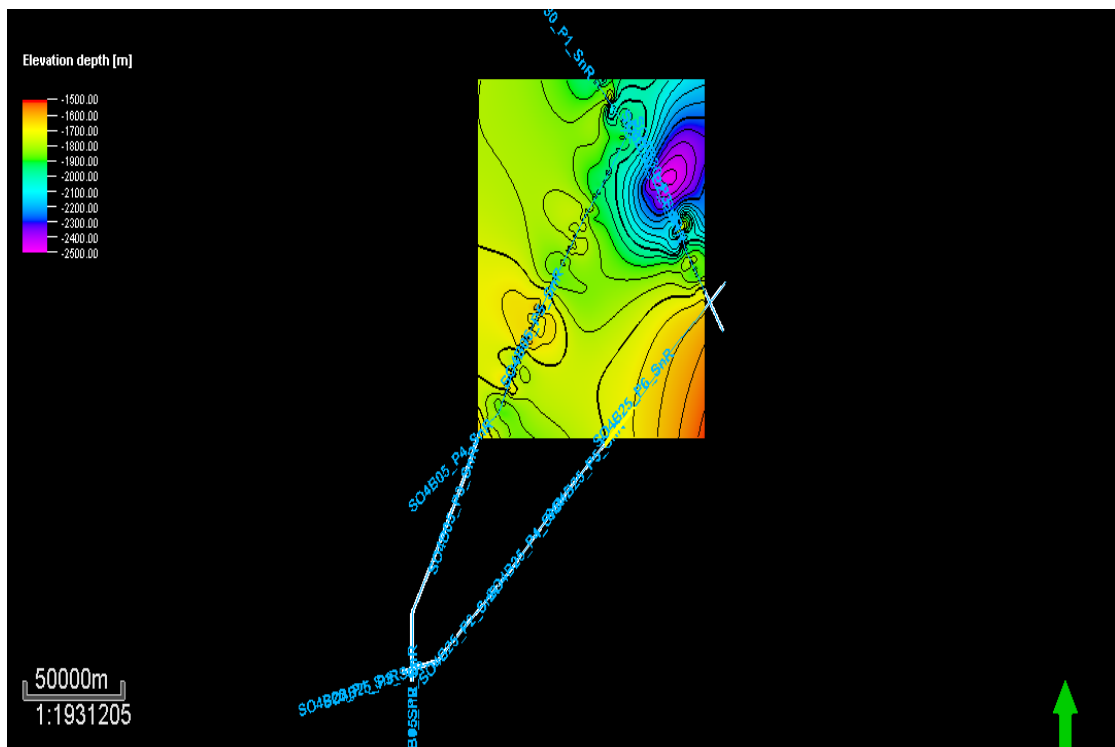
Figure 4.29: 2D view of the Callovian - Oxfordian base surface map (Upper Hamenlei=Anole Formation).
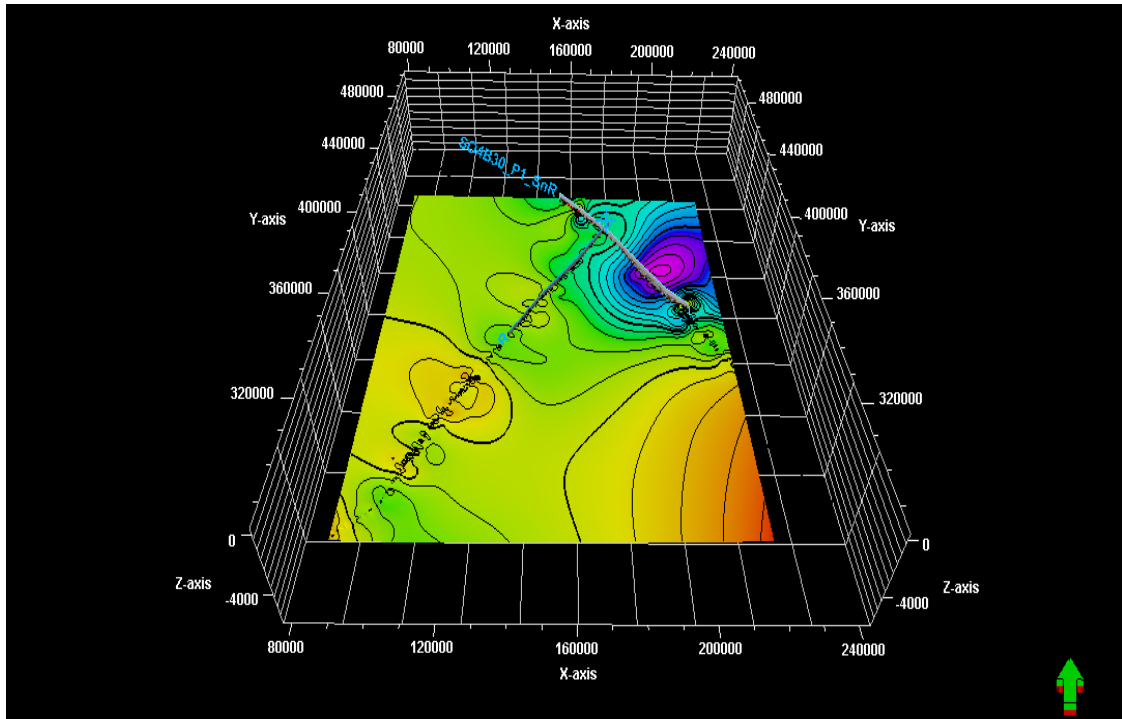
Figure 4.30: 3D view of the Callovian - Oxfordian base surface map (Upper Hamenlei= Anole Formation).
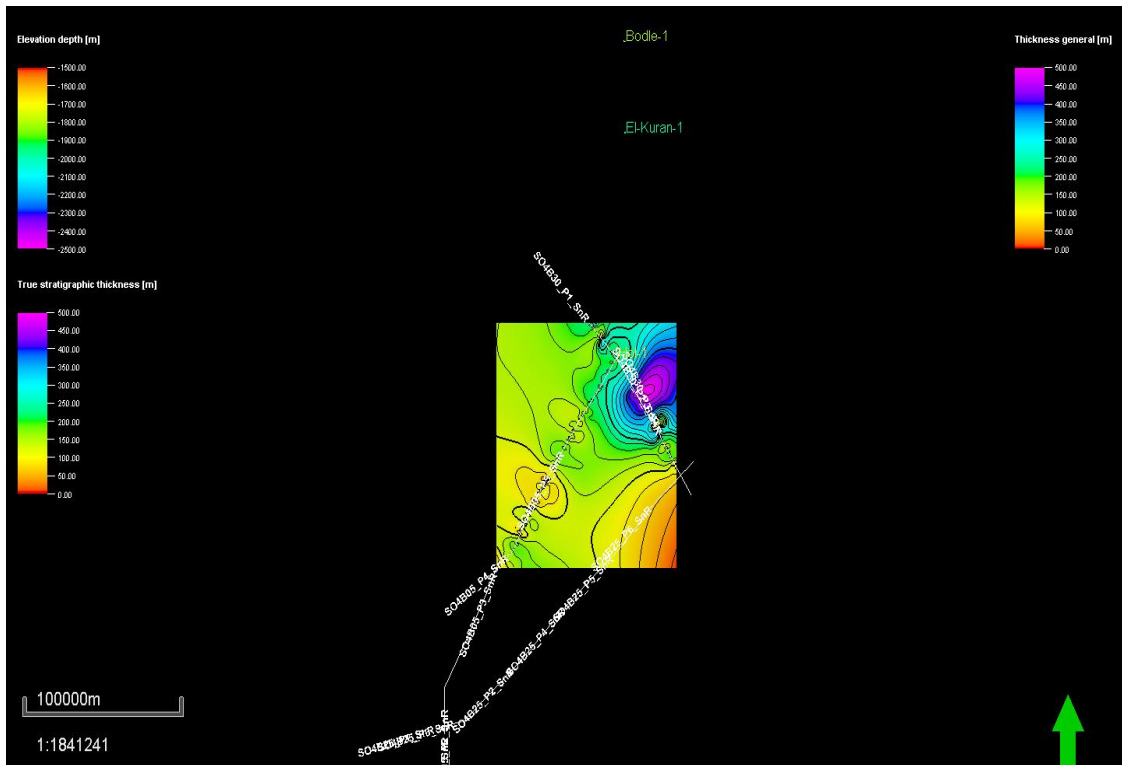
Figure 4.31: Callovian - Oxfordian base surface map (Upper Hamenlei= Anole Formation) with seismic profiles and exploration wells from neighboring Ogaden basin.

f) Oxfordian Base Surface Map (Upper Hamenlei =? Lower Uegit Formations).

The depth contour map for the Upper Hamenlei formation is given in Figure 4.32. The depocenters and source rock kitchen zones located at the northeastern side of the study area. Two structural highs can be observed from the southeastern and western side of map, which may act as a good hydrocarbon traps that was generated and expelled from the Uarandab shale source rocks that located below it.

These depth values were designated in a color line, which can be utilized to classify the difference in thickness formations. On the color line, red indicate the uplifted area and purple-blue indicate the kitchen zones.

Figures 4.33 and 4.34, presents a 3D view of the Oxfordian base surface map and the locations of the seismic profiles and exploration wells from neighboring Ogaden basin.
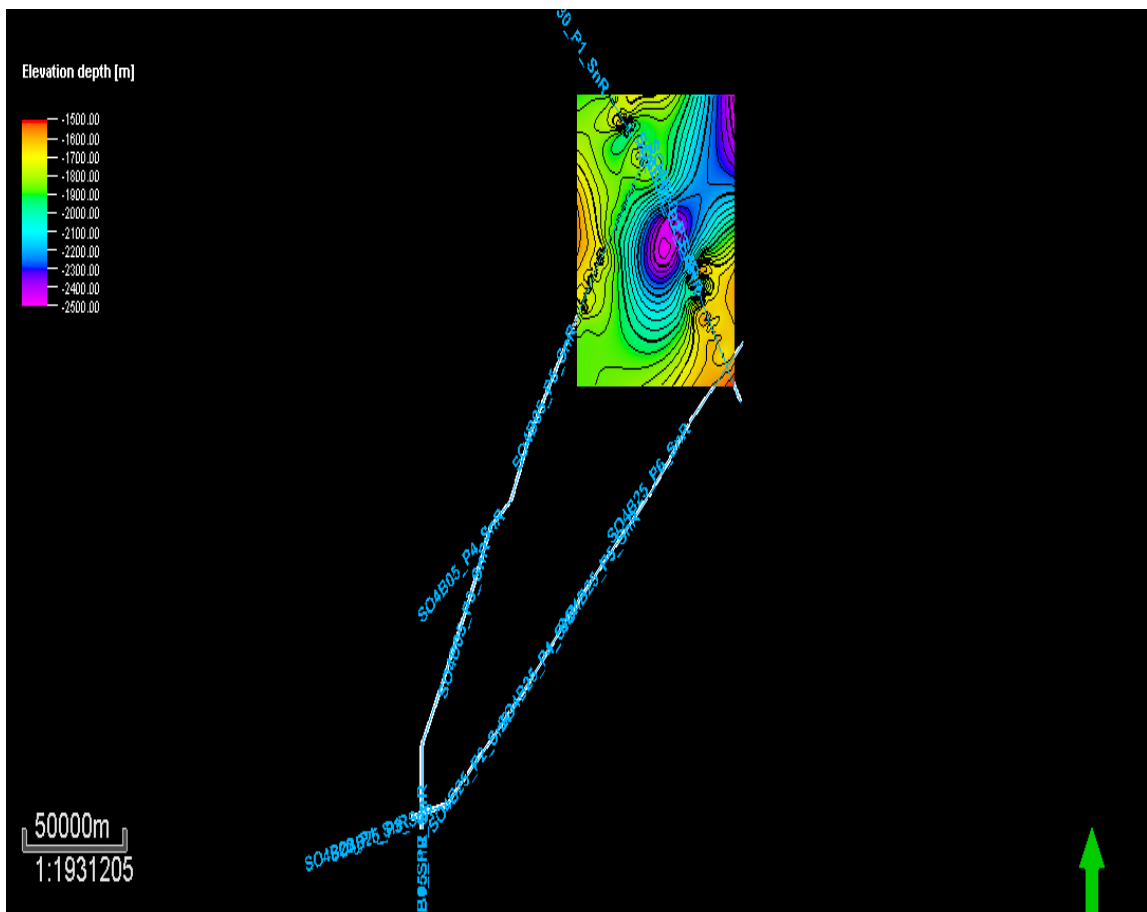
Figure 4.32: 2D view of the Oxfordian base surface map (Upper Hamenlei = ? Lower Uegit Formations)
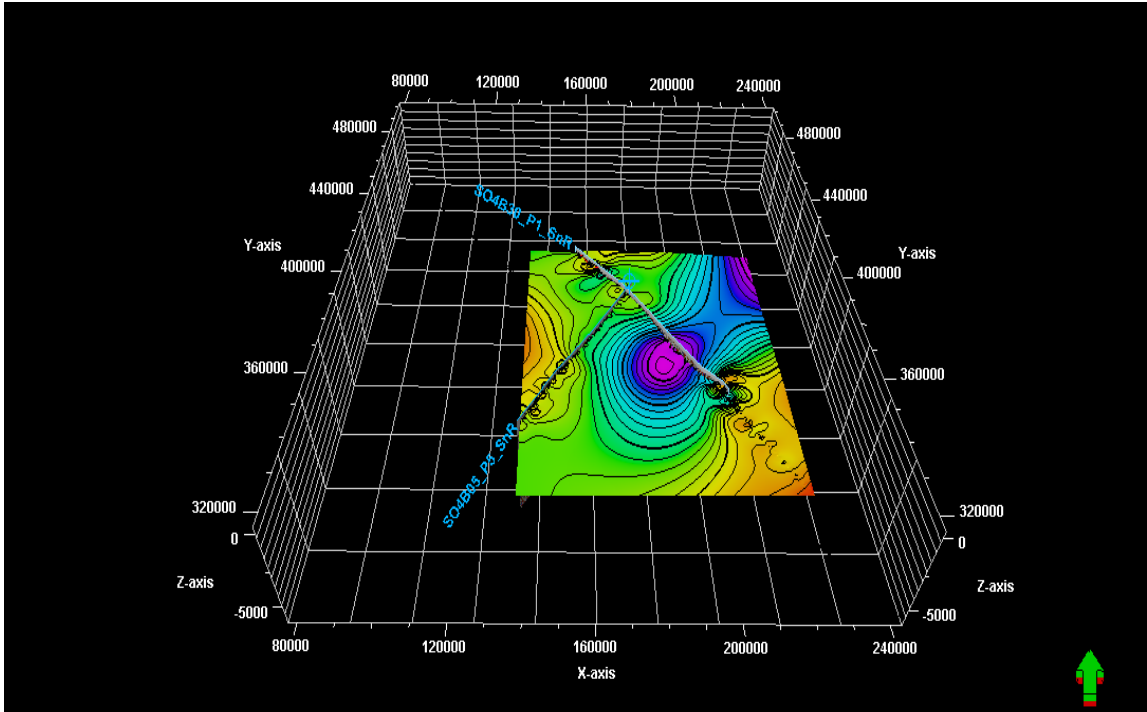
Figure 4.33: 3D view of the Oxfordian base surface map (Upper Hamenlei = ? Lower Uegit Formations)
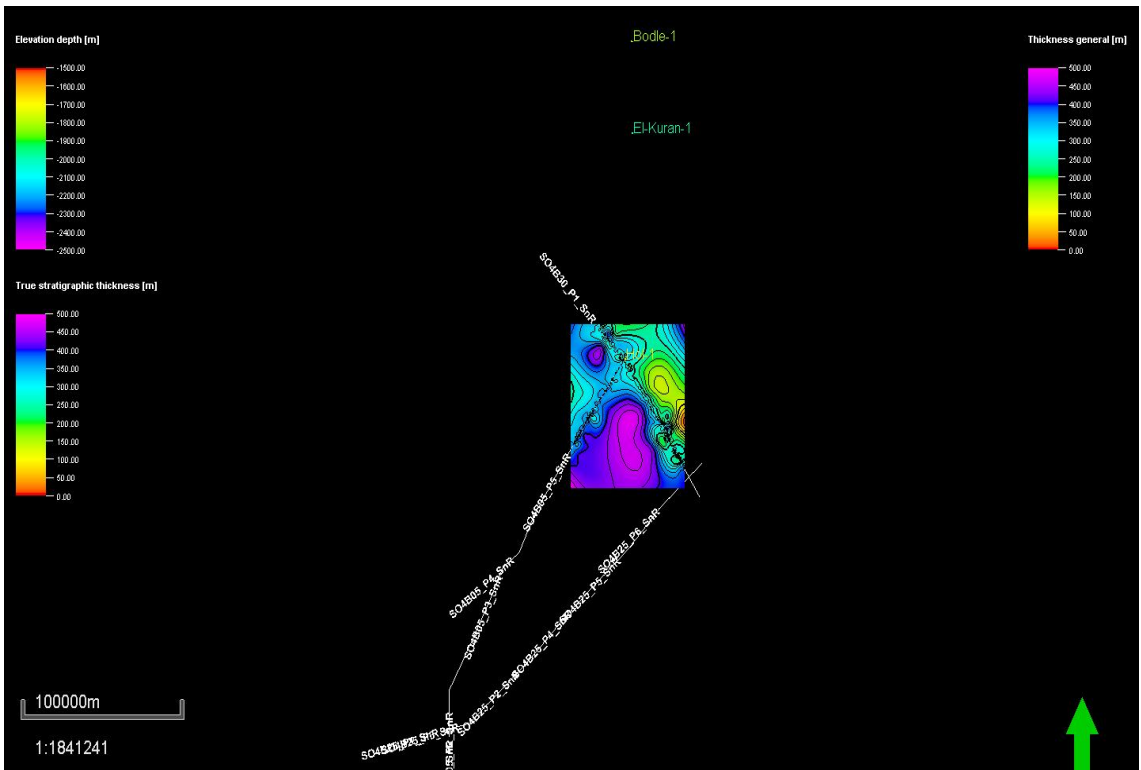
Figure 4.34: Oxfordian base surface map (Upper Hamenlei = ? Lower Uegit Formations) with seismic profiles and exploration wells from neighboring Ogaden basin.

4.4.3. 3D View of the Jurassic Formation Surfaces from the Somalian Sector of the Lugh-Mandera basin

A total of six (6) 3D view surface formations maps are provided below. A striking feature is observed by comparing the geographical extent of the mapped chrono- and seismostratigraphic surfaces. The Pliensbachian-Hettangian (Figure 4.35)-Toarcian (Figure 4.36) surfaces are developed through the entire survey area, however starting from the Bajocian (Figure 4.37) to Oxfordian (Figure 4.40) time surfaces, their surface areas decrease and are concentrating mainly at the north-eastern corner of the survey area or the Ogaden basin itself. We interpret this as a part of the change of the depositional environment, influenced by the sea level changes, reflecting the transgressional-regressional phases that took place here during the Jurassic-Cretaceous times.
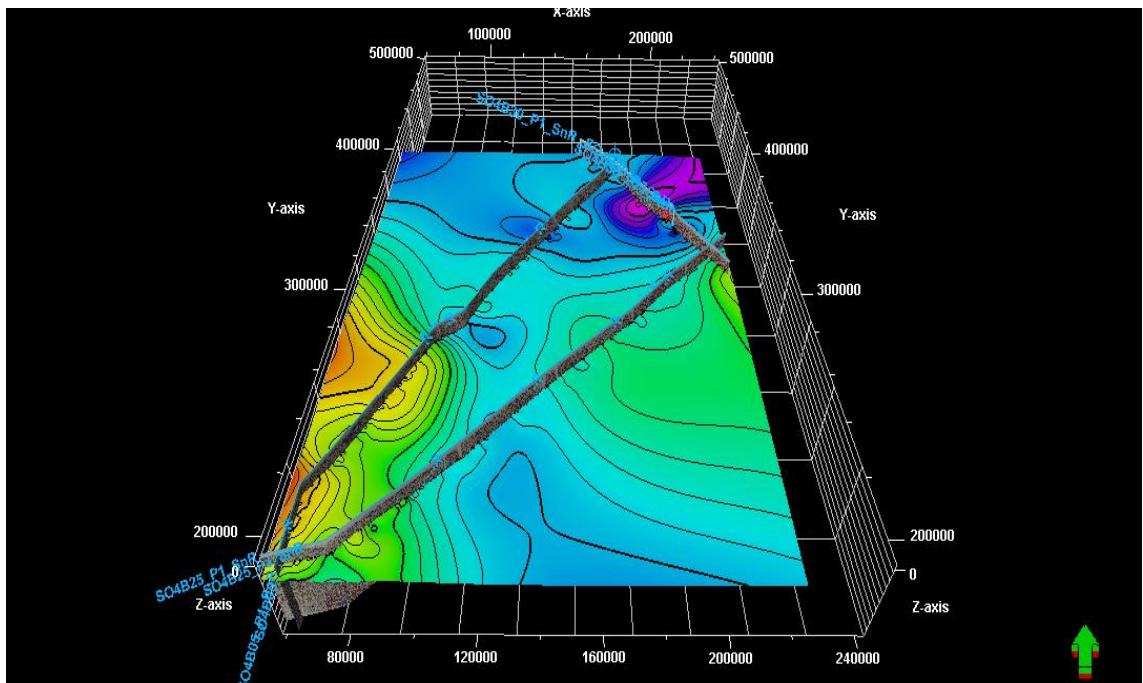
Figure 4.35: 3D view of Pliensbachian-Hettangian base (top Adigrat- base Lower Hamenlei Formation) surface map
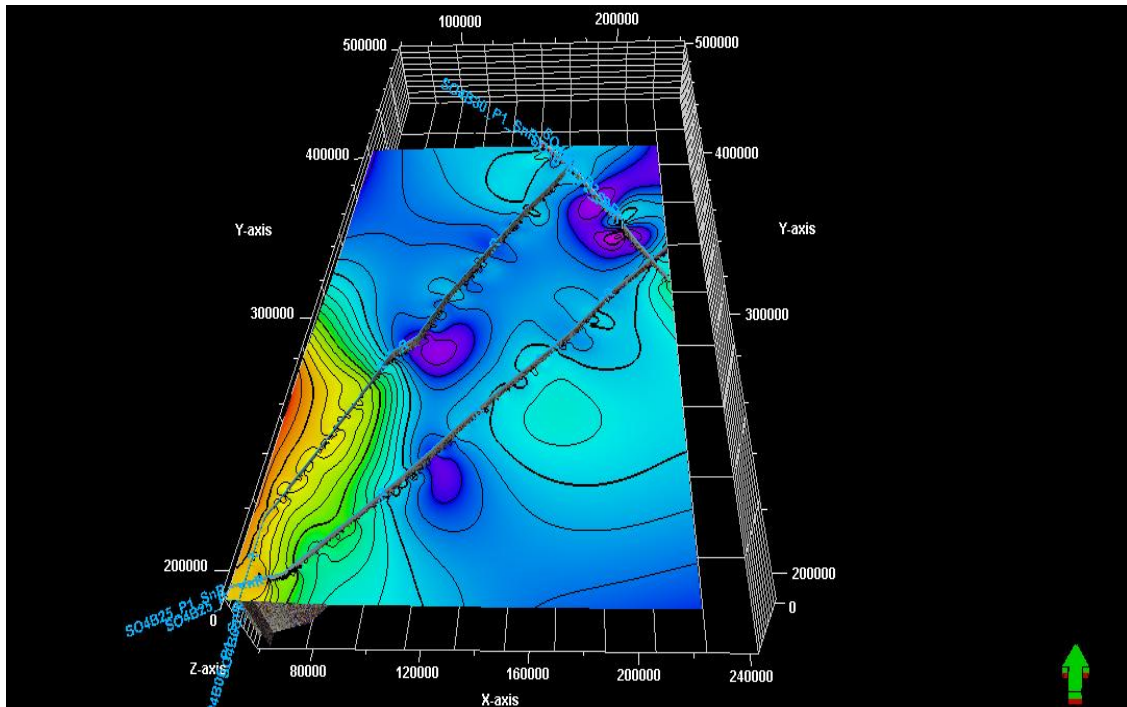
Figure 4.36: 3D view of Toarcian (mid Uanei) Member base surface map
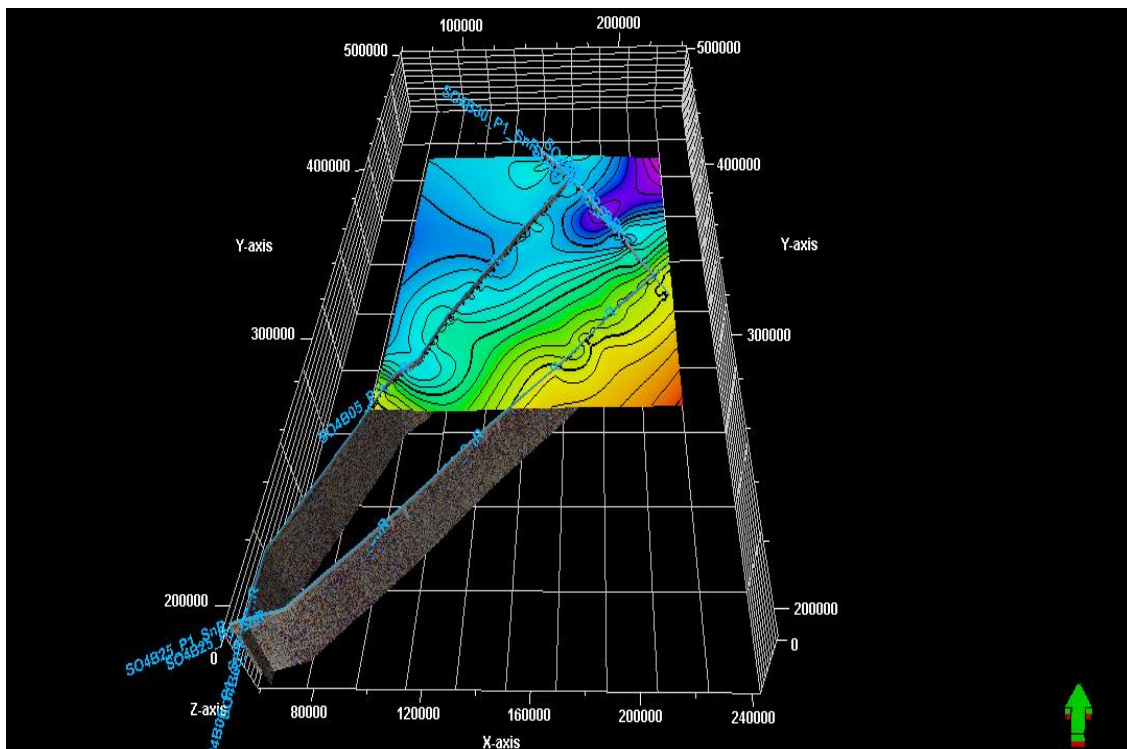
Figure 4.37: 3D view of Bajocian base (Baidoa) Member surface map
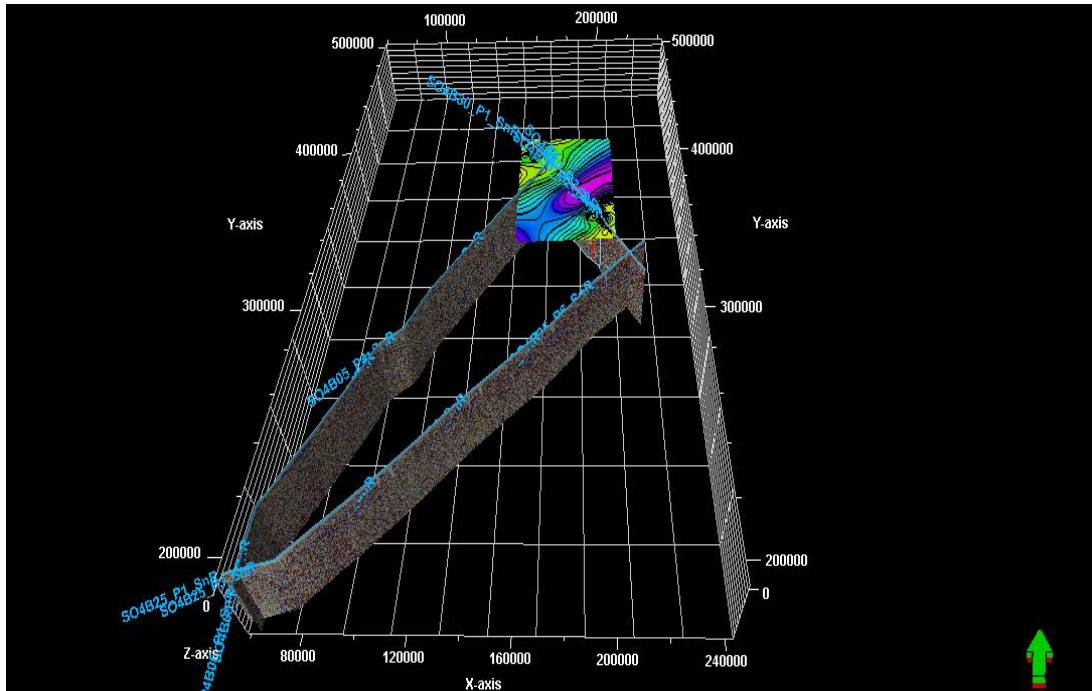
Figure 4.38: 3D view of Lower Callovian -Bathonian (bottom Goloda Member) base surface map
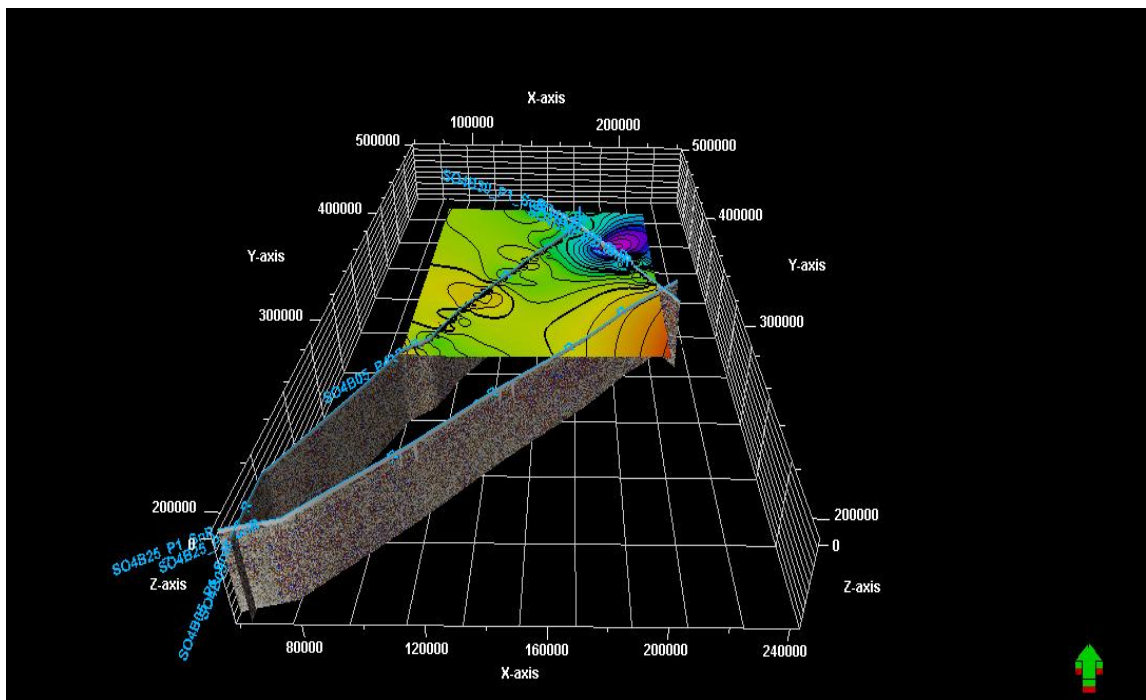
Figure 4.39: Oxfordian-Callovian (top Anole Formation) base surface map
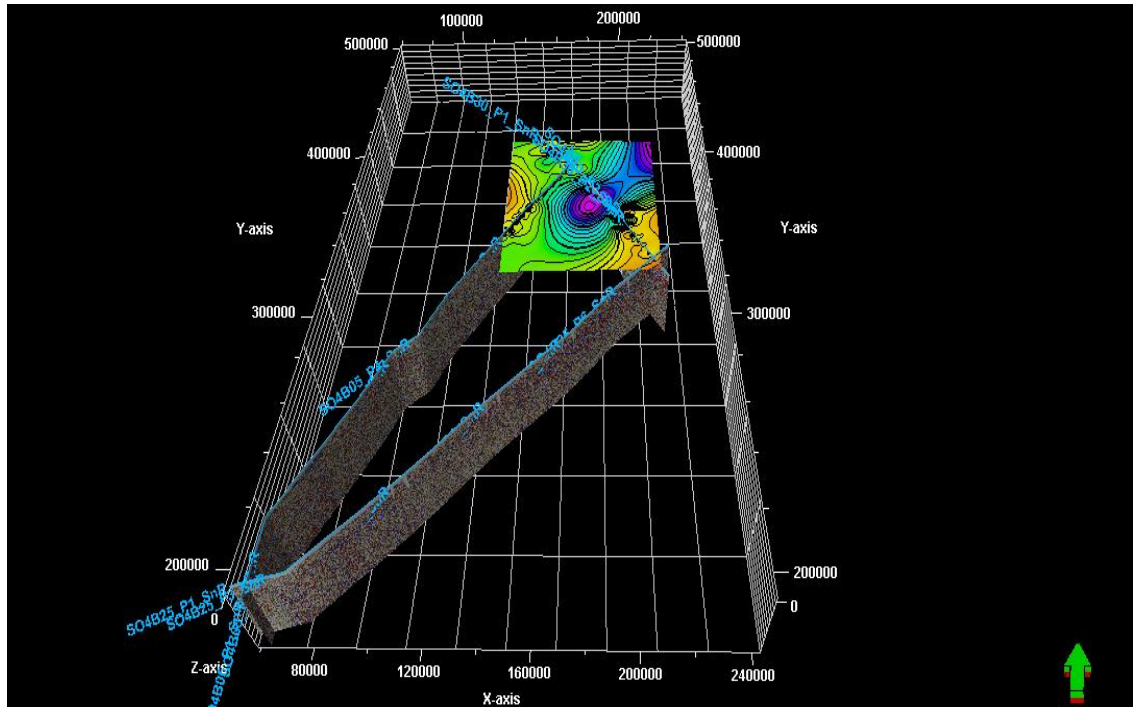
Figure 4.40: 3D view of Oxfordian (Upper Hamenlei/ base Lower Uegit) base surface map

These generated maps enable us to suggest that the study area was under a transgressional stage through most of the Liassic time (Hettangian-Sinemurian-Plensbachain-Toarcian stages). A regressional phase probably commenced during the Aalenian-Bajocian times, and accelerated with a maximum during the Bathonian–Early Callovian times (Mid Hamenlei/ Late Anole), before once again experiencing another less progressive transgression in the Late Callovian-Oxfordian (Dogger/Malm transition) time, and finally regressing again towards the larger Ogaden basin to the north in the Early Oxfordian (see Figures above). The Lugh-Mandera basin remained submerged under marine conditions until the Early Cretaceous (Neocomian) times before completely retreating and becoming an area of denudation over since (Al Kassim et al., 1993; Ali Kassim et al., 2002). These time series maps also demonstrate the increasing impact of the uplifting occurring at the south-eastern part of the survey area which is probably related to the elevation of the Bur Acaba basement high along the bounding faults.

4.4.4. Thicknesses (Isochore and Isopach) Structural Maps

The two most common subsurface geological maps used in oil and gas exploration practice are: *isopach* and *isochore maps* as shown in (figure 4.41). For a long time there has been a general confusion among the geological community on what each one of them stands for. The difference between these two thicknesses is provided below (after Teapork & Bischke, 2002).

> "An *isochore map delineates the **true vertical thickness** of a stratigraphic interval, whereas an **isopach map** illustrates the **true stratigraphic thickness** of a stratigraphic interval".*
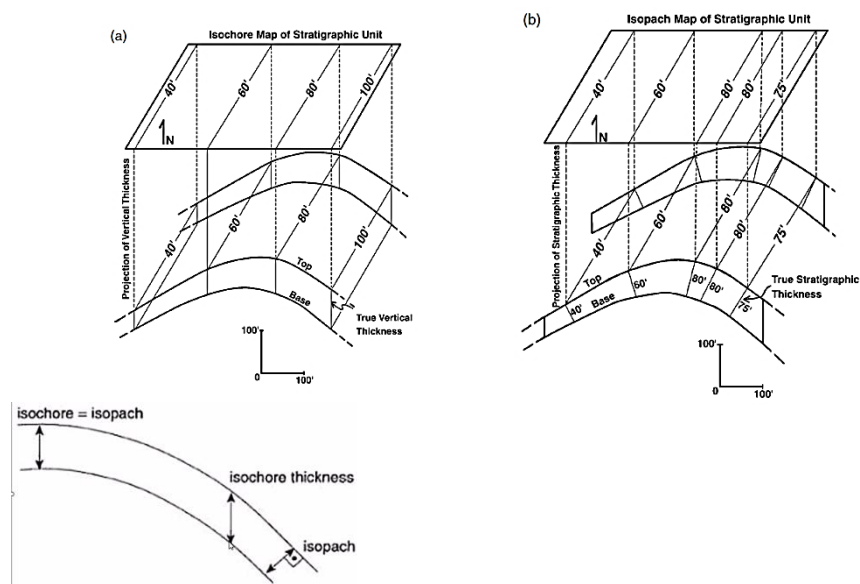
Figure 4.41: Showing the principle difference between an isochore (a) and isopach (b) maps.

According to web dictionary (**https://en.wiktionary.org/wiki**), the word Isopach originates from Ancient Greek, **πάχος** (páchos; *plural* **πάχη** o*r* **πάχια**) meaning **thickness**, **corpulence** or **fatness**. In geology, a line on a map joining parts of a stratigraphic unit that have the same stratigraphic thickness is termed as an ***isopachous line***.

The word isochore derives from words iso- + Ancient Greek χώρα (*khṓra*, "place"; *plural* isochores. In geology, a contour line showing points of equal vertical thickness of strata is called ***isochore line***.

Isochores will be equal to ***isopach***s if the strata are horizontal. ***Isopach maps*** seem to be the most important as they provide the correct (stratigraphic) thicknesses, and hence, depth of the formations of interest. Until the late 1940s, the full application was not well realized or employed in daily subsurface interpretations. However, even at that time they were used for predetermining drilling depths to a specific horizon of interest, for locating buried structures in areas where formations would become thinner over the crestal parts of such structures and also estimating the elevation of a datum bed below the drill bit that has been encountered higher other known stratigraphic horizons or datum layers (Low, 1949).

Below are the results of generating a series of ***isochore*** and ***isopach maps*** between the following base surfaces:

i)   Isochore and isopach thicknesses maps (?) between Pliensbachian –Hettangian and Toarcian base surfaces (Adigrat-mid Middle Hamenlei Formations = almost entire Iscia Baidoa Member);

j)   Isochore and isopach thicknesses maps (?) between Toarcian and Bajocian base surfaces (mid Middle Hamenlei = top Iscia Baidoa Formation= upper Uanei Member)

k)   Isochore and isopach Thicknesses map (?) between Bajocian –Lower Callovian-Bathonian base surfaces (topmost Middle Hamenlei-lower Upper Hamenlei=Baidoa Formation).

l)   Isochore and isopach thicknesses maps (?) between Lower Callovian-Bathonian and Callovian-Oxfordian base surfaces (mid Upper Hamenlei=top Anole Formation=Goloda Member), and

m) Isochore and isopach thicknesses maps between Callovian-Oxfordian and Oxfordian base surfaces (top Upper Hamenlei = top Anole/bottom Lower Uegit Formations).

The last two characterize the attitude of the promising reservoir (Goloda Member) and source rock (top Anole/ bottom Uegit Formations?) intervals.

As a result of consistent dips of the formations and almost entire horizontal layering of the studied formations, both isochore and isopach maps with an exception of a few chrono and seismo-stratigraphic horizons in general show similar thickness distributions. Areas of decreased thicknesses are attributed to deformation zones due to folding and faulting. These deformations occurred as a result of wrench (strike-slip) tectonics.

a) **Thicknesses Maps between Pliensbachian –Hettangian and Toarcian Base Surfaces**

The isochore (Figure 4.42) and isopach (Figure 4.43) maps between Pliensbachian – Hettangian and Toarcian base surfaces (Adigrat-mid Middle Hamenlei formations = almost entire Iscia Baidoa Formation) demonstrate some slight differences between them, especially at the central deformed area. The formation dips were incorporated to generate the filtered isopach (true stratigraphic) thickness map. As a result, the last map (Figure 4.43) shows lesser values of thicknesses than the one of isochores. The isopach map thicknesses are within the 10-250 m range. Two consistent deformed structures occur in the south-western and north-eastern corners of the study area. The south-western structure consists of two highs divided by a saddle, and an approximate vertical closure of 120 meters, while the one in the north-east has a less closure of only about 70 meters (Figure 4.43). Additionally, the two structures differ by their trends: south-western has a 310 NW trend, while the north-eastern has a 50 NE trend. This is a result of different strain regimes involved in their formation with the first one representing a deformation above a buried basement high (?) or folded structure (probably portion of the Sengif or Garbaharey fold belt), while the north-eastern developed above a depressed area (Bodle deep). The central area seems to share the same trend as the south-western structural closure (310 NW). We assume that this area was increasingly affected by wrench tectonics, in particular through its orthogonal (oblique) transpressional deformational component. This is seen through the interpretation seismic profiles with all showing evidence of flower structures of different orientations. Both generated Pliensbachian-Hettangian and Toarcian subsurface maps specify the priority of infill drilling within the south-western corner of the study area. The subsurface formation base and thicknesses maps for the Pliensbachian-Hettangian to Toarcian include the Adigrat-mid Middle Hamenlei sections are provided in (Figures 4.42-4.43).
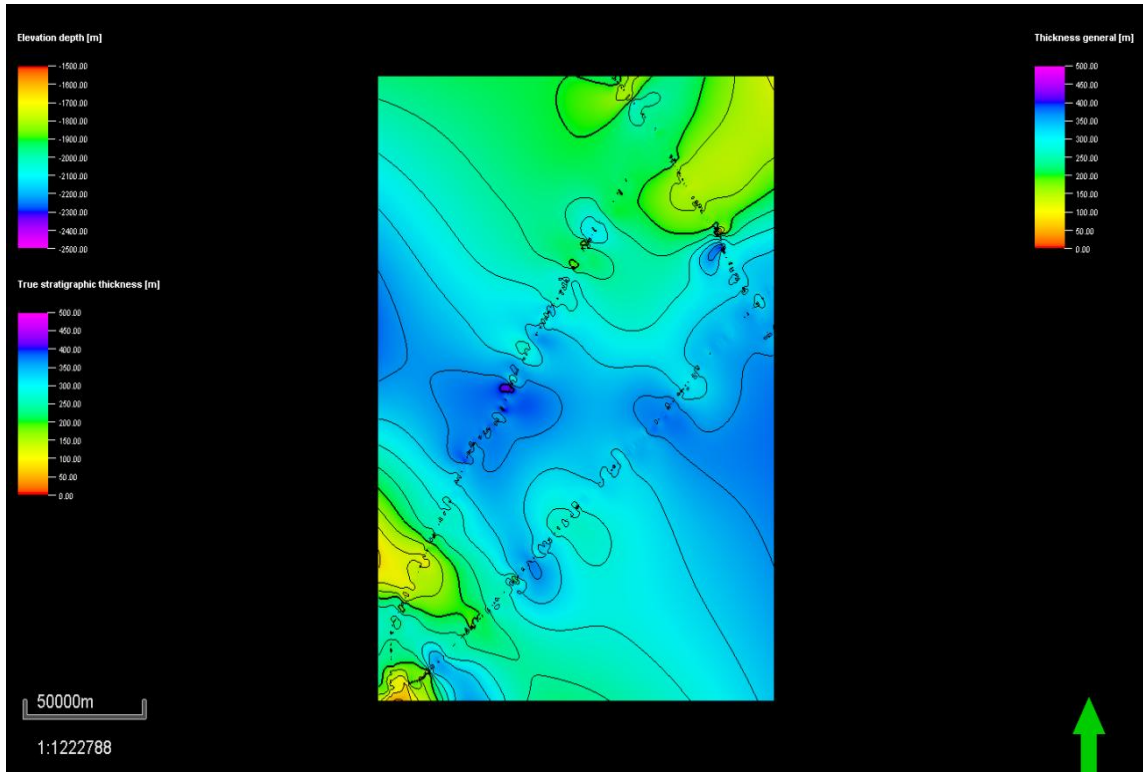
Figure 4.42: Isochore map between Hettangian-Pliensbachian and Toarcian base surfaces
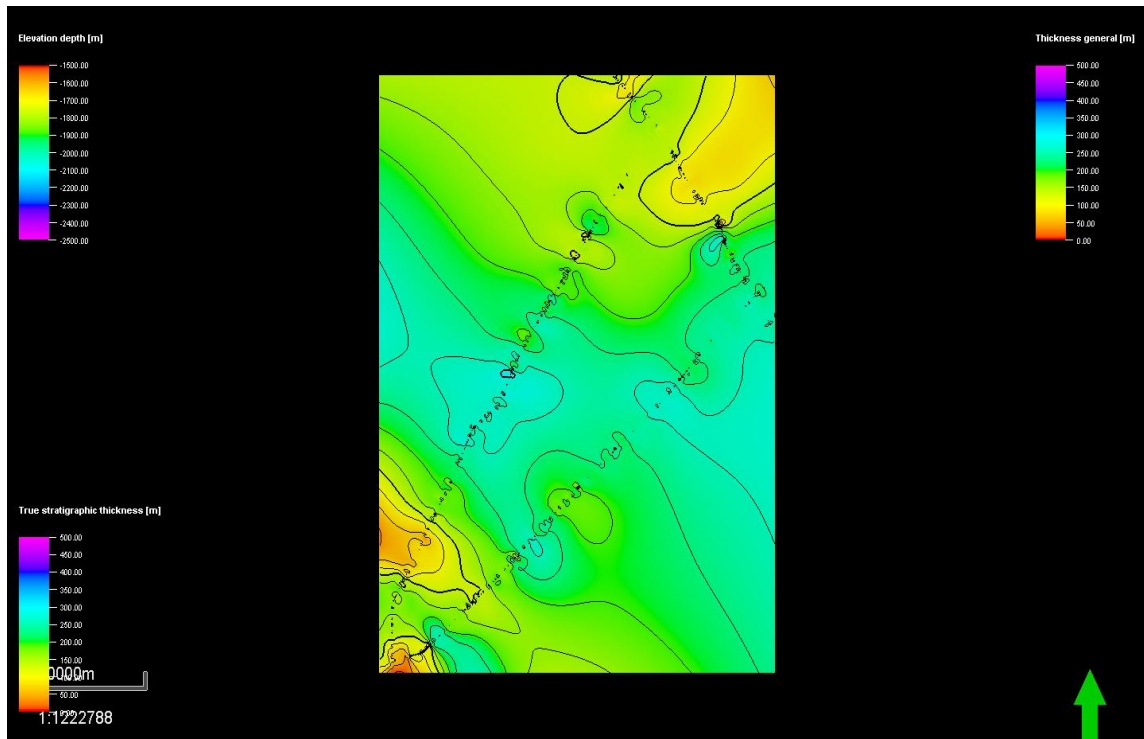
Figure 4.43: Isopach map between Hettangian-Pliensbachian and Toarcian base surfaces.

In the northern Ogaden basin, the Adigrat formation has a wider geographical distribution than the previous Carboniferous-Permian Calub formation. Here it has a maximum thickness of 135 meters and shows fairly good porosity (10-20%) and permeability (up to 100 mD) reservoir qualities. Oil and gas accumulations of commercial production are associated with this formation (Hunegnaw et al., 1998). Reservoir characteristic maps for the Adigrat formation demonstrate a decrease of porosity values towards the southern part of the Ogaden basin (Bodle deep and South Calub saddle) as a result of increased shale, mica, calcite and anhydrite content resulting in the decrease of porosities to the values of 2-12% and permeabilities of 0.1-4 mD. Unpublished petrophysical data from Hol-1 well identified the presence of excellent former intergranular, solution moldic and fracture porosity which is now filled with sparite (Berry, 1974). Figure 4.44 represents the Isopach map between Hettangian-Pliensbachian and Toarcian base surfaces with seismic profiles and exploration wells from neighboring Ogaden basin.
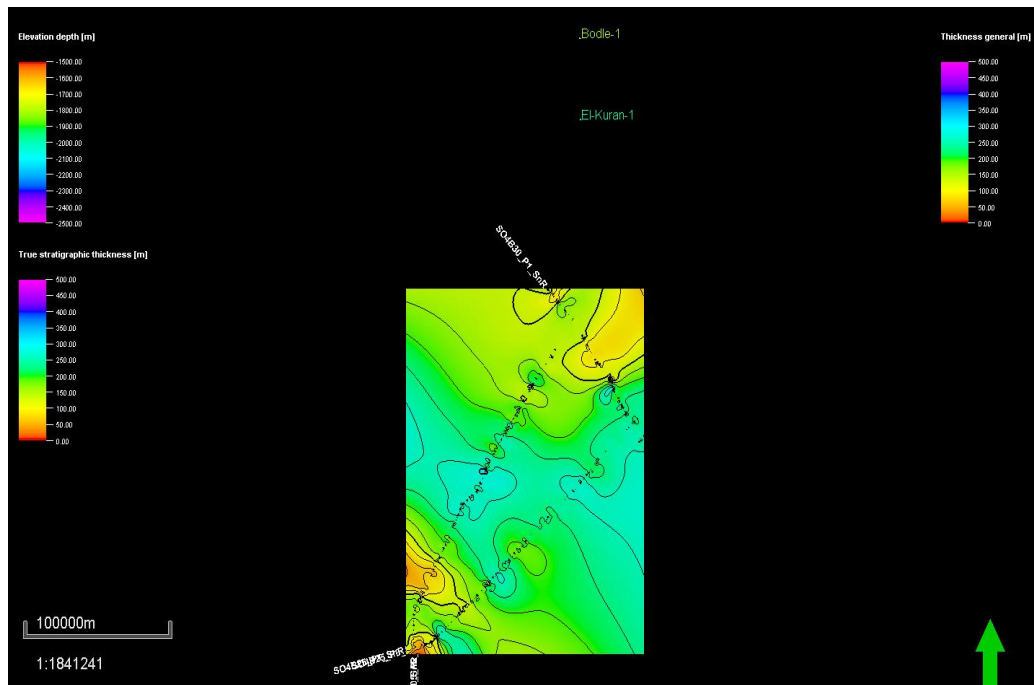
Figure 4.44: Isopach map between Hettangian-Pliensbachian and Toarcian base surfaces

The increased shaliness of Adigrat formation is probably responsible for the increased TOC values (>0.5%) in the 12880-13190' interval of Hol-1 well. The Lower Hamenlei and top Adigrat also referred as the Transition zone (Hunegnaw et al., 1998) act both as a source and seal rock in the Ogaden basin. Here they have thicknesses ranging between

50-120 m and contain Type II and III kerogens. They are mature enough to generate various hydrocarbon products, including wet and gas products in the deeper sections of the Bodle Deep. Our TTI modeling indicates that the rock is within the dry gas window at present. The value for cumulative TTI is 1,319, and the expulsion began 172Ma ago in the Middle Jurassic.

In the Ogaden basin, hydrocarbon traps occurring within the Adigrat formation are commonly structural in origin and are presented either as drag folds associated with large faults and/or domal features related to basement highs (Hunegnaw et al., 1998). Both of these types occur within the Somalian sector of the Lugh-Mandera basin.

b) **Thicknesses maps between Toarcian and Bajocian base surfaces (mid Middle Hamenlei = top Iscia Baidoa Formation= Upper Uanei Member).**

Both isochore (Figure 4.45) and isopach (Figure 4.46) thickness maps show that the thicknesses are increased in the central and northern parts of the survey area. The true stratigraphic thicknesses (isopach map) range between 20 (south-east) to approximately 450 (at the north) meters. These values range between 100 (Calub area) to 195 m (Bokh area) in the Ogaden basin of Ethiopia (Hunegnaw et al., 1998).

The average TOC values for this section are estimated at 0.204% which characterizes it as a poor quality source rock (Peters, 1986). Nonetheless, the source rock interval has a considerable thickness (2260' or 689 m) which could give it some potential considering its wide geographical distribution both in Somalia and Ethiopia. The best reservoir rock properties of the Middle Hamenlei formation are observed in Ethiopia within the Calub Saddle and eastern part of the Ogaden basin, located to the north and north-east from the survey area. Better characteristics were encountered in dolomitic beds with porosities of over 11-26% and permeabilities of 5-60 mD. However, the reservoir quality decreases towards the Bodle Deep where the Bodle-1 and Hol-1 wells are located (Hunegnaw et al., 1998).
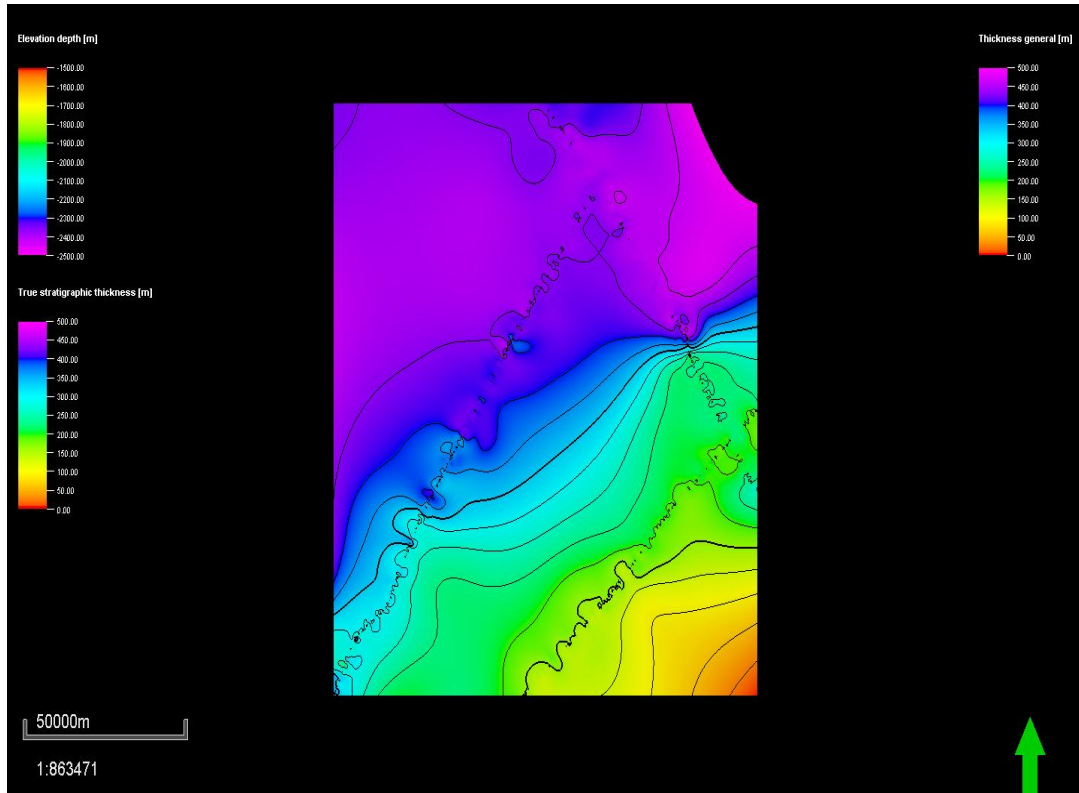
Figure 4.45: Isochore map between Toarcian and Bajocian base surfaces
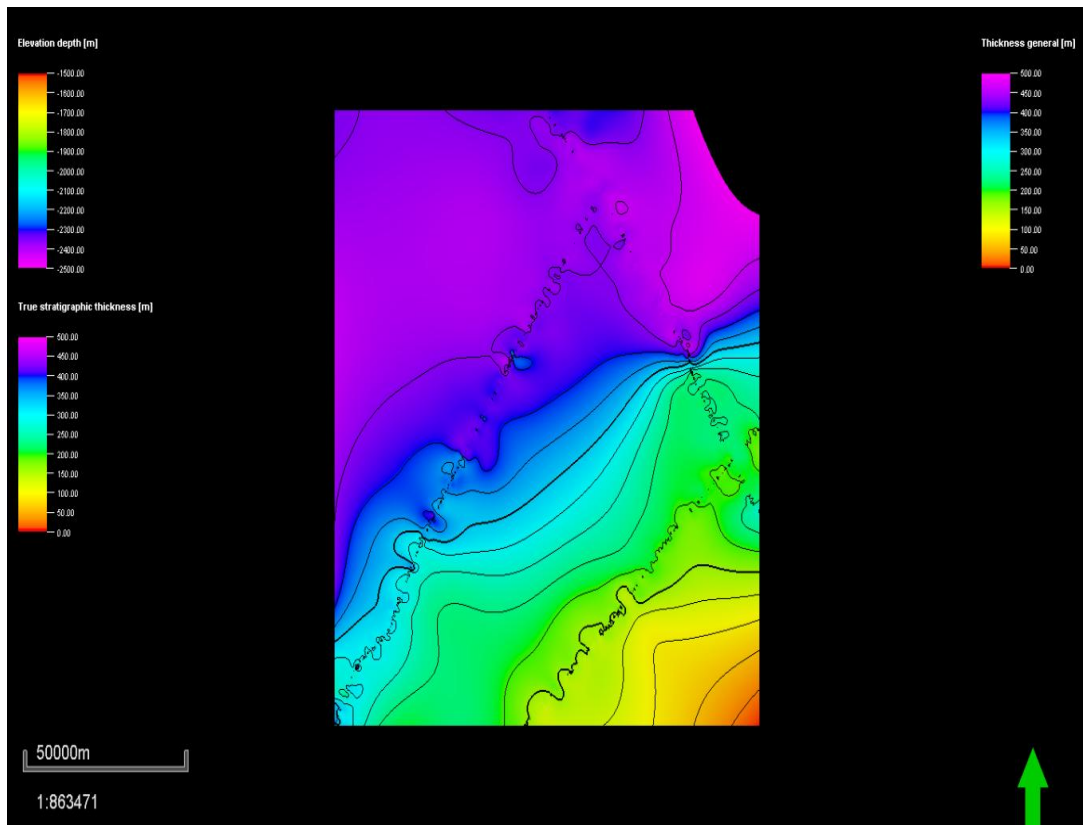
Figure 4.46: Isopach map between Toarcian and Bajocian base surfaces

The petrophysics from Hol-1 shows that this interval is characterized by the filling of the former intergranular and moldic pores by sparry calcite and anhydrite (Berry, 1974). The shale components of Middle Hamenlei in Ogaden basin have the II type kerogen and appear to be mature, but are generally thin (less than 3 m). They are believed to have generated wet gas in the Ethiopian sector of the Bodle Deep (Hunegnaw et al., 1998). Potential trapping mechanisms of this section are located at the south-eastern part of the survey area (towards the Bur Acaba high) where an approximately 50 sq. km structure with an average 200 meter vertical closure is developed. This offers an additional infill drilling location. Hunegnaw et al. (1998) state that there are three types of hydrocarbon traps associated with Middle Hamenlei Formation. These are stratigraphic, mixed (combinational) and structural (gentle anticlines in the Calub saddle and eastern Ogaden basin).

Figures 4.47 and 4.48 show Isopach maps between Toarcian and Bajocian base surfaces /with seismic profiles and the neighboring wells from the Ogaden basin.
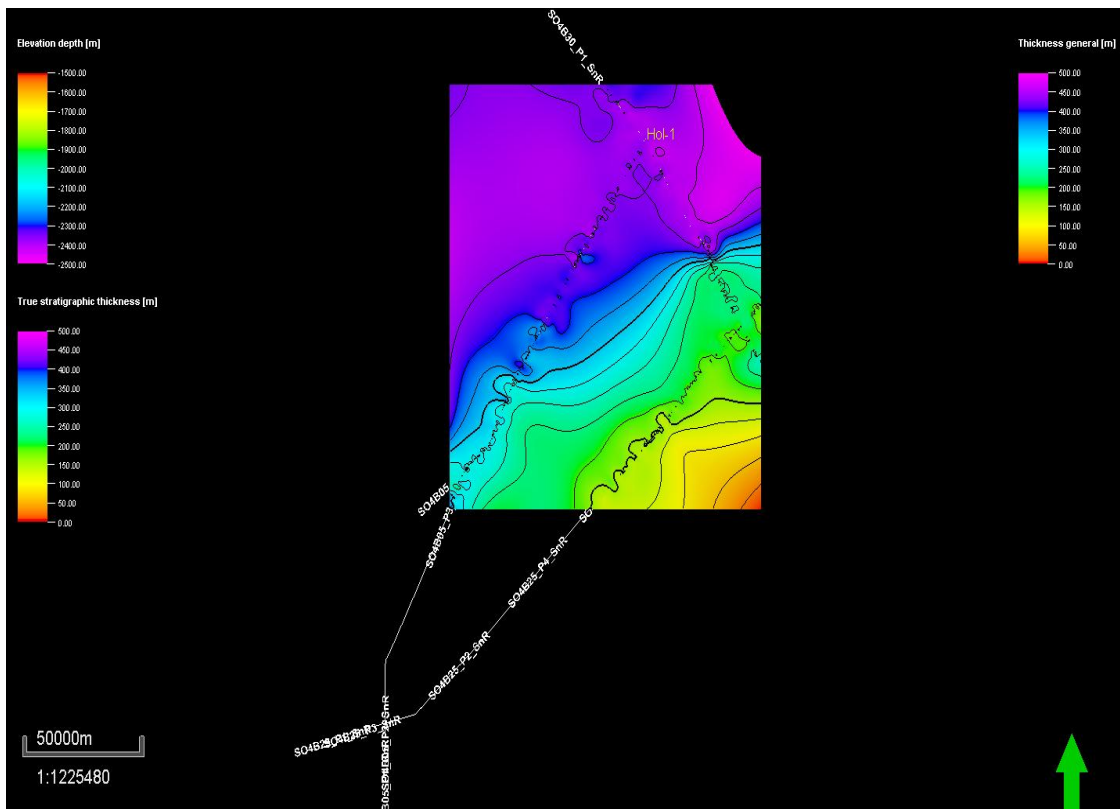
Figure 4.47: Isopach map between Toarcian and Bajocian base surfaces with seismic profiles.

129
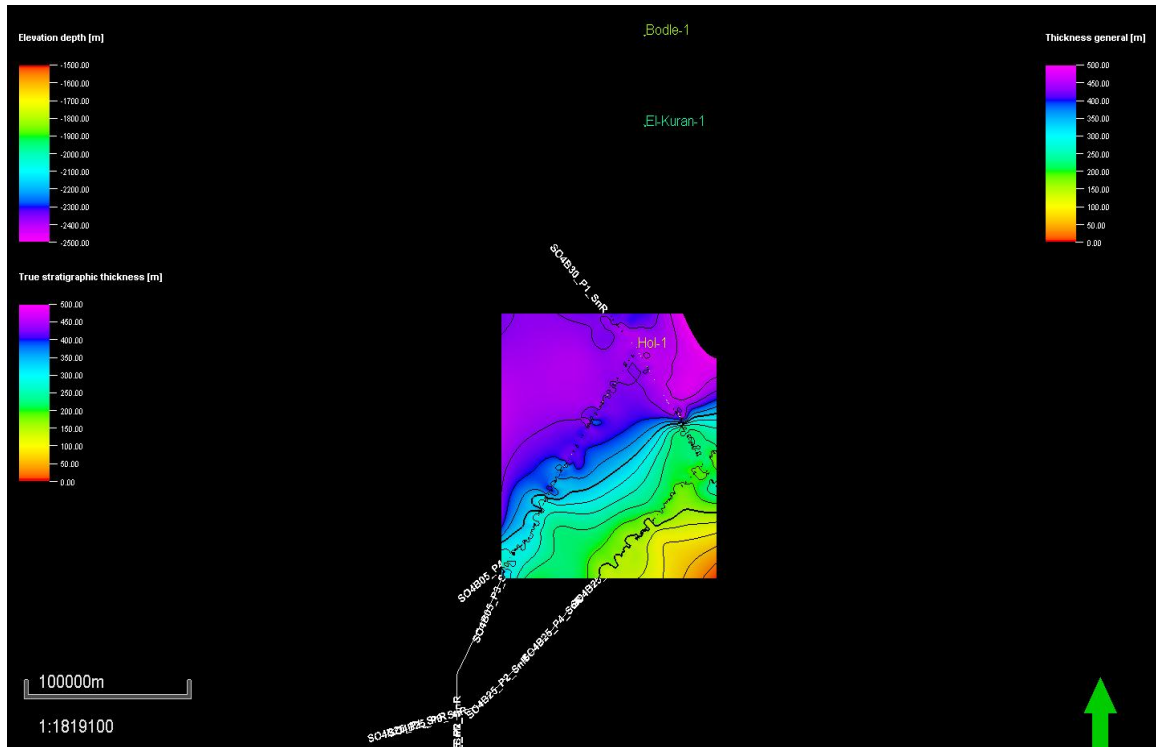
Figure 4.48: Bajocian surface map with seismic profiles and the neighborig wells

c) **Thicknesses map (?) between Bajocian –Lower Callovian-Bathonian base surfaces (topmost Middle Hamenlei-lower Upper Hamenlei=Baidoa Formation).**

Both isochore (Figure 4.49) and isopach (Figure 4.50) maps for the Bajocian –Lower Callovian-Bathonian base surfaces (topmost Middle Hamenlei-lower Upper Hamenlei-Baidoa formation) are identical, thus, indicating horizontal layering between these two surfaces.

In the Ogaden basin, the Mid Hamenlei Formation is presented by grainstones and dolomites which provide excellent reservoir properties, especially in the Calub Saddle and the eastern part of the basin. These qualities again deteriorate towards the Bodle Deep (Hunegnaw et al., 1998).
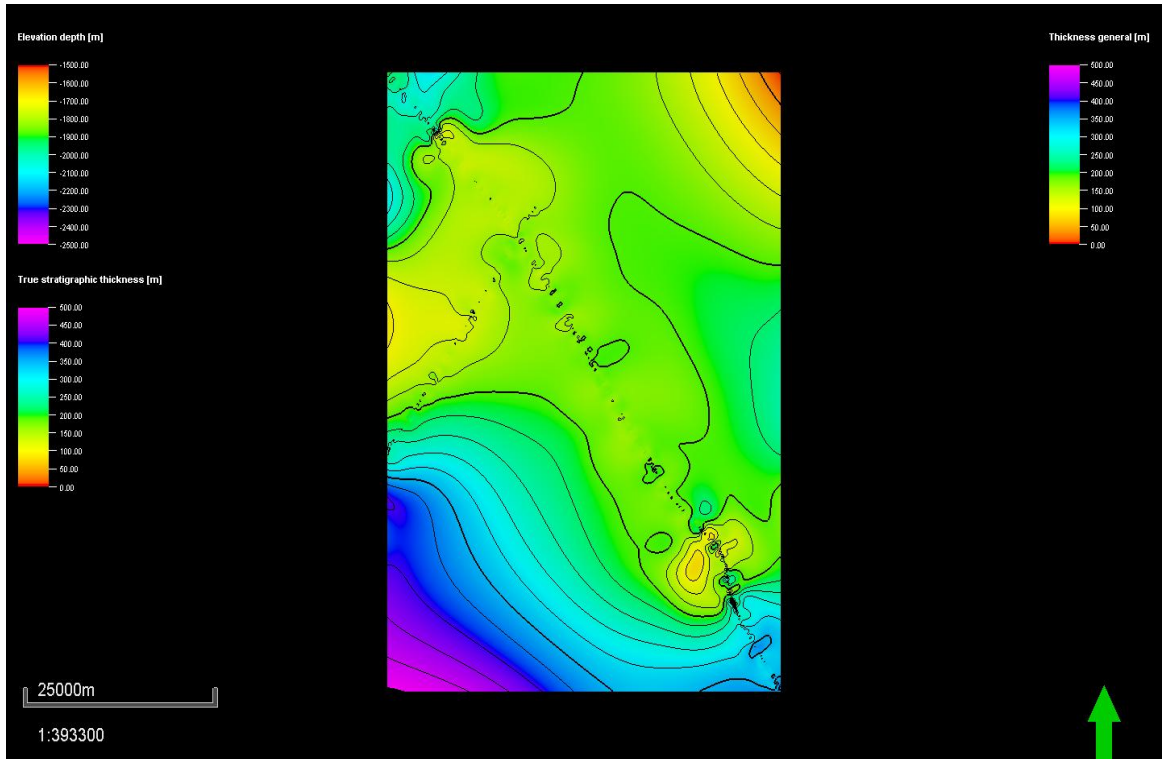
Figure 4.49: Isochore map between Bajocian and Bathonian-Lower Callovian base surfaces
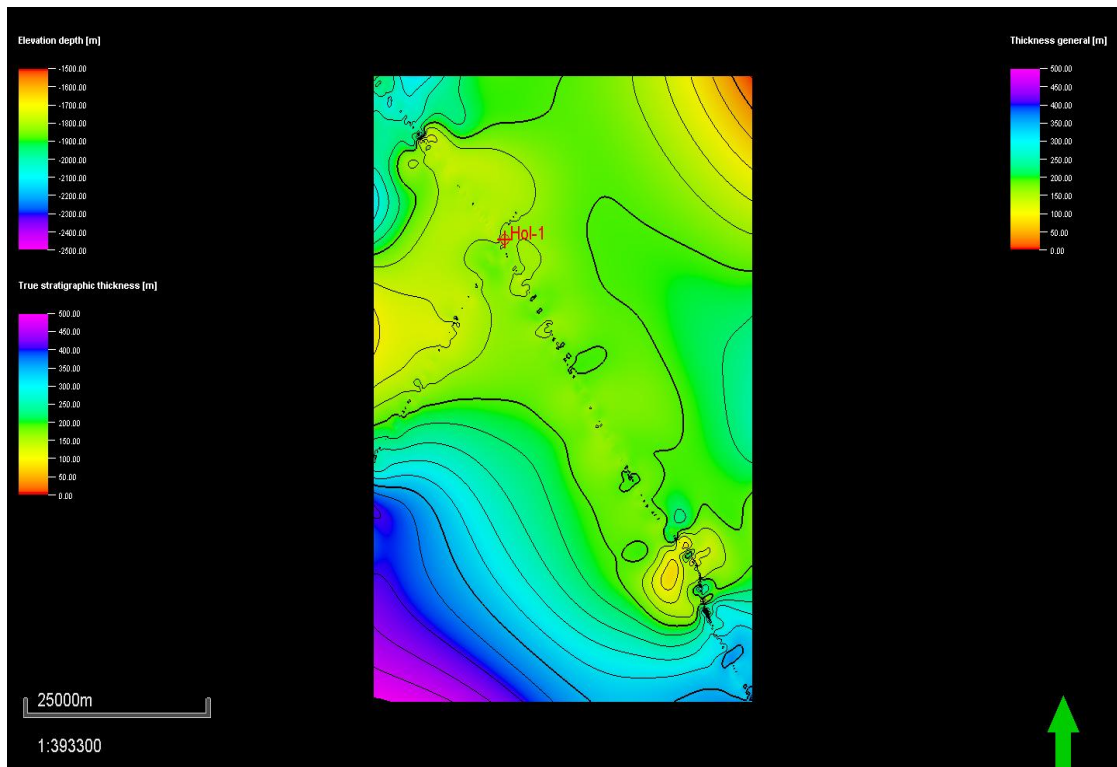
Figure 4.50: Isopach map between Bajocian and Bathonian-Lower Callovian base surfaces.

In the Hol-1 section, the Bajocian –Lower Callovian-Bathonian interval corresponds to the Baidoa formation with increased average TOC values (>0.5 %) for the lower portion suggesting increased shaliness. In the Ogaden basin, the shales that are intercalated among the carbonates contain kerogen of Type II and are mature enough to generate wet gas in the Bodle Deep (Hunegnaw et al., 1998). TTI modeling demonstrates that the interval is within the oil window at present since the value of cumulative TTI is 20. The expulsion began ~ around 156 Ma ago (Kimmeridgian) stage.

Figures 4.51 and 4.52 illustrate the Isopach maps between Bajocian and Bathonian-Lower Callovian base surfaces /with seismic profiles and well locations from neighboring wells from the Ogaden basin.
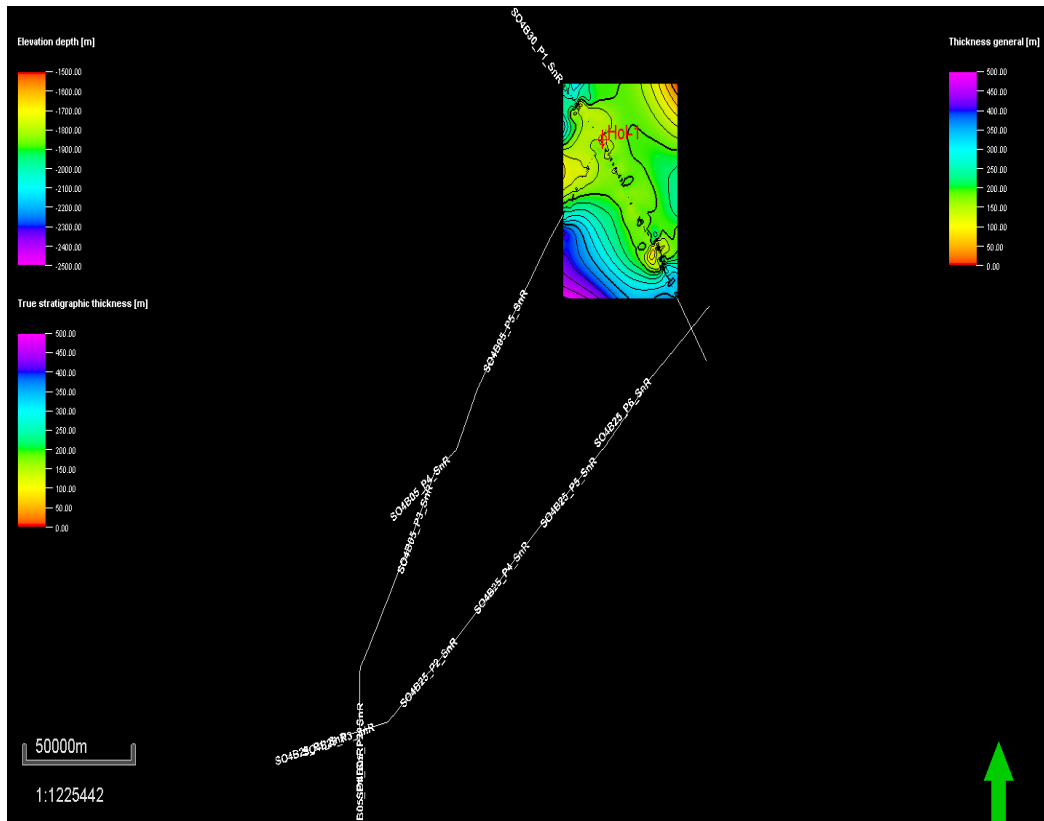
Figure 4.51: Isopach map between Bajocian and Bathonian-Lower Callovian base surfaces with seismic profiles
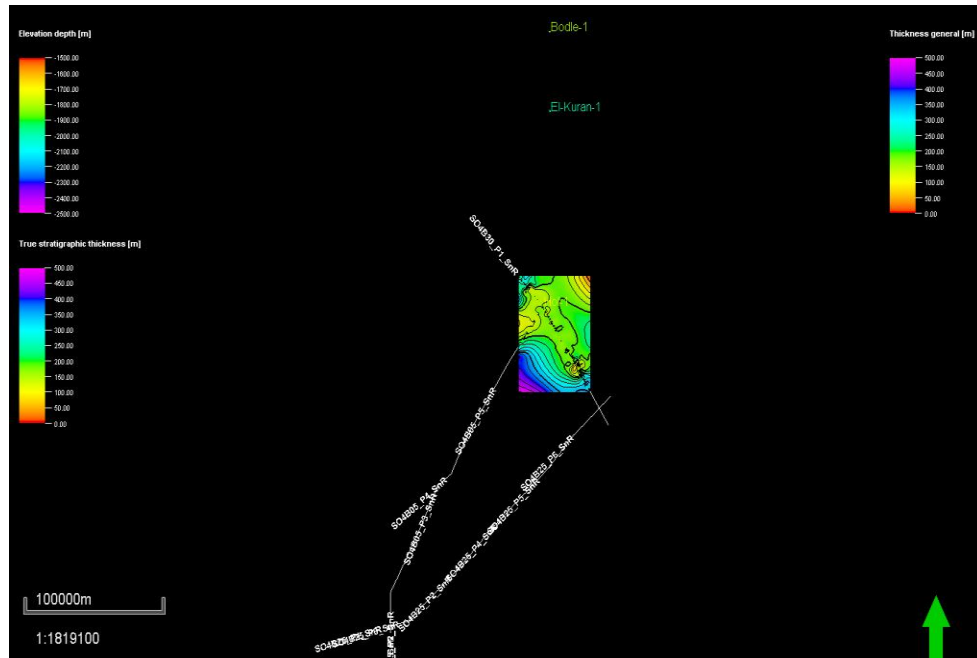
Figure 4.52: Isopach map between Bajocian and Bathonian-Lower Callovian base surfaces with seismic profiles and well loctions from neighboring wells from the Ogaden basin.

➢ **Reservoir Rock (Topmost Iscia Baidoa Formation: Baidoa and Goloda Members; Upper Hamenlei)**

According to Benvenuti et al. (1993), the Iscia Baidoa formation is one of the most important water aquifers of the Bay region in south-western Somalia. Outcrops of this formation occur further to the south east where they transgressively overlay the Bur crystalline basement. Here, the Goloda Member of the Baidoa formation is characterized by high permeability properties due to increased fracturing and karstism. Additionally, this same research concluded that the prevailing flow direction of the subterranean waters was to the south-east (towards the Bur Acaba high). As such, it seems very likely that the distribution of some hydrocarbon accumulations may have been controlled by the hydrodynamic forces. This option offers the development of a supplementary, hydrodynamic type of trap. This trap would contain a water drive oil and gas reservoir.

d) Thickness map (?) between Lower Callovian-Bathonian and Callovian-Oxfordian base surfaces (mid Upper Hamenlei=top Anole Formation=Goloda Member).

Both isochore and isopach (Figures 4.53 &4.55) maps for the Lower Callovian-Bathonian and Callovian-Oxfordian base surfaces (mid Upper Hamenlei=top Anole Formation=Goloda Member) are identical, thus, indicating that rectified isochore (Fig 4.54) and Isopach (Figure 4.56) thickness maps show that the thicknesses are increased in the north and eastern parts of the survey area.

The maps demonstrated development of several highs, it is largely possible, that the hydrocarbons might have been redistributed and accumulated towards the northern-western and south-western parts of the study area. At least two closed structures (anticlinal crests/dorms?) have been mapped to the north-west and south-west of the survey area (Figure 4.55). The orange area represents the most elevated parts of the reservoir with arrows indicating the likely directions of hydrocarbons migration.
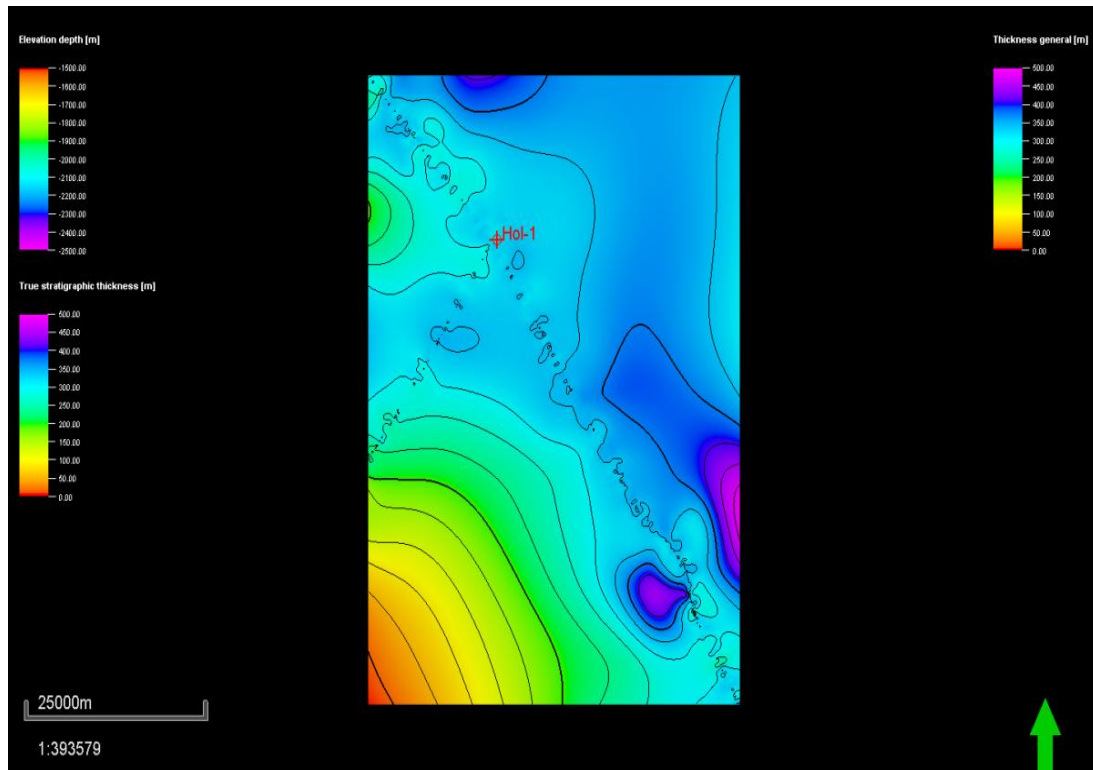
Figure 4.53: Isochore map between Bathonian-Lower Callovian and Callovian-Oxfordian base surfaces.
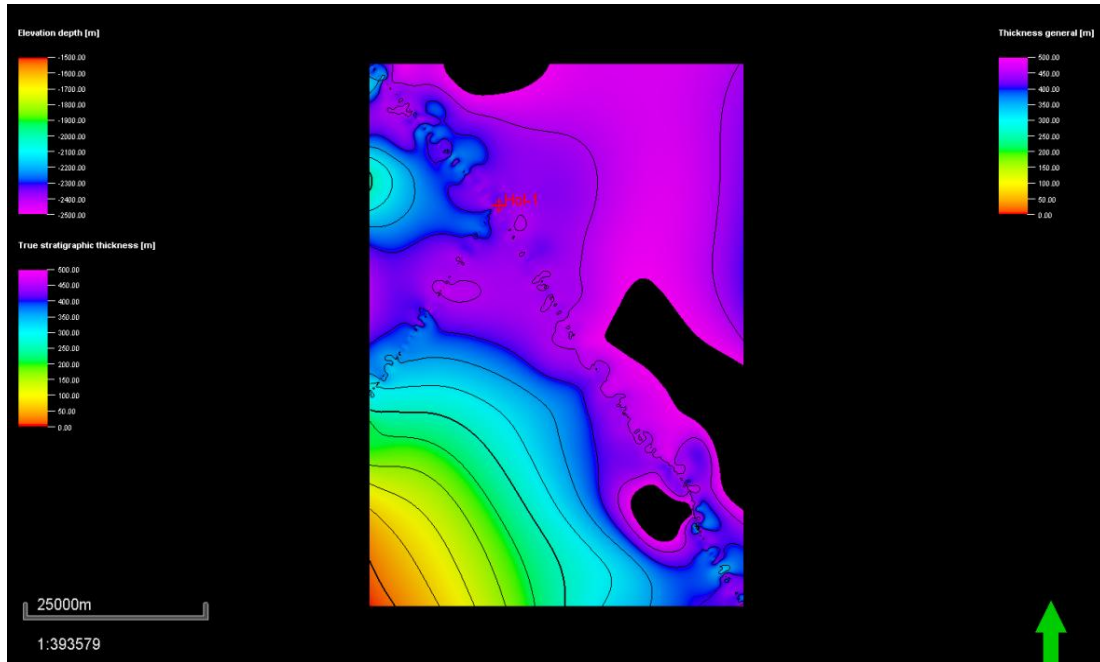
Figure 4.54: Rectified Isochore map between Bathonian-Lower Callovian and Callovian-Oxfordian base surfaces after eliminating negative elevation depth values
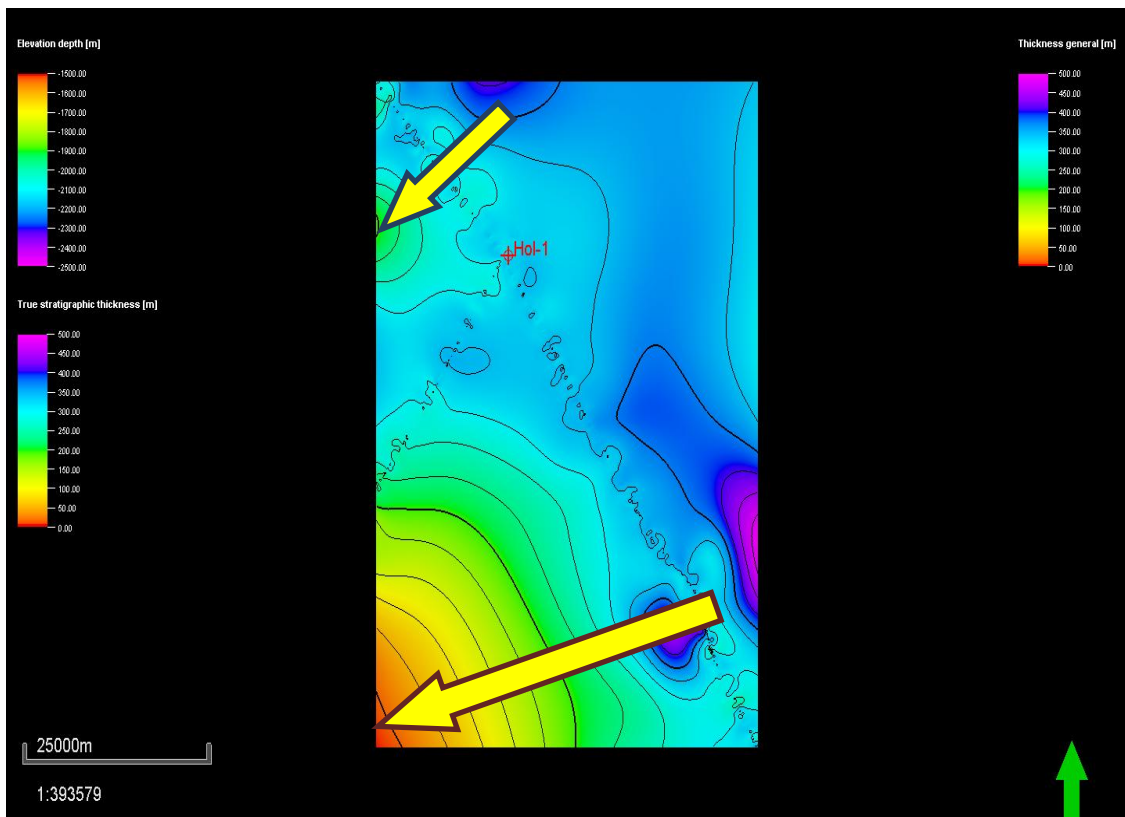
Figure 4.55: Isopach thickness map of the Goloda Member with evidence of fold structures at the north-western and south-western part of the survey area.
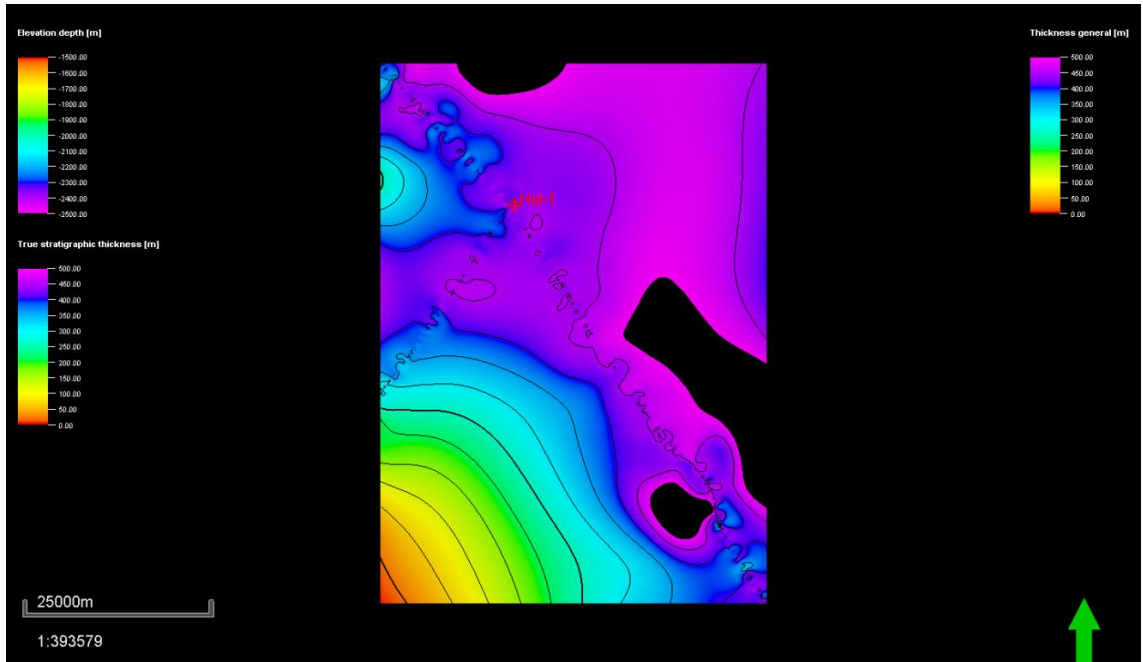
Figure 4.56: Rectified Isopach map between Bathonian-Lower Callovian and Callovian-Oxfordian base surfaces (Goloda Member) after eliminating negative elevation depth values.

Figures 4.57 and 4.58, shows Isopach maps between Bathonian-Lower Callovian and Callovian-Oxfordian base surfaces (Goloda Member) with seismic profiles and well locations from neighboring wells from the Ogaden basin respectively.
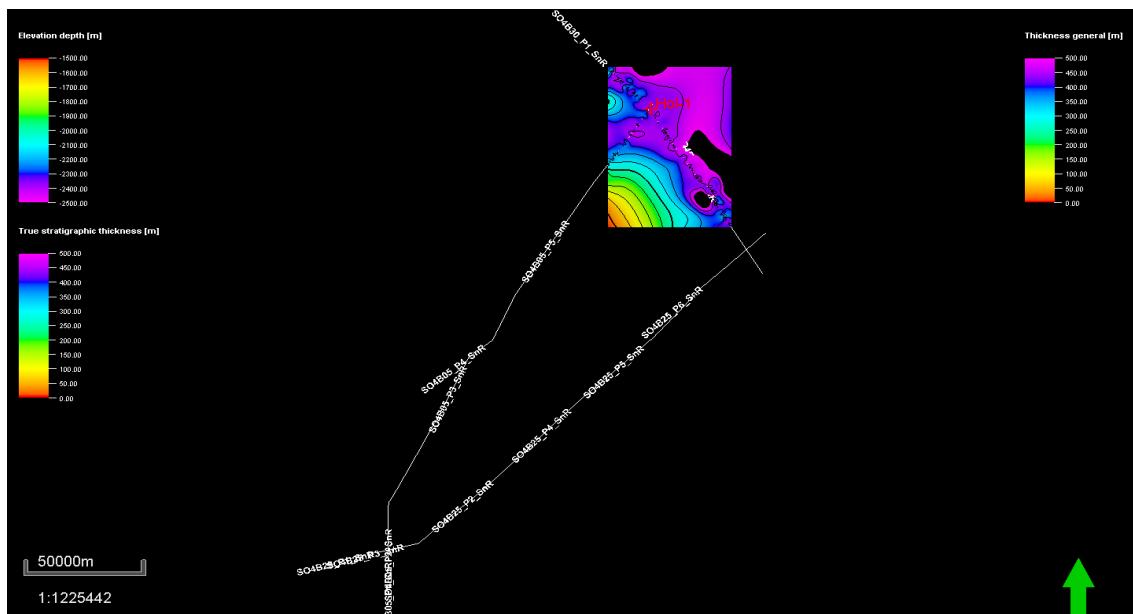
Figure 4.57: Isopach map between Bathonian-Lower Callovian and Callovian-Oxfordian base surfaces (Goloda Member) with seismic profiles.
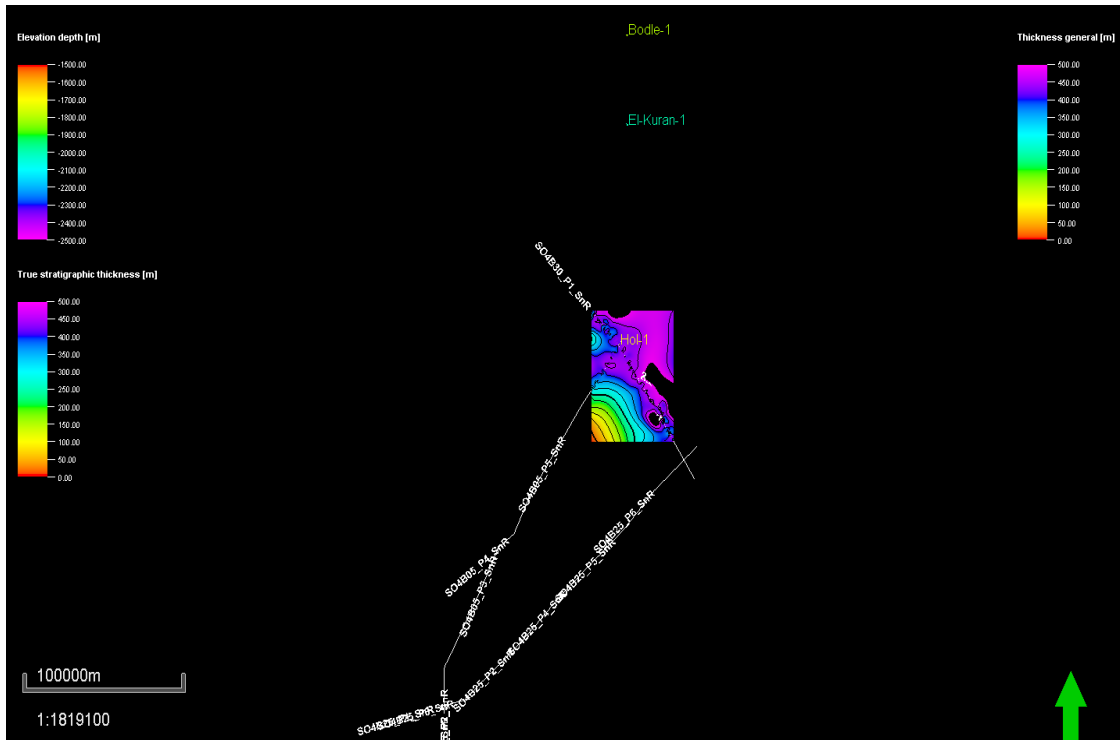
Figure 4.58: Thickness map of the Goloda Member with the location seismic profiles and exploration wells from neighboring Ogaden basin.

The Mesozoic formations of Lugh-Mandera basin experienced folding and faulting during Late Cretaceous around 80 Ma, due to the compressive phase associated with right transpressional strike slip movement, in conjunction with NE-SW dipping rift zone (Boccaletti et al., 1988) as shown in Figure 4.59.
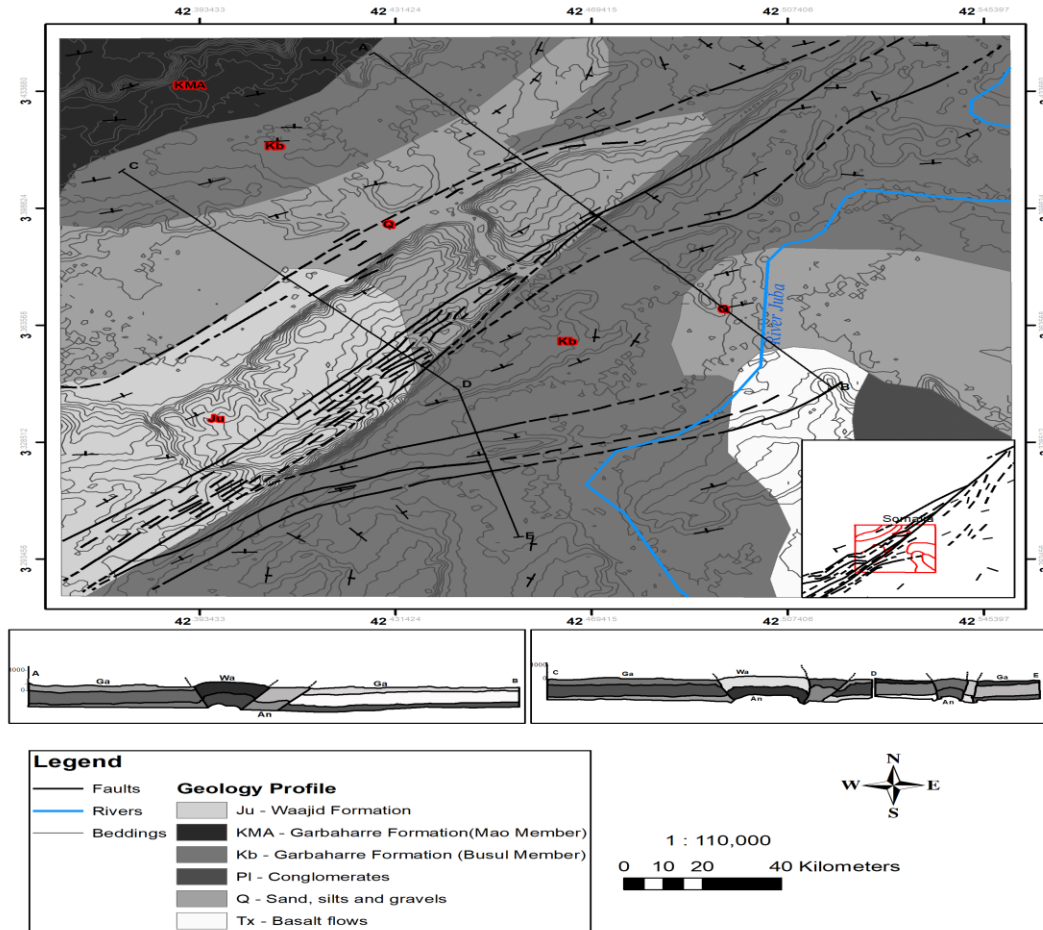
Figure 4.59: Modified Schematic section of the Lugh-Mandera basin (after Beltrandi and Pyre, 1973).

A TTI modeling for this interval gives a value of 5.1 which equivalent to a Vitrinite Reflectance (Ro) of 0.6%. This indicates that the Upper Jurassic source rock is located within the early oil window zone, which began expulsion in the Oxfordian (approximately 161.5 Ma) ago. When correlating the expulsion events of hydrocarbons with the structure formations, it indicates that the structure were not in place to entrap the expelled oil. Re-distribution of hydrocarbons is the only way to get hydrocarbon accumulation within the structures formed in Late Cretaceous.

➢ **Source Rock Element**

• **Thickness map between Callovian-Oxfordian and Oxfordian base surfaces (top Upper Hamenlei = top Anole/bottom Lower Uegit Formations).**

According to the log and driller's report data, the 2349-2973' interval in well Hol-1 data characterizes the topmost Anole and bottom Lower Uegit or top Upper Hamenlei. The paleontology refers this section to the Mid-Late Jurassic (Callovian-Oxfordian stages). These stages include the Uarandab depositional sequence in the chronostratigraphic chart of Somalia (Bosellini, 1992) that developed during the major marine transgression and coeval final breakup of Africa and Madagascar. On the other hand, Ali Kassim et al. (2002) considers the early Kimmeridgian-Callovian successions in Lugh-Mandera basin within the Anole formation. Geochemical studies undertaken for this selected sections from Hol-1 well have indicated the average TOC values of >0.5% that qualifies it as a poor quality source rock. The predominant lithological composition of the Callovian – Oxfordian (Top Anole Formation) section is presented by limestones as shown in Figure 4.60) suggesting a potential carbonate and fracture reservoir type.
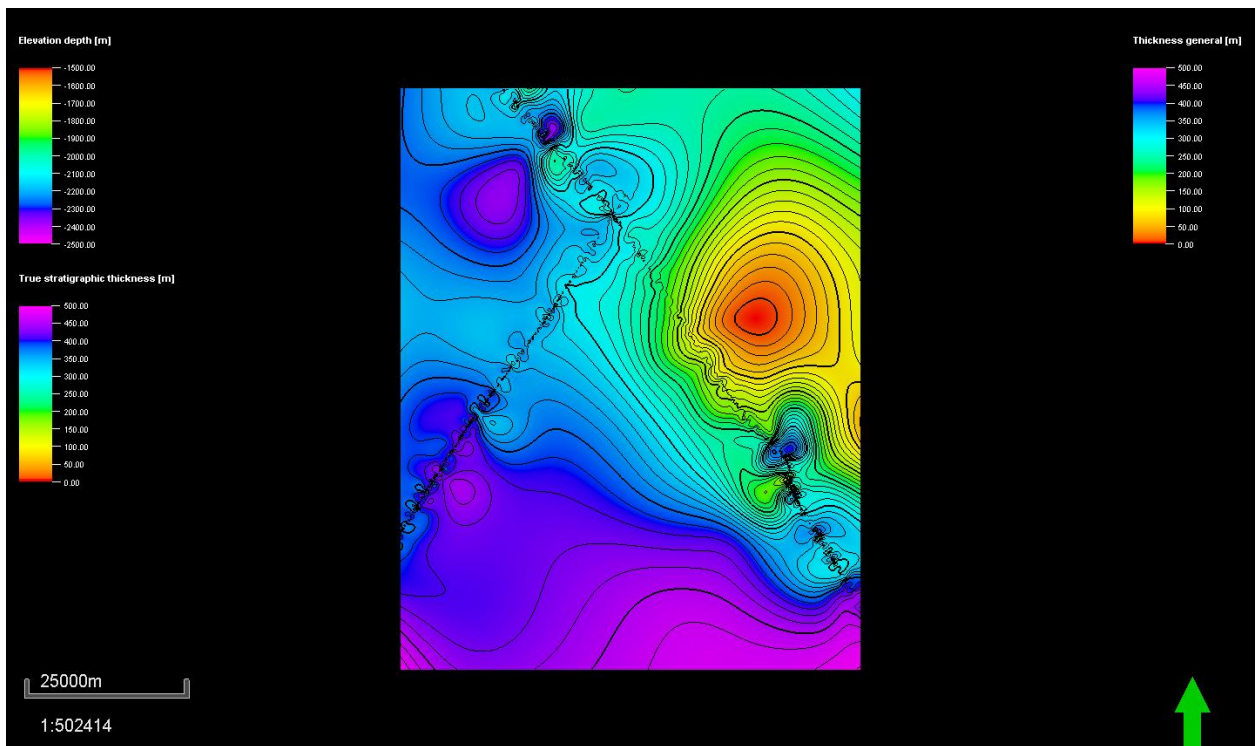
Figure 4.60: Isochore map between Callovian-Oxfordian and Oxfordian base surfaces

This same interval recorded the presence of a gas show at the depth of 2900` which also suggests some reservoir properties. However, as Benvenuti et al. (1993) mention, the Uegit formation found outcropping further at the south-east near the Bur Acaba basement high is characterized by low permeabilities. As such, this formation can only store natural gas accumulations. Alternatively, these strata could have a potential for generating permeability barriers of heavier hydrocarbons in the south-east of the survey area as shown by the arrows in figure 4.61.
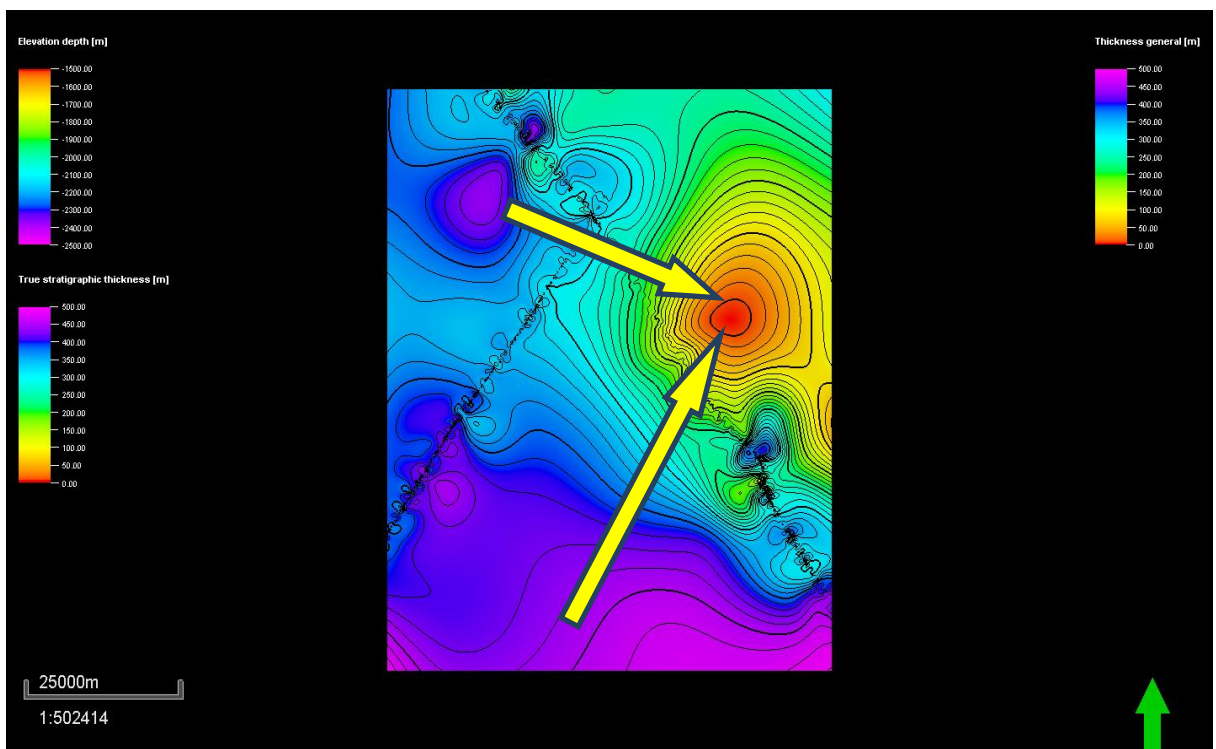
Figure 4.61: Isopach map between Callovian-Oxfordian and Oxfordian base surfaces with arrows indicating probable hydrocarbon migration pathways.

The thicknesses of Callovian-Oxfordian (top Anole-lower Uegit? Upper Hamenlei) strata are thicker and are located deeper in the western and southern parts (500 m) and become thinner towards the eastern and south-eastern area of the survey area (0-200 m). The concentric configuration of the surface characterizes a broad domal structure with shallow dipping limbs. The structure has a vertical closure of approximately 200 meters and areal closure of 25 sq. km. This structure should be tested by some infill drilling. The

140

thicknesses mapped here are higher than those reported further to the north, within the Ogaden basin (Hunegnaw et al., 1998).

3D view Isopach map between Callovian-Oxfordian and Oxfordian base surfaces can be seen in (fig 4.62).
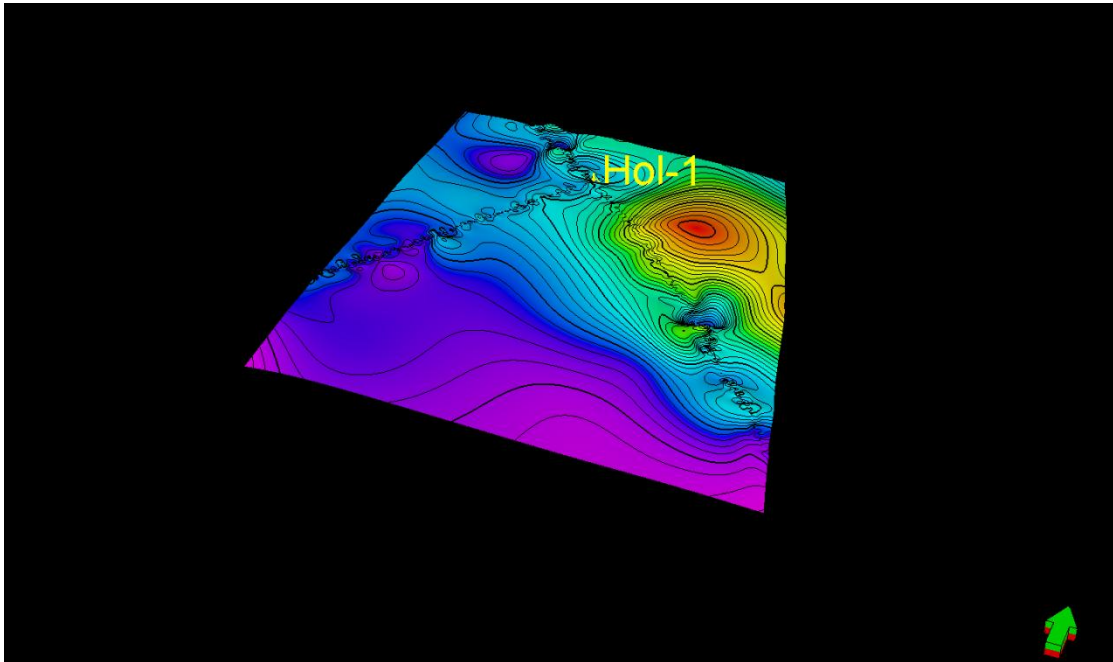
Figure 4.62: 3D view Isopach map between Callovian-Oxfordian and Oxfordian base surfaces.

Upper Hamenlei carbonate reservoirs from the Ogaden basin located further to the north from the survey area are represented by uncemented grainstones and packstones with good porosities (10-23%) and permeabilities (10mD-1 Darcy) values (Hunegnaw et al., 1998). In the Calub Saddle and eastern part of Ogaden, these reservoir units have a constant thickness distribution (40-135 m) and are overlain by dark, organic rich shales of the Kimmeridgian Uarandab formation that acts as both as a source and seal rock. This formation is considered as the best quality source rock in the Ogaden basin with type II kerogen. Unfortunately, the quality of the seismic data from the shallower depths and the issues with the reference data used for the seismic well tie does not allow us to map the extent of the Uarandab, Gabradarre and Busul formations which equivalent to Upper Uegit and Garbaharey formations in accordance to mud logger's report in Hol-1 well.

Figures 4.63 and 4.64, shows Isopach maps between Callovian-Oxfordian and Oxfordian base surfaces with seismic profiles and exploration wells from neighboring Ogaden basin respectively.
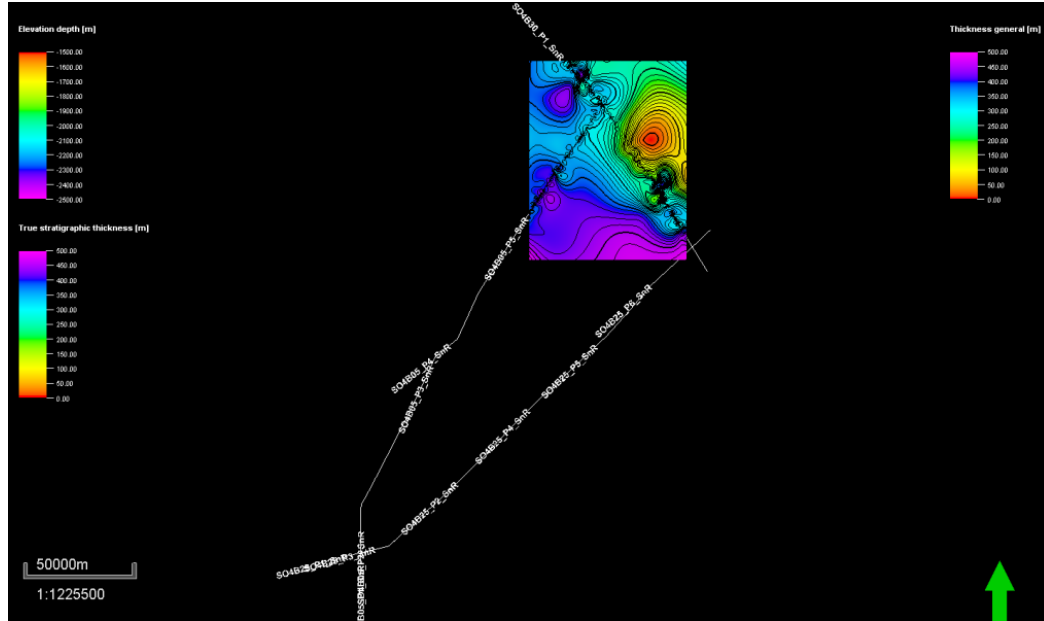
Figure 4.63: Isopach map between Callovian-Oxfordian and Oxfordian base surfaces with seismic profiles.
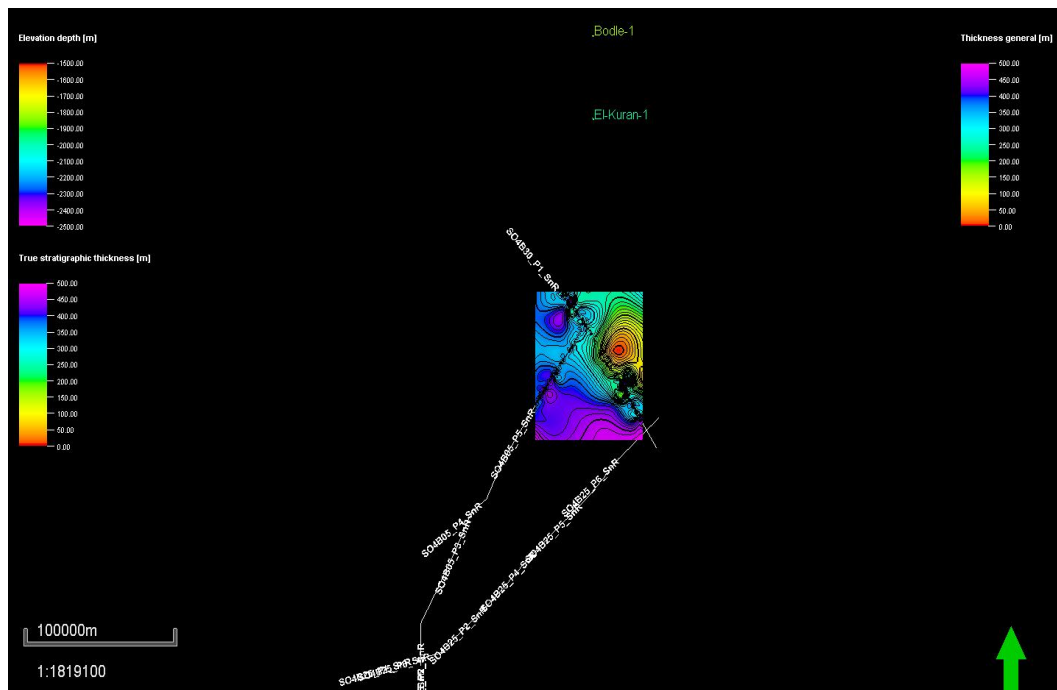
Figure 4.64: Isopach map between Callovian-Oxfordian and Oxfordian base surfaces with seismic profiles and exploration wells from neighboring Ogaden basin.

The nature of this dormal structure is seen through the interpreted seismic profiles of SO4B30_P1_SnR, SO4B30_P2_SnR and SO4B30_P3_SnR (See below). In all cases the importance of flower structures is obvious.
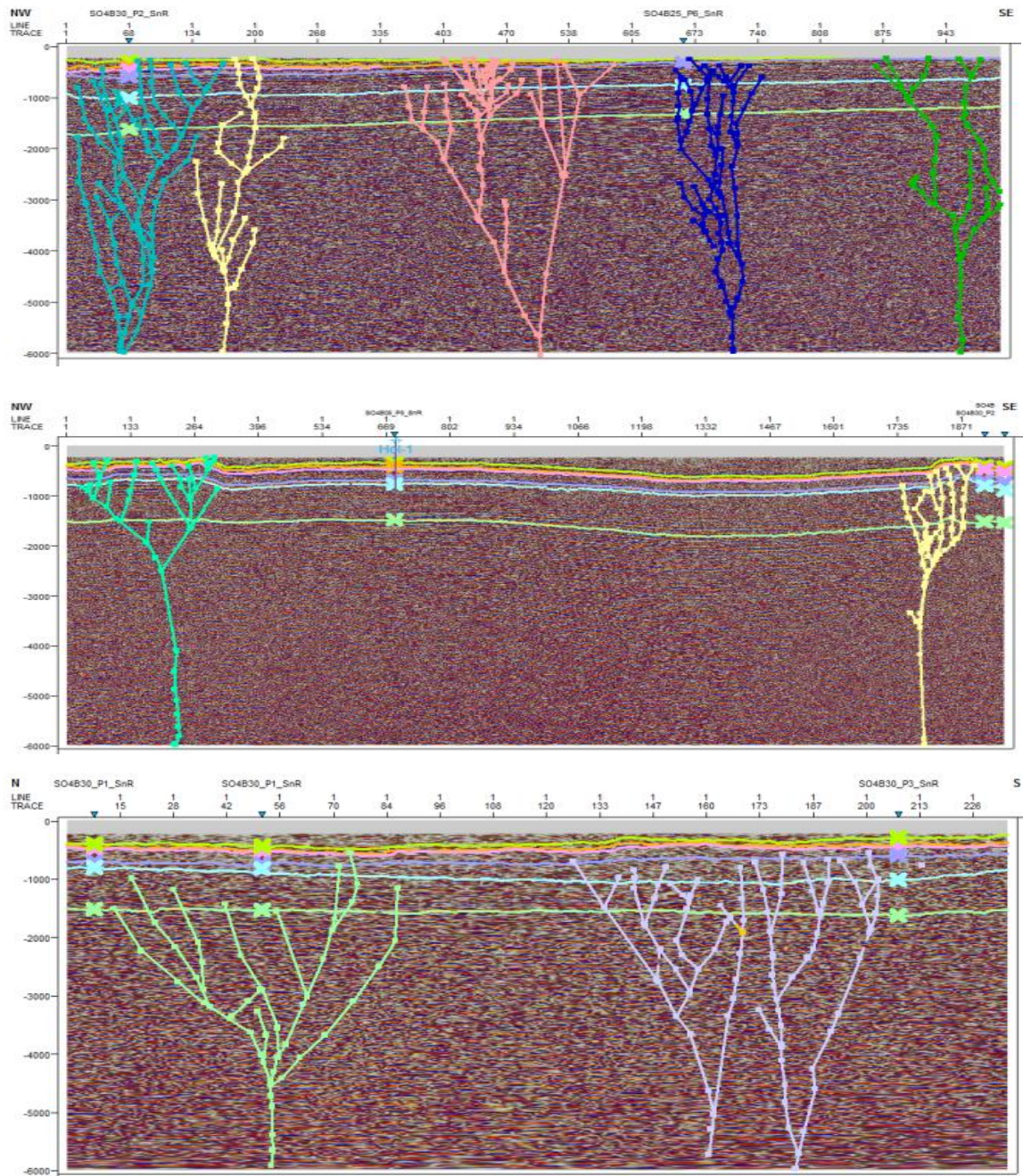
Figure 4.65: Summarized interpretations for SO4B30_P1_SnR, SO4B30_P2_SnR and SO4B30_P3_SnR seismic profiles demonstrating broad anticlinal (dormal) and syncline structures seen in the Callovian-Oxfordian and Oxfordian base subsurface maps.

4.5. Time-Temperature Index Source Rock Maturation Modeling for Hol-1 well

4.5.1. Sedimentation rate

The Lower Jurassic accumulated during a rapid sedimentation rate condition (525'/1Ma) from about 196 Ma to about 182.7 Ma, and the upper curve is represented by 62.9'/Ma from about 182.7 Ma to about 170Ma in the Hol area. It was followed by small uplift around (170Ma) Aalanian age. These are represented by Adigrat and Iscia-Baidoa Formations.

Middle/Upper Jurassic experienced the highest sedimentation rate of (1005'/1Ma) within two years starting from 170Ma, and the slowest sedimentation rate recorded were 23'/Ma from about 152Ma to about 130Ma. These are represented mostly by Anole, Uegit, and the upper part of Iscia-Baidoa Formations as shown in (figure 4.66). From about 130 Ma up to present, deposited at the lowest rate of 0.8'/Ma, which indicate the withdrawal of sea from south western to northeastern of Somalia and Ogaden vicinity.
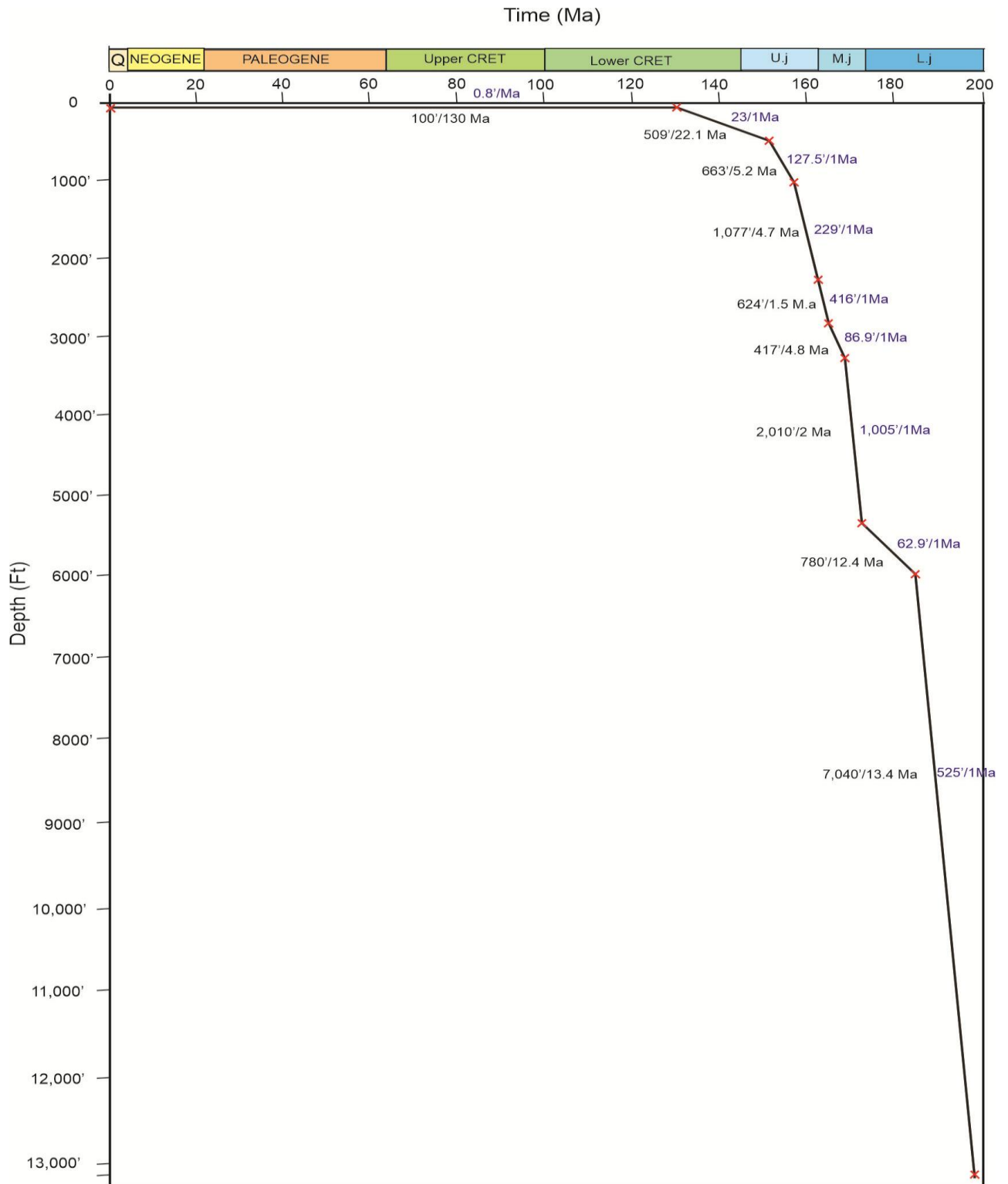
Figure 4.66: Hol-1 well Sedimentation Rate Curve.

4.5.2. Time-Temperature Index (TTI) for Hol-1 Well

The TTI curves for Hol-1 well consist of a family of eight burial history curves; each of them represents subsidence rates of sedimentary package.

The general tectonic setting has been one of extension; first occurred during the Permo-Triassic Karroo times, while the second occurred during the Jurassic separation of Madagascar and India from Africa along the Indian Ocean coast, and finally the formation of EARS during Oligocene (Bosellini, 1992, Hunegnaw et al., 1998).

The lowest TTI curve in the lower Jurassic shows more rapid subsidence due to the Karoo rifting. It was followed by small uplift around Aalenian age which is reflected only the lowest curve as shown in Figure 4.67.

The subsidence rate where at the pick during the Middle and Upper Jurassic times due to the separation of Madagascar from Africa, as the basin began to subside rapidly again, before ending with the cessation of subsidence around 130 Ma ago. During this period the following formations has been deposited; Iscia-Baidoa carbonates, evaporates, the marls and shales of Anole, the shallow marine limestone, and the Lower member of Garbaharey busul, and they all represent the syn-rift sequence.

The last TTI curves show relative stability from about 130 Ma till present which characterize the cease of sedimentation in south-western Somalia.

B.H.T= 140 °C

S.T= 29 °C

T.D= 13,258' (4,042 m)

Time-Temperature Index Curve for Hol-1 Well

State	Formations	Age (M.a)	Depth (Ft)	TTI
Immature		0	0'	
		130	100'	
		152,1	609'	
	Tith-Kim	157.3	1272'	1.2
	Oxfordian	162	2349'	2.5
Early Oil	Oxf-Cal	163.5	2973'	4.9
	L.Cal-Bath	168.3	3390'	5.1
Normal Oil	Bajocian	170.3	5400'	20
	Toarcian	182.7	6180'	20.8
Dry Gas	Plien-Het	196.1	13,258'	1,319

Figure 4.67: Superposition of temperature grid on the Time-Temperature Index (TTI) curve for Hol-1 well.

4.5.3. TTI Calculation for the Lower Jurassic Sediments of Hol-1 well

A Vitrinite Reflectance of greater than 2 equates to a TTI value of 1,319, suggesting that high Jurassic source rocks are fully mature and at present are within dry gas window, which started at 182.7 Ma (Pliensbachian) and is located between 6180' - 13,258' (1,884-4,042m) interval.

From Table 4.1 it is clear that the rock is currently still within the dry gas window since the value for cumulative TTI is 1,319 which corresponds to the occurrence of dry gas window. But the generation of hydrocarbons (HC's) began when the temperature got

close to 90 ~ degrees Celsius corresponding to 172Ma ago (Aalenian stage, Middle Jurassic).

Table 4.1: TTI Calculation for the Lower Jurassic Sediments from Hol-1 well

Temperature interval	n	Time factor	r^n	TTI Interval	TTI Cumulative	Ages M.A
20-30C^o	-8	0.125	$1/256$	0.0005	0.0005	196
30 – 40C^o	-7	0.5	$1/128$	0.005	0.0045	196 – 195.5
40 – 50C^o	-6	0.5	$1/64$	0.008	0.0125	195.5– 195
50 – 60C^o	-5	1	$1/32$	0.03	0.0425	195 – 194
60 – 70C^o	-4	1	$1/16$	0.063	0.1055	194 – 193
70 – 80C^o	-3	1	$1/8$	0.125	0.2305	193 – 192
80 – 90C^o	-2	20	$1/4$	5	5.2305	192– 172
90 – 100C^o	-1	1	$1/2$	0.5	5.7305	172 – 171
100 – 110C^o	0	0.8	1	0.8	6.5305	171 – 170.2
110- 120C^o	1	6.2	2	12.4	18.9305	170.2 – 164
120 – 130C^o	2	3	4	12	30.9305	164 – 161
130 – 140C^o	3	161	8	1,288	1,319	161– 0

4.5.4. TTI Calculation for the Middle Jurassic Sediments of Hol-1 well

A Vitrinite Reflectance of less than 0.9 equates to a TTI of 20. This means that Middle Jurassic source rocks are fully matured and are presently within the typical oil window, which lies between 3,390 and 5,400 ft, and began expulsion 170.3 Ma ago, in the Bajocian.

Table 4.2 shows that the rock is still in the oil window at present since the value for cumulative TTI is 20 which define the top level occurrence of normal oil window. The generation of hydrocarbons (Hc's) began 156 Ma ago (Kimmeridgian stage, Late Jurassic).

Table 4.2: TTI Calculation for the Middle Jurassic sediments from Hol-1 well

Temperature interval	N	Time factor	r^n	TTI Interval	TTI Cumulative	Ages M.A
20-30C°	-8	0.0125	$1/256$	0.0005	0.0005	170
30 – 40C°	-7	0.0125	$1/128$	0.001	0.0015	170 – 170
40 – 50C°	-6	3	$1/64$	0.047	0.0485	170 – 167
50 – 60C°	-5	5	$1/32$	0.156	0.2045	167– 162
60 – 70C°	-4	6	$1/16$	0.379	0.5795	162 – 156
70 – 80C°	-3	156	$1/8$	19.5	20	156 – 0

4.5.5. TTI Calculation for the Upper Jurassic Sediments of Hol-1 well

A TTI value of 5.1 which is equivalent to a Vitrinite Reflectance (Ro) of 0.6% indicates that the Upper Jurassic source rock is within the early stages of the oil window zone, into which it entered in Oxfordian time (approximately 161.5 Ma) ago. The sediments within the early oil window are located between well depths of 2,400' - 2,973' (732- 906.4m) interval.

Table 4.3 it shows the distribution of TTI values corresponding to the early oil window. The cumulative TTI value is very low 5.1 which defines that the source rock interval is in the onset zone.

Table 4.3: TTI Calculation for the Upper Jurassic Sediments from Hol-1 well

Temperature interval	n	Time factor	r^n	TTI Interval	TTI Cumulative	Ages M.A
20-30C°	-8	0.125	$1/256$	0.0005	0.0005	168
30 – 40C°	-7	5	$1/128$	0.039	0.0395	168 – 163
40 – 50C°	-6	4	$1/64$	0.063	0.1025	163 – 159
50 – 60C°	-5	159	$1/32$	4.968	5.1	159 – 0

4.6. Time-Temperature Index Source Rock Maturation Modeling for Bodle-1 well (Ogaden basin, Ethiopia)

4.6.1. Sedimentation Rate

The Upper Triassic and Lower Jurassic shows a more rapid subsidence of 65'/1Ma from about 210 Ma to about 196 Ma, followed by Pleinsbachian time when the rates dropped to 39.5'/1Ma from about 196 Ma to about 157 Ma in the Bodle deep rift area. These are represented Adigrat-Lower Hamenlei formations. The Middle/Upper Jurassic experienced the highest sedimentation rate of about 83.9'/ 1Ma from about 157 Ma to about 152 Ma. These are represented by Uarandab and Gabredarre formations (figure 4.68). Lastly Qorahei formation shows relative stability up to day. For the last 145 Ma, the Bodle-1 area is a denudation zone with no evidence of deposition.

Bodle-1 well Sedimentation Rate Curve
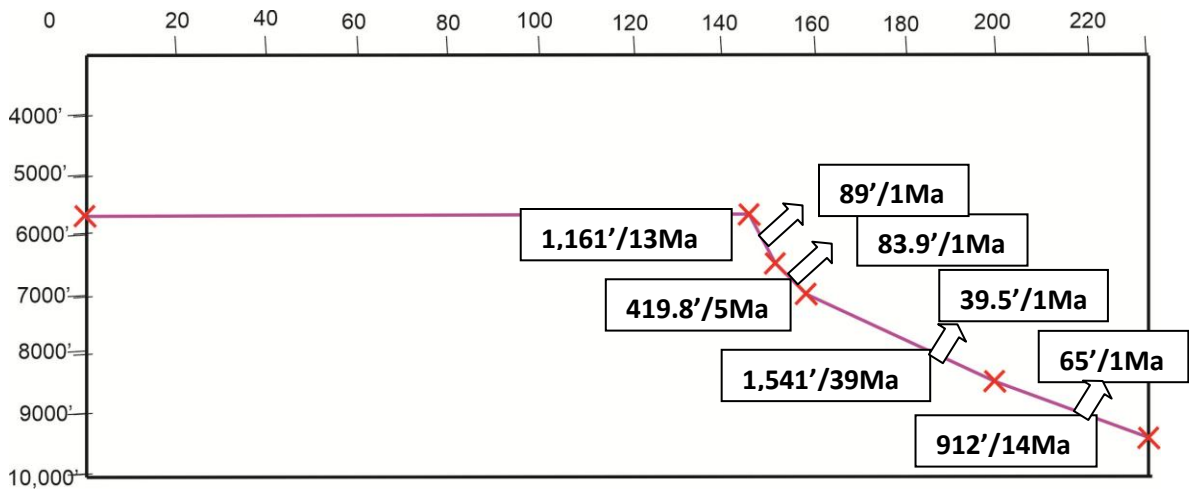
Figure 4.68: Sedimentation rate for Bodle-1 well

4.6.2. Time-Temperature Index (TTI) for Bodle-1 Well

The TTI curve for Bodle-1 well contains a family of four burial history curves; each of which represents the depositional history of the sedimentary packages figure 4.69.

The lowest TTI curve in the Upper Triassic shows more rapid subsidence due to the Karoo rifting. Increased subsidence rates are typical for the Middle and Upper Jurassic due to separation of Madagascar from Africa. The last TTI curves show relative stability from about 145 Ma up to day, which represent the cessation of sedimentation from Ogaden basin in Ethiopia.

Time-Temperature Index Curve for Bodle-1 well

State	TTI	Age	Depth
		145	5,523'
Normal Oil	73	152	6,684'
Late Oil	146	157	7,104'
Wet Gas	294	196	8,645'
	587	210	9,557'

B.H.T = 130 ºC
S.T = 28 ºC
T.D = 9,557' (2,911 m)
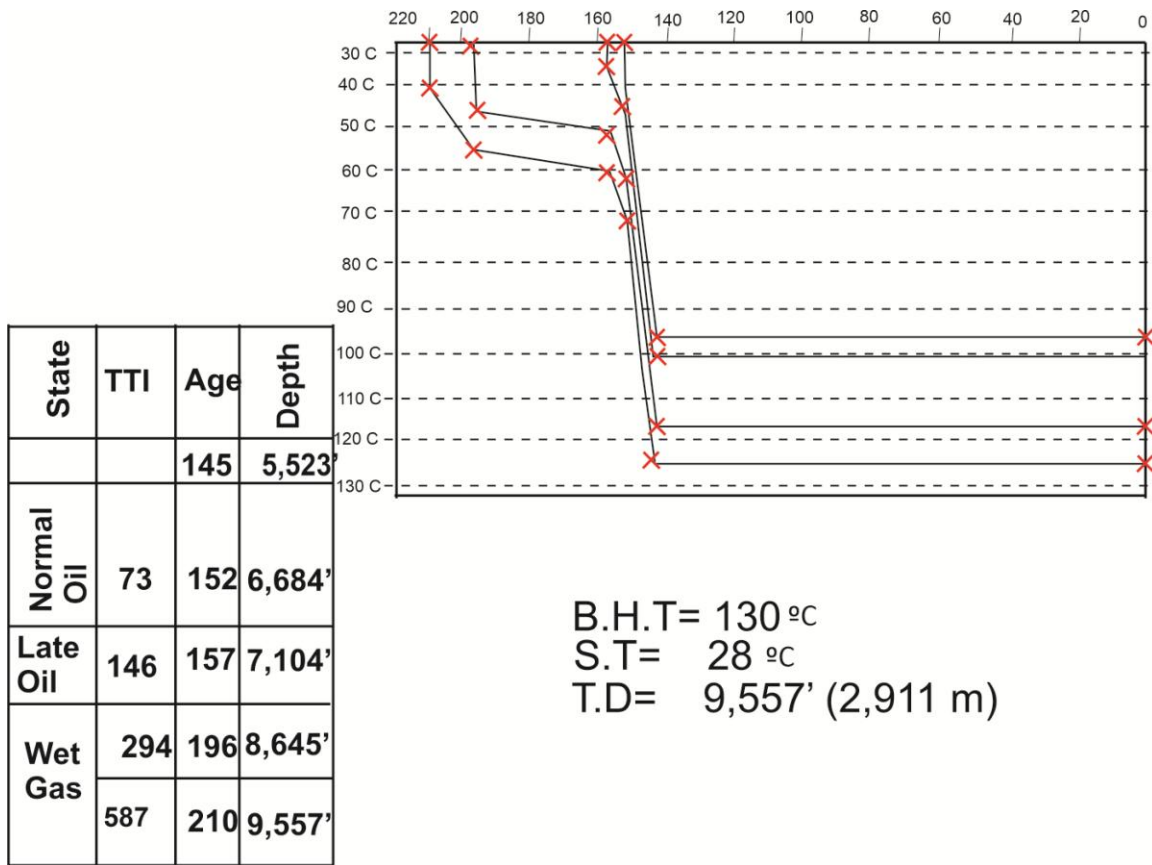
Figure 4.69: Superposition of temperature grid on the Time-Temperature Index (TTI) curve for Bodle-1 well.

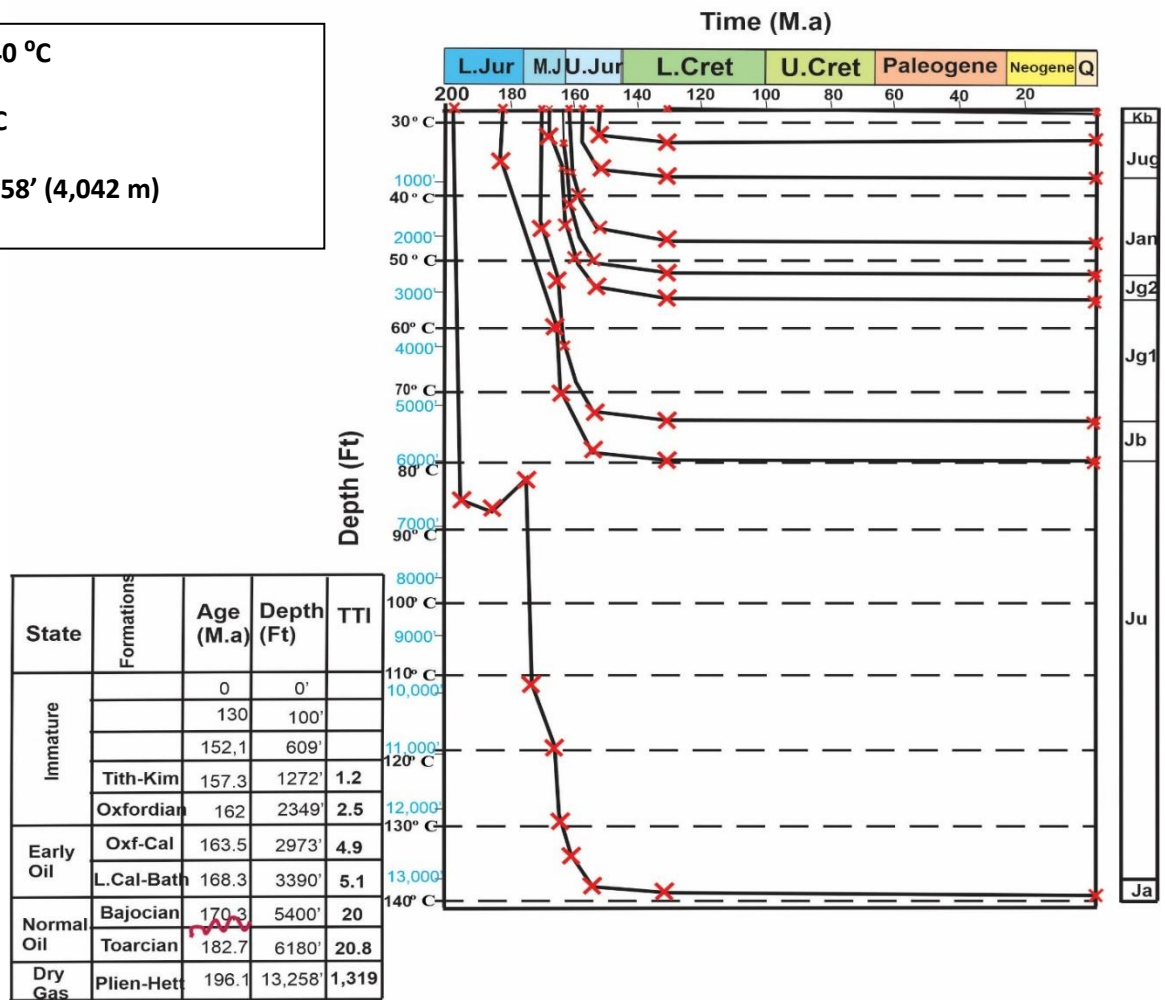### 4.6.3. TTI Calculation for the Upper Triassic Sediments of Bodle-1 well

A TTI value of 586.9 corresponds to a Vitrinite Reflectance (Ro) 1.75, suggesting that Upper Triassic source rocks are fully mature and are currently within the wet gas window which was initiated during the 210 Ma. The wet gas zone ranges between 8,645'- 9,557' (2,636 – 2,914m) interval.

Table 4.4 shows that the rock is still in the wet gas window zone at present since the value for the cumulative TTI is 586.9. But the generation of gas began 146Ma ago (Tithonian stage, Late Jurassic).

Table 4.4: TTI Calculation for the Upper Triassic sediments from Bodle-1 well

Temperature interval	n	Time factor	r^n	TTI Interval	TTI Cumulative	Ages M.A
20-30C^o	-8	0.125	$^1/_{256}$	0.0005	0.0005	210
30 – 40C^o	-7	0.5	$^1/_{128}$	0.004	0.0045	210 – 209.5
40 – 50C^o	-6	9.5	$^1/_{64}$	0.148	0.1525	209.5– 200
50 – 60C^o	-5	44	$^1/_{32}$	1.4	1.5525	200 – 156
60 – 70C^o	-4	4	$^1/_{16}$	0.25	1.8025	156 – 152
70 – 80C^o	-3	1	$^1/_8$	0.125	1.9275	152 – 151
80 – 90C^o	-2	2	$^1/_4$	0.5	2.4275	151– 149
90 – 100C^o	-1	1	$^1/_2$	0.5	2.9275	149 – 148
100 – 110C^o	0	2	1	2	4.9275	148 – 146
110- 120C^o	1	1	2	2	6.9275	146 – 145
120 – 130C^o	2	145	4	580	586.9	145 – 0

4.6.4. TTI Calculation for the Upper Jurassic Sediments of Bodle-1 well

A TTI value of 146 corresponds to a Vitrinite Reflectance (Ro) of 1.35, suggesting that the Upper Jurassic source rocks are completely mature and are currently within the Late oil window zone, which ranges between 6,684'-7,104' (2,038-2,166m), and entered into this condition at 157 Ma ago (Oxfordian stage, Late Jurassic).

Table 4.5 shows that the source rock is still within the Late oil window zone at present corresponding to a cumulative TTI value of 146. The oil generation began 145 Ma ago (Tithonian stage, Late Jurassic).

Table 4.5: TTI Calculation for the Upper Jurassic sediments from Bodle-1 well

Temperature interval	N	Time factor	r^n	TTI Interval	TTI Cumulative	Ages M.A
20-30C°	-8	0.125	$1/256$	0.0005	0.0005	157
30 – 40C°	-7	3	$1/128$	0.0234	0.0239	157 – 154
40 – 50C°	-6	3	$1/64$	0.468	0.0707	154 – 151
50 – 60C°	-5	1	$1/32$	0.0313	0.102	151– 150
60 – 70C°	-4	1	$1/16$	0.0625	0.1645	150 – 149
70 – 80C°	-3	2	$1/8$	0.25	0.4145	149 – 147
80- 90 C	-2	1	1/4	0.25	0.6645	147—146
90-100 C	-1	1	1/2	0.5	1.1645	146-145
100-110 C	0	145	1	145	146	145-0

4.7. Time-Temperature Index Source Rock Maturation Modeling for El Kuran-1 well (Ogaden basin, Ethiopia)

4.7.1. Sedimentation Rate

The Upper Triassic and Lower Jurassic shows rapid sedimentation rates of 66'/ 1Ma from about 210 Ma to about 196 Ma, followed by Pleinsbachian ages with a rate of which is represented by 95.3'/ 1Ma from about (196 Ma to about 157 Ma). These are represented Adigrat and Hamenlei formations. The Middle/Upper Jurassic experienced the highest sedimentation rate of about 910'/ 1Ma from about (157 Ma to about 152 M.a). subsequently by another curve which deposited 84.3'/ 13 Ma. These are represented by Uarandab and Gabredarre formations. Qorahei formation shows relative stability up to day as shown in (figure 4.70).

Denudation processes in the El-kuran area dominate for the last 152 Ma (stage).

El Kuran-1 well Sedimentation Rate Curve
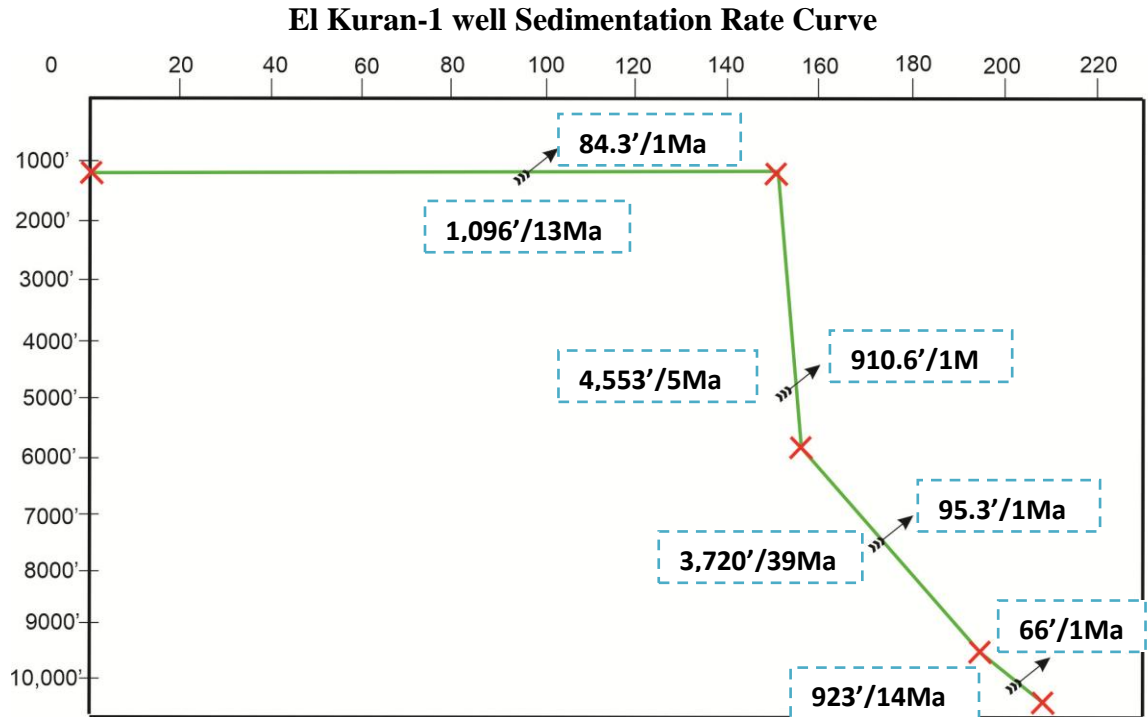
Figure 4.70: Sedimentation rate for El Kuran-1 well

4.7.2. Time-Temperature Index (TTI) for El Kuran-1 Well

The TTI curve for El Kuran-1 well contains a family of four burial history curves; each of them represents subsidence rates of sedimentary package as shown in (figure 4.71).

The lowest TTI curve in the Upper Triassic shows more rapid subsidence due to the Karoo rifting. The subsidence rate where at the top during Middle and Upper Jurassic due to separation of Madagascar from Africa. The last TTI curves show relative stability from about 145 Ma up to day, which represent the cessation of sedimentation from Ogaden basin in Ethiopia.

Time-Temperature Index Curve for El Kuran-1 well

State	TTI	Age	Depth
		145	161'
Immature	1.2	152	1,257'
Early Oil	19.3	157	5,810'
Normal Oil	84	196	9,530'
Late Oil	165.3	210	

B.H.T= 104.76ºC
S.T= 28 ºC
T.D= 10,462' (3189 m)
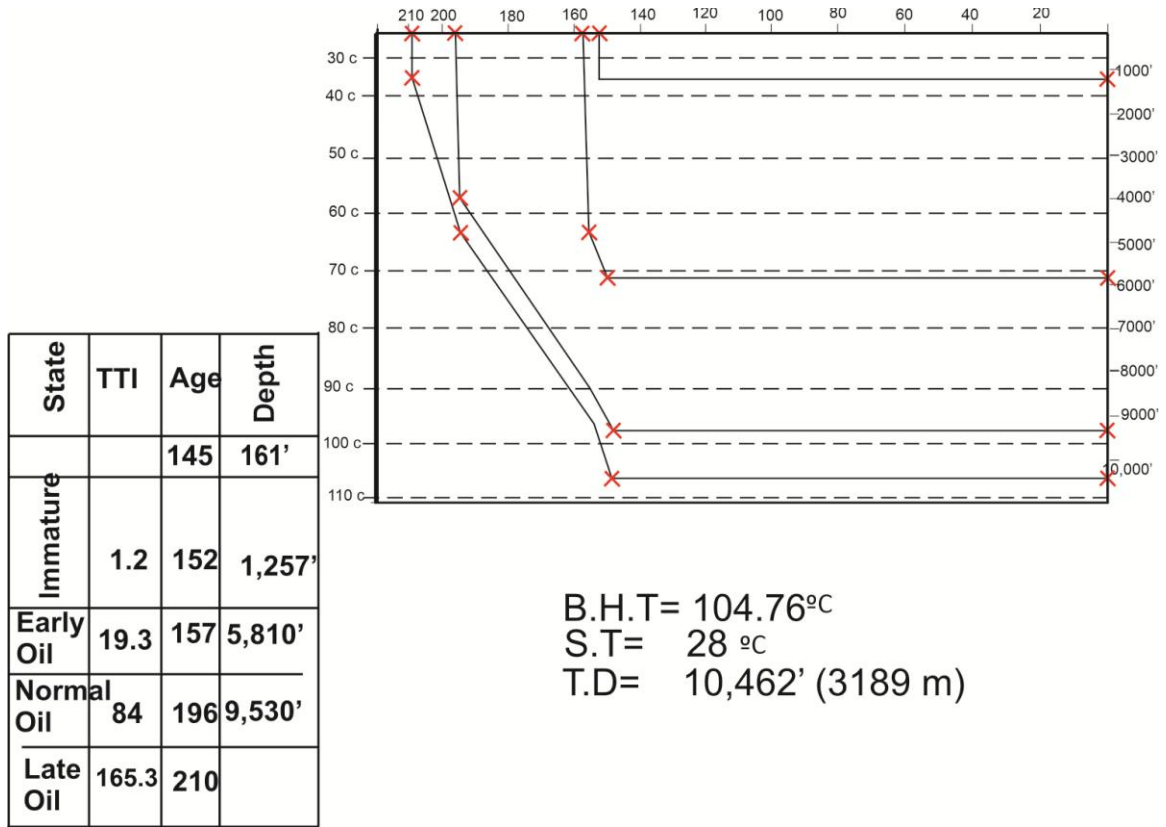
Figure 4.71: Superposition of temperature grid on the Time-Temperature Index (TTI) curve for El kuran-1 well.

4.7.3. TTI Calculation for the Upper Triassic Sediments from El Kuran-1 well

A TTI of 165.3 corresponds to a Vitrinite Reflectance of 1.35, suggesting that the Upper Triassic source rocks are completely mature and are presently even within Late oil window zone which was initiated some at 210 Ma ago (Norian stage). The Late oil window zone ranges between 9,530'-10,462'(2,905-3,189m) interval.

Table 4.6 demonstrates that the source rock is still within the Late oil window at present corresponding to a cumulative TTI value of 165.3. The oil generation began 165Ma ago Middle Jurassic (Callovian stage).

Table 4.6: TTI Calculation for the Upper Triassic sediments from El-Kuran-1 well

Temperature interval	N	Time factor	r^n	TTI Interval	TTI Cumulative	Ages M.A
20-30C°	-8	0.125	$\frac{1}{256}$	0.0005	0.0005	210
30 – 40C°	-7	2	$\frac{1}{128}$	0.0156	0.0161	210 – 209.5
40 – 50C°	-6	5	$\frac{1}{64}$	0.0781	0.0942	209.5– 200
50 – 60C°	-5	6	$\frac{1}{32}$	0.1875	0.2817	200 – 156
60 – 70C°	-4	8	$\frac{1}{16}$	0.5	0.7817	156 – 152
70 – 80C°	-3	12	$\frac{1}{8}$	1.5	2.7817	152 – 151
80 – 90C°	-2	12	$\frac{1}{4}$	3	5.7817	151– 149
90 – 100C°	-1	10	$\frac{1}{2}$	5	10.2817	149 – 148
100 – 110C°	0	155	1	155	165.3	148 – 146

4.7.4. TTI Calculation for the Lower Jurassic Sediments of El kuran-1 well

A TTI of 84 corresponds to Vitrinite Reflectance of 1. This means that Lower Jurassic source rock is fully mature and is currently within the normal light oil window, which lies between 5,810'- 9,530' (1,771-2,905 m) interval, and began at 196 Ma in the Sinemurian stage.

Table 4.7 it shows that the source rock is still in the normal light oil window zone at present corresponding to a cumulative TTI value of 84, which define the occurrence of normal light oil window zone. The oil generation began at around 157 Ma ago (Oxfordian stage, Late Jurassic).

Table 4.7: TTI Calculation for the Lower Jurassic sediments from El Kuran-1 well

Temperature interval	N	Time factor	r^n	TTI Interval	TTI Cumulative	Ages M.A
20-30C°	-8	0.125	$\frac{1}{256}$	0.0005	0.0005	196
30 – 40C°	-7	0.125	$\frac{1}{128}$	0.0009	0.0014	196 – 195.8
40 – 50C°	-6	0.125	$\frac{1}{64}$	0.0019	0.0033	195.8– 195.75
50 – 60C°	-5	2.75	$\frac{1}{32}$	0.09375	0.09705	195.75– 193
60 – 70C°	-4	11	$\frac{1}{16}$	0.6875	0.78455	193 – 182
70 – 80C°	-3	12	$\frac{1}{8}$	1.5	2.28455	182 – 170
80- 90 C	-2	13	1/4	3.25	5.53455	170—157

90-100 C	-1	157	1/2	78.5	84	157-0

4.8. Discussion

According to stratigraphic studies, the Lugh-Mandera basin has a thick Lower and Middle Jurassic strata and thinner Upper Jurassic to Early Cretaceous layers, according to stratigraphic studies. The basin's Jurassic sediments thicken in the northern half of the basin, where the deposit layers are found deeper than 13,258' (4,040m). The Jurassic and Early Cretaceous strata appear to be more deformed than the pre-Jurassic sediments, indicating that wrench fault tectonics has affected mostly the top sequences with flower structure.. The basement rocks are located much deeper probably at depth of around 8 km, under the thick formations of the Karoo group.

Lower and Middle Jurassic successions comprise interbeding layers of sands, silty shales, dark grey limestones, grey green clays locally fossilfereous, dolomites and evaporites with fluvio-deltaic, shallow marine with intertidal and lagoonal episodes. This section has two potential petroleum system intervals, i.e, the first interval located in the lower part indicating grey lime mudstone zone between 12,980'-13,250' (3,957-4,042 m) interval. It has a marginal source rock quality, which could also act as a seal for the Deleb-Adigrat sandstone reservoir rock.

The second interval is developed in the Middle Jurassic, and is widely distributed across the basin, consisting of grainstones, packstones, and dolomites which serves as excellent reservoir rocks. Due to the heavy calcitic precipitation and infilling of the pores, the quality is fairly poor in the Hol-1 region. Dolomitic beds with high porosities may be the best reservoirs. The lime mudstone source rock beneath the reservoir rock serves as an ideal kitchen zone for hydrocarbon generation, while the evaporate beds found above the source and reservoir intervals could serve as a seal.

A TTI modeling results for the Lower Jurassic source rocks correspond to a value of 1,319 that correlate to a Vitrinite Reflectance (Ro) value of more than 2. This shows that the source rocks are over mature and located within the dry gas window, that began to develop in the Sinemurian time (approximately 196 Ma) ago. The wet gas window's

sediments are found between well depths of 6180'- 13,220' (1,884- 4,030m) interval. Maturation and expulsion began at Aalenian (172 M.a). A TTI analysis For the same Lower Jurassic source rock from the neighboring Ogaden basin in Ethiopia (Bodle-1 well) yields a value of 580, suggesting that they are also located within the wet gas window. Elkuran_1 well obtained maturation values corresponding to the Late Oil window, with TTI values of 165.3 for the Hettangian source rock.

Maturation of the Lower and Middle Jurassic source rocks peaked during Toarcian, Sinemurian sediments in Hol-1, and Elkuran wells, the TTI values obtained were 21 and 84 respectively. This shows that the source rocks are mature and located within the peak oil window, while the thicknesses of the normal oil window's sediments of Toarcian and Sinemurian are 2,790' and 3,720' respectively. Table 4.8 compares the TTI values of Lugh-Mandera basin and neighboring wells from Ogaden basin in Ethiopia.

The Upper Jurassic sediments are 4240' (1,290m) thick and represented by Interbeddings of grey limestone, shales, sandstones, and sandy limestones. The rahmu section of the Upper Jurassic contains dark grey limestone with shale interbeds. From the geochemical data it shows a mature kerogen type II for this zone, with increased organic content. The TOC was around 0.46 wt% at 3000 feet. This serves as an excellent source rock for the Upper Jurassic sediments.

The Upper Jurassic source rock is within the early oil window, as indicated by TTI values of 5.1. Which is equivalent to a Vitrinite Reflectance (Ro) of 0.6 %? These sediments are found between 2,400'-2,973' (732-906 m) deep, and mature. The oil generation began 159 Ma ago (Oxfordian). TTI analysis of the Upper Jurassic strata in Elkuran-1 well obtains a value of 19.3 predicting that the maturation is also within the early oil window. However, the Bodle-1 well, which is closer to both Hol-1 and Elkuran-1, gives TTI values of 146, indicating that the Upper Jurassic source rock matured within the Late oil window. Table 4.8 illustrates the comparison of the TTI values obtained from the Hol-1 well from Lugh-Mandera basin of Somalia and the neighboring Elkuran-1 and Bodle-1 wells from Ogaden basin of Ehiopia.

The TTI Modeling results reveal that Lugh-Mandera basin has mature source rocks that have produced both oil and gas. The following are the average maturation depths in the Lugh-Mandera basin (based on TTI modeling): Immature: 699'-2,349'; Early oil: 2,400'-3,390'; Peak light oil: 3,570'-6,180'; and Dry gas: 6,360'-13,220' as indicated in figure 4.72.
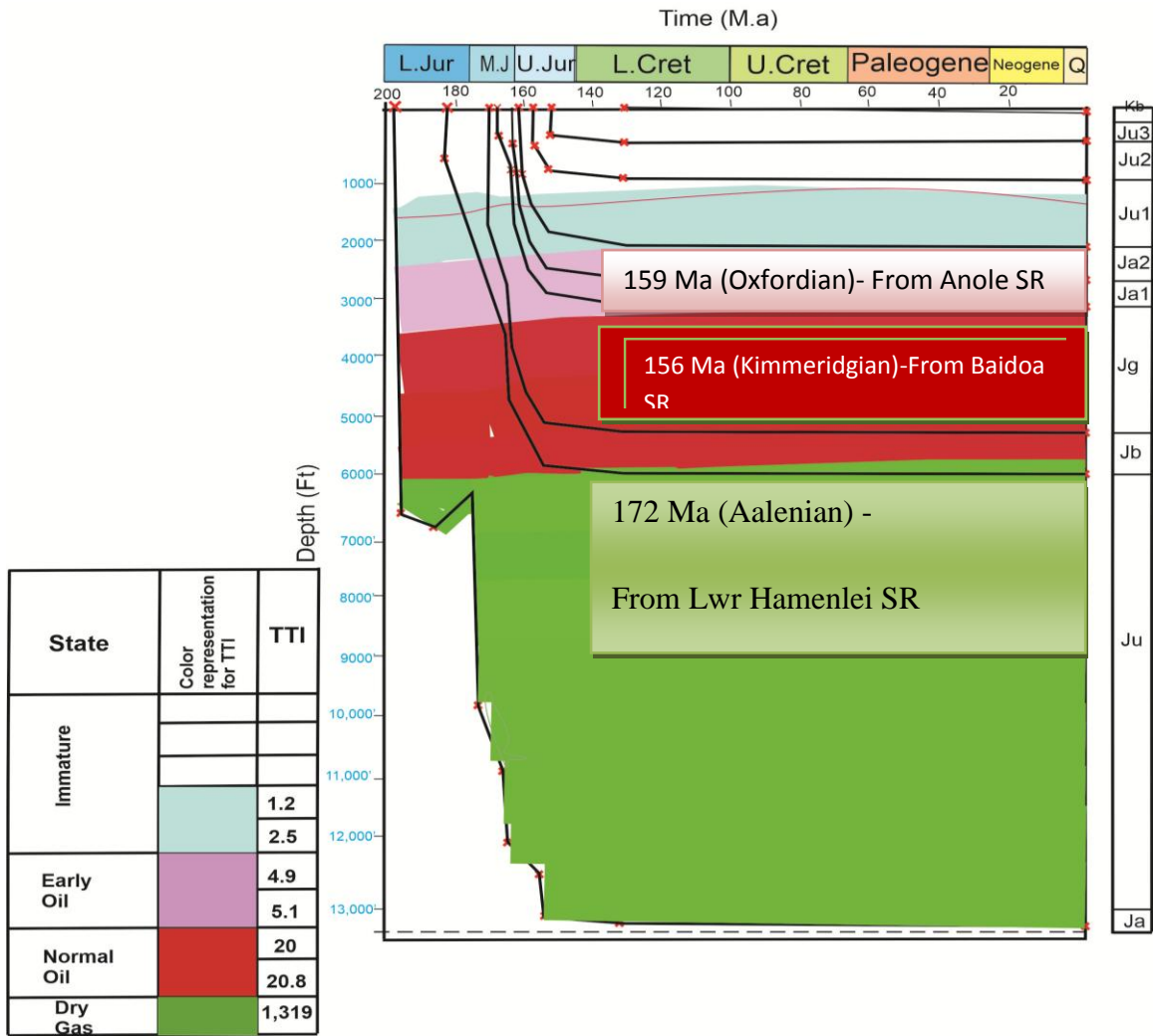
Figure 4.72: TTI Modeling results and the state of hydrocarbon products interims of depth

While neighboring Bodle-1 well has produced oil and wet gas, and El kuran-1 well produced mostly normal light oil. Table 4.8.These results demonstrate that the basin has promising potential. Especially, when compared to the neighboring Ogaden basin in Ethiopia. There are similarities between the petroleum systems of Lugh-Mandera basin and Bodle rift zone. In terms of increased shaliness of the Lower Hamenlei-Adigrat formation that probably blocked the permeability of the Deleb-Adigrat sandstone in both basins.

Epoch		Age	Hol-1	Bodle-1	El Kuran-1
L. Cretaceous		Albian			
		Aptian			
		Barremian			
		Hauterivian			
		Valanginian			
		Berriasian			
U.Jurassic		Tithonian		73	1.2
		Kimmerdigian	2.5	146 / 146 M.a	19.3
		Oxfordian			
M.Jurassic		Callovian	5.1 / 159 M.a		84 / 157 M.a
		Bathonian			
		Bajocian	20.8 / 156 M.a	587 / 146 M.a	
		Aalenian			
L.Jurassic		Toarcian			
		Pliensbachian	1,319 / 172 M.a		
		Sinemurian			
		Hettangian			165.3 / 151 M.a
Triassic		Upper			
Oil Window (m)			1884- 1646 TD		2905-1771 TD
Gas Window (m)				2913- 2165 TD	

Immature	Early Oil	Normal Oil	Late Oil	Wet Gas	Dry Gas

Table 4.8: A comparison of the TTI values obtained from this study area and the neighboring Ogaden basin in Ethiopia. The numbers of wells are three (3).

160

The results of the fourteen (14) seismic profiles with a general length of 650.5 kms revealed the presence of positive flower patterns along the vertical display of most seismic sections from the Lugh-Mandera basin. The concentration of positive flower structures increased in number towards the Hol-1 well, and reduces towards the southwest and especially become dominated on the SO4B-05-P5 and SO4B-05-P4 as indicated in Figures 4.3 & 4.4.

As such, the interpretations revealed the development of minimal deformed folds that have been observed in SW Somalia LMB sector as a result of a transpressive event that occurred during the Early-Late Cretaceous periods linked to the dextral wrench faults that trend to NE-SW (Beltrandi and Pyre, 1973; Carmignani *et* al., 1983).

Beside the dominating structural entrapment configuration presented by flower structures and folds, the south-eastern part of the study area seems to demonstrate some characteristics typical for stratigraphic and hydrodynamic types of oil and gas traps. The stratigraphic type of entrapment is presented by permeability barriers (Selley, 1998), where initially porous and permeable strata loose these properties updip, and thus, impede further movement of the subsurface fluids. The entire section of the Hol-1 wellcat is presented by thick layers of limestones, marls, dolostones and other evaporates lithologies, and thus, the major of reservoir type expected to develop here is *carbonate*.

The studies of Benvenuti et al. (1993) have demonstrated that these thick carbonate sediments are characterized by different petrophysical properties. They distinguished four permeability complexes in the Bay region of south-west Somalia. Among them, two are of specific interest, since they have been encountered in the section of Hol-1 well, and are considered as potential reservoir rock components for the Petroleum system. These are: a) the marly limestone complex of Uegit formation, sandstone (Deleb-Adigrat) and a marly-limestone (Uanei) member of the Baidoa formation that has poor permeability properties towards the south-east from the survey area (near the Bur Acaba basement high), and b) limestone complex presented by the Goloda member of the Baidoa formation that has high permeability values due to extensive fracturing and karstism. The reservoir characterization of such reservoirs is a challenging effort which requires 3D seismic data and increased drilling density.

The available biostratigraphy results seem to indicate stable sources of sediment supply and rates of deposition without any evidence of drastic erosion or truncation during the Jurassic and before the Early Cretaceous when the marine conditions began to retreat from the area (possibly northwards as seen from the interpreted formation base surfaces). The topmost section of the local stratigraphy is composed of a mixture of evaporitic-carbonate lithologies with subordinate sandstone (clastic) material all of which suggests the development of a local hydrocarbon seal capacity. This largely increases the potential of preservation of the generated and entrapped hydrocarbons.

CHAPTER 5 : CONCLUSIONS AND RECOMMENDATIONS

5.1. CONCLUSIONS

The Lugh-Mandera basin has thick Lower and Middle Jurassic strata and thinner Upper Jurassic and Early Cretaceous layers. The results also indicated that these sediments are thicker at the northern end of the basin and thin off towards the western and eastern ends. As a result, the geometry of the sedimentary basin is asymmetrical. The petroleum system of the Lugh-Mandera basin is similar to the ones developed in the neighboring Ogaden basin of Ethiopia. The major source rock interval is related to the Lower, Middle, and Upper Jurassic lime mudstones and shales, while the primary reservoir rocks are the Middle Jurassic fractured limestones and dolomites. The thick Middle Jurassic evaporites and Upper Jurassic Uarandab shales may have good sealing capabilities, while the thin marine carbonates of Uegit and Garbaharey formations act as Overburden rock.

The existence of a wrench fault tectonics in the Lugh-Mandera basin was suggested by earlier studies and has been verified structurally. The subsurface geological maps and the seismic data interpretation confirm that wrench fault structures (Traps) could be favorable for the accumulation of hydrocarbons if re-distribution of Hc's occurred.

In this study a wrench fault tectonics generated positive flower structures in the Lugh-Mandera basin. Across the strike of the Lugh-Mandera basin some related wrench tectonic anticlines with a wavelength of about 10 km have been mapped. Sub-vertical angle faults dominate in the basin. They link up with planar faults to generate positive flower structures that serve as viable hydrocarbon traps. These together with antiforms characterize a positive flower structures. They arise in convergent or transpression fault zones, as well as in the combination of compression and strike slip faults. The existence of an anticline on the vertical seismic display of seismic lines S04B05-P5, SO4B30_P3, as shown in (Figures 4.3 & 4.14) represents folding.

The Implication of Wrench Tectonics on the Petroleum System:

- Wrench related structure can have significant impact on hydrocarbon dolomite reservoirs.

- On both sides of faults, facies and thickness may vary dramatically for the same stratigraphic strata.

- Broad anticlinal (dormal) and numerous flower structures create potential hydrocarbon traps.

- Faulted anticlines formed after the initial hydrocarbon expulsion and migration occurred and entrapment relies on only re-distribution of hydrocarbons.

TTI modeling shows that the source rocks are within situated at different levels of maturation. For instance, the Lower Jurassic Pleinsbachian-Hettangian source rock is located within the dry gas window and develops between depths of 6,360'-13,220' (1,939-4,030 m) interval. Their maturation and expulsion has been estimated to have occurred in the Aalenian stage (172 Ma) ago. The Middle Jurassic Bajocian source rock is located within the peak oil window and is present between the depths of 3,570'-6,180' (1,088-1,884 m) interval. Maturation and expulsion from these source rocks interval began around 156 Ma ago (Kimmeridgian).

5.2. RECOMMENDATIONS

Future exploration activities should be driven by the recognition of the general tectonic and structural setting of the survey area. The available surface and subsurface data and interpretations reveal that the Lugh-Mandera basin developed under the prevailing influence of wrench (strike-slip) tectonics. This conclusion is proved by the high density of flower structures which commonly develop due to shearing and tangential compressional and transtentional deformations along large strike-slip faults. However, hydrocarbon exploration and later production from these complex geological areas requires increased attention on their structural geological aspects.

More infill drilling would be necessary to evaluate the hydrocarbon potential of the Somalian sector of the Lugh-Mandera basin. It will be largely beneficial if more 2D and locally 3D seismic lines are acquired along the Garbaharrey and Sengif fold deformation belts, and also areas to the south-east from the survey area, in the proximity of the Bur Acaba basement high, and some interior locations of the broad Tomalo syncline.

Due to time constraints and lack of 3D seismic data we were not able to undertake a complete fault modeling of the basin, especially the study of the fault geometries and the entrapping mechanisms related to them. As Tearpock et al and Bischke (2002) mention it is impossible to undertake a scrupulous fault modeling of vertically dipping faults, including flower structures using only 2D seismic survey data. As seen from our interpretations, steeply dipping fault surfaces will be projected on 2D surface maps as dots (!). Therefore, it is advisable to set a special programme and acquire a 3D seismic survey, especially near the deformation fold structures that have extents exceeding 100 km (Ali Kassim et al., 1993; Ali Kassim et al., 2002).

The current study proposes infilling drilling locations that target the possible hydrodynamic traps. The analysis of the position of springs, hydrostructural conditions of complexes, geometry of rock bodies suggest that the prevailing flow direction of subterranean waters in the Bay region is south-east, and towards the Bur Acaba high. The

165

flow direction is perpendicular to the contact between the limestone complex (reservoir) and the impermeable layer of the crystalline complex (Benvenuti et al., 1993).

Future research should incorporate these results and focus on advanced reservoir characterization and fault modeling. These would help in understanding the nature and amount of the fluid content, size and shape of the reservoir. The migration pathways and entrapment potential of the faults will also provide future infill drilling sites. The reservoir characterization of carbonate reservoirs is much complicated than that for sandstone lithologies. One of the reasons is that limestones are more prone to various postdepositional lithological changes (including karst and stylolites) the effects of fracturing which is difficult in assessment when core and well log data are limited, or absent.

Target zones for drilling have been estimated and therefore recommended on the subsurface depth structure map in figures (4.55 & 4.61), arrows indicating the likely directions of primary and secondary hydrocarbon migration.

REFERENCES

Abbate, E., Sagri, M., Sassi, F.P., (1993). *In: Geological Map of Somalia,* vol. 113. Istituto Agronomico per l'Oltremare, Relazionie Monografie Agrarie Subtropicali e Tropicali, Nuova Serie, Firenze, P. 19-30.

Acacia Consultants (2008), *Mid-term evaluation of the Agricultural Rehabilitation and Diversification of High Potential Irrigation Schemes (ARDOPIS).* OSRO/SOM/510/EC and OSRO/SOM/511/EC.

Ali Kassim, M., Carmignani, L., Fazzuoli, M., (1987). In: Geology of the Luuq-Mandera basin. *International Meeting Geology of Somalia and Surrounding Regions, Excursion A Guidebook, Mogadisho*, 43P.

Ali Kassim, M., Carmignani, L., Fantozzi, P., (1993a). *Tectonic traspression in the Gedo region southern Somalia*. In: Abbate, E., Sagri, M., Sassi, F.P. (Eds.), Geology and Mineral Resources of Somalia and Surrounding Regions, vol. 113, P. 67-234.

Ali Kassim M., L. Carmignani, P. Conti, P.L. Fantozzi, (2002) *Geology of the Mesozoic-Tertiary sedimentary basins in southwestern Somalia,* P. 1-6.

Aloisi, P., & De Angelis, A. M. (1938). *Le Rocce della Somalia. Rendicont della Societ_a Geografica*, Geologia della Somalia 2, P.16-63.

Al-Thour, K. A. (1997). Facies sequences of the Middle-Upper Jurassic carbonate platform (Amran Group) in the Sana'a region, Republic of Yemen. *Marine and Petroleum Geology*, 14(6), P. 643-660.

Anderson, E. M. (1951). *The Dynamics of Faulting, Etc.(Revised.).* Edinburgh: London.

Angelucci, A. B., Cabdulqaadir, M., Faaduma, C., Franco, F., Carush, M., & Piccoli, G. (1983). The Jurassic stratigraphic series in Gedo and Bay regions (Southwestern Somalia). *Memorie di Scienze Geologiche*, 36, P. 73–94.

Arkell, W. J. (1956). Comments on stratigraphic procedure and terminology. *American Journal of Science*, 254(8), P. 457-467.

Azzaroli, A., Merla, C., (1959). A *Geological Map of Ethiopia and Somalia and Comment with a Map of Major Landforms*. CNR, Firenze, P. 95-99.

Azzaroli, P., & De Angelis, A. M. (1965). Lineamenti geologici della regione dei Bur in Somalia. *Atti della Societa Toscana di Scienze Naturali, Memorie, Serie A*, 72, P. 537-547.

Baker, B.H and Saggerson, E.P (1958). Geology of the E1.Wak-Aus   Mandula area. *Rep* .No.44. prepared by the ministry of commerce and industry, the geological survey of kenya. P.7-36.

Barbieri, F. (1968). Jurassic microfacies in western Somalia. *Rivista Italiana Paleontologica Stratigrafica*, v. 74, P. 805-826.

Barker. C. (1996) *Thermal Modeling of Petroleum Generation. Theory and Application*. Elsevier, P. 225-297.

Barnes, S. U. (1976). Geology and oil prospects of Somalia, East Africa. *AAPG Bulletin*, 60(3), P. 389-413.

Beck, M. E., JR, (1983). On the mechanism of tectonic transport in zones of oblique subduction. *Tectonophysics*, 93, P. 1–11.

Bellieni, G., Hayder, A., Ibrahim, H., Sassi, F., & Zirpoli, G. (1980). Caratteri geochimico-petrografici dei graniti dei Buur (Somalia meridionale). *Quaderni di Geologia della Somalia, Universitia Nazionale Somala* , 4, P. 98–114.

Beltrandi, M., & Pyre, A. (1973). Geological Evolution of Southwest Somali, Sedimentary Basins of the African coasts. South. *Blant, G., Ed.*, vol. 2, P. 159-178.

Benvenuti, G., Hussein Salad M., Omar S.Yusuf and Vallario, A- (1993). *Preliminary hydrogeologic balance of the Baidoa formation (Bay region, South West Somalia) in Geology and Mineral Resources of Somalia and surrounding regions (with a*

geological map of Somalia 1:1,5oo,000). B-Mineral and Water Resources . Instituto agronomico per L'oltremare.Firenze.P. 671-678.

Berry, G. (1974). '*Sedimentological Studies on Carbonate rocks from the Hol-1 well and on Carbonate field samples from Somalia*'. South. *Blant, G., Ed.*, vol. 2, P. 139-158.

Bignell, R. (1977). Petroleum developments in Central and Southern Africa. *American Association of Petroleum Geologists Bulletin*, 61, P. 1746-1794.

Billings, M. P. (1954). *Structural geology (2d ed.).* New York: Prentice-Hall.

Biro, P. (1975). Petroleum developments in central and southern Africa in 1974. *AAPG Bulletin 59*, 10, P. 1904-1949.

Bjorlykke, K. (2010). *Petroleum geoscience: From sedimentary environments to rock physics.* Springer Science & Business Media.

Bocal (1972). *Palynological Report on Burmah oil Somalia Ltd.* Hol N-1 well. Bopal/32 Report.

Boccaletti, M., Dainelli, P., Angelucci, A., Arush, M. A., Cabdulqaadir, M. M., Nafissi, P., & Robba, E. (1988). Folding of the Mesozoic Cover in SW Somalia: a Compressional Episode Related to teh early Stages of Indian Ocean Evolution. . *Journal of Petroleum Geology,*, 11(2), P. 157-168.

Borsi, S., Ferrara, G., & Mazzuoli, R. (1965). *Petrographic study and dating with the K / Ar and Rb / Sr methods of a granite rock near Bur Somalia*.

Bosellini, A. (1986). East Africa continental margins. *Geology*, 14, P. 373-205.

Bosellini. (1989). The continental margins of Somalia: Their structural evolution and sequence stratigraphy. *Memorie di Scienze Geologiche*, 41, P. 373-458.

Bosellini. (1992). *The Continental Margins of Somalia: Structural Evolution and Sequence Stratigraphy: Chapter 11.* African and Mediterranean Margins.

Buck, W. R., Lavier, L. L., & Poliakov, A. N. (1999). How to make a rift wide. Philosophical Transactions of the Royal Society of London. Series A Mathematical. *Physical and Engineering Sciences*, 357(1753), P. 671-693.

Burmah Oil Co. (1973). *Hol No. 1. Complete Report, Mogadishu.* Mogadishu: unpublished.

Buscaglione, L., Fazzuoli, M., Chiocchini, M., & Pavia, G. (1993). *Contributions to the stratigraphy of the Early to Middle Jurassic formations of the eastern side of the Luuq-Mandera basin Bay and Gedo regions southwestern Somalia.* (In: Abbate, E., Sagri, M., Sassi, F.P. (Eds.), Geology and Mineral Resources of Somalia and Surrounding Regions, vol. 113. Istituto Agronomico per l'Oltremare, Relazioni e Monografie Agrarie Subtropicali per l'Oltremare, Relazioni e Monografie Agrarie Sub ed.). Nuova Serie: Firenze, P. 153–168.

Canuti, P., Fazzuoli, M., Ficcarelli, G., & Venturi, F. (1983). Occurrence of Liassic faunas at Waaney (Uanei), Province of Bay, South-western Somalia. *Rivista Italiana di Paleontologia e Stratigrafia*, 889, P. 31–46.

Carmignani, L., Kassim, M., & Fantozzi, P. (1983). *Preliminary note on the survey of the Gedo region (upper valley of Juba-southern Somalia).* Somalia Geology Papers.

Catuneanu, O., Wopfner, H., Eriksson, P.G., Cairncross, B., Rubidge, B.S., Smith, R.M.H. & Hancox, P.J. (2005). The Karoo basins of south-centralAfrica. *Journal of African Earth Sciences*, 43, P. 211–253.

Cloos, E. (1955). Experimental analysis of fracture patterns. *Geological Society of America Bulletin*, 66(3), P. 241-256.

Coffin, M.F., Rabinowitz, P.D., (1983). East African continental margin transect. In: Bally, A.W. (Ed.), Seismic Expression of Structural Styles. Volume Two Studies in Geology. *American Association of Petroleum Geologists, 15, Lamont-Doherty Geological Observatory, Columbia University, Columbia*, P. 22–33.

Coffin, M. F., & Rabinowitz, P. D. (1987). Reconstruction of Madagascar and Africa: Evidence from the Davie fracture zone and western Somali basin. *Journal of Geophysical Research: Solid Earth*, 92(B9), P. 9385-9406.

Coffin, M.F., Rabinowitz, P.D., (1988). Evolution of the Conjugate East African-Madagascan Margins and the Western Somali basin. *Geological Society of America*, 64, P. 37-178.

Coffin, M.F. and Rabinowitz, P.D, (1992). The Mesozoic East African and Madagascan Conjugate Continental Margins. Stratigraphy and Tectonics. In: Geology and Geophysics of Continental Margins. *AAPG Memoir* 53, P. 207-240.

Currie, E.D., (1925). *Jurassic and Eocene Echinoidea (from Jubaland)*. Monograph Geology Department Hunterian Museum Glasgow University 1, P . 46–76.

Dal Piaz, G., & Sassi, F. (1986). *The crystalline basement of Somalia*: a review. 31, P. 351–361.

Daniels, J. L. (1965). A photogeological interpretation of the Bur region, Somalia. *Geol. & Min. Res, Oxford*, 9 (4): P. 427-436.

Dobrin, M. B., & Savit, C. H. (1988). *Introduction to Geophysical Prospecting.* New York: McGraw-Hill Book Co. 867P.

Domino, E. (1966, July 28). *Geology of the Garbe Harre area Burmah.* Retrieved from Oil Somalia Ltd. Reports Environment, P. 235-251: http://www.springerlink.com/index/10.1007/978-3-642-02332-3

Eagles, G. & König, M. (2008). A model of plate kinematics in Gondwana break up. *Geophysical Journal International*, 173, P.703–717.

Fantoli, A., (1960). Le precipitazioni atmosferiche in Somalia. *Rivista di Agricoltura Subtropicale e Tropicale* 54, P. 4–9.

Freudenthal and Hochuli (1985). *Paleontology and Stratigraphy of Hol-1* well, South Western Somalia (unpublished).

Friedman G. (1972) *Significance of Red Sea in Problem of Evaporites and Basinal Limestones.* AAPG Vol 56/6.

Gadallah, M. R., & Fisher, R. (2009). *Seismic Interpretation. In Exploration Geophysics,.* Heidelberg: Springer, Berlin, P. 149-221.

Gaede, V. F., (1964), *Central area of Whittier oil field: California Div. Oil and Gas, California Oil Fields*—Summ. Operations, v. 50, no. 1, P. 59-67.

Haider, A., (1983). Contributo alla conoscenza delle masse granitoidi dei Buur (Somalia meridionale). *Quaderni di Geologia della Somalia, Universita Nazionale Somalia* 7, P. 39–53.

Haider, A., (1993). Preliminary data on the magmatic origin and emplacement context of the Precambrian amphibolites of the Buur region (Southern Somalia).). In: Abbate, E., Sagri, M., Sassi, F.P. (Eds.), *Geology and Mineral Resources of Somalia and Surrounding Regions*, vol. 113, P. 34-112.

Harms, J.C and Brady, M.J., (1989). *Oil and Gas Potential of the Somali Democratic Republic: Volume I. South-West. Juba-Lamu and Mandera-Lugh Basins.* Prepared for the Ministry of Mineral and Water Resources.

Harms, J.C & Naleye, A., (1993). Petroleum exploration in Somalia; Geology and mineral resources of Somalia and the surrounding regions; First Agron; Oltremare, Firenze. *Relaz e Monogr.*, 113, P. 417 – 428.

Harms, J.C and Brady, M.J., (2002). *Exploration history and hydrocarbon potential of Somalia: presentation for* Kansas Geological Society; Technical Talk 2002.

Harding, T. P., (1973a). Newport-Inglewood trend, California— an example of wrenching style of deformation: *Am. Assoc. Petroleum Geologists Bull.,* v. 57, no. 1, P. 97-116.

Harding T.P., (1985). Seismic characteristics and identification of negative flower structures, positive flower structures, and positive structural inversion. *Bulletin of the American Association of Petroleum Geologists* 69 (4), P.582-600.

Hill, P. (1947) Classification of faults: *Am. Assoc. Petroleum Geologists Bull*., v. 31, P. 16-99.

Holdsworth, R. E., Dewey, J. F., & Strachan, R. A. (1998). Transpression and transtension zones. . *Geological Society, London. Special Publications*, 135(1), P. 1-14.

Hunegnaw, A., Sage, L., & Gonnard, R. (1998). Hydrocarbon potential of the intracratonic Ogaden Basin, SE Ethiopia. *Journal of Petroleum Geology*, *21*(4), P. 401-425.

Ilyin, A. (1967). *Geology of the Buur area. Explanatory Note to the Geological Map of the Buur area, Scale 1:200.000.* Unpublished Report: Geological Survey of Somalia, Muqdisho.

Kamen-Kaye & Barnes. (1979). Exploration geology of Northeastern Africa- Seychelles basin. *Journal of Petroleum Geology*, 2, P. 23-45.

Kamen-Kaye, M., (1978). Permian to Tertiary faunas and paleogeography: Somalia, Kenya, Tanzania, Mozambique, Madagascar, South Africa. *Joum Petrol. Geof*., 1 (1) P. 79-101.

Keary, P., Brooks, M., & Hill, I. (2002). *An Introduction to Geophysical Exploration.* Blackwell Science, 2002. ISBN0632049294, P. 21-118.

Kennedy, W. Q. (1946). The Great Glen Fault. *Quarterly Journal of the Geological Society*, 102(1-4), P. 41-76.

Kent, P. E. (1982). *The Somali ocean basin and the continental margin of east Africa. In The Ocean Basins and Margins. .* Boston, MA.: Springer, P. 185-204.

Klemme, H.D., (1980) *Petroleum Basin: Classification and characteristics. J.Petrol. Geol. V.2(3), P. 187-207.*

Lavier, L. L., & Manatschal, G. (2006). A mechanism to thin the continental lithosphere at magma-poor margins. *Nature*, 440(7082), P. 324-328.

Low, J. (1949). *Subsurface maps and illustrations in Subsurface Geologic Methods.Ed.L.W., LeoRoy and H.M. Crain.* Department of Publication, Colarado School of Mines, Golden, Colorado, P. 627-682.

Marillier, F., Eichenberger, U., Sommaruga, A., (2006). Seismic synthesis of the Swiss Molasse Basin. *Schweizerische Geophysilaische Kommission SGPK, Annual Report*., P. 1–16.

McKenzie, D. (1978). 'The evolution of the Indian Ocean since the Late Cretaceous, *Geophs.J.R.Astron.Soc.*, 24, P. 437-528.

Migliorini, C.I. (1948) *Geology and oil prospects of Eastern Ethiopia: AGIP Mineraria, Rome*. (unpublished Sinclair Petroleum Report).

Moody, J., & Hill, M. (1956). Wrench faults tectonics. . *Geological Society of America Bulletin*, 67, P. 1207–1246.

Morgan, P and Davies, T.D., (1985). *Geochemical Study of Hol-1 well*, Somalia (unpublished).

Norton, I., & Sclater, J. (1979). A model for the evolution of the Indian Ocean and the break-up of Gondwanaland. *Journal of Geophysical Research*, 84, P. 6803-6830.

Paleoservices (1973). *Paleontological final report Hol-1*. Confidential (unpublished report).

Paleoservices (1975). *Field samples burmah oil Ltd*. Confidential unpublished Paleontological Report 1.

Peters, K. E. (1986). Guidelines for evaluating petroleum source rock using programmed pyrolysis. *AAPG bulletin*, 70(3), P. 318-329.

Piccoli, G. (1986). *Geological history of Central and Southern Somalia since the Triassic*. P. 31-111.

Pichi-Sermolli, R. E. (1957). Una carta geobotanica dell'Africa Orientale (Eritrea, Ethiopia, Somalia). . *Webbia* , 13: P. 15–132 & 1 map.

Purcell, P. G. (1979). *The geology and petroleum potential of the Ogaden Basin, Ethiopia.* unpublished report.

Rabinowitz, P.D., Coffin, M.F., Falvey, D., (1983). The separation of Madagascar and Africa. *Science*, 220, P. 67–69.

Rapolla, A., Cella, F., Dorre, A.S., (1995a). Gravity study of the crustal structures of Somalia along International Lithosphere program geotransects. *Journal of African Earth Sciences* 20, P. 3–4.

Rapolla, A., Cella, F., Dorre, A.S., (1995b). Moho and lithosphere–astenosphere boundaries in East Africa from regional gravity data, *Journal of African Earth Sciences* 25, P. 8-14.

Rizzo, G., (1977). Appunti sul clima della Somalia. In: Cuman Shire, Y. (Ed.), *Quaderni di Geologia della Somalia, vol. 1. Universita` Nazionale della Somalia*, P. 94–101.

Schuck, A., & Lange, G. (2007). *Seismic methods. In Environmental Geology.* Heidelberg: Springer, Berlin, P. 337-402.

Selley, R. C. (1998). *Elements of petroleum geology.* Gulf Professional Publishing *(P.98-167).*

St John, W. (2016). Synopsis of geology of Ethiopia. *AAPG Search and Discovery Article*, P. 70-215.

Stefanini, G., & Paoli, G. (1916). *Hydrogeological, botanical and entomological researches: carried out in southern Italian Somalia (1913) (No. 7). .* Italian colonial agricultural institute.

Stefanini, G. (1931d). Fossili del Giuralias. Premessa: cenni sulle localitia fossilifere giurassiche della Somalia. *Palaeontographia Italica*, 32, P. 35–48.

Suess, E., (1885). Face of the earth (Das Antlitz der Erde): English translation by H. B. C. Sollas under direction W. J. Sollas, N. Y., *Oxford Univ. Press*, v (5), P. 1904-1925.

Swalim. October (2007). *The Climate of Somalia.* Report No. WO1 SWALIM.

Swalim. December (2007). *Status of Medium to Large Irrigation Schemes in Southern Somalia*. Technical Report No. W-05. Nairobi, Kenya.

Sylvester, A.G., Smith, R.R., (1976). Tectonic transpression and basement-controlled deformation in San Andreas Fault Zone, Salton Trough, California. *American Association of Petroleum Geologists Bulletin* 60, P. 2081–2102.

Sylvester, A. (1988). *Strike-slip faults.* Geological Society of America, P.123-150.

Tearpock, D. J., & Bischke, R. E. (2002). Applied subsurface geological mapping with structural methods. *2nd Ed. Prentice-Hall PTR.822P.*

Van Hinte, J.E. (1978)' Geohistory Analysis-Application of Micropaleontology in Exploration Geology. *The American Association of Petroleum Geology Bulletin,* 62 (2), P. 201-222.

Walters, R., and Linton, R. E., (1973). The sedimentary basins of coastal Kenya, in Sedimentary basins of the African coasts, part 2: *Association of African Geological Surveys*, P. 133-158.

Waples.D.W. (1980) ' Time and Temperature in Petroleum formations Application of Lopatin's Method to Petroleum Exploration' *American Association of Petroleum Geologists Bulletin*, 64(6), P. 916-926.

Waples.D.W. (1985) ' *Predicting thermal Maturity' in Geochemistry in Petroleum Exploration*, P. 121-154.

Warden, A., & Horkel, A. (1984). The geological evolution of the NE branch of the Mozambique belt (Kenya, Somalia, Ethiopia). *Mitteilungen der Osterrichischen Geologischen Gesellschaft*, 77, P. 161–184.

Weir, J., (1929). *Jurassic fossils from Jubaland, East Africa*. Monograph Geology Department Hunterian Museum Glasgow University 3, P. 1–63.

Whiteman. (1981). East Africa basins: Reserves, resources and prospects, in petroleum exploration strategies in developing countries: United Nations meeting, Hague, Proceedings. *United Nations Natural Resources and Energy Division*, Hague, P. 51-98.

Wilcox, R., Harding, T., & Seely, D. (1973). Basic wrench tectonics. *American Association of Petroleum Geologists Bulletin*, 57, P. 74–96.

Wilson, J. T. (1965). A new class of faults and their bearing on continental drift. *Nature*, 207(4995), P. 343-347.

Woodcock, N. H., (1986). Strike-slip duplexes. *Journal of structural geology*, 8(7), P. 725-735.

Yeats, R. S. McNeill, L. C., Piper, K. A., Goldfinger, C., Kulm, L. D., (1997). Listric normal faulting on the Cascadia continental margin. *Journal of Geophysical Research: Solid Earth*, 102(B6), P. 12123-12138.